FLUORESCENCE RESPONSE OF SOME STRUCTURALLY SIMPLE MULTICOMPONENT SYSTEMS TOWARDS THE TRANSITION METAL IONS

A Thesis
Submitted for the Degree of
DOCTOR OF PHILOSOPHY

By

B. Ramachandram

School of Chemistry
UNIVERSITY OF HYDERABAD
Hyderabad 500 046
INDIA

July 1999

Dedicated to my

Parents,
Teachers,
Brothers, Sisters
and Vijaya

CONTENTS

DECLARATION

I hereby declare that the matter embodied in this Thesis is the result of investigation carried out by me in the School of Chemistry, University of Hyderabad, Hyderabad, India under the supervision of Dr. Anunay Samanta.

In keeping with the general practice of reporting scientific observations due acknowledgements have been made wherever the work described is based on the findings of other investigators.

B. Ramachandram
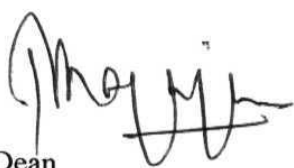
CERTIFICATE

Certified that the work contained in the Thesis entitled *"Fluorescence Response of Some Structurally Simple Multi-component Systems Towards the Transition Metal Ions"* **has been** carried out by B. Ramachandram under my supervision and that the same has not been submitted elsewhere for a degree.

July, 1999

Dr. Anunay Samanta

(Thesis Supervisor)

Dean

School of Chemistry

ACKNOWLEDGEMENTS

I thank...

...my supervisor, Dr. Anunay Samanta for his excellent guidance and encouragement throughout my research period. He guided me in the real sense, in all aspects. Working with him is pleasant.

...the dean, Prof. M. Nagarajan for letting me avail the facilities and for useful discussions and timely suggestions.

...Prof. PS. Zacharias for his constant help both academically and non academically.

... Dr. Bhaskar G. Maiya for his timely help during my research period.

...all the faculty members for their help during the various occasions.

...my labmates Soujanya, Saroja, Satyen, Sankaran, Rana, and Sreenivasamurthy for their help during my research work.

...Satyen and Sankaran who made my work easy in all respects, moving with them is pleasant and memorable.

...Anthony, Chandrakala and Krishnama Chary for their useful discussions at various stages of the synthesis part.

...my friends, Srinivas, Arounagouri, Giri, Ramana, Prasad, Ravi, Barathi, Ramanathan, Vijaya Prakash, Ramalakshmi, D S . Reddy, Rajesh, Dharma, Das, Ram, Srinivasan, Srinivas (G), Palas, Senthil, Sampath, Sreenivas Bandaru, Malikajun Reddy Jr. Ram, Sailaja, Sonika, Mangaya, Madhavi, Padmaja, Sumod, Venu, Praveen, Pal, who made my stay in the campus memorable.

...Dr. K.V. Reddy, of CIL for his good cooperation in using the fluorimeter.

...Raghava for his cooperation in collecting crystal data.

List of publications:

(i) Work presented in the Thesis:

1. Modulation of metal-fluorophore communication to develop structurally simple fluorescent sensors for transition metal ions; B. Ramachandram and A. Samanta, J. Chem. Soc. Chem. Comai un. 1037, 1997.

2. How important is the quenching influence of the transition metal ions in the design of fluorescent PET sensors?; B. Ramachandram and A. Samanta, Chem. Phys. **Lett.** *290,* 9, 1998.

3. Transition metal ion induced fluorescence enhancement of 4-(N,N-dimethylethylenediamino)-7-nitrobenz-2-oxa-l,3-diazole; B. Ramachandram and A. Samanta, J. Phys. Chem. A. *102,* 10579, 1998.

4. Fluorescence response of structurally simple *fluorophore - spacer - receptor* systems towards transition metal ions and protons; B. Ramachandram, NB. Sankaran and A. Samanta, Res. **Chem. Interm**. **In** Press.

5. Unusually high fluorescence enhancement of structurally *simple fluorophore - spacer - receptor* systems induced by transition metal ions; B. Ramachandram, G. Saroja and A. Samanta, To be communicated.

(ii) Work not related to the Thesis:

6. An investigation of the triplet state properties of 1,8-naphthalimide: a laser flash photolysis study; A. Samanta, B. Ramachandram and G. Saroja, J. Photochem. Photobiol. A: Chem. *101,* 29, **1996**.

7. 4-Aminophthalimide derivatives as environment sensitive probes; G. Saroja, T. Soujanya, B. Ramachandram and A. Samanta, J. **Fluoresc.** *8,* 405, 1998.

8. The fluorescence response of a structurally modified 4-aminophthalimide derivative covalently attached to a fatty acid in homogeneous and micellar environment; G. Saroja, B. Ramachandram, S. Saha and A. Samanta, J. Phys. Chem. B. *103,* 2906, 1999.

FLUORESCENCE SIGNALLING SYSTEMS: AN OVERVIEW

1.1. Introduction

Just as binary logical and arithmetic operations in the computers are performed by the semiconductors, information processing or computation at the molecular level is possible when molecular devices are developed that can function as wires, gates, memory elements, sensors, etc. It is this realisation that has led to a widespread activity in the development of molecular systems capable of performing functions of various kinds.[1-3] A molecular device is essentially an assembly of suitably organised molecular components and is capable of performing one or more complex logic functions characteristic of the assembly. The specific function performed by a molecular device is the result of individual functions performed by its constituent components. When a molecular device is capable of performing light-induced function, it is termed as a photonic molecular device (PMD). In molecular photochemistry, a molecule performs simple intramolecular or intermolecular photoinduced acts such as emission, electron transfer, bond-breaking, etc, while more complex light-induced functions such as vectorial election transfer, migration of electronic energy, etc can only be performed by an assembly of suitable molecular components or PMDs. A few simple PMDs are schematically illustrated in fig. 1.1.

Currently, there is a paramount need for the detection and measurement of the concentration of specific ions or small molecules such as lead, arsenic and carbon monoxide to monitor increasing water or air pollution. Continuous monitoring of the level of calcium ion, potassium ion or glucose in the body is also often required. All these can be achieved by the design and construction of appropriate molecular systems capable
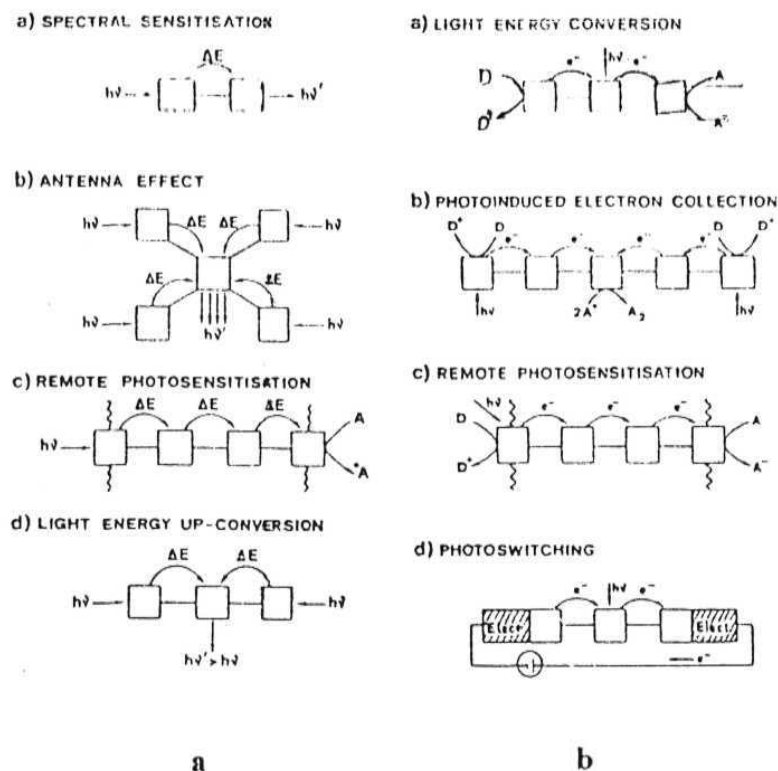
Fig. 1.1. Schematic representation of the function of some photonic molecular devices based on (a) electronic energy transfer and (b) photoinduced electron transfer.

of sensing and reporting the concentration of the required ion or molecule. Molecular devices that function as sensors can possess various signal transduction systems such as UV-visible absorption, circular dichroism, NMR, redox potential and fluorescence.[1-5] Perhaps, the most useful response systems for optical readout are based on fluorescence. This is primarily because of enormous sensitivity of fluorescence in detecting very low concentration of the analyte using less-expensive instrumentation. Further, since the fluorescence response of a given system towards the analytes is almost instantaneous, there is hardly any time lag between the sampling and readout. The sensors based on

fluorescence signalling are commonly termed as fluorosensors. One of the most frequently used mechanisms to vary the fluorescence signal of the sensors in the presence of a guest is photoinduced electron transfer (PET).[1-8] Several researchers have contributed to the development of PET fluorosensors for a variety of guest molecules or ions. Notable among them are the contributions from the research groups of Lehn,[1b,c,d,h] Czarnik,[2] de Silva,[3] Shinkai,[4] Valeur,[6] Balzani[1c,f,g] and Fabbrizzi.[8] The sensing principle involving PET and a few other mechanisms along with representative sensor systems belonging to different classes have been outlined in the following sections of this chapter. In view of the fact that the number of sensor systems reported in the literature is rather large and quite a few excellent and contemporary review articles are already available,[1-6] the discussion presented here is aimed at providing the necessary background of the research undertaken and the discussion has been restricted to a limited number of systems.

1.2.   Fluorescence Signalling Based on Photoinduced Electron Transfer (PET)

1.2.1.   Design principle

That the PET is undoubtedly the most commonly used mechanism for the development of fluorosensors is clearly evident from the volume of the literature available on the PET fluorosensors.[1-8] A fluorescence signalling system usually consists of three components.[†] A 'fluorophore' is essential for the absorption and emission of photons. A 'receptor'[*] moiety is required for the complexation and decomplexation of the

---

Systems with two or more receptor components have also been reported.[2,3] However, the most commonly used PET sensors are three-component systems comprising a fluorophore, a spacer and a receptor.

Strictly speaking, receptors are higher order structures with recognition features. However, since the metal ion binding sites of the PET fluorosensors are generally termed as receptors in the literature, without taking into consideration whether or not the binding site contains any recognition feature, we have followed the same terminology throughout the thesis.

guest. A 'spacer' is often used which, apart from connecting the fluorophore and the receptor, plays a key role in establishing the electronic communication between them.
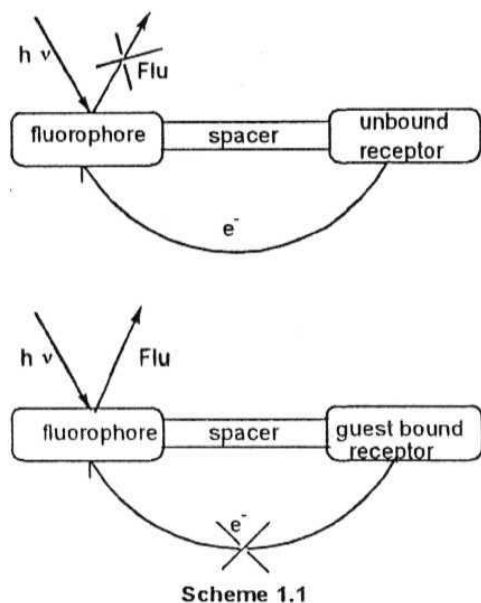
The operating principle of the multi-component *fluorophore-spacer-receptor* fluorosensors has been illustrated in Scheme 1.1. In the absence of the guest, the receptor (usually a group containing one (or more) amino nitrogen atom(s)) is arranged such that it can transfer an electron to the excited fluorophore. The fluorescence of the system is quenched ('switched off) as a result of PET. Thus in the absence of a guest the system is non-fluorescent or weakly fluorescent. On the other hand, since the election donating ability of a guest-bound receptor is drastically lower than that of the unbound receptor, the PET communication between the fluorophore and receptor gets cut-off in the presence of the guest. As a consequence, the fluorescence is 'switched on'. The sensors that are based on this principle are known as fluorescence 'off-on' systems. A few examples of 'off-on' fluorescence signalling systems are shown in the following sections.

On the other hand, as illustrated in Scheme 1.2, PET fluorosensors with the same *'fluorophore - spacer - receptor* architecture but with signalling of an opposite kind can be constructed, where PET is unfavourable in guest-free condition and favourable in the presence of guest. This kind of fluorescence signalling systems, not so common as the previously described ones, are called 'on-off' sensors as the initial guest-free condition is fluorescent and the final guest-bound system is non-fluorescent. Compound 1 falls in this category of signalling systems.[8a,8b] In the presence of the metal ions such as Cu^{+2} or Ni^{+2},
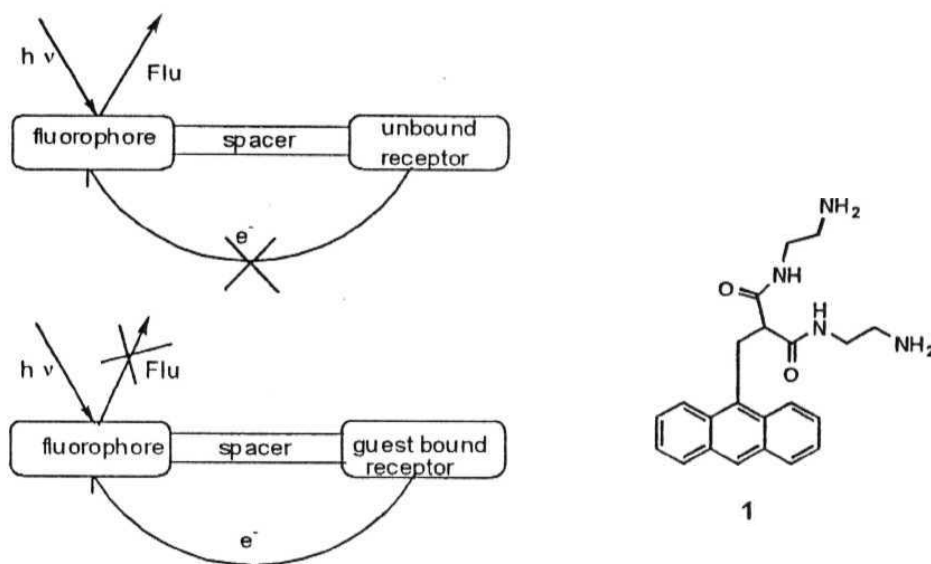
Scheme 1.2

when the amide nitrogen atom of the receptor moiety is deprotonated, conditions become favourable for PET in the system. Few other systems are also present in the literature.[8]

It is evident from the design principles stated above that for the construction of an efficient PET sensor with fluorescence 'off-on' function, one needs to select the fluorophore and the receptor components such that PET between them is thermodynamically feasible.[9] Redox potentials of the components and the lowest singlet state energy of the fluorophore are often helpful in finding out whether the free energy change (vide section 2.5) associated with intramolecular PET is exergonic or not. The chosen receptor should bind the guest as tightly as possible and should be optically transparent at the exciting wavelength of the fluorophore. The chosen fluorophore should have high fluorescence efficiency. Finally, the fluorophore and receptor should be attached through a spacer such that PET is maximised in the *fluorophore-spacer-receptor* system. Generally, a short flexible spacer unit is better than a long one with rigid structure for efficient PET in the system.

1.2.2. *Fluorosensors responsive to protons*

Most of the PET fluorosensors for protons are constituted with a simple amino group as the receptor moiety.[2,3] The phenylalkylamino derivatives such as 2 are perhaps the simplest systems reported two decades ago whose fluorescence signal could be

2   3   4   5

6   7   8
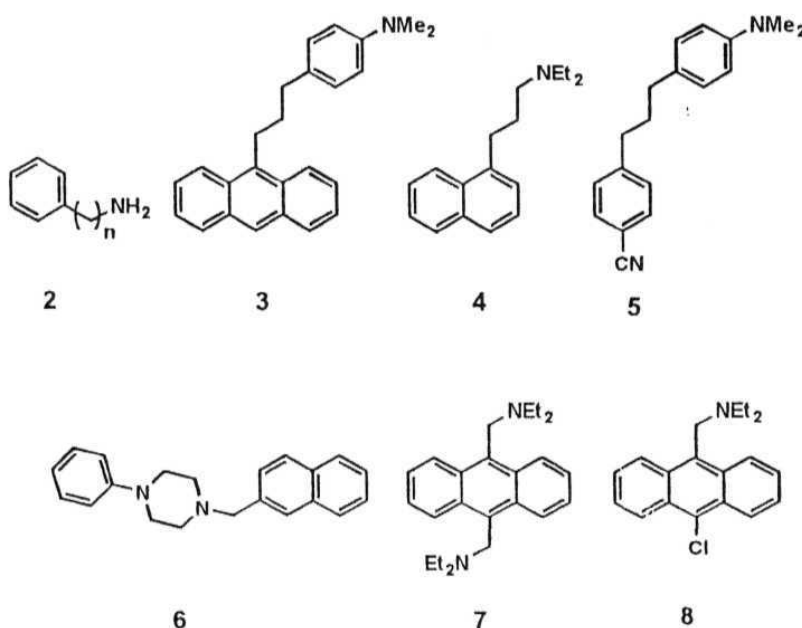
modulated by the presence of the protons.[10] The fluorescence yield (ϕ_f) and lifetime (τ_f) of 2, when protonated, are very similar to those observed for the parent fluorophore (toluene). On the other hand, ϕ_f and τ_f values are quite different from those of the parent fluorophore when the pH of the medium is increased. In the higher pH range, most of the receptor moieties are free from the protons and PET process is thermodynamically feasible in the system. A decrease in the pH of the medium increases the number of molecules with protonated receptor. Since the protonated receptors can no longer quench the fluorescence, one observes an enhancement of the fluorescence intensity of 2 in acidic medium. A similar behaviour has been reported for systems 3 - 8.[1f,11-15]

Utilisation of two or more receptor units in the multi-component system is expected to make intramolecular PET more efficient in the guest-free state. On complete protonation of both the receptors, one can expect fluorescence enhancement (FE) much higher than that observed for a sensor system containing only one receptor moiety. 7 belongs to this category of systems.[14]

Fluorophores containing an electron donor as well as an acceptor group usually fluoresce from a ICT state that is more polar than the ground state.[16] Multi-component
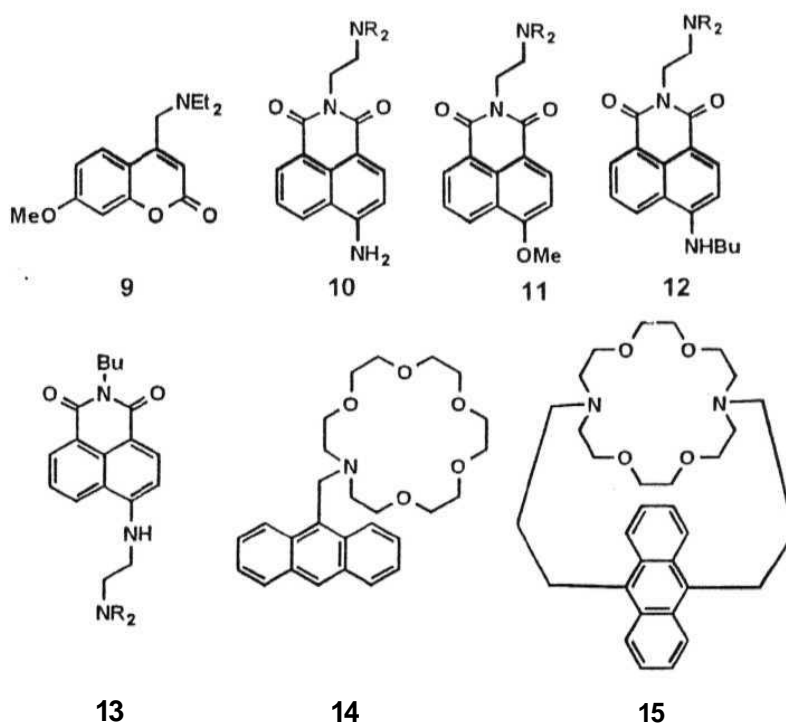
PET fluorosensors involving these fluorophores most often exhibit not only fluorescence enhancement but also a shift (vide section 1.3.4 for details) in the wavelength of the absorption and emission maxima in the presence of protons (or other guests). Compounds 9-12, for example, exhibit proton induced red shift along with fluorescence

enhancement.[17-19] Fluorescence enhancement coupled with a blue shift of the spectral maxima has been reported for sensor systems **13**.[19]

        Macrocyclic crown ethers are known to be excellent receptors for the alkali metal ions.[20] An azacrown moiety, formed on replacement of one of the oxygen atoms of the crown skeleton by nitrogen, can act as a receptor component for the protons as well. **14** and 15 are typical systems that show both metal ion and pH dependent fluorescence.[21,22]

1.2.3.   Fluorosensors responsive to alkali metal ions

        The discovery of the macrocyclic crown ether compounds has opened up a new avenue in the research on sensor design and development. This is mainly due to the fact

        16   **17**   **18**

        19   **20**   **21**
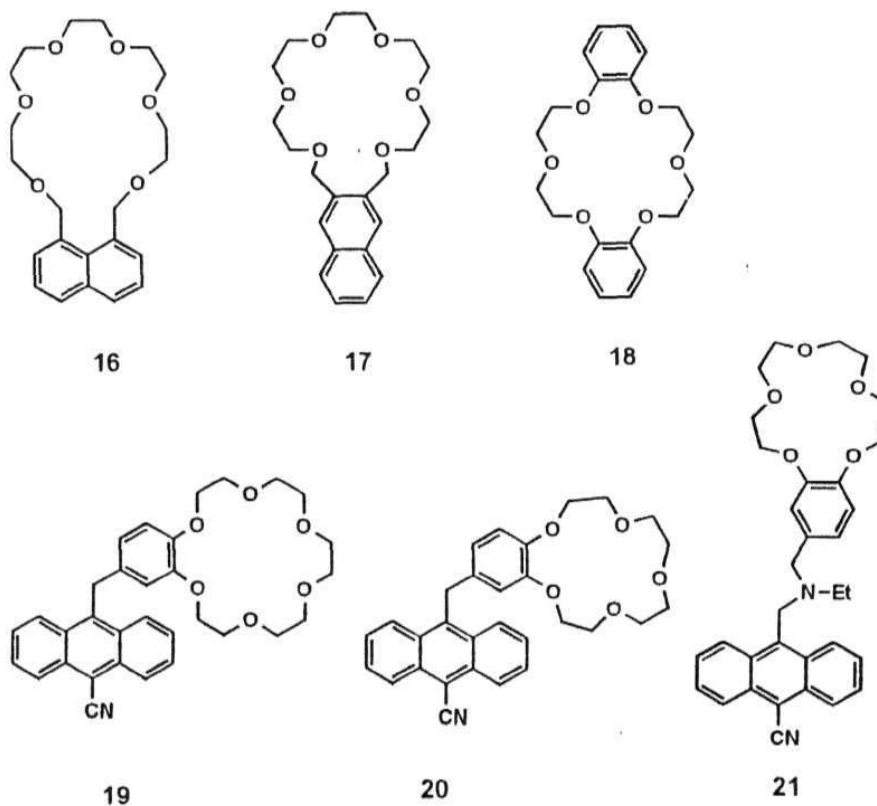
that the crown ether compounds with definite cavity size and orientation bind one metal ion more effectively over the other, thereby allowing ion discrimination. Naphtho- and

benzocrown ether systems such as 16-18 show small but significant alkali metal ion induced fluorescence and phosphorescence modulations.[23-25] 19 and 20 are PET sensors in which the crown ether moieties are capable of binding selectively K^4 and Na^+ respectively.[26,27] The sensor 21, developed by de Silva's group, belongs to this category.[3g] However, this system does more than just detecting a specific metal ion. This is truly a novel system containing two receptor moieties for two different guests; one for the protons and the other for sodium ions. Therefore, maximum FE could be observed only when both Na^+ and protons are present in the medium. In molecular electronics terminology, this system represents an AND gate.

1.2.4. Systems responsive to alkaline earth metal ions

Hard multi-anionic receptors are most suitable for complexation of the alkaline earth metal ions. Even though the crown ether receptors are mainly useful in sensing the alkali cations, the dipositive nature of the alkaline earth metal ions can perturb the charge density in the crown system leading to modulation of the fluorescence of the system. 22
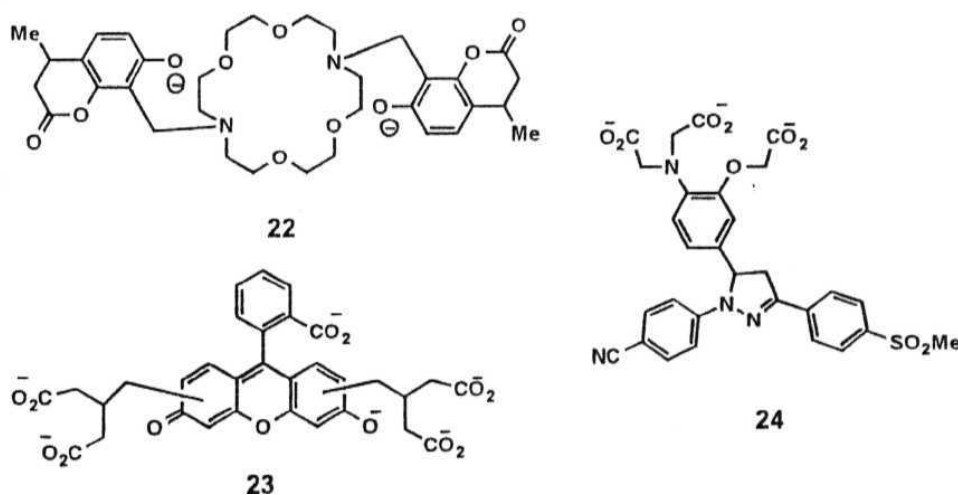
is an example of this class, where the anionic phenolate oxygens also participate in the binding of the alkaline earth metal ions.[28] Other systems with multi-carboxylate anion

structure as the receptor unit for the alkaline earth metal ions such as Ca^+ and Mg are 23 and 24 respectively.[29,30]

I. 2.5. Fluorosensors *responsive to other metal ions*

Diamine receptor containing system, 25 is one of the PET fluorosensors, developed quite early by Czarnik and coworkers, for metal ions such as Zn^+, Cd^+, Hg^{+2}, etc.,[2,31,32] The binding ability of the polyamine receptors such as the cyclam and its higher homologues with the heavy metal ions has been utilised in 26.
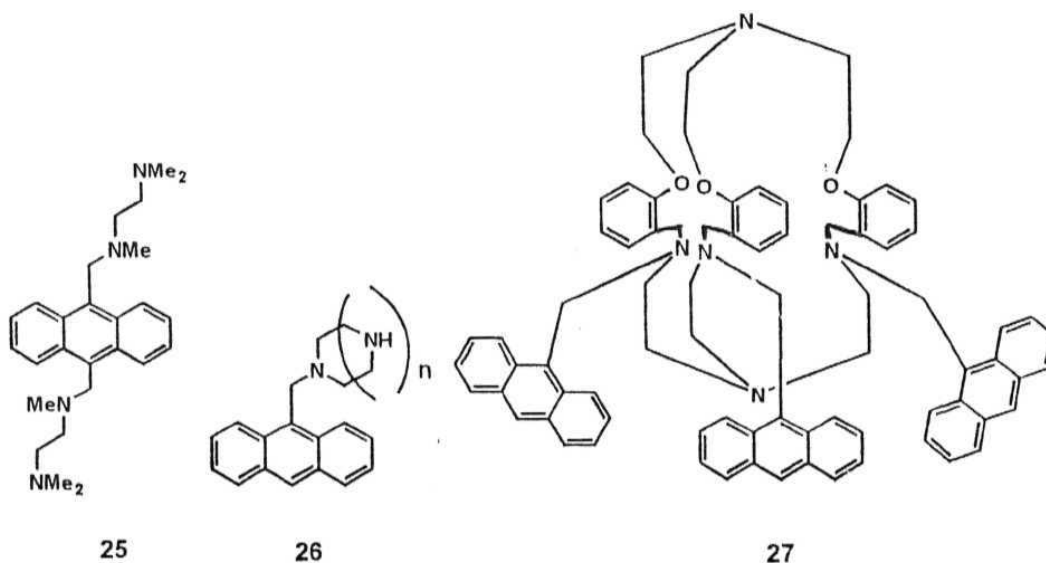
The fluorescence 'off-on' PET systems, described here so far and many others quoted in the review articles, are capable of sensing different type of metal ions that do not have any significant fluorescence quenching ability. However, the PET fluorosensors for redox active metal ions such as the transition metal ions with incomplete d-shell was not available until very recently. Fluorescence quenching ability of the transition metal ions is believed to be the reason for the nonavailability of the fluorescence 'off-on' signalling systems for these metal ions. 27, is reported to be the first system to exhibit fluorescence enhancement in the presence of quenching metal ions such as Cu^{+2}, Ni^{+2},

etc.[7] In this system, a specially designed cryptand moiety acts as the receptor component. The cavity of the receptor moiety, where the added metal ions get bound, insulates the quenching metal ions from the fluorophore components.

1.2.6. *Fluorosensors responsive to anions*
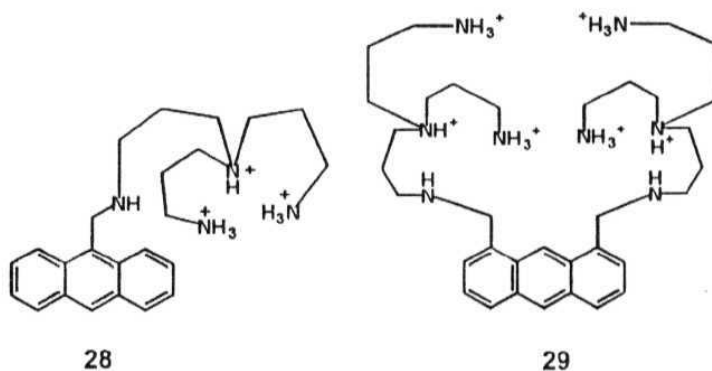
PET fluorosensors for the anions must involve a receptor component that should contain at least one positive center. Partially protonated polyamine receptors such as those used in 28 and 29 are ideal for sensing the phosphate anion.[2,33,34]

1.2.7. *Fluorosensors responsive to neutral molecules*
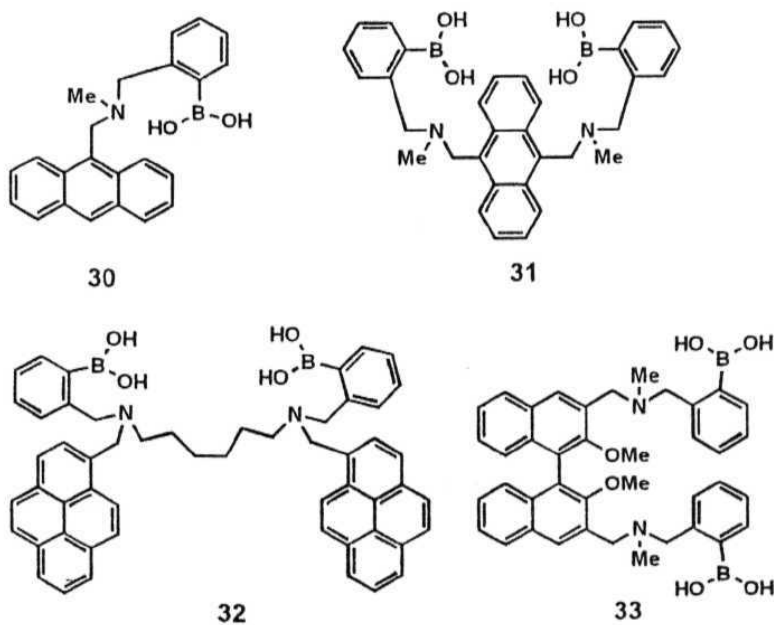
As stated earlier, one is often required to measure the level of various neutral molecules in the environment and in the body. Quite naturally, sensor development for the neutral molecules is an important area in the current research.

Czarnik,[35a] Aoyama[35b] and Shinkai[35c-g] developed PET fluorescence 'off-on' signalling systems for the sugar molecules. In these *fluorophore - spacer - receptor* systems, an amine group with an adjacent boronic acid serves as the receptor (30-33). In the absence of the sugar molecules, the boron atom is in sp^2 hybridization that is not favourable for the acceptance of the electrons from the adjacent amine lone pair of electrons. In this situation, the electron of the amino moiety is transferred to the excited fluorophore leading to fluorescence quenching. In the presence of the sugar, which gets bound to the boronic acid moiety, there occurs a change in the hybridisation of the boron center. A change in the hybridization from sp^2 to sp^3 makes the boron atom more favourable for the acceptance of the electron from the amine moiety, which in turn reduces the PET process in the system leading to fluorescence enhancement of the total system. Scheme 1.3 is an illustration of this design logic.
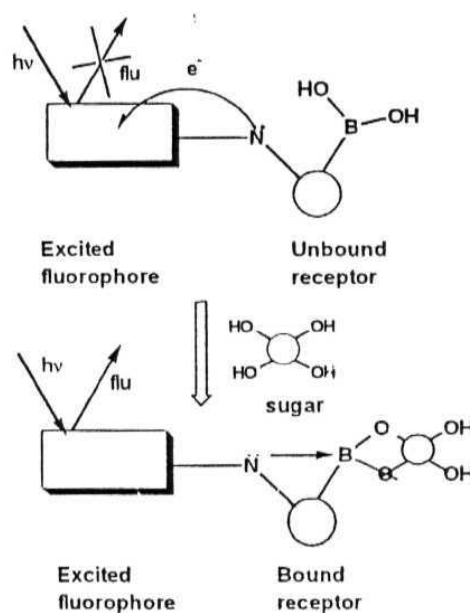
Scheme 1.3

Other molecules such as amines,[36] thiols,[37] quinone[38] and imidazole and histidine[3940] etc., are also successfully traced using the fluorosensors based on PET phenomenon.

1.3.   Other Mechanisms for the Design of Fluorosensors

Like PET, many other mechanisms such as double bond torsion, reversal of the ordering of the n-π* and rc-7t* excited states, heavy atom effect, electronic energy transfer, solvent polarity, etc. influence the fluorescence efficiency of a system and

hence, can be used for the development of fluorosensors. A few fluorosensors based on some of these mechanisms have been illustrated below.

1.3.1.   Low energy n-π* excited states

Molecules with lowest excited singlet states of the n-π* type are usually nonemissive in non-polar solvents because of the forbidden nature of the transition to the ground state.[16,41] Many of these molecules also possess a π-π* state slightly above the n-π* state. Since the solvent polarity has an opposite effect on the energetics of these states, what often happens, when the polarity of the medium is increased, is a reversal of the ordering of these states.[16,41] Since the emission from a π-π* state is allowed, an increase in the polarity of the medium results in fluorescence enhancement.[16,41-45] In other words, an increase in the polarity of the medium is observable through the 'off-on' fluorescence signalling. Therefore, one can utilise such systems as fluorosensors for the polarity of the medium. Pyrene-1-carboxaldehyde shows nearly 100-fold increase in the fluorescence intensity when the medium is changed from n-hexane to methanol.[43] Other compounds such as 7-alkoxycoumarin,[43a,44] and nile red[45] fall in this category of fluorosensors.

1.3.2.   Double bond obstruction

Conjugated alkenes with flexible structures are generally non-emissive in fluid media. Internal twisting (torsion) around the double bond is responsible for rapid
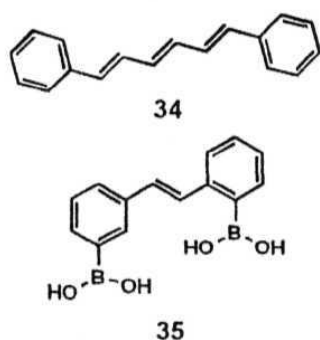
nonradiative decay of the excited molecules.[41] However, when incorporated into structures with rigid configuration like membranes, cyclodextrins, the barrier to internal twisting is increased resulting in an enhancement of the fluorescence efficiency of the systems. 34 is perhaps one of the classic systems that displays significant fluorescence only in semi-rigid environments where the double bond torsion is obstructed.[41,46] 35 is another system of this class for which the internal twisting

is obstructed in the presence of sugar molecules that bind with the system forming borate macrocyclic esters.[47]

1.3.3.   Metal-centered excited states and energy transfer

Rare earth metal ions are generally poor absorbers.[16,41] In order to populate the excited states of such metal ions, one requires special techniques like laser pumping.[48] One can avoid this situation using an appropriate sensitiser or molecular antenna that transfers the excitation energy into the metal ion excited state.[49] 36, for example, is one of the systems belonging to this class, for which an enhancement of europium emission is observed in the presence of benzene as the guest molecule.

36
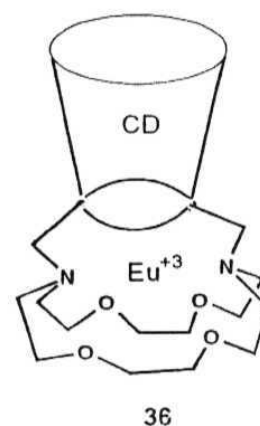
Energy transfer from cyclodextrin encapsulated benzene to azacrown-bound Eu^{3+} is believed to be responsible for the fluorescence enhancement.[50]

1.3.4.   Charge transfer excited states

The lowest singlet excited state of the electron donor-acceptor (EDA) molecules is most often intramolecular charge transfer (ICT) in nature.[16,41] Electronic excitation of the EDA molecules is associated with significant changes in the dipole moment. The excited state dipole moment of a majority of the EDA compounds is higher than that in the ground state,[16,41,51,52] although, the opposite is true for a few systems such as betaines.[3] Because of their significant dipole moments, these systems are highly solvated in polar media. Moreover, since electronic excitation is accompanied by a change in the dipole moment of the system, the extent of stabilisation due to solvation is different for the ground and excited states. As a result of this, one observes a shift in the wavelength corresponding to the ICT emission maximum on change of the polarity of the media. In addition, a change in the polarity of the medium is also associated with changes in the fluorescence yield and lifetime of these systems. Since for EDA systems, 37-40, the

dipole moment increases on electronic excitation, a Stokes shift of the fluorescence maximum could be observed on increase in the polarity of the medium.[52,54,56]
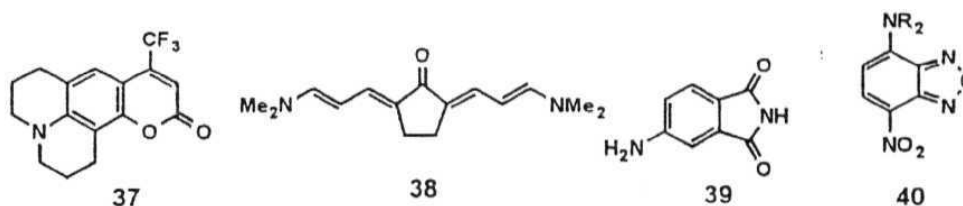
Unlike the neutral molecules, the ions can exert a strong electric field on the ICT state of the EDA molecules. However, the effect of the ions, usually present in low concentration, is masked by the influence of large number of solvent molecules around the fluorophore. Therefore, simple EDA systems as such can not be used as fluorosensors for the ions. However, when the ions present in the medium are trapped near the fluorophore by a suitably placed receptor (as in 41 - 44) to exert maximum electric field on the fluorophore, the effect is observable through the changes in the fluorescence
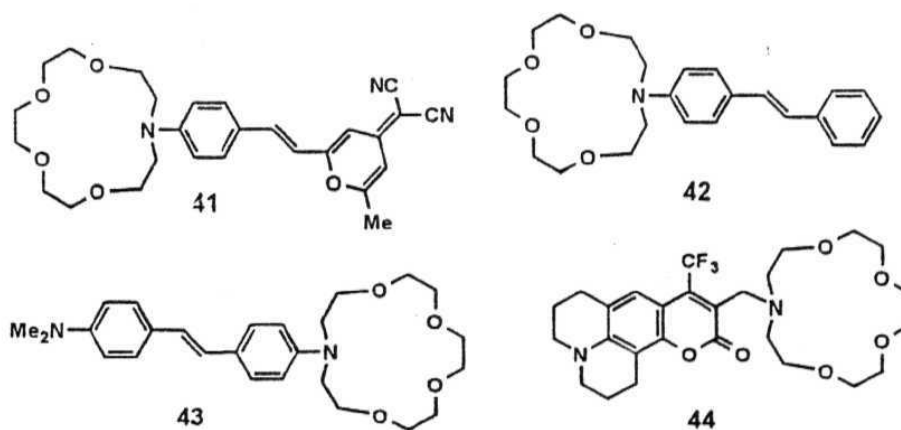
properties. 41 - 44 are typical examples of ion responsive ICT fluorosensors. In 41 and 42, the receptor moiety is connected to the electron rich site (i.e. the donor moiety) of the molecule. This type of systems display a blue shift of the fluorescence maxima upon guest binding.[57,58] On the other hand, systems, where the receptor is connected to the electron deficient acceptor moiety (as in 43 and 44), display a red shift of the emission

maxima.[59,60] This can be rationalised as follows with the help of fig 1.2. In the case of the first category of systems, guest (a cation) binding results in a decrease in the separation of charge between the donor and the acceptor moieties leading to a reduction in the dipole moment of the ground and excited states. Since the excited state dipole moment of these EDA fluorophores is higher than the ground state moment, the excited state will be destabilised more than the ground state. This leads to a blue shift of the spectral maxima. In the case of second category of systems, since the receptor for the cations is connected to the acceptor moiety, charge separation between

Fig 1.2

the donor and the acceptor moieties increases in the presence of the guest. As stated above, the effect will be relatively larger for the excited state that has a higher excited state dipole moment. Greater stabilisation of the excited state (compared to the ground state) in the presence of the guest leads to a red shift of the spectral maximum.

1. 3.5. Twisted intramolecular charge transfer states (TICT)

Complete charge separation in the EDA systems can be achieved by decoupling of the HOMO of the donor and the LUMO of the acceptor by twisting the donor (or the acceptor moiety) through 90° with respect to the acceptor (or donor) moiety. This phenomenon is commonly known as twisted intramolecular charge transfer (TICT) process. The enhanced separation of charge makes the fluorescent TICT state highly sensitive to the polarity of the environment. 4-N,N-dimethylaminobenzonitrile (DMABN) is the most extensively studied molecule of this class.[61,62] Compound 45 and its relatives are another set of molecules of this class that are being used as polarity

sensors in biochemical research for over five decades.[63] 46, 47 and 48 belong to **this** class of ion responsive fluorosensors.[64-66] .
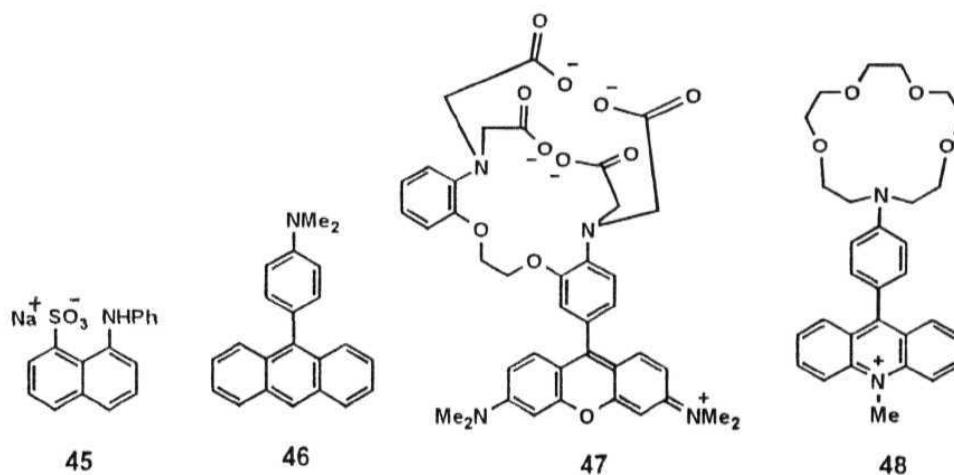
1.3.6. Modulation of monomer and excimer emission intensity

Most of the multi-component systems discussed so far consisted of a single fluorophore moiety. Systems containing two identical fluorophores often exhibit an additional Stokes-shifted broad emission band that originates from an intramolecular excimer, formed between an excited and a ground state fluorophore.[67] The equilibrium between the excimer and the monomer is sensitive to the concentration of the species and the polarity of the media. A suitable guest molecule capable of perturbing this equilibrium can yield a signal transduction of interest. 1,3-bis-(1-pyrenyl)propane is one of the most extensively studied systems belonging to this class. For this system, the monomer/excimer equilibrium can be shifted on encapsulation by cyclodextrins.[68,69] y-Cyclodextrin, with a large cavity that can accommodate two pyrene moieties, shifts the equilibrium towards the excimer resulting in an enhancement of the intensity of the excimer band relative to the monomer emission. In contrast, β-cyclodextrin, because of

its small cavity that can accommodate only one pyrene moiety enhances the monomer emission at the cost of the excimer emission.

1.4.   Motivation of the Thesis

While a wide variety of sensors for the cations, anions and neutral molecules have been developed in recent years exploiting the design principles outlined above, fluorescence 'off-on' PET systems for the transition metal ions remained elusive for a long period. This observation is commonly rationalised taking into consideration of strong fluorescence quenching ability of the d-block metal ions.[70] Perhaps, for the *fluorophore-spacer-receptor* systems, the fluorescence *enhancement* resulting from the binding of these metal ions with the receptor is compensated by fluorescence *quenching* resulting from the fluorophore-metal ion interaction. One possible approach to circumvent the quenching influence of the transition metal ions is perhaps to specially design a receptor such that the metal ion in the bound condition is not accessible to the fluorophore for quenching. Based on tin's receptor design approach, Ghosh et al[7] have developed a *fluorophore-spacer-receptor* system (27) that shows fluorescence enhancement even in the presence of the quenching metal ions. The ability of this system to function as an 'off-on' switch for the transition metal ions (reportedly the first system to do so) results from the special topology of the receptor. The receptor, a cryptand moiety in this case, contains a cavity wherein the quenching metal ions are trapped and thus become unavailable for fluorescence quenching. In other words, in this approach, the metal ion - receptor interaction has been increased to reduce indirectly the communication between the metal ion and the fluorophore that leads to fluorescence quenching.

While the above approach is an elegant one, it requires considerable synthetic skill for the development of fluorosensors of this kind. Further, the systems so developed

are fairly complex. Since the quenching interaction between the fluorophore and the metal ions is known to be predominantly redox in nature,[70] we thought that it might be possible to reduce this interaction simply by making the fluorophore electronically deficient by suitable substitution or simple structural modifications. Such modification not only minimises the fluorophore-metal ion quenching interaction in the metal-bound state, but also enhances the PET communication between the fluorophore and the receptor in the unbound state; both favouring an increase in the efficiency of the sensor system. We have undertaken this investigation primarily to find out whether it is possible to develop structurally simple fluorescence 'off-on' systems for the, quenching transition metal ions following a design logic that is based on right selection of the fluorophore component of the multi-component sensor systems.

Multi-component systems, ANPDEA and ANPPED employing 4-amino-1,8-naphthalimide (ANP) as the fluorophore component and a dimethylamino and an aniino moiety as the receptor units have been synthesised and their fluorescence response has been investigated in the presence of d-block metal ions. Poor metal ion sensing ability of the two systems has been attributed to the electron rich nature of the fluorophore and inefficient PET in these systems. Since 4-aminophthalimide (AP) is expected to be relatively electron deficient, APDEA, APDPA, APPED and APNED have been synthesised and their fluorescence output has been studied in the presence of quenching metal ions. Interestingly, these structurally simple systems exhibit metal ion induced excellent fluorescence enhancement. Enhanced PET communication between the fluorophore and the receptor and reduced redox activity between the fluorophore and the metal ions are responsible for improved performance of these systems as fluorosensors for the quenching metal ions compared to ANPDEA and ANPPED.

Since the redox behaviour of 4-methoxy-1,8-naphthalimide is clearly indicative of its election deficient nature (compared to 4-amino-1,8-naphthalimide), multi-

component systems such as OMNPDEA, OMNPDPA, OMNPPED and OMNPNED have been prepared and the fluorescence signalling abilities of these systems have been investigated.

ANPDEA

ANPPED

APDEA

APDPA

APPED

APNED

OMNPDEA

OMNPDPA

OMNPPED

OMNPNED
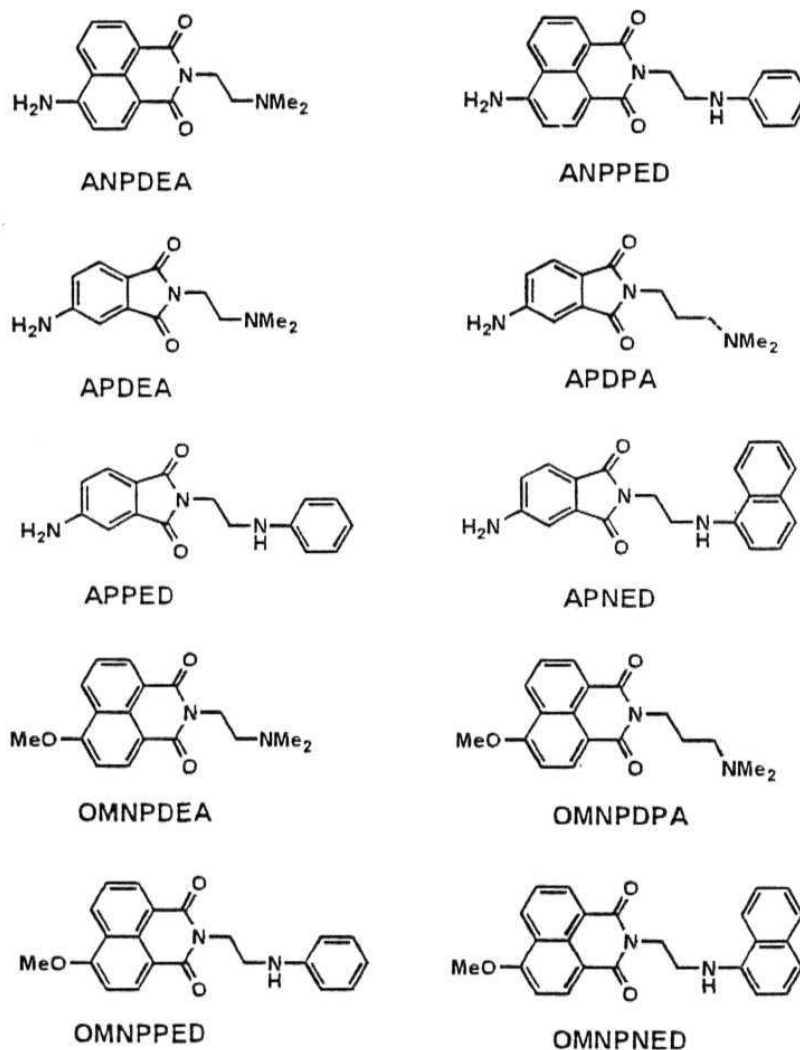
We then turned our attention to 4-alkylamino-7-nitrobenz-2-oxa-l,3-diazole (4-alkylamino NBD), a fluorophore that has been extensively used in biological studies.[56g]

NAM   NEA
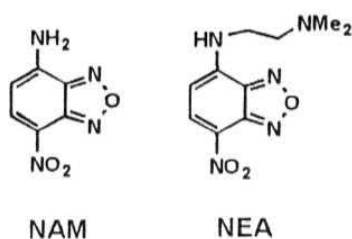
However, the redox properties of 4-amino-NBD (NAM) indicate its electron rich nature and quenching studies on this fluorophore with the transition metal ions confirmed a strong interaction between the fluorophore and the metal ions. In a situation like this, even though one does not expect metal ion-induced fluorescence enhancement of the multi-component system (NEA) comprising this fluorophore moiety, interestingly, fluorescence studies indicate reasonably good fluorescence signalling of the transition metal ions by this system. This apparently unusual observation has been accounted for taking into consideration of short fluorescence lifetime of the PET quenched fluorophore.

Since a number of independent mechanisms of fluorescence enhancement, other than the commonly exploited PET suppression principle, are known, we thought that it might be possible to improve the fluorescence signalling ability of a given multi-component system by incorporating one of these mechanisms in the PET design principle. Taking into consideration that most of the transition metal ion salts are available in hydrated form, one can expect, for studies in non-aqueous media, an increase in the polarity of the microenvironment around the fluorophore on the addition of the metal salts. Therefore, if the chosen fluorophore component is such whose fluorescence quantum yield is higher in aqueous environment than that in non-aqueous media, then, on the addition of the hydrated metal salts to the *fluomphore-spacer-receptor* system, one can expect fluorescence enhancement much higher than that expected from consideration of PET mechanism alone. In order to realise the objective that a cooperative interaction of two independent mechanisms of fluorescence enhancement should make a fluorosensor to glow brighter (or transmit a stronger signal) than that predicted by PET design principle alone, studies have been carried out on derivatives of 1,8-naphthalimide (NPDEA, NPDPA, NPDBA, NPPED and NPNED) and 4-chloro-1,8-naphthalimide

(CNPDEA, CNPDPA, CNPPED and CNPNED), whose fluorescence efficiency in aqueous media is significantly higher than that in non-aqueous environment.
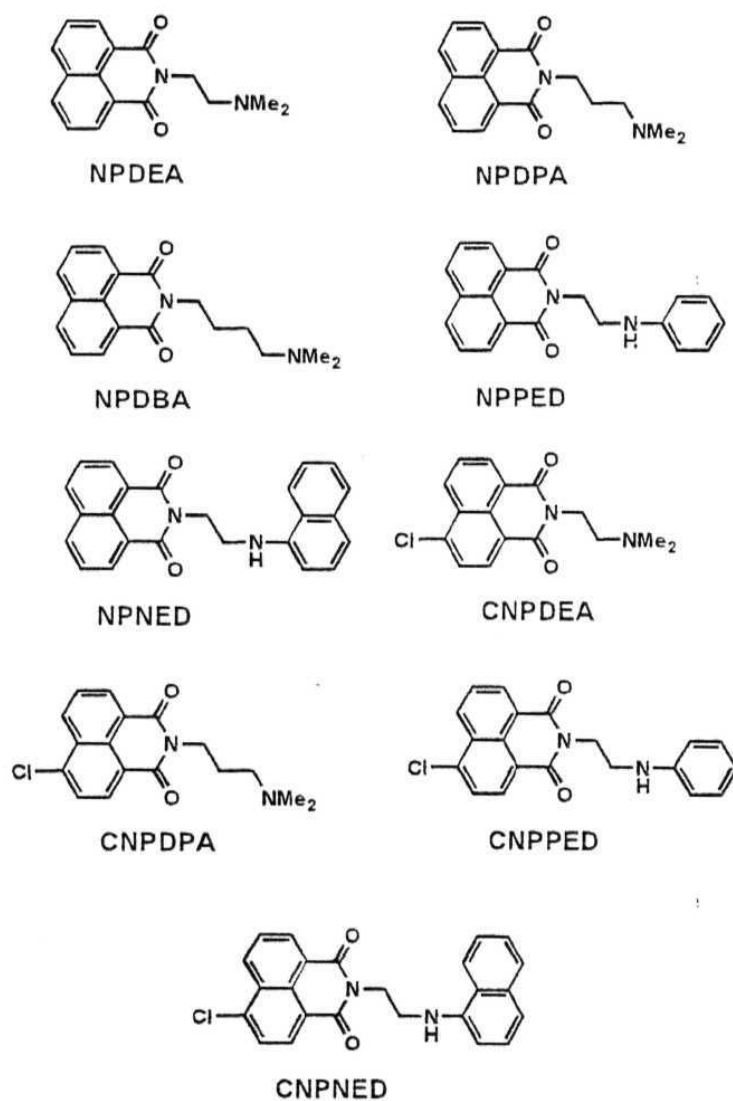
1.5.   Layout of the Thesis

The thesis has been divided into seven chapters. First chapter provides a brief introduction on various signalling systems based on different mechanism of fluorescence

modulation. The second chapter provides details of the experimental procedures for the preparation of the key systems, analytical data of these systems and the methodologies followed for the Photophysical studies. Third chapter consists of two sections. While the first section deals with 4-aminonaphthalimide derivatives, the second section is concerned with the signalling ability of the 4-aminophthalimide derivatives. Fourth chapter of the thesis is devoted to transition metal ion sensing studies on multi-component systems based on 4-methoxy-1,8-naphthalimide fluorophore. Fifth chapter describes the fluorescence response of the NBD derivatives towards the transition metal ions. Sixth chapter provides the results of the investigation performed on *fluorophore-spacer-receptor* systems involving 1,8-naphthalimide and 4-chloro-1,8-naphthalimide as fluorophores. The last chapter summarises the results.

1.6. References

1. a) *Molecular Electronic Devices*, Eds., F.L. Carter, R.E. Siatkowski, H. Wohltjen, Elsevier, Amsterdam, 1988; b) J.M. Lehn, *Angew. Chem. Int. Ed. Engl.* 1988, *27,* 89; c) J.M. Lehn, *Angew. Chem. Int. Ed Engl.* 1990, *29,* 1304; d) J.M. Lehn, *Supramolecular Chemistry,* VCH, Weinheim, 1995; e) *Supramolecular Photochemistry,* Ed., V. Balzani, Reidel, Dordrecht, 1987; f) V. Balzani, F. Scandola, *Supramolecular Photochemistry,* Ellis-Horwood, Chichester, **1991;** g) V. Balzani, A. Juzis, M. Venturi, S. Campagna, S. Serroni, *Chem. Rev.* **1996,** *96,* 759; **h)** S. L. Gilat, S.M. Kawai, J.M. Lehn, *Chem. Eur. J.* 1995, *1*, 275; i) M.R. Wasielewski, M.P. O'Neil, D. Gosztola, M.P. Niemczyk, W.A. Svec, *Pure Appl. Chem.* **1992,** *64,* 1319.

2. *a) Chemosensors of Ion and Molecular Recognition,* NATO ASI Series, Eds., J.-P. Desvergene, A.W. Czarnik, Kluwer Academic, Dordrecht, Vol. C492, **1997;** b) *Fluorescent Chemosensors for Ion and Molecule Recognition*, ACS Symposium Series 538, Ed., A.W. Czarnik, American Chemical Society, Washington, DC, 1993;

c) A.W. Czarnik, *Acc. Chem. Res.* **1994,** *27,* 302; d) A.W. Czarnik, In *Topics in Fluorescence Spectroscopy*, Ed., J.R. Lakowicz, Plenum Press, New York, 1994, Vol. IV, p. 49; e) M.E. Huston, K.W. Haider. A.W. Czarnik, *J. Am. Chem. Soc.* **1988,** *1 10,* 4460.

3. a) A.P. de Silva, H.Q.N. Gunaratne, T. Gunnlaugsson, A.J.M. Huxley, C.P. McCoy, J.T. Rademacher, T.E. Rice, *Chem. Rev.* 1997, *97,* 1515 and references therein; b) R.A. Bissel, A.P. de Silva, H.Q.N. Gunaratne, P.L.M. Lynch, G.E.M. Maguire, K.R.A.S. Sandanayake, *Chem. Soc. Rev.* 1992, *21,* 187; c) R.A. Bissel, A.P. de Silva, H.Q.N. Gunaratne, P.L.M. Lynch, G.E.M. Maguire, K.R.A.S. Sandanayake, *Top. Curr. Chem.* 1993, *168,* 223; d) A.P. de Silva, H.Q.N. Gunaratne, G.E.M. Maguire, *J. Chem. Soc. Chem. Commun.* **1994,** 1213; e) A.P. de Silva, H.Q.N. Gunaratne, T. Gunnlaugsson, M. Nieuwenhuizen, *J. Chem. Soc. Chem. Commun.* **1996,** 1967; f) A.P. de Silva, H.Q.N. Gunaratne, C. McVeigh. G.E.M. Maguire, P.R.S. Maxwell, E. Hanlon, *J. Chem. Soc. Chem. Commun.* 1996, 2191; g) A.P. de Silva, H.Q.N. Gunaratne, C.P. McCoy, *Nature,* 1993, *364,* 42; h) A.P. de Silva, H.Q.N. Gunaratne. C.P. McCoy, J. *Chem. Soc. Chem. Commun.* 1996, 2399; i) A.J. Bryan, A.P. de Silva, S.A. de Silva, R.A.D.D. Rupasinghe, K.R.A.S. Sandanayake, *Biosensors,* 1989, *4,* 169.

4. a) Y. Siomi, K. Kondo, M. Saisho, T. Harada, K. Tsukagoslii, S. Shinkai, *Supra. Mol. Chem.* **1993,** *2,* 11; **b)** Y. Siomi, M. Saisho, T. Harada, K. Tsukagoshi, S. Shinkai, *J. Chem. Soc. Perkin Trans. 1,* **1993,** 2111; c) T.D. James, P. Linnane, S. Shinkai, *J. Chem. Soc. Chem. Commn.* 1996, 281.

5. R. Deans, A. Niemz, E.C. Breinlnger, V.M. Rotello, *J. Am. Chem. Soc.* **1997,** *119,* 10863.

6. B. Valeur, In *Topics in Fluorescence Spectroscopy,* Ed., J.R. Lakowicz, Plenum Press, New York, **1994,** Vol. **IV, p.** 21.

7. a) P. Ghosh, P.K. Bharadwaj, S. Mandal, S. Ghosh, *J. Am. Cham. Soc.* 1996, *118*, 1553; b) P. Ghosh, P.K. Bharadwaj, J. Roy, S, Ghosh, *J. Am. Chem. Soc.* 1997, *119*, 11903.

8. a) L. Fabbrizzi, M. Licchelli, P. Pallavicini, D. Sacchi, *Angew. Chem. Int. Ed. Engl.* 1994, *33,* 1975; b) L. Fabbrizzi, M. Licchelli, P. Pallavicini, A. Perotti, A. Taglietti, D. Sacchi, *Chem. Eur. J.* 1996, *2,* 75; c) M. Gubelmann, J.M. Lehn, J.L. Sessler, A. Harriman, *J. Chem. Soc. Chem. Commun.* 1988, 77; d) V. Krishnan, *J. Photochem. Photobiol. A: Chem.* 1994, *84,* 233; e) S.P. McGlynn, T. Azumi, M. Kinoshita, *Molecular Spectroscopy of the Triplet States,* Prentice Hall, Englwood Cliffs, NJ, 1969; 1) S.D. Lytton, Z.I. Cabantchik, J. Libman, A. Shanzer, *Mol. Pharmacol.* 1991, *40,* 584; g) S.D. Lytton, B. Mester, J. Libman, A. Shanzer, Z.I. Cabantichik, *Anal. Biochem.* 1992, *205,* 326; h) A. Shanzer, J. Libman, *Croat. Chim. Acta.* 1996, *69,* 709; i) H. Weizman, O. Ardon, B. Mester, J. Libman, O. Dwir, Y. Hadar, Y. Chen, A. Shanzer, *J. Am. Chem. Soc.* 1996, *118*, 12368; j) B. Bodenant, F. Fages, *Tetrahedron Lett.* 1995, *36,* 1451; k) F. Fages, B. Bodenant, T. Weil, *J. Org. Chem.* 1996, *61,* 3956; 1) M. Chae, A.W. Czarnik, *J. Fluoresc.* 1992, *2,* 225.

9. a) A. Weller, *Pure Appl. Chem.* 1968, *16,* 115; b) D. Rehm, A. Weller, *Isr. J. Chem.* 1970, *8,* 259.

10. a) H. Shizuka, M. Nakamura, T. Morita, *J. Phys. Chem.* 1979, *83,* 2019; b) Y.C. Wang, H. Morawetz, *J. Am. Chem. Soc.* 1976, *98,* 3611.

11. a) B.K. Sclinger, *Ami. J. Chem.* 1977, *30,* 2087; b) M. Migita, T. Okada, N. Mataga, Y. Sakata, S. Misumi, N. Nakashima, K. Yoshihara, *Bull. Chem. Soc. Jpn.* 1981, *54,* 3304; c) Y. Wang, M.C. Crawford, K.B. Eisenthal, *J. Am. Chem. Soc.* **1982,** *104,* 5874.

12. G.S. Cox, NJ. Turro, N.C. Yang, M.J. Chem, *J. Am. Chem. Soc.* **1984,** *106, All.*

13. a) R.M. Hermant, N.A.C. Bakker, T. Scherer, B. Krijnen, J.W. Verhoeven, *J. Am. Chem. Soc.* 1990, *112,* 1214; b) H.J. Verhey, J.W. Hofstraat, C.H.W. Bekker, J.W. Verhoeven, *New. J. Chem.* 1996, *20,* 809; c) L.W. Jenneskens, H. J. Van Ramesdonk, H.J. Verhey, G.D.B. Van Houwelingen, J.W. Verhoeven, *Rec. Trav. Chem. Pays. Bas.* 1989, *108,* 453; d) H.J. Van Ramesdonk, M. Vos, J.W. Verhoeven, G.R. Mohlmann, N.A. Tissink, A.W. Meesem, *Polymer,* 1987, *28,* 951; e) G.F. Mes, H.J. Van Ramesdonk, J.W. Verhoeven, *J. Am. Chem. Soc.* **1984**, *106*, 1335.

14. a) A.P. de Silva, R.A.D.D. Rupasinghe, S.L.A. Peiris, *Proc. Srilanka. Assoc. Advmt, Sci. Abst.* 1982, *38,* 68; b) A.P. de Silva, R.A.D.D. Rupasinghe, *J. Chem. Soc. Chem. Commun.* 1985, 1669.

15. a) A.P. de Silva, S.A. de Silva, *Proc. Srilanka. Assoc. Advmt. Sci. Abst.* 1986, *41,* 83; b) A.P. de Silva, S.A. de Silva, *J. Chem. Soc. Chem. Commun.* 1986, 1709.

16. a) J.R. Lakowicz, *Principles of Fluorescence Spectroscopy,* Plenum Press, New York, 1986; b) B.M. Krasovitskii, B.M. Bolotin, *Organic Luminescent Materials,* VCH, Weinheim, 1989.

17. A.P. de Silva, H.Q.N. Gunaratne, P.L.M. Lynch, A.L. Patty, G.L. Spence, *J. Chem. Soc. Perkin Trans 2,* 1993, 1611.

18. a) A. Pardo, J.M.L. Poyato, E. Martin, J.J. Camacho, D. Reyman, M.F. Brana, J.M. Castellano, *J. Photochem. Photobiol. A: Chem.* 1986, *36,* 323; b) A. Pardo, E. Martin, J.M.L. Poyato, J.J. Camacho, M.F. Brana, J.M. Castellano, *J. Photochem. Photobiol. A: Chem.* 1987, *41,* 69; c) A. Pardo, E. Martin, J.M.L. Poyato, J.J. Camacho, J.M. Guerra, R Weigand, M.F. Brana, J.M. Castellano, *J. Photochem. Photobiol. A: Chem.* 1989, *48,* 259; d) A. Pardo, J.M.L. Poyato, E. Martin, J.J. Camacho, D. Reyman, *J. Lumin.* 1990, *46,* 381; e) D. Yuan, R.G. Brown, *J. Chem. Res (M).* 1994, 2337; f) M.S. Alexiou, V. Tychopoulos, S. Ghorbanian, J.H.P.

Tyman, R.G. Brown, P.l. Brittain, *J. Chem. Soc. Perkin Trans. 2,* 1990, 837; g) E. Martin, R. Weigand, *Chem. Phys. Lett.* **1998,** *288,* 52.

19. A. P. de Silva, H.Q.N. Gunaralnc, J.L. Habib-Jiwan, C.P. McCoy, T.E. Rice, J.P. Soumillion, *Angew. Chem. Int. Ed. Engl.* 1995, *34,* 1728.

20. a) E. Weber, J.L. Tom, 1. Coldberg, F. Vogltc, DA. Laidler, T.F. Staddent, R.A. Bartsels, C.L. Liotta, *Crown Ethers and Analogy,* Interscience Publications, New York, 1989; b) F. de Jones, D.N. Rainhoud, *Stability and Reactivity of the Crown Compounds,* Academic Press, London, 1981; c) C.J. Pederson, *J. Am. Chem. Soc.* 1967, *89,* 2495; d) C.J. Pederson, *J. Am. Chem. Soc.* 1967, *89,* 7017.

21. A.P. de Silva, S.A. de Silva,*./. Chem. Soc. Chem. Commun.* 1986, 1709.

22. a) J.P. Konopelski, F. Kootzyba-Hibert, J.M. Lehn, J.-P. Desvergne, F. Fages, A. Castellan, H. Bouas-Laurent,*./. Chem. Soc. Chem. Commun.* 1985, 433; b) F. Fages, J.-P. Desvergne, H. Bouas-Laurent, P. Marsau, J. M. Lehn, F. Kotzyba-Hibert, A.M. Albercht-Gary, M. Al-Joubbeh, *J. Am. Chem. Soc.* 1989, *111,*8672.

23. L.R. Sousa, J.M. Larson, *J. Am. Chem. Soc.* 1977, *99,* 307.

24. J.M. Larson, L.R. Sousa, *J. Am. Chem. Soc.* 1978,*100,* 1943.

25. a) H. Shizuka, K. Takada, T. Morita, *J. Phys. Chem.* 1980, *84,* 994b) G.J. Kavarnos, T. Cole, F. Scribe, J.C. Dolton, NJ. Turro, *J. Am. Chem. Soc.* 1971, *93,* 1032; c) N.J. Turro, G.J. Kavarnos, V. Fung, A.L. Lyons, T. Cole, *J. Am. Chem. Soc.* 1972, *94,* 1392.

26. A.P. de Silva, K.R.A.S. Sandanayake, *Tetrahydron Lett.* 1991, *32,* 421.

27. A.P. de Silva, K.R.A.S. Sandanayake, *J. Chem. Soc. Chem. Commun.* 1989, 1183.

28. H. Nishida, Y. Katayama, H. Katsuki, H. Nakamura, M. Tagaki, K. Ueno, *Chem. Lett.* 1982, 1853.

29. D.F.H. Wallach, T.L. Steck,*Anal. Chem.* 1963, *35,* 1035.

30. A.P. de Silva, H.Q.N. Gunaratne,*J. Chem. Soc. Chem. Commun.* 1990, 186.

31. a) E.U. Akkaya, M.E. Huston, A.W. Czarnik, *J. Am. Chem. Soc.* 1990, *112*, 3590; b) M.E. Huston, C. Engleman, A.W. Czarnik, *J. Am. Chem. Soc.* 1990, *112*, 7054; c) F. Fages, J.-P. Desvergne, H. Bousa-Laurent, P. Marsau, J.M. Lehn, F. Kotzyka-Hibert, A.M. Albrecht-Gary, M. Al-Joubbeh, *J. Am. Chem. Soc.* 1989, *111*, 8672.

32. R.D. Hancock, A.E. Martell, *Chem. Rev.* 1989, *89,* 1875.

33. M.E. Huston, E.U. Akkaya, A.W. Czarnik, *J. Am. Chem. Soc.* 1989, *111*, 8735.

34. a) D.H. Vance, A.W. Czarnik, *J. Am. Chem. Soc.* 1994, *116*, 9397; b) A.W. Czarnik, *ACS Symp. Ser.* 1994, *561*, 314.

35. a) J. Yoon, A.W. Czarnik, *J. Am. Chem. Soc.* 1992, *114,* 5874; b) Y. Nagai, K. Kabayashi, H. Toi, Y. Aoyama, *Bull. Chem. Soc. Jpn.* 1993, *66*, 2965; c) T.D. James, K.R.A.S. Sandanayake, S. Shinkai, *J. Chem. Soc. Chem. Commun.* 1994, 477; d) T.D. James, K.R.A.S. Sandanayake, S. Shinkai, *Angew. Chem. Int. Ed. Engl.* 1994, *33,* 2207; e) T.D. James, K.R.A.S. Sandanayake, S. Shinkai, *Nature,* 1995, *374,* 345; f) T. Grady, S.J. Harris, M.R. Smyth, D. Diamond, P. Hailey, *Anal. Chem.* 1996, *68,* 3775; g) P. Linnane, T.D. James, S. Imazu, S. Shinkai, *Tetrahedron Lett.* 1995, *36,* 8833.

36. A.P. de Silva, H.Q.N. Gunaratne, T. Gunnlaugsson, *Tetrahedron Lett.* 1998, *39,* 5077.

37 J.K. Weltmen, R.P. Szaro, A.R. Frackelston, R.M. Dowben, J.R. Bunting, R.E. Cathou, *J. Biol. Chem.* 1973, *218*, 3173.

38. F. D'Souza, G.R Deviprasad, Y.Y. Hsieh, *J. Chem. Soc. Chem. Commun.* 1997, 533.

39. L. Fabbrizzi, G. Francese, M. Licchelli, A. Perotti, A. Taglietti, *J. Chem. Soc. Chem. Commun.* 1997, 581.

40. K. Niikura, A. Metzger, A.V. Anslyn, *J. Am. Chem. Soc.* 1998, *120*, 8533.

41. a) N.J. Turro, *Modern Molecular Photochemistry,* University Science Books, Mill Valley, CA, 1991; b) J. Kopecky, *Photochemistry: A Visual Approach,* VCH, New

York, 1992; c) R.P. Wayne, *Principles and Applications of Photochemistry*, Oxford University Press, Oxford, 1988; d) J.A. Barltrop, J.D. Coyle, *Excited slates in Organic Chemistry*, Wiley, London, 1975; e) K. Kalyanasundaram, *Photochemistry in Microheterogeneous Systems,* Academic Press, New York, 1983; f) *Photochemistry in Organised and Constrained Media,* Ed., V. Ramamurthy, VCH, New York, 1991.

42. a) A.D. Hamilton, *Adv. Supramol. Chem.* 1990, *1*, 1; b) M.J. Kamlet, J.L.M. Abboud, M.H. Abraham, R.W. Traft, *J. Org. Chem.* 1983, *48*, 2877.

43. a) K. Kalyanasundaram, J.K. Thomas, *J. Phys. Chem.* 1977, *81*, 2176; b) P. Lianos, B. Lux, D. Gerard, *J. Chem. Phys.* 1988, *77*, 907; c) S. Ogawa, S. Tsuchiya, *Chem. Lett.* 1996, 709; d) K. Hirtani, M. Nomoto, H. Sugihara, T. Okada, *Chem. Lett.* 1990, 43; e) K. Hirtani, M. Nomoto, S. Ohuchi, K. Taguchi, *Bull. Chem. Soc. Jpn.* 1990, *63*, 1349; f) O.S. Wolfbeis, H. Offenbacher, *Monatsh. Chem.* 1984, *115*, 647.

44. a) N.J. Tuno, T. Okubo, *J. Phys. Chem.* 1982, *86*, 159; b) K.P. Ananthapadmanabhan, E.D. Goddard, N.J. Turro, P.L. Kuo, *J. Colloid. Interface Sci.* 1985, *1*, 352.

45. a) D.L. Sackett, J.R. Knutson, J. Wilff, *J. Biol. Chem.* 1990, *265*, 14899; b) D.L. Sackett, J. Wilff, *Anal Biochem.* 1989, *167*, 228.

46. a) R.H. Bisby, R.B. Cundall, L. Davenport, ID. Johnson, E.W. Thomas, In *Fluorescent Probes,* Eds., G.S. Beddard, M.A. West, Academic Press, London, 1981, p. 97; b) D.H. Waldeck, *Chem. Rev.* 1991, *91*, 415; c) D.G. Whitten, *Acc. Chem. Res.* 1993, *26*, 502; d) L.G. Duveneck, E.V. Sitzmann, K.B. Eisenthal, N.J Turro, *J. Phys. Chem.* 1989, *93*, 7166; e) J. Saltiel, J. D'Agostino, E. D. Megarity, L. Metto, K.R. Neuberger, M. Wrighton, O.C. Zafiriou. *Org. Photochem.* 1973, *3*, 1; f) J. Saltiel, Y.P. Sun, In *Photochromism: Molecules and Systems,* Eds., H. Durr, H. Bouas-Laurent, Elsevier, Amsterdam, 1990, p. 64.

47. K.R.A.S. Sandanayake, K. Nakashima, S. Shinkai, *J. Chem. Soc. Chem. Commun.* 1994, 1621.

48. W. DeW. Horrocks, D.R. Sudnick, *Acc. Chem. Res.* 1981, *14*, 384.

49. a) F.H. Richardson, *Chem. Rev.* 1982, *82*, 541; b) N. Sabbatini, M. Guardigli, J.M. Lehn, *Coord. Chem. Rev.* 1993, *123*, 201; c) V. Balzani, N. Sabbatini, F. Scandola, *Chem. Rev.* 1986. *86*, 319.

50. a) Z. Pikramenou. D.G. Nocera, *Inorg. Chem.* 1992, *31*, 532; b) Z. Pikramenou, K.M. Johnson, D.G. Nocera, *Tetrahedron Lett.* 1993, *34*, 3581; c) M.A. Mortellaro, D.G. Nocera, *Chemtech.* 1996, February, 17; d) D.G. Nocera, *New Sci.* 1996, 13, January, 24; e) I. Fujii. R. Kiyama, K. Kanematsu, *Bioorg. Chem.* 1989, *17*, 240; f) B.G. McLachlan. JR Kavandi, J.B. Callis, M. Gouterman, E. Green, G.E. Khalil, D. Burns, *Exp. Fluids.* 1993, *14*, 33; g) J. Gallery, M. Gouterman, E. Green, G.E. Khalil, *Rev. Sci. Instrum.* 1994, *65*, 712.

51. T.C. Werner. In *Modern Fluorescence Spectroscopy,* Ed., E.L. Wehry, Plenum, New York, 1977, Vol. II, p. 277.

52. a) H.Z. Langhals. *Phys. Chem. Neue Folge,* 1981, *127*, 45; b) H.Z. Langhals, *Angew. Chem. Int. Ed. Engl.* 1982, *21*, 724.

53. C. Reichardt, *Chem. Rev.* 1994, *94*, 2319.

54. G. Jones, W.R Jackson, S. Kanoktanaporn, W.R. Bergmark, *Photochem, Photbiol.* 1985, *42*, All.

55. M.A. Kessler. O.S. Wolfbeis, *Spectrochim.Acta.* 1991, *47A*, 187.

56. a) T. Soujanya, RW. Fessenden, A. Samanta, *J. Phys. Chem.* 1996, *100*, 3507; b) T. Soujanya, T.S.R Krishna, A. Samanta, *J. Photochem. Photobiol. A: Chem,* 1992, *66*, 185; c) T. Soujanya, T.S.R. Krishna, A. Samanta, J. *Phys. Chem.* 1992, *96*, 185; d) G. Saroja, A. Samanta, *Chem. Phys. Lett.* 1995, *246*, 506; e) G. Saroja, A. Samanta, J. *Chem. Soc. Faraday Trans.* 1996, *92*, 2697; f) G. Saroja, T. Soujanya, B.

Ramachandram, A. Samanta, *J. Fluoresc.* 1998, *8,* 405; g) A. Chattopadhyay, *Chem, Phys. Lipids* 1990, *53,* 1; h) S. Mukherjee, A. Chattopadhyay, A. Samanta, T. Soujayna, *J. Phys. Chem.* 1994, *98,* 2809; i) S. Saha, A. Samanta, *J. Phys. Chem.* 1998, 102,7903.

57. a) J.F. Letard, R. Lapouyade, W. Rettig, *Mol. Cryst. Liq. Cryst.* 1993, *36,* 41; b) J.F. Letard, R. Lapouyade, W. Rettig, *Pure Appl. Chem.* 1993, *65,* 1705.

58. a) P. Dumon, G. Jonasauskas, F. Dupuy, P. Pee, C. Rulliere, J.F. Létard, R. Lapouyade, *J. Phys. Chem.* 1994, *98,* 10391; b) R. Mathevet, G. Jonusauskas, C. Rulliere, J.F. Letard, R. Lapouyade,*J Phys. Chem.* 1995, *99,* 15709.

59. S. Delmond, J.F. Letard, R. Lapouyade, R. Mathevet, G. Jonusauskas, C. Rulliere, *New J. Chem.* 1996,*20,* 861.

60. J. Bourson, M.N. Borrel, B. Valeur,*Anal. Chim. Acta.* 1992, *257,* 180.

61. a) Z.R. Grabowski, K. Rotkiewicz, A. Siemiarczuk, D.J. Cowely, W. Baumann, *Nouv. J. Chim.* 1979, *3,* 443; b) Z.R. Grabowski, J. Dobokowski, *Pure Appl. Chem.* 1983,55,245.

62. a) Z.R. Grabowski, *Pure Appl, Chem.* 1992, *64,* 1249; b) W. Rettig, *Angew. Chem. Int. Ed. Engl.* 1986, *25,* 971; c) E.M. Kosower, D. Huppert, *Ann. Rev. Phys. Chem.* 1986, *37,* 127; d) K. Bhattacharyya, M. Chowdhury, *Chem. Rev.* 1993, *93,* 507; e) W. Rettig, *Top. Curr. Chem.* 1994, *169,* 253.

63. a) E.M. Kosower, *Acc. Chem. Res.* 1982, 75, 266; b) G. Weber, D.J.R. Laurence, *Biochem. J.* 1954, *31,* 56; c) D.J. Cowley, *Nature,* 1986, *319,* 14.

64. H. Shizuka, T. Ogiwara, E. Kimura,*J. Phys. Chem.* 1985, *89,* 4302.

65. A. Minta, J.P.Y. Kao, R.Y. Tsien, *J. Biol. Chem.* 1989,*164,* 8171.

66. S.A. Jonker, F. Ariese, J. W. Verhoeven, *Recl. Trav. Chim. Pays-Bas,* 1989, *108,* 109.

67. *The Exciplex,* Eds., M. Gordon, W.R Ware, Academic Press, New York, 1975 and references therein.

68. a) J. Emert, D. Kodali, R. Catena, *J. Chem. Soc. Cheat Commun.* 1981, 758; b) N.J. Turro, T. Okubo, G.C. Weed, *Photochem. Photobiol.* 1982, *35,* 325; c) F. Diederich, *Cyclophanes,* Royal Society of Chemistry, Cambridge. 1991, p 113; d) D. Marquis, J.-P. Desvergne, *Chem. Phys. Lett.* 1994, *230,* 131; e) D. Marquis, J.-P. Desvergne, H. Bous-Laurent, *J. Org. Chem.* 1995, *60,* 7984; f) F. Fages, J.-P. Desvergne, K. Kampke, H. Bous-Laurent, J.M. Lehn, M. Meyer, A.M. Albrecht-Gary, *J. Am. Chem. Soc.* 1993, 775, 3658.

69. a) I. Aoki, Y. Kawahara, T. Sakaki, T. Harada, S. Shinkai, *Bull. Chem. Soc. Jpn.* 1993, *66,* 927; b) C.J. Broan, *J. Chem. Soc. Chem. Commun.* 1996, 699; c) A. Ueno, F. Moriwaki, T. Osa, F. Hamada, K. Murai, *J. Am. Chem. Soc.* 1988, 770, 4323; d) T. Saika, T. Iyoda, K. Honda, T. Shimidzu, *J. Chem. Soc. Chem. Commun.* 1992, 591.

70. a) A.W. Varnes, R.B. Dodson, E.L. Wehry, *J. Am. Chem. Soc.* 1972, *94,* 946; b) J.A. Kemlo, T.M. Shepherd, *Chem. Phys. Lett.* 1977, *47,* 158.

EXPERIMENTAL DETAILS

This chapter provides details of the experimental procedures that have been followed at various stages of this investigation. Specifically, the methods of synthesis of various systems, purification procedures and the analytical data of the compounds have been provided. The instrumental details and methodologies employed for the study of the Photophysical behaviour of the systems are also described in this chapter.

2.1.   Materials and Purification

4-Aminophthalimide (AP) and 4-aminonaphthalimide (ANP) were procured from Kodak and Aldrich respectively and recrystallised several times from ethanol-water mixture for Photophysical studies but used as received for the synthesis. N,N-Dimethylethylenediamine, N,N-dimethylpropylenediamine, N-phenylethylenediamine, N-(l-naphthyl)ethylenediamine hydrochloride and 4-aminonaphthalic anhydride were purchased from Aldrich and used as procured. 4-Chloronaphthalic anhydride and 4-chloro-7-nitrobenz-2-oxa-l,3-diazole (4-chloro-NBD) were obtained from Acros Organics Limited and used for synthesis without any further purification. NaN_3 was obtained from Loba Chemicals (India). Coumarin dye (C-153, Molecular Probes, Laser grade) was used as received for the fluorescence quantum yield measurements.

The following metal salts were used in the investigation: $Zn(H_2O)_6(ClO_4)_2$, $Cu(H_2O)_3(NO_3)_2$, $Ni(H_2O)_6(ClO_4)_2$, $Co(H_2O)_6(NO_3)_2$, $Fe(H_2O)_6(ClO_4)_3$, $Fe(H_2O)_6(ClO_4)_2$, $Mn(H_2O)_6(ClO_4)_2$, $Cr(H_2O)_6Cl_3$ and $Co(H_2O)_6Cl_2$. The metal salts used in this study were of analytical grade (procured locally) and were employed without any purification.

However, for some specific experiments freshly recrystallised metal salts were used. The anhydrous metal salts were prepared using the following procedure.[1]

The hydrated metal salts (usually metal chlorides) were refluxed in appropriate amount of 2,2-dimethoxypropane (Merck, India) for 6 hours and subsequently the solvent was removed under vacuum. The perfectly dried salt under vacuum was stored in a desiccator.

Silica gel and basic alumina used for column chromatography were obtained from Acme Scientific Chemicals (India). The drying agents used at various stages of the purification procedures, anhydrous CaO, $CaCl_2$, $MgSO_4$, CaH_2. K_2CO_3, P_2O_5 and Mg turnings were procured from local companies.

$CDCl_3$ from Sigma or Acros Organics Limited (India), methanol-d_4 from Acros Organics Limited (India) and acetone-d_6 from Aldrich were used for the NMR spectral measurements.

2.7.7.   *Solvent purification*

Extremely pure and dry solvents are essential for the spectroscopic investigation of the systems as contamination of the solvent by impurities such as water, and acids affects the spectral behaviour of the compounds significantly. Even though the solvents (Merck, India) were of spectral grade, extreme care was taken for the purification and drying of the solvents. Each solvent was purified following standard procedures outlined below. To avoid the contamination on storing, only freshly purified solvents were used for spectral measurements.

Tetrahydrofuran (THF): Preliminary drying was done over ignited $CaCl_2$. Subsequently, the solvent containing the blue ketyl radical, formed from the reaction of Na with small amount of benzophenone, was distilled.

Acetonitrile (AN): Most of the water was eliminated by shaking the solvent with pre-dried silica gel blue. Subsequent stirring with CaH_2, until no further evolution of

hydrogen gas observed, left only traces of water in the solvent. This was followed by fractional distillation over CaH_2.

Methanol (MeOH): First dried over CaH_2 by stirring overnight. Then to 50-75 ml of methanol, clean dry magnesium turnings (5 g) and iodine (0.5 g) were added and warmed until all the Mg was converted into the magnesium methoxide. To this about 1 litre of methanol was added, refluxed for 2-3 hours and distilled.

N,N-Dimethylformamide (DMF) and *dimethylsulfoxide (DMSO)* used for synthesis were purified using standard procedures.[2]

Water: Triply distilled water was used for the preparation of buffer solutions used in the spectroscopic measurements.
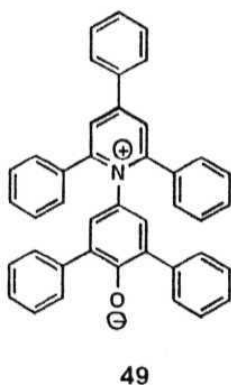
The extent of dryness of each solvent was checked by monitoring the wavelength of the absorption maxima of the betaine dye 49 in a given solvent.[3] 49 was introduced by Dimorth and Reichardt[4] as a polarity indicator of the solvent in view of the extreme sensitivity of the intramolecular charge transfer band of the dye. Based on the transition energy of the longest wavelength, solvatochromic absorption band of the dye, a solvent polarity scale in terms of a polarity parameter, $E_T(30)$ was proposed. $E_T(30)$ was defined as

49

$$E_T(30) \text{ (kcal/mol)} = 28591/\lambda_{max} \text{ (nm)} \qquad 2.1$$

Where, $E_T(30)$ is the molar transition energy of 49 measured in kcal/mol at room temperature (25°C) and 1 atmospheric pressure and λ_{max} is the wavelength of the longest absorption band in nanometers. We measured the $E_T(30)$ values of the solvents and compared with the literature $E_T(30)$ values of the respective solvents[3] to ensure that the solvents are not contaminated by polar impurities. 49 was a kind gift from Prof. C. Reichardt of Philips University and was used without any further **purification**. All the

purified solvents were found to be optically transparent in the spectral region of interest (usually 300-700 nm).

2.2.   Synthesis of the Sensor Systems

2.2.1.   *2-(N,N-Dimethylamino)-1-(4-aminophthalimido)ethane(APDEA):*
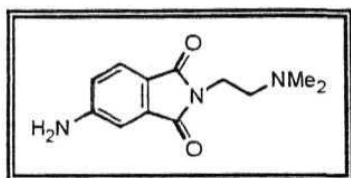
4-Aminophthalimide (0.5 g, 3.08 mmol) and N,N-dimethylethylenediamine (0.4 ml, 3.69 mmol) placed in a 25 ml round bottomed flask fitted with a water condenser and potassium hydroxide guard tube. Then the reaction mixture was heated at 80-90°C with constant stirring for about 4-5 hours. The thick product thus obtained was purified by column chromatography (basic alumina, hexane (HX): ethyl acetate (EtOAc)/30: 70). The desired product was confirmed by the following analytical data. Yield 80%.

IR (KBr, cm^{-1}): 3429, 3350, 2926, 2852, 1759, 1697, 1396. 1010 and 748.
^{1}H NMR (MeOH-d$_4$): 8 2.6 (s, 6H). 3.0 (t, 2H), 3.6 (t, 2H). 5.2 (s, 2H), 6.9 (dd, 1H), 7.2 (d, 1H) and 7.6 (d, 1H).

2.2.2.   *3-(N,N-Dimethylamino)-1-(4-aminophthalimido)propane(APDPA):*
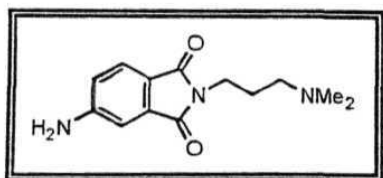
3-N,N-Dimethylamino-1-(4-aminophthalimido) propane (APDPA) was obtained by following a procedure similar to that employed for the synthesis of APDEA by treating 4-aminophthalimide (0.5 g, 3.08 mmol) with N,N-dimethylpropylenediamine (0.47 ml, 3.7 mmol). The final purified product (basic alumina, HX: EtOAc/50: 50) gave the following satisfactory analytical data. Yield. 80%.

IR (KBr, cm⁻¹): 3425, 3352, 2925, 2852, 1755, 1699, 1396, 1020 and 746.

¹H NMR (MeOH-d₄): δ 2.1 (m, 2H), 2.8 (s, 6H), 3.1 (t, 2H), 3.7 (t, 2H), 5.2 (s, 2H), 6.9 (dd, 1H), 7.1 (d, 1H) and 7.6 (d, 1H).

2.2.3. *2-Anilino-1-(4-aminophthalimido)ethane (APPED):*
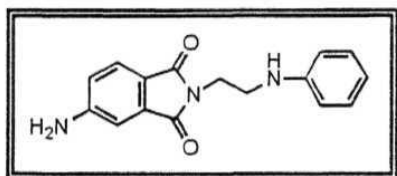
4-Aminophthalimide (0.5 g, 3.08 mmol) was treated with N-phenylethylenediamine (0.48 ml, 3.7 mmol) at 80-90°C to obtain APPED. The product was purified by column chromatography (basic alumina, HX: EtOAc/70: 30). The obtained product gave the following analytical data. Yield. 75%.

IR (KBr, cm⁻¹): 3477, 3373, 3250, 3040, 2922, 1759, 1687, 1008 and 745.

¹H NMR (CDCl₃): δ 3.4 (t, 2H), 3.9 (t, 2H), 4.4 (s, 1H), 5.2 (s, 2H) 6.6 (m, 3H), 6.8 (dd, 1H), 7.0 (d, 1H), 7.2 (t, 2H) and 7.6 (d, 1H).

2.2.4. *2-(1-Naphthylamino)-1-(4-aminophthalimido)ethane (APNED):*
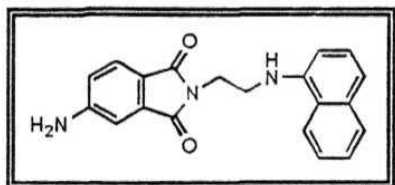
N-(1-Naphthyl)ethylenediamine hydrochloride (0.48 g, 2.59 mmol) was dissolved in ethanol (5 ml). The solution was neutralised using K₂CO₃ (0.18 g, 1.3 mmol) with constant stirring at room temperature for 1 hour. 4-aminophthalimide (0.35 g, 2.15 mmol) was added to the reaction mixture and refluxed for 24 hours. After complete reaction the mixture was allowed to cool and the solvent was evaporated under vacuum. The obtained residue was purified by column chromatography (basic alumina HX: EtOAc/80: 20) to yield a yellowish material which was characterised by IR and ¹H NMR spectral data. Yield 70%.

IR (KBr, cm⁻¹): 3477, 3385, 3371, 3043, 2945, 1755, 1693, 1624, 1398, 773 and 752.

^{1}H NMR (CDCl₃): δ 3.6 (t, 2H), 4.1 (t, 2H), 4.3 (s, 2H), 5.2 (s, 1H), 6.6 (d, 1H), 6.8 (dd, 1H), 7.1 (d, 1H), 7.25 (d, 1H), 7.4 (d, 1H), 7.5 (m, 2H), 7.7 (d, 1H), 7.8 (dd, 1H) and 8.0 (dd, 1H).

2.2.5.   2-(N,N-Dimethylamino)-1-(4-amino-1,8-naphthalimido)ethane (ANPDEA):
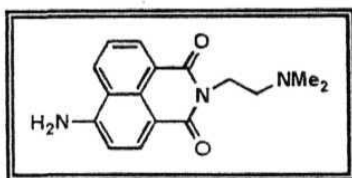
4-Amino-1,8-naphthalic anhydride (0.1 g, 0.47 mmol) and N,N-dimethylethylenediamine (0.062 ml, 0.56 mmol) placed in 10 ml round bottomed flask. Ethanol (2 ml) was added to the above reaction mixture and refluxed for 24 hours. After complete reaction the solvent was removed. The obtained residue was purified by column chromatography (silica gel, HX: EtOAc/50: 50). The final product was characterised by IR and ^{1}H NMR spectral data. Yield 75%.

IR (KBr, cm⁻¹); 3402, 3211, 2943, 2813, 1672, 1639, 1375, 771 and 754.

^{1}H NMR (CDCl₃): δ 2.5 (s, 6H), 2.7 (t, 2H), 4.2 (t, 2H), 5.1 (s, 2H), 6.8 (d, 1H), 7.6 (t, 1H), 8.0 (d, 1H), 8.3 (d, 1H) and 8.6 (d, 1H).

2.2.6.   2-Anilino-1-(4-amino-1,8-naphthalimido)ethane (ANPPED):
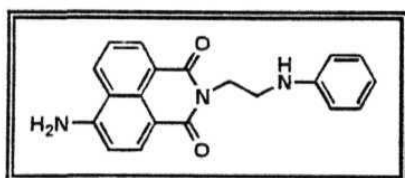
ANPPED was obtained from, 4-aminonaphthalic anhydride (0.1 g, 0.47 mmol) on treatment of N-phenylethylenediamine (0.075 ml, 0.56 mmol). The procedure employed for the synthesis and purification of ANPPED was similar to that used for ANPDEA. The product was characterised by IR and ^{1}HNMR spectral data. Yield 70%.

IR (KBr, cm⁻¹): 3468, 3350, 3234, 3040, 2831, 1670, 1639, 1365, 769 and 752.

¹H NMR: δ 3.6 (t, 2H), 4.2 (s, 1H), 4.5 (t, 2H), 5.0 (s, 2H), 6.6 (m, 3H), 6.9 (d, 1H), 7.1 (t, 2H), 7.7 (t, 1H), 8.1 (d, 1H), 8.4 (d, 1H) and 8.6 (d, 1H).

2.2.7. 2-(N,N-Dimethylamino)-1-(1,8-naphthalimido)ethane (NPDEA):
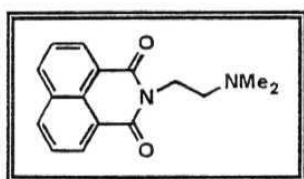
1,8- Naphthalic anhydride (0.5 g, 2.53 mmol) and N,N-dimethylethylenediamine (0.335 ml, 3.036 mmol) was suspended in ethanol (5 ml) in a 25 ml round bottomed flask and refluxed for 5 hours. After complete reaction the solvent was evaporated to dryness. The obtained residue was purified by column chromatography (silica gel, HX: EtOAc/20: 80). The purified compound underwent satisfactory analytical experiments to yield the following spectral data. Yield 90%.

IR (KBr, cm⁻¹): 2941, 2852, 1695, 1657, 1383 and 779.

¹H NMR (CDCl₃): δ 2.4 (s, 6H), 2.6 (t, 2H), 4.3 (t, 2H), 7.7 (t, 2H), 8.2 (d, 2H), and 8.6 (d, 2H).

2.2.8. 3-(N,N-Dimethylamino)-1-(1,8-naphthalmido)propane (NPDPA):
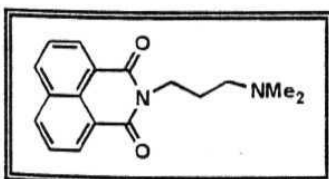
NPDPA was obtained by similar method employed for the synthesis of NPDEA wherein 1,8-naphthalic anhydride (0.5 g, 2.53 mmol) was treated with N,N-dimethylpropylenediamine (0.38 ml, 3.0 mmol) instead of N,N-dimethylethylenediamine. The purified compound gave satisfactory analytical data as given below. Yield 85%.

IR (KBr, cm⁻¹): 2943, 2812, 1697, 1655, 1342 and 779.

^{1}H NMR (CDCl$_3$): δ 1.9 (m, 2H), 2.4 (s, 6H), 2.6 (t, 2H), 4.4 (t, 2H), 7.7 (t, 2H), 8.6 (d, 2H) and 8.6 (d, 2H).

2.2.9. 2-Anilino-1-(1,8-naphthalmido)ethane (NPPED):

NPPED was obtained by a similar method employed for NPDEA. The purified product gave the following analytical data. Yield 90%.

IR (KBr, cm^{-1}): 3377, 3050, 2961, 1701, 1657, 1383 and 781.

^{1}H NMR (CDCl$_3$): δ 3.5 (t, 2H), 4.3 (s, 1H), 4.6 (t, 2H), 6.7 (m, 3H), 7.2 (t, 2H), 7.8 (t, 2H), 8.2 (d, 2H) and 8.6 (d, 2H).

2.2.10. 2-(1-Naphthylamino)-1-(1,8-naphthalimido)ethane (NPNED):
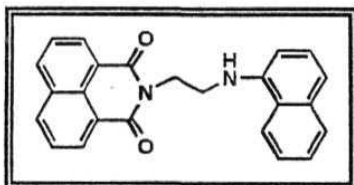
1,8-Naphthalic anhydride (0.5 g, 2.53 mmol) was dissolved in ethanol (5 ml) and treated with previously neutralised N-(1-naphthyl)ethylenediamine hydrochloride (0.56 g, 3.0 mmol) in ethanol at refluxing temperature for 24 hours. After complete reaction the reaction mixture was allowed to cool and the solvent was evaporated under vacuum. Thus obtained solid was purified by column chromatography (silica gel, HX: EtOAc/80: 20) to yield a reddish material which was characterized by IR and ^{1}H NMR. Yield 80%.

IR (KBr, cm^{-1}): 3408, 3050, 2950, 2852, 1689, 1655, 1385 and 771.

^{1}H NMR (CDCl$_3$): δ 3.7 (t, 2H), 4.7 (t, 2H), 5.3 (s, 1H), 6.6 (d, 1H), 7.3-7.5 (m, 4H), 7.6-7.9 (m, 4H), 8.2 (d, 2H) and 8.6 (d, 2H).

2.2.11. 4-(N,N-Dimethylamino)-1-(1,8-naphthalimido)butane (NPDBA):
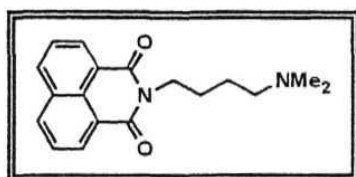
The desired compound (NPDBA) was obtained by following a two step method in which first step is the preparation of the 1-(1,8-naphthalimido)-4-bromobutane and second step involves the treatment of the N,N-dimethylamino hydrochloride with 1-(1,8-naphthalimido)-4-bromobutane.

Step 1: 1,8-Naphthalimide (0.5 g, 2.53 mmol) was treated with previously washed NaH (0.245 g, 10 mmol) in dry DMF (3 ml) at room temperature with constant stirring for 1 hour. Subsequently to the sodium salt of naphthalimide dibromobutane (0.333 ml, 2.78 mmol) was added and the reaction mixture was stirred at room temperature for 24 hours. After complete reaction, the excess sodium hydride present in the reaction mixture was quenched with water (1 ml) and the solvent was removed under vacuum. Thus obtained solid was purified by column chromatography (basic alumina, HX: EtOAc/85: 15). The purified compound gave satisfactory spectral data. Yield 60%.

IR (KBr, cm^{-1}): 2926, 1697, 1664, 1587, 1342 and 781
^{1}H NMR (CDCl$_3$): δ 1.6 (m, 2H), 1.8 (m, 2H), 2.4 (t, 2H), 4.2 (t, 2H), 7.8 (t, 2H) 8.2 (d, 2H) and 8.6 (d, 2H).

Step 2: 1-(1,8-naphthalimido)-4-bromobutane (0.1 g, 0.3 mmol) was dissolved in dry acetonitrile (5 ml). N,N-Dimethylamine hydrochloride (0.03 g, 0.36 mmol) and K$_2$CO$_3$ (0.083 g, 0.6 mmol) were added to the above solution. Catalytic amount of potassium iodide was added and the reaction mixture was allowed to stir for 24 hours at room temperature. After complete reaction the inorganic residue was filtered. The obtained filtrate gave a colourless residue on evaporation of the solvent under vacuum. Finally the residue was purified by column chromatography (basic alumina, HX:

EtOAc/30: 70) to obtain fine cólourless compound. The overall yield was 55%. The final product gave the following analytical data.

IR (KBr, cm⁻¹): 2941, 1697, 1658, 1346 and 779.

¹H NMR (CDCl₃): δ 1.6-1.8 (m, 4H), 2.2 (s, 6H), 2.4 (t, 2H), 4.2 (t, 2H), 7.7 (t, 2H) 8.2 (d, 2H) and 8.6 (d, 2H).

2.2.12. N-Ethyl-1,8-naphthalimide (NPNE):
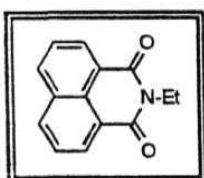
NPNE was obtained from 1,8-naphthalimide (0.5 g, 2.53 mmol) on treatment with previously washed sodium hydride (0.36 g 15 mmol) followed by ethylbromide (0.23 ml, 3.0 mmol) in dry DMF (5 ml) at room temperature for 24 hours with constant stirring. The obtained residue was purified by column chromatography after water work-up (silica gel, HX: EtOAc/80: 20) to yield a light yellow crystalline material. Yield 60%. The following analytical data support the structure of the compound.

IR (KBr, cm⁻¹): 2974, 1695, 1653, 1587, 1363, 1051 and 771.

¹H NMR (CDCl₃): δ 0.9 (t, 3H), 4.3 (q, 2H), 7.7 (t, 2H), 8.2 (d, 2H) and 8.6 (d, 2H).

2.2.13. 2-(N,N-Dimethylamino)-1-(4-chloro-1,8-naphthalimido)ethane (CNPDEA):
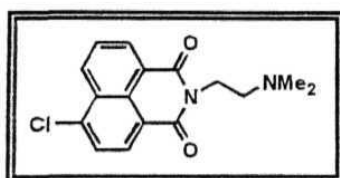
4-Chloro-1,8-naphthalic anhydride (0.5 g, 2.15 mmol) was suspended in ethanol (5 ml) and to this N,N-dimethylethylenediamine (0.29 ml, 2.6 mmol) was added. Then the reaction mixture was refluxed for 6 hours. The suspended 4-chloro-1,8-naphthalic anhydride was slowly dissolved in ethanol as the reaction proceeds. After complete reaction the reaction mixture was allowed to cool to

room temperature. The desired product was crystallised out on cooling. Then the reaction mixture was filtered through a buckner funnel. The product thus obtained was crystallised several times from ethanol to obtain the spectroscopic purity. Yield 95%. The following analytical data was obtained for the pure product.

IR (KBr, cm^{-1}): 2968, 2858, 1697, 1658, 1379, 1037 and 779.

^{1}H NMR (CDCl$_3$): δ 2.4 (s, 6H), 2.6 (t, 2H), 4.3 (t, 2H), 7.9 (t, 2H) and 8.5-8.7 (m, 3H).

2.2.14. 3-(N,N-Dimethylamino)-1-(4-chloro-1,8-naphthalimido)propane (CNPDPA):
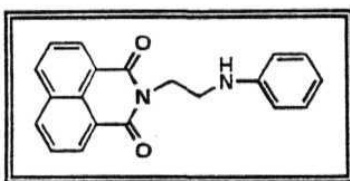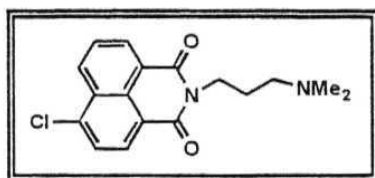

CNPDPA was obtained by the similar method employed for CNPDEA, yield 90%. The pure compound gave the following analytical data.

IR (KBr, cm^{-1}): 2947, 2780, 1699, 1653, 1348 and 783.

^{1}H NMR (CDCl$_3$): δ 1.9 (m, 2H), 2.3 (s, 6H), 2.4 (t, 2H), 4.2 (t, 2H), 7.8 (t, 2H) and 8.5-8.7 (m, 3H).

2.2.15. 2-Anilino-1-(4-chloro-1,8-naphthalimido)ethane (CNPPED):
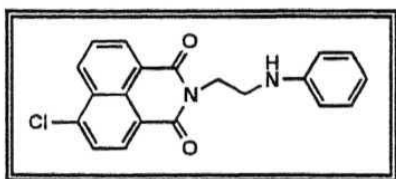
Similar method as employed for CNPDEA was used to obtain CNPPED in good yield (90%) and purity. The analytical data are presented below.

IR (KBr, cm^{-1}): 3391, 3026, 2957, 1701, 1657, 1340 and 783.

^{1}H NMR (CDCl$_3$): δ 3.5 (t, 2H), 4.2 (s, 1H), 4.5 (t, 2H), 6.6 (dd, 3H), 7.1 (t, 2H), 7.8 (t, 2H) and 8.4-8.6 (m, 3H).

2.2.16. 2-(1-Naphthylamino)-1-(4-chloro-1,8-naphthalimido)ethane (CNPNED):
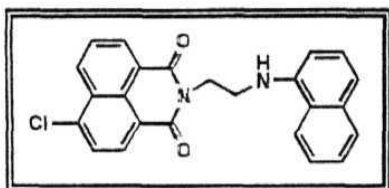
N-(1-naphthyl)ethylenediamine hydrochloride (0.48 g, 2.59 mmol) was dissolved in dry DMF (5 ml) and neutralised with anhydrous K_2CO_3 (0.18 g, 1.3 mmol) by constant stirring at room temperature for 1 hour. 4-Chloro-1,8-naphthalic anhydride (0.5 g, 2.15 mmol) was added to the above reaction mixture. Then the reaction mixture was heated at 80-90°C for 24 hours. After complete reaction the reaction mixture was allowed to cool to room temperature and the solvent was removed under vacuum. The obtained residue was purified by column chromatography (silica gel, HX: EtOAc/80: 20) to yield a yellowish material, which was characterised by IR and NMR. Yield. 50%.

IR (KBr, cm^{-1}): 3369, 3030, 2960, 2850, 1697, 1658, 783 and 763.
^{1}H NMR (CDCl$_3$): δ 3.7 (t, 2H), 4.7 (t, 2H), 5.2 (s, 1H), 6.6 (d, 1H), 7.2 (d, 1H), 7.3-7.5 (m, 3H), 7.7-7.9 (m, 4H), and 8.5-8.7 (m, 3H).

2.2.17. N-Butyl-4-chloro-1,8-naphthalimide (CNPNB):
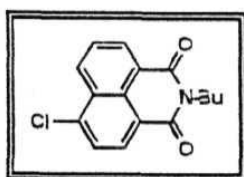
The desired product CNPNB was obtained by a very similar method employed for the preparation of CNPDEA. Yield 90%. The purified product gave the following analytical data.

IR (KBr, cm^{-1}): 2955, 1699, 1655, 1348, 1230, 1076 and 784.
^{1}H NMR (CDCl$_3$): δ 0.9 (t, 3H), 1.5 (m, 2H), 1.7 (m, 2H), 4.2 (t, 2H), 7.8 (t, 2H) and 8.5-8.7 (m, 3H).

2.2.18. 4-(2-N,N-Dimethylethylenediamino)-7-nitrobenz-2-oxa-1,3-diazole (NEA):
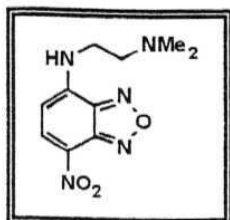
N,N-Dimethylethylenediamine (0.33 ml, 3 mmol) solution in toluene (3 ml) was added drop-wise to a toluene (3 ml) solution of 4-chloro-7-nitrobenz-2-oxa-1,3-diazole (0.5 g, 2.5 mmol) at 0°C. The reaction mixture was stirred for 1 hour at 0° C and then for another 2 hours at room temperature. The solid product obtained was purified by repeated recrystallisation from methanol. The structure of the compound was established by the following analytical data. Yield 60%.

IR (KBr, cm^{-1}): 3447, 3030, 2962, 1587, and 1332.

^{1}H NMR (CDCl$_3$): δ 2.3 (s, 6H), 2.7 (t, 2H), 3.5 (t, 2H), 3.7 (s, 1H), 6.15 (d, 1H) and 8.5 (d, 1H).

2.2.19. 4-Amino-7-nitrobenz-2-oxa-1,3-diazole (NAM):
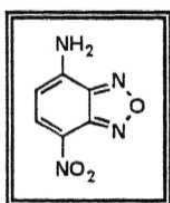
NAM was prepared from 4-chloro-7-nitrobenz-2-oxa-1,3-diazole by following a standard two-step procedure as described below.[5] 4-Chloro-7-nitrobenz-2-oxa-1,3-diazole   (0.5   g,   2.5   mmol)   in dimethylsulfoxide (10 ml) containing sodium azide (0.3 g, 4.6 mmol) was heated on a steam bath for 5 minutes. Dilution with water (40 ml) and crystallisation of the precipitate from aqueous ethanol (1:1 and charcoal) gave yellow needles of 4-azido-7-nitrobenz-2-oxa-1,3-diazole. To obtain NAM, 4-azido-7-nitrobenz-2-oxa-1,3-diazole (0.5 g, 2.42 mmol) was refluxed for 30 minutes in toluene (25 ml). Addition of light petroleum (5 ml) to the hot solution on sublimation under vacuum (120°/0.5 mm Hg) gave 4-amino-7-nitrobenz-2-oxa-1,3-diazole. The analytical data for the final product was found to be in accordance with its structure. Yield 43%.

IR (KBr, cm^{-1}): 3425, 3337, 1643, 1554, 1261, 1097 and 800.

^{1}H NMR (Acetone-d$_6$): δ 6.5 (d, 1H), 7.9 (s, 2H) and 8.5 (d, 1H).

2.2.20. 4-Methoxy-N-butyl-1,8-naphthalimide (OMNPNB):
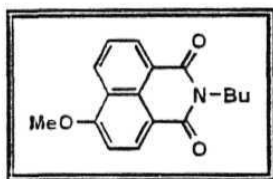
OMNPNB was obtained from CNPNB (0.1 g, 0.35 mmol) on treatment with sodium methoxide (0.1M solution in methanol, 5 ml) at room temperature for 6 hours. After complete reaction the solvent was removed under vaccum and the product was purified by column chromatography (silica gel. HX: EtOAc/85: 15). Yield 70%. The structure of the compound was established with the following analytical data.

IR (KBr, cm^{-1}): 2957, 2850, 1693, 1657, 1593, 1026 and 781.

^{1}H NMR (CDCl$_3$): δ 0.9 (t, 3H), 1.5 (m. 2H), 1.7 (m, 2H), 4.1 (s, 3H), 4.2 (t, 2H), 6.9 (d, 1H), 7.6 (t, 1H), and 8.4 (m, 3H).

2.2.21. 2-(N,N-Dimethylamino)-1-(4-methoxy-1,8-naphthalimido)ethane (OMNPDEA):
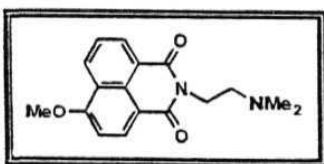
CNPDEA (0.1 g, 0.33 mmol) was reacted with sodium methoxide (0.1M solution in methanol, 5 ml) at room temperature for 6 hours. After complete reaction the solvent was evaporated under vaccum and the residue was purified by column chromatography (silica gel, HX: EtOAc/60: 40) yield 70%. The structure of the compound was established on the basis of the following analytical data.

IR (KBr, cm^{-1}): 2943, 1697, 1657, 1593, 1388, 1028 and 779.

^{1}H NMR (CDCl$_3$): δ 2.3 (s, 6H), 2.6 (t, 2H), 4.1 (s, 3H), 4.4 (t, 2H), 7.0 (d, 1H), 7.6 (t, 1H) and 8.5 (m, 3H).

2.2.22. 3-(N,N-Dimethylamino)-1-(4-methoxy-1,8-naphthalimido)propane (OMNPDPA):
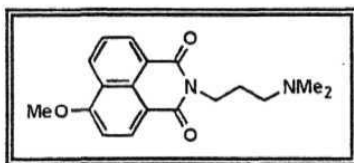
CNPDPA (0.1 g, 0.31 mmol) was treated with sodium methoxide (0.1 M solution in methanol, 5 ml) at room temperature for 6 hours. After complete reaction the product was purified by column chromatography (silica gel HX: EtOAc/50: 50). Yield 80%. The compound gave the following analytical data.

IR (KBr, cm^{-1}): 2941, 1699, 1655, 1597, 1385, 1030 and 775.

^{1}H NMR (CDCl$_3$): δ 1.9 (m, 2H), 2.25 (s, 6H), 2.4 (t, 2H), 4.0 (s, 3H), 4.2 (t, 2H), 6.9 (d. 1H), 7.6 (t, 1H) and 8.5 (m, 3H).

2.2.23. 2-Anilino-1-(4-methoxy-1,8-naphthalimido)ethane (OMNPPED):
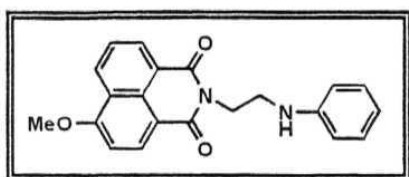
CNPPED (0.1 g, 0.28 mmol) was allowed to react with sodium methoxide (0.1 M solution in methanol, 5 ml) at room temperature for 6 hours. After complete reaction the solvent was evaporated and the product was purified by column chromatography (silica gel, HX: EtOAc/80: 20). Yield 60%. The final compound gave the following spectral data.

IR (KBr, cm^{-1}): 3275, 3030, 2960, 1697, 1651, 1388, 1263, 1053 and 781.

^{1}H NMR (CDCl$_3$): δ 3.5 (t, 2H), 4.1 (s, 3H), 4.3 (s, 1H), 4.6 (t, 2H), 6.6 (dd, 3H), 6.9 (d. 1H), 7.1 (t, 2H), 7.5 (t, 1H) and 8.5 (m, 3H).

2.2.24. 2-(1-Naphthylamino)-1-(4-methoxy-1,8-naphthalimido)ethane (OMNPNED):

CNPNED (0.1 g, 0.29 mmol) was stirred in dry DMF (5 ml) containing sodium methoxide in methanol (0.1 M, 1 ml) at 80°C for 24 hours. After complete reaction the
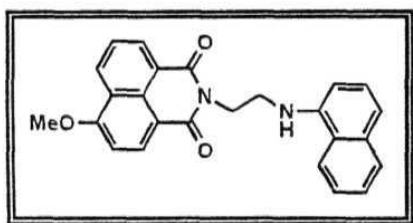
solvent was removed under vacuum and the reaction mixture was purified by column chromatography (silica gel, HX: EtOAc/80: 20). Yield 40%. The resultant yellowish product gave satisfactory analytical data as given below.

IR (KBR, cm^{-1}): 3410, 1689, 1657, 1383 and 769.

^{1}H NMR (CDCl$_3$): δ 3.8 (t, 2H), 4.1 (s, 3H), 4.7 (t, 2H), 5.4 (s, 1H), 6.6 (d, 1H), 7.0 (d, 1H), 7.2 (d, 1H), 7.3-7.5 (m, 3H), 7.7 (m, 2H), 7.9 (dd, 1H) and 8.5-8.7 (m, 3H).

2.3.   Solution Preparation for Spectral Measurements

Dilute solutions with optical density of 0.1-0.2 at the longest wavelength absorption maximum, which corresponded to a concentration of 2-8 x 10^{-5} M, were used for the absorption and fluorescence measurements. The stock solutions of the metal salts were prepared by dissolving a known amount of the salt in a known volume of the solvent. The concentrations of the stock solutions were such that not more than 100 μl of this solution was required for 2 ml solution of the systems. Since the addition was limited within 100 μl (to 2 ml of solution in the cuvette), no volume correction was employed for the calculation of the final concentration of the metal ions.

The tris buffer solution was prepared by addition of appropriate amount of 0.1N HCl solution to an aqueous solution of trisamine (trishydroxymethylaminomethane) so as to obtain a pH of 7.5.[6]

2.4.   **Fluorescence Quantum Yield** Measurements

4-Aminophthalimide (ϕ_f = 0.63 in AN)[7] was used as the reference compound for the measurement of the fluorescence quantum yield of the multi-component systems

involving 4-aminophthalimide. On the other hand, coumarin dye, C-153, (ϕ_f = 0.89 in acetonitrile)[8] was used as the reference for NBD and ANP derivatives. For the measurement of the fluorescence quantum yield of 1,8-naphthalimide and 4-chloro-1,8-naphthalimide derivatives, 1,8-naphthalimide (ϕ_f = 5.0 x 10^{-2} in acetonitrile)[9] was used as the reference compound. The fluorescence quantum yields were determined using the following expression.[10]

$$\phi_{sample} = \frac{I_{sample} \times O.D_{standard}}{I_{standard} \times O.D_{sample}} \times \phi_{standard}$$
2.2

Where, I is the area under the emission curve, O.D is the optical density of the compound at the exciting wavelength. For actual measurement, optically matched solutions of the reference and the sample at the exciting wavelength were used and areas were determined either by the program available with the spectrofluorimeter or by 'cut and weigh' method. No solution of O.D more than 0.2 at the exciting wavelength was used and no correction for the solvent refractive indices was made.

2.5.   Calculation of AG* Values

The feasibility of the electron transfer between the two components participating in the electron transfer process is dictated by the overall change in the free energy (ΔG), which accompanies the reaction.[11,12] The exothermicity (AG < 0) is the primary requisite for an efficient electron transfer process. For the bimolecular electron transfer between two ground state species the standard free energy change in the gas phase is given by the following equation.

$$\Delta G = IP_D - EA_A$$
2.3

where, IP_D is the ionisation potential of the donor and EA_A represents the electron affinity of the acceptor. In order to calculate the AG, one needs to estimate the values of IP_D and EA_A from the energies of the highest occupied molecular orbital (HOMO) and lowest

unoccupied molecular orbital (LUMO) of the donor and acceptor respectively. Since the absorption of light energy reduces the ionisation potential of the donor and increases the electron affinity of the acceptor, equn. 2.3 can be modified in the following manner where the donor is electronically excited.

$$\Delta G^* = IP_D - EA_A - E_D^* \qquad\qquad \textbf{2.4}$$

When the acceptor is electronically excited, then equn. 2.3 turns into the following equation.

$$\Delta G^* = IP_D - EA_A + E_A^* \qquad\qquad 2.5$$

where, E_D^* and E_A^* are the singlet state energies of the donor and acceptor respectively.

While considering the free energy change for the electron transfer process between the two components in the solution phase, one must take into account the coulombic interactions and solvent stabilisation effects of the charge transfer intermediates formed in electron transfer.[11,12] These stabilising factors can be incorporated into the equn. 2.4 to yield

$$\Delta G^* = IP_D - EA_A - E_D^* - \underbrace{\frac{e^2}{2}\left(\frac{1}{r_D} + \frac{1}{r_A}\right)\left(1 - \frac{1}{\varepsilon}\right)}_{\text{solvation}} - \underbrace{\frac{e^2}{\varepsilon d_{SSIP}}}_{\text{coulombic}} \qquad 2.6$$

where, r_D and r_A are the radii of the donor and the acceptor, z is the dielectric constant of the solvent and d_{SSIP} is the distance between the solvent separated ion pair. The ionisation potential and electron affinity in solution are related to the redox potentials of the donor and the acceptor:

$$IP_D = E(D^+/D) - \Delta G(D^{+\cdot}) + \text{constant} \qquad 2.7$$

$$EA_A = E(A/A^-) + \Delta G(A^-) + \text{constant} \qquad 2.8$$

Where, $\Delta G(D^+)$ and $\Delta G(A^-)$ are the individual solvation energies;

$$\Delta G(D^+) + \Delta G(A^-) = \frac{e^2}{2}\left(\frac{1}{r_D} + \frac{1}{r_A}\right)\left(1 - \frac{1}{\varepsilon}\right) \qquad 2.9$$

Combining equns. 2.6-2.9 we obtain the following equn.

$$\Delta G^*{}_{SSIP} = [E(D^+/D) - E(A/A^-) - e^2 / \varepsilon d_{SSIP}] - E_D^* \qquad 2.10$$

Replacing $E(D^+/D)$ by E_{ox}(donor), $E(A/A^-)$ by E_{red}(acceptor), d_{SSIP} by d and E_D^* by $E_{0,0}$ we obtain.

$$\Delta G^* = [E_{ox}(donor) - E_{red}(acceptor) - e^2 / \varepsilon d] - E_{0,0} \qquad 2.11$$

If the solvent separated ion pair dissociate into free ions and because of this the ion pairs are separated beyond their respective coulombic fields or if the solvent has a large dielectric constant, the coulombic energy term can be neglected. In polar solvents like acetonitrile, the coulombic energy is less than or equal to 0.1 V and which can be neglected. Then the equation 2.11 transforms as

$$\Delta G^* = [E_{ox}(donor) - E_{red}(acceptor)] - E_{0,0} \qquad 2.12$$

As we are mainly interested in the construction of the fluorosensors utilising the photoinduced electron transfer mechanism, the donor and the acceptor in equn. 2.12 are the receptor and the fluorophore respectively. Therefore, equn. 2.12 can be written as

$$\Delta G^* = [E_{ox}(receptor) - E_{red}(fluorophore)] - E_{0,0} \qquad 2.13$$

2.6. Estimation of Fluorescence Enhancement (FE)

The fluorescence enhancement (FE) values were obtained using the following equation.

$$FE = I_F \text{(optimum)} / I_F \text{(zero)} \qquad 2.14$$

Where, I_F (optimum) is the area under the fluorescence curve with an optimum amount of the metal salt (concentration of the metal ion for which highest fluorescence intensity was

observed). I_F (zero) is area under the fluorescence curve with zero concentration of the metal salt.

2.7.   Instrumentation

The IR and NMR spectra were recorded on JASCO FT-IR / 5300 and on Brucker ACF 200 MHz spectrophotometer respectively. The voltammetric measurements were performed with Cypress System computer controlled electroanalytical set-up, model CS-1090. Tne experiments were carried out in a standard three-component cell, which was equipped with a glassy carbon working electrode, a platinum wire as the auxilliary electrode and a Ag/AgCl as reference electrode. The cyclic voltammograms were recorded in N_2 bubbled acetonitrile solutions containing 0.1 M tetrabutylammonium perchlorate (TBAP) as the supporting electrolyte. The scan speed was 100 mV / sec.

The absorption spectra were recorded on a JASCO Model 7800 spectrophotometer. Fluorescence spectra were recorded either on a JASCO FP-777 or Hitachi. Model 3100 spectrofluorimeter. The fluorescence spectra were not corrected for the instrumental characteristics.

The fluorescence lifetimes were measured on IBH 5000 single photon counting spectrofluorimeter.[13] Fig. 2.1 shows the layout of a typical time correlated single photon counting fluorimeter. A hydrogen flash lamp of pulse width 1.4 ns and frequency of 40 KHz was employed as the excitation source. A small fraction of the excitation pulse was detected by a photo-multiplier tube (1P28) and the photo-multiplier signal was fed into a constant fraction discriminator (CFD) to discriminate the background noise and generate a precise timing pulse. The output of CFD served as the START pulse of the time to amplitude converter (TAC). A fluorescence photon recorded by the emission photo-multiplier (Hamamatsu 3235), as determined by discriminator, generated a pulse, which served as the STOP signal for TAC. The TAC signal produced was proportional to the

time taken from the excitation event to the first photon recorded. The signal from
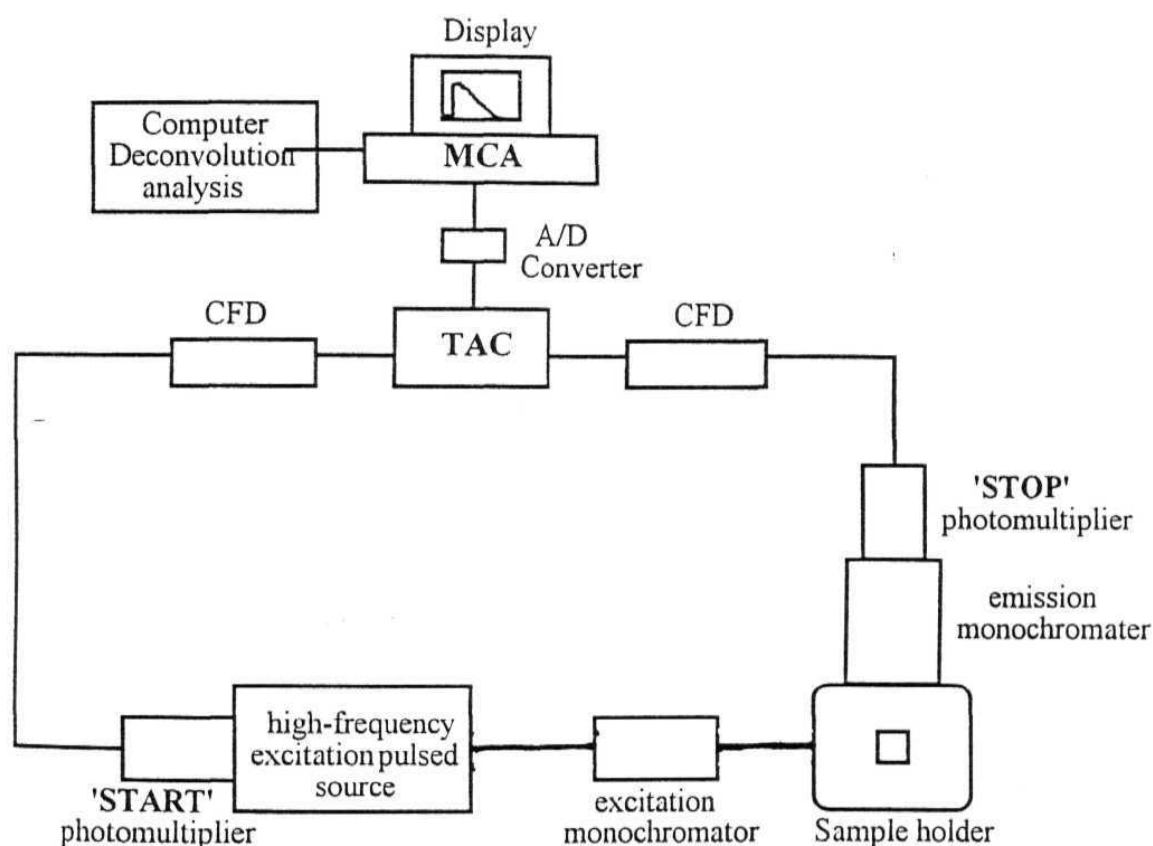
Fig 2.1. Schematic representation of the single-photon counting apparatus.

TAC was digitised by the analog to digital converter (A/D converter) and sent to the appropriate channel, depending on the digitised value of the TAC voltage of a multi-channel analyser (MCA). The whole process was repeated so that the MCA counts represented the number of photon events as a function of time. After many excitation pulses, the MCA memory contents represented a histogram of the emission decay i.e.

time profile of the fluorescence intensity. For recording the lamp profile, a scatterer (dilute solution of MgO in H_2O) was placed in the place of the sample.

Data analysis:

The program used for the estimation of fluorescence lifetimes from the fluorescence decay curves was based on reconvolution least squares method.[14] When the decay time is long compared to the decay time of the excitation pulse, the excitation may be described as a function. However, when the lifetime is short, distortion of the experimental data occurs by the finite decay time of the lamp pulse and response time of the photomultiplier and associated electronics. Since the measured decay function is convolution of the true fluorescence decay, it is necessary to analyse the data by deconvolution in order to get the fluorescence lifetime.

The mathematical statement of the problem is given by the following equation

$$D(t) = \int_0^t P(t')G(t-t')dt' \qquad\qquad 2.15$$

Where D(t) is the fluorescence intensity at any time t. P(t') is the intensity of the exciting light at time t, G(t-t') is the response function of the experimental system. The experimental data D(t) and P(t) from the MCA are fed into a computer (IBM PC, 80486, 50 MHz) to determine the lifetime. We have used the IBH program to analyse the multi-exponential decays.

An excitation pulse profile was recorded and then deconvolution started with mixing of the excitation pulse and a projected decay to form a new reconvoluted set. The data was compared with the experimental set and the difference between the data points summed, generating χ^2 function for the fit. The deconvolution proceeded through a series of such iterations until an insignificant change of χ^2 occurs between iterations. The quality of the fit was normally assessed by the inspection of reduced χ^2, plot of weighted

residuals and autocorrelation function of the residuals. The data points and the fitted curves were finally recorded using a plotter.

2.8.   X-Ray Crystallography

Crystal structure of NPDPA, NPPED and NPNED were determined as described below. The fine crystals for all the compounds could be obtained from methanol solution. The tiny single crystal was fixed to a capillary head by an appropriate fixing material and mounted to the instrument (Enraf-Nonius CAD4 Diffractometer with Mo-Ka radiation). Primary unit cell constants were determined with a set of 25 narrow frame scans. The data were collected at room temperature using CAD4 software. Absorption correction was not applied to the data. XT AL 3.4[15] version was employed for the data reduction. The solution and refinement for the crystal data was obtained using SHELXS-97[16] and SHELXL-97[17] program respectively. The crystallographic parameters of NPDPA, NPPED and NPNED are collected in Table 6.1-6.4 of chapter VI respectively, and necessary data for these structures have been provided as appendix.

Standard error limits involved in various measurements are:

λmax (abs/flu)	± 1 nm
ϕ_f	$\pm 10\%$
τ (> 1 ns)	$\pm 5\%$
τ (< 1 ns)	$\pm 15\%$
FE	$\pm 10\%$

2.9.   References

1.   F.A. Cotton, G. Wilkinson, *Advanced Inorganic Chemistry: A Comprehensive Text,* Wiley-Interscience, New York, 1998, p. 552.

2. D.D. Perrin, W.L.F. Armarego, D.R. Perrin, *Purification of Laboratory Chemicals*, II Ed., Pergamon Press, New York, 1980.

3. C. Reichardt, *Solvents and Solvent Effects in Organic Chemistry*, VCH, Weinheim, 1988, Chapt. 7 and references therein.

4. K. Dimorth, C. Reichardt, T. Siepmann, F. Bohlmaun, *Liebigs Ann. Chem.* 1963, *661,* 1.

5. A.J. Boulton, P.B. Gosh, A.R. Katritzky, *J. Chem. Soc. B,* 1966, 1004.

6. G. Gomori, *Methods in Enzymology,* Vol. I, 1955, p. 138.

7. T. Soujanya, R.W. Fessenden, A. Samanta, *J. Phys. Chem.* 1996, *100,* 3507.

8. K. Rechtaler, G. Köhler, *Chem. Phys.* 1994, *189,* 99.

9. G. Saroja, A. Samanta, J. *Photochem. Photobiol. A: Chem.* 1994, *84,* 19.

10. E. Austin, M. Goutermann, *Bioinor. Chem.* 1978, *9,* 281.

11. a) A. Weller, *Pure Appl. Chem.* 1968, *16,* 115; b) D. Rehm, A. Weller, *Isr. J. Chem.* 1970, *8,* 259.

12. a) G.J. Kavarnos, N.J. Turro, *Chem. Rev.* 1986, *86,* 401 and references therein; b) G.J. Kavarnos, *Top. Curr. Chem.* 1990, *156,* 20.

13. a) D.V. O'Connor, D. Phillips, *Time-correlated Single Photon Counting,* Academic Press, New York, 1984; b) J.R. Lakowicz, In *Topics in Fluorescence Spectroscopy,* Ed., J.R. Lakowicz, Vol. I, Plenum Press, New York, 1991.

14. a) P.R. Bevington, *Data Reduction and Error Analysis for Physical Science,* McGraw-Hill, New York, 1964, b) D.F. Eaton, *Pure Appl. Chem.* 1990, *62,* 1631.

15. *Xtal 3.4. User's Manual.* Eds., S. R. Hall, G. S. D. King, J. M. Stewart, University of Western Australia, Lamb, Perth, 1995.

16. G. M. Sheldrick, *Acta Cryst.* 1990, *A46,* 467.

17. G. M. Sheldrick, *SHELXL-97, Program for the Refinement of Crystal Structures,* Universitat of Gottingen, Germany, 1997.

MULTI-COMPONENT SYSTEMS INVOLVING 4-AMINO-1,8-NAPHTHALIMIDE AND 4-AMINOPHTHALIMIDE FLUOROPHORES

The Photophysical behaviour and transition metal ion sensing ability of some *fluorophore-spacer-receptor* systems involving 4-amino-1,8-naphthalimide (ANP) and 4-aminophthalimide (AP) as the fluorophore component have been described in this chapter. The first section of this chapter deals with the ANP derivatives and the second section is devoted to the derivatives of AP. The structural formulae of the various *fluorophore-spacer-receptor* systems studied along with those of the constituting fluorophores are shown in Chart 3.1. Even though some Photophysical studies have been made on ANPDEA,[1] no report is available on the transition metal ion sensing ability of this system or others shown in Chart 3.1.

ANP, AP and their derivatives are known to be highly fluorescent, particularly in aprotic media.[1-6] These systems fluoresce from an intramolecular charge transfer (ICT) state that is more polar than the ground state. The fluorescence is characterised by a broad band that exhibits solvatochromism typical of a charge transfer transition. Further, since these fluorophores interact strongly with the hydrogen bond donating solvents in the excited state, the fluorescent state is stabilised significantly in protic solvents leading to a large Stokes shift of the fluorescence maximum. The hydrogen bonding interaction with the solvents leads to a decrease in the fluorescence quantum yield of the systems. A number of studies have been made where AP and its derivatives have been employed as fluorescence probe for the organised media such as micelles and cyclodextrins.[4-5] The solvation of the excited state of AP has also been investigated extensively in various media.[3,6] In the case of dimethylamino derivative of AP, a low-lying nonfluorescent

twisted intramolecular charge transfer (TICT) state has been identified recently.[2] This TICT state acts as an efficient nonradiative deactivation pathway in polar media.
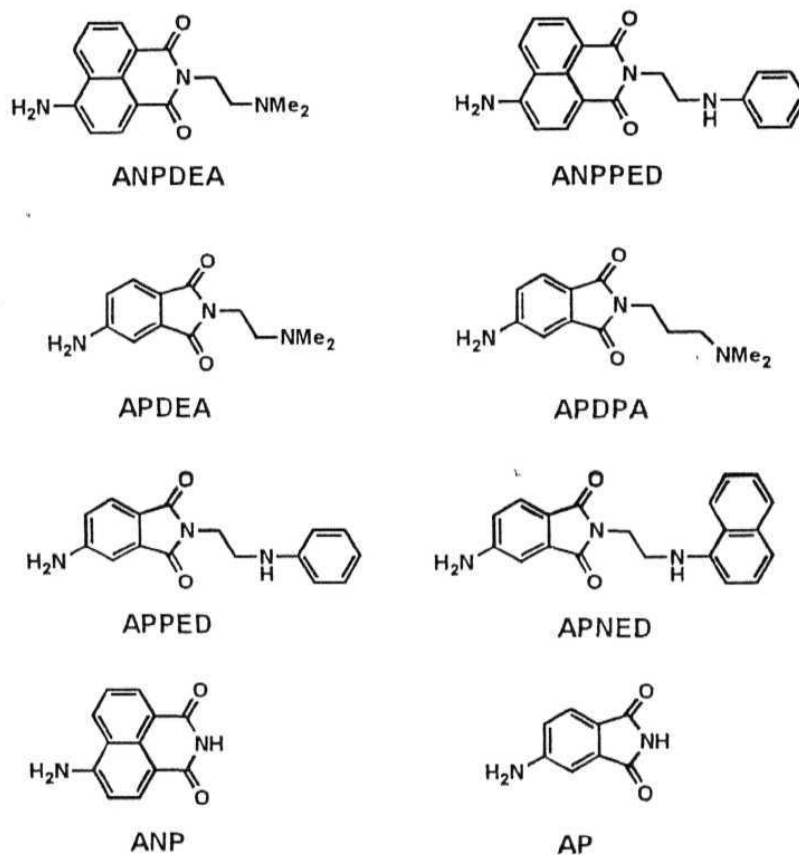
Chart 3.1

3.1.   ANP DERIVATIVES

3. J. J. Spectral features

The absorption and fluorescence spectra of ANPDEA in acetonitrile are depicted in fig 3.1. That the absorption band shown in this figure arises from an intramolecular charge transfer (ICT) transition within the fluorophore is evident from its broad, structureless feature and also from a comparison with the spectral behaviour of ANP.

Fluorescence intensity (arb. units)
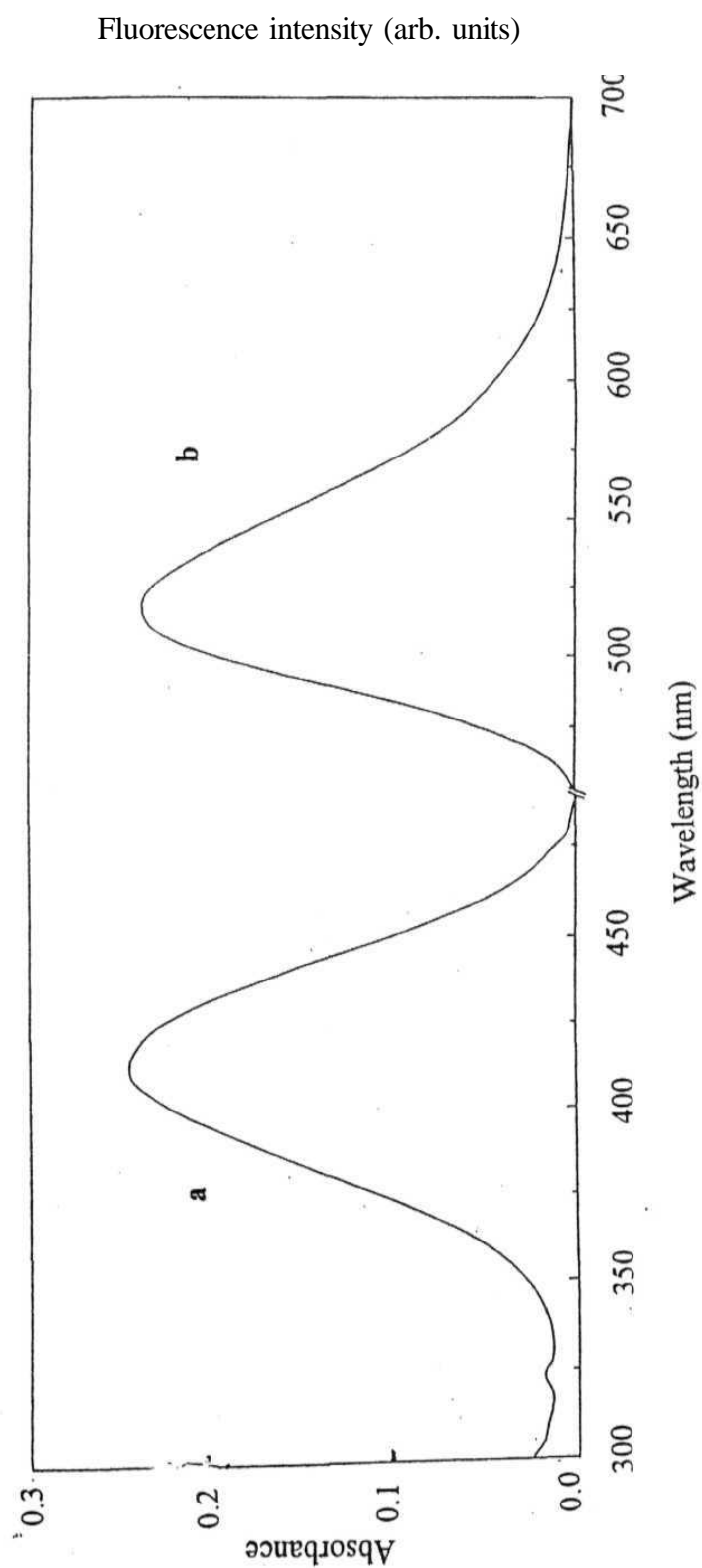
Fig. 3.1. Absorption (a) and fluorescence (b) spectra of ANPDEA in acetonitrile. The fluorescence spectrum was obtained by exciting the solution at 425 nm.

The disappearance of this band in acidic medium (where the lone pair of the amino nitrogen gets protonated) further confirms the ICT nature of this band. The wavelengths corresponding to the absorption band maxima of the multi-component systems and the constituent fluorophore are shown in Table 3.1. The fluorescence spectra of ANP and its derivatives consist of a broad band whose location is highly dependent on the polarity of the medium. Enhanced solvatochromism of the fluorescence band compared to the ICT absorption band (Table 3.1) suggests that the excited state of the fluorophore is more polar than the ground state.

Table 3.1. Spectral properties of ANP, ANPDEA and ANPPED in THF and AN.

Compound	THF		AN	
	λ_{max} (abs)[a] in nm	λ_{max} (flu)[b] in nm	λ_{max} (abs)[a] in nm	λ_{max} (flu)[b] in nm
ANP	412	498	420	510
ANPDEA	415	510	422	520
ANPPED	417	512	421	520

[a]*The concentration of the solutions for the spectral measurements was between 2-5 $\times 10^{-5} M$;* [b]*the excitation wavelength was 425 nm.*

3.1.2. *Feasibility of PET in ANPDEA and ANPPED*

Electron deficiency in the fluorophore is essential for an efficient PET in the *fluorophore-spacer-receptor* system and also, to minimise likely redox interaction between the fluorophore and the quenching transition metal ions. The redox behaviour of ANP has been studied to find out how electron rich the fluorophore is and whether PET in the *fluorophore-spacer-receptor* systems is allowed thermodynamically. The oxidation of ANP was observed at 1.27 V and the reduction at -1.61 V. The free energy changes (AG*) for PET in ANPDEA and ANPPED, calculated using equation 2.13,[7] are

displayed in Table 3.2. The exergonic free energy changes indicate that PET is thermodynamically allowed in these systems.

Table 3.2. Thennodynamic driving force (AG*) for PET in the sensor systems involving ANP and AP.

System	E_{red} (fluor) (V)[a]	$E_{0,0}$ (kcal/mol)[b]	ΔG^* (kcal/mol)[c]
ANPDEA			-6.6
ANPPED	-1.61	55.04	-6.4
APDEA			
APDPA			-12.7
APPED	-1.66	62.2	-12.4
APNED			-12.9

[a] E_{red} *values (vs Ag/AgCl electrode) of the fluorophore components (ANP and AP) were measured following procedures as described in sec. 2.7, the cyclic voltammetric traces for the reduction of ANP and AP were found to be irreversible;* [b] $E_{0,0}$ *was estimated from the mean position of the absorption and fluorscence maxima of the fluorophore components in acetonitrile.* [c]ΔG^* *calculations were made using equn.2.13, E_{ox} values of the receptor moieties (0.49, 0.50 and 0.48 V for triethylamine, N-methylaniline and N,N-dimethyl-1-aminonaphthalene respectively) were obtained from ref. 8. The oxidation potential of triethylamine was corrected for Ag/AgCl electrode by subtracting 0.27V from the measured potential against SCE electrode. The free energy change values are applicable in polar solvents such as acetonitrile.*

3.1.3. *Fluorescence quantum yield and decay behaviour*

The measured fluorescence quantum yields (ϕ_f) of ANP, ANPDEA and ANPPED in AN and THF are shown in Table 3.3. Eventhough the ϕ_f values of ANP in THF and AN are close to unity, those for ANPDEA and ANPPED are rather low. Clearly, this is a reflection of PET between the receptor and the fluorophore moieties in these multi-component systems. Further, the quantum yield values indicate that PET is more efficient in ANPPED. A study of the fluorescence decay behaviour of these systems confirms PET

in ANPDEA and ANPPED. While the fluorescence decay of ANP is single exponential
with a lifetime of 11.0 ns in both THF and AN, the fluorescence decay curves of
ANPDEA and ANPPED could be best fitted to a biexponential decay function. The
fluorescence decay parameters of the systems are collected in Table 3.3 and a few
representative decay curves are illustrated in fig 3.2. There can be hardly any doubt that
the short-lived component arises from the PET-quenched fluorophore. The long-lived
species perhaps originates from one or more conformers of the multi-component systems
where PET is not favourable either due to an unfavourable distance between the
fluorophore and the receptor or because of an unfavourable orientation of the two. The
fluorescence decay parameters also suggest that of the two systems PET is more efficient
in ANPPED.

Table 3.3. *Fluorescence quantum yield* $(\phi_f)^a$ *and lifetime* $(\tau_f)^b$ *of ANP, ANPDEA and ANPPED in THF and AN.*

Solvent	Property	ANP	ANPDEA	ANPPED
THF	ϕ_f	1.0	0.67	2.9×10^{-2}
	F^c	1.0	1.5	34.5
	τ_1/ns	11.0	0.8 (7.0%)	0.8 (99.99%)
	τ_2/ns	---	6.9 (93%)	7.4 (0.01%)
AN	ϕ_f	0.97	0.74	3.0×10^{-2}
	F^c	1.0	1.3	32.0
	τ_1/ns	11	2.2 (2.0%)	0.4 (99.99%)
	τ_2/ns	---	7.4 (98%)	7.5 (0.01%)

[a]Coumarin 153 was used as the reference compound (ϕ_f of 0.89 in acetonitrile),[9] [b]the quantities shown within the brackets represent the relative weightages of the components, [c]F represents the ratio of the fluorescence quantum yield of the constituent fluorophore to that of the multi-component system.
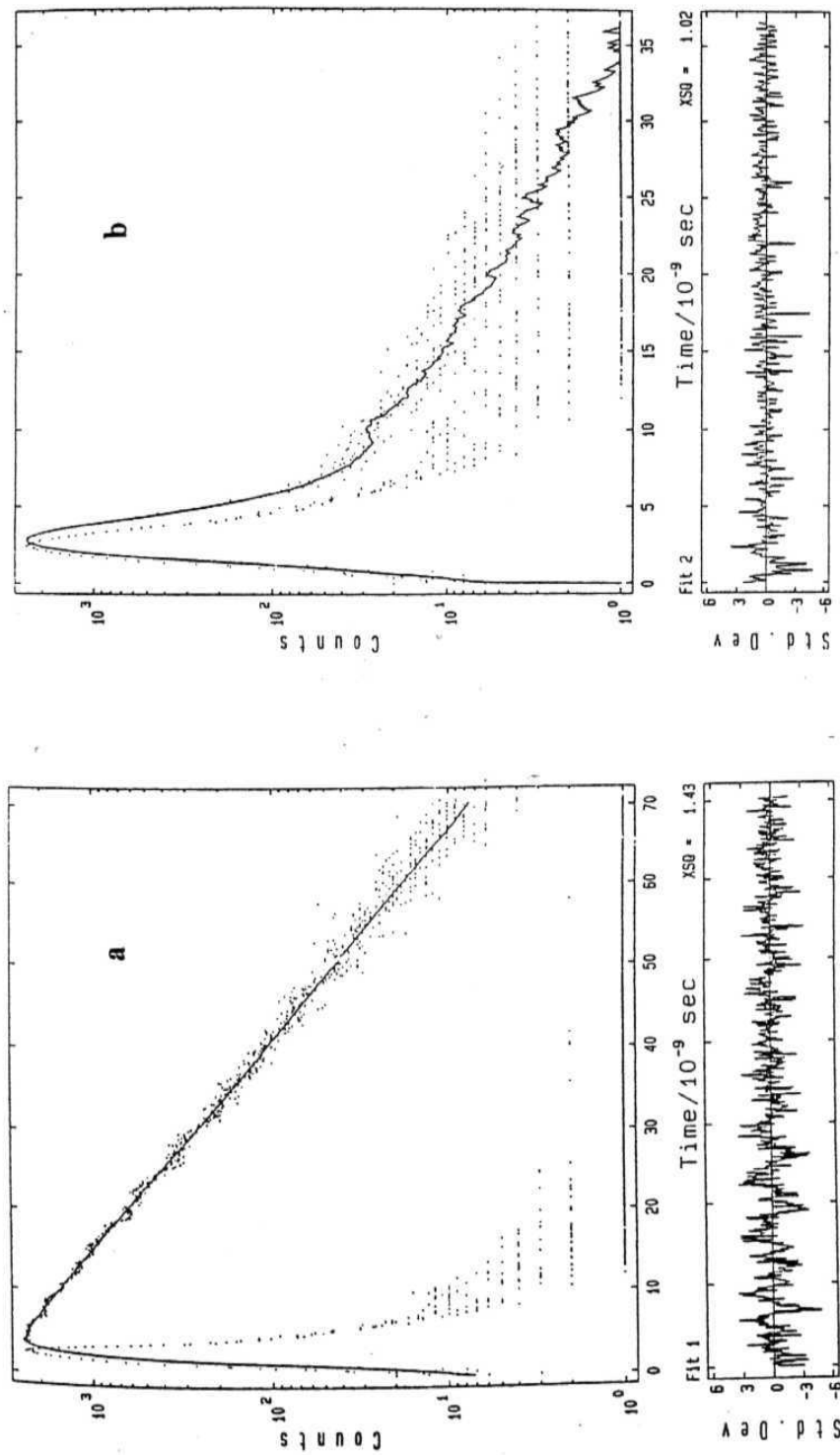
Fig 3.2. Fluorescence decay curves of (a) ANP and (b) ANPPED in AN. The excitation wavelength was 425 nm. The solid lines indicate the best fit to the measured decay curves. The decay curve shown in the figure for ANPPED was fitted to a biexponential decay function while that of ANP was analysed using a single exponential decay function. The exciting lamp profiles are also shown in the figure. The fluorescence was monitored at 520 nm.

3.1.4. *Effect of metal ions*

Quenching of fluorescence by the transition metal ions is a common phenomenon.[10] However, it can be seen from fig 3.3 that the addition of the transition metal salts to solutions of ANPDEA and ANPPED leads to an increase in the fluorescence intensity of the systems. The observed fluorescence enhancement (FE) values of the two systems are collected in Table 3.4. Higher FE values observed for ANPPED are in agreement with the fact that PET is more efficient in this system (vide Table 3.3). Apart from FE, the addition of the metal salt leads to a Stokes shift of the fluorescence maxima of the systems. Since the location of the emission maximum of ANP is sensitive to the polarity of the medium, the Stokes shift can in principle be due to the salt-induced increase in the polarity of the medium surrounding to the fluorophore. However, since the addition of the metal salts to ANP does not lead to any shift of its fluorescence maximum, one can rule out the possibility that the spectral shift is due to salt induced change in the microscopic polarity around the fluorophore moiety. Therefore, it is quite likely that the red shift of the spectral maxima of the multi-component systems is due to the involvement of the carbonyl oxygen atom(s), in addition to the amino nitrogen of the receptor moiety, in coordination with the metal ions (which enhances the charge separation in the fluorophore).

Typical changes in the fluorescence decay behaviour of the systems on addition of the metal ions have been depicted in fig 3.4. The fluorescence decay profile changes from the biexponential to a single exponential one with gradual disappearence of the short-lived component. It is interesting to note that at higher concentration of the metal ions, corresponding to almost complete recovery of the fluorescence, the decay curve is clearly single exponential with a lifetime not very different from that of the fluorophore. With further increase in the concentration of the metal salts, one can, however, observe quenching of the fluorescence.
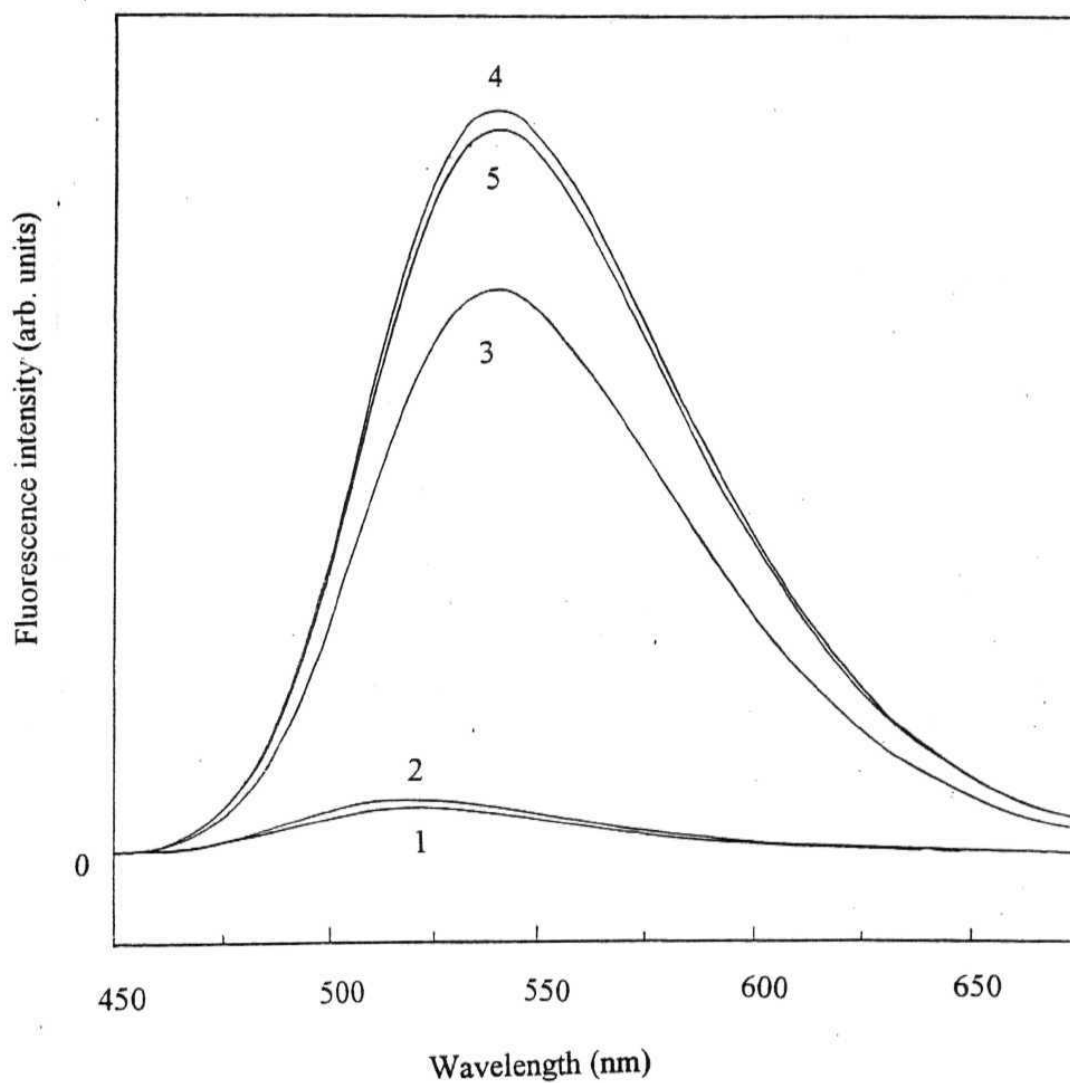
Fig 3.3. Fluorescence spectra of ANPPED (10^5 M) in AN for different concentrations of Mn(H$_2$O)$_6$(ClO$_4$)$_2$; the concentrations of Mn^{+2} corresponding to the spectra labelled 1 to 5 are 0, 2.0 x 10^{-4}, 4.0 x 10^{-4}, 6.0 x 10^{-4}, and 8.0 x 10^{-4} M respectively. λ_{ex} was 425 nm.

Table 3.4. Fluorescence enhancement (FE) values of ANPDEA and ANPPED in the presence of the transition metal ions and protons.

Metal ion	ANPDEA				ANPPED			
	THF		AN		THF		AN	
	$[Salt]/M^a$	FE^b	$[Salt]/M^a$	FE^b	$[Salt]/M^a$	FE^b	$[Salt]/M^a$	FE^b
Zn^{+2}	2.5×10^{-5}	1.3	2.2×10^{-4}	1.3	2.9×10^{-3}	1.1	5.7×10^{-3}	2.0
Cu^{+2}	9.0×10^{-4}	1.3	2.6×10^{-5}	1.2	1.5×10^{-3}	1.1	8.8×10^{-4}	7.0
Ni^{+2}	2.8×10^{-4}	1.2	1.7×10^{-5}	1.1	4.8×10^{-4}	23.0	1.0×10^{-3}	5.0
Co^{+2}	1.3×10^{-4}	1.4	1.1×10^{-5}	1.1	7.9×10^{-3}	6.0	3.1×10^{-4}	15.0
Fe^{+3}	4.2×10^{-5}	1.3	2.6×10^{-5}	1.1	1.7×10^{-4}	5.0	2.2×10^{-4}	21.0
Mn^{+2}	7.8×10^{-5}	1.3	8.5×10^{-5}	1.5	3.5×10^{-3}	17.0	6.0×10^{-4}	14.0
Cr^{+3}	2.9×10^{-4}	1.4	4.3×10^{-5}	1.1	2.9×10^{-3}	4.0	3.0×10^{-3}	8.0
H^+	6.3×10^{-4}	1.6	6.3×10^{-4}	1.4	1.0×10^{-2}	6.0	2.5×10^{-3}	18.0

[a]The concentration of the metal salt/proton for which maximum fluorescence enhancement has been observed. A further increase in the concentration of the metal ions led to fluorescence quenching. [b]FE values are calculated from the areas under the fluorescence curves of two solutions; one corresponding to the concentration of the metal ion/proton indicated in the second column of the Table and the other with no metal ion/proton (using eq.n. 2.14).

Fig 3.4. The fluorescence decay curve of ANPPED (10^5 M) in AN in the presence of 7.0 x 10^{-4} M of $Fe(H_2O)_6(ClO_4)_3$. Shown also in the figure are the exciting lamp profile and the single exponential fit ($\tau = 6.5$ ns) to the fluorescence decay curve. The exciting wavelength was 425 nm and the fluorescence was monitored at 525 nm.

3.2.   AP DERIVATIVES

Low FE values of the ANP derivatives, ANPDEA in particular, in the presence of the metal ions suggest that intramolecular PET in these multi-component systems is not very efficient. Since the most convenient approach to enhance PET and to improve the fluorescence signalling ability of the multi-component system is to make the fluorophore component electronically deficient, we have synthesised *fluorophore-spacer-receptor* systems employing relatively electron deficient AP as the fluorophore component and studied their signalling ability.

That AP is relatively electron deficient (hence, a better fluorophore component compared to ANP) is evident from the fact that oxidation of AP could be observed at 15 V while that for ANP was observed at a lower potential (1.27 V) under the same measurement condition (section 2.7). The reduction of AP could be observed at -1.66 V (Table 3.2). The free energy changes associated with PET in the multi-component systems involving AP, shown in Table 3.2. are clearly more favourable compared to systems involving ANP.

3.2.1. Spectral features

The absorption spectral features of APDEA, APDPA and APPED are quite similar to those of AP except that the longest wavelength absorption band (ICT transition within the fluorophore) of the multi-component systems appears at a higher wavelength. Interestingly, the absorption spectrum of APNED looks quite different (fig 3.5) from the others presumably due to the contribution to absorption in the 300 - 350 nm range by the naphthylamino moiety.

The fluorescence spectra of APDEA, APDPA and APPED are quite similar to that of AP except for the fact that the fluorescence maxima of the multi-component systems appear at a longer wavelength in any given solvent. The spectral data of the systems are shown in Table 3.5. Interestingly, the fluorescence spectrum of APNED
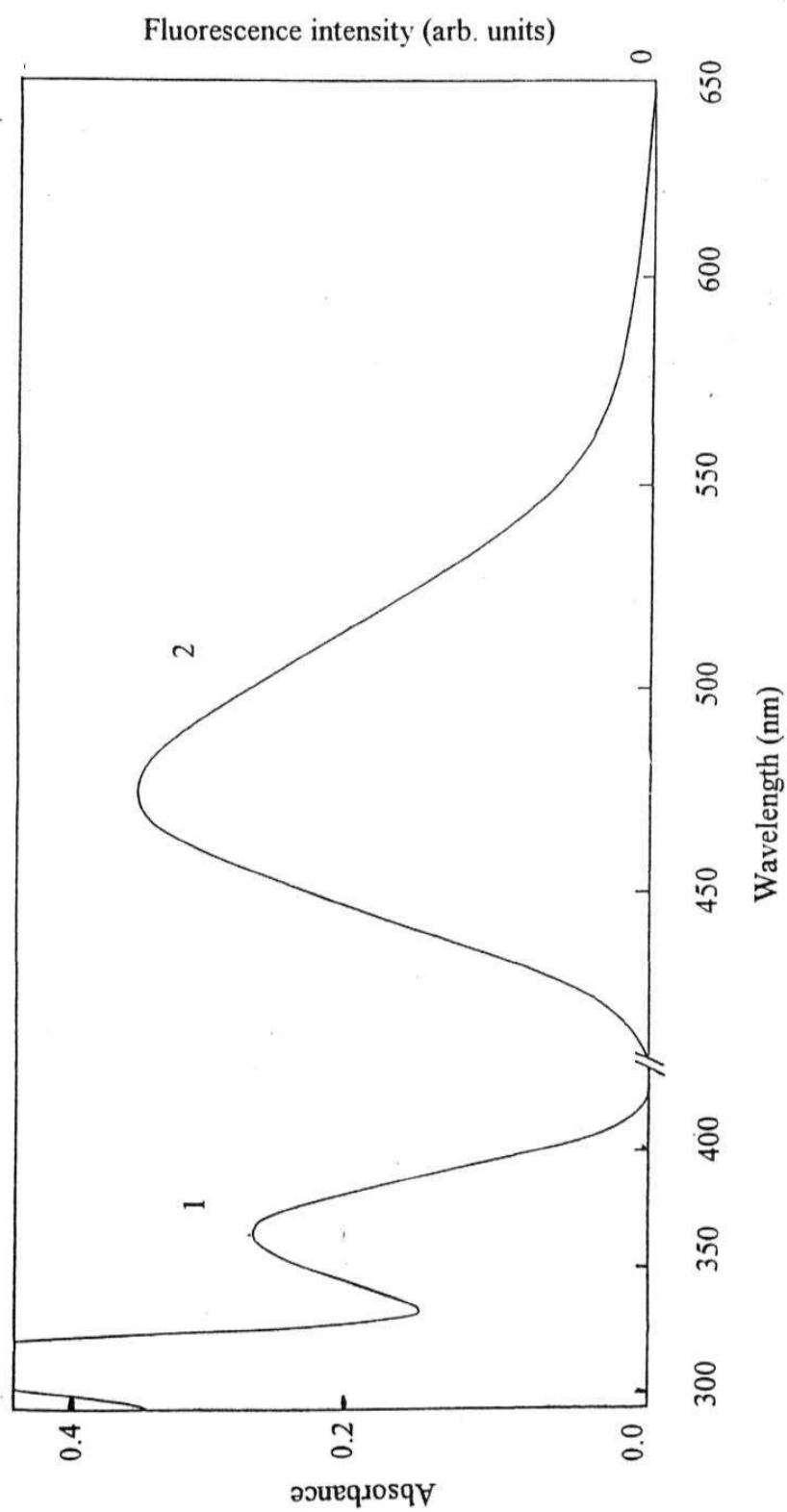
Fig 3.5(a). Absorption(1) and fluorescence(2) spectra of APPED in AN. The solution was excited at 380 nm for recording the fluorescence spectrum.
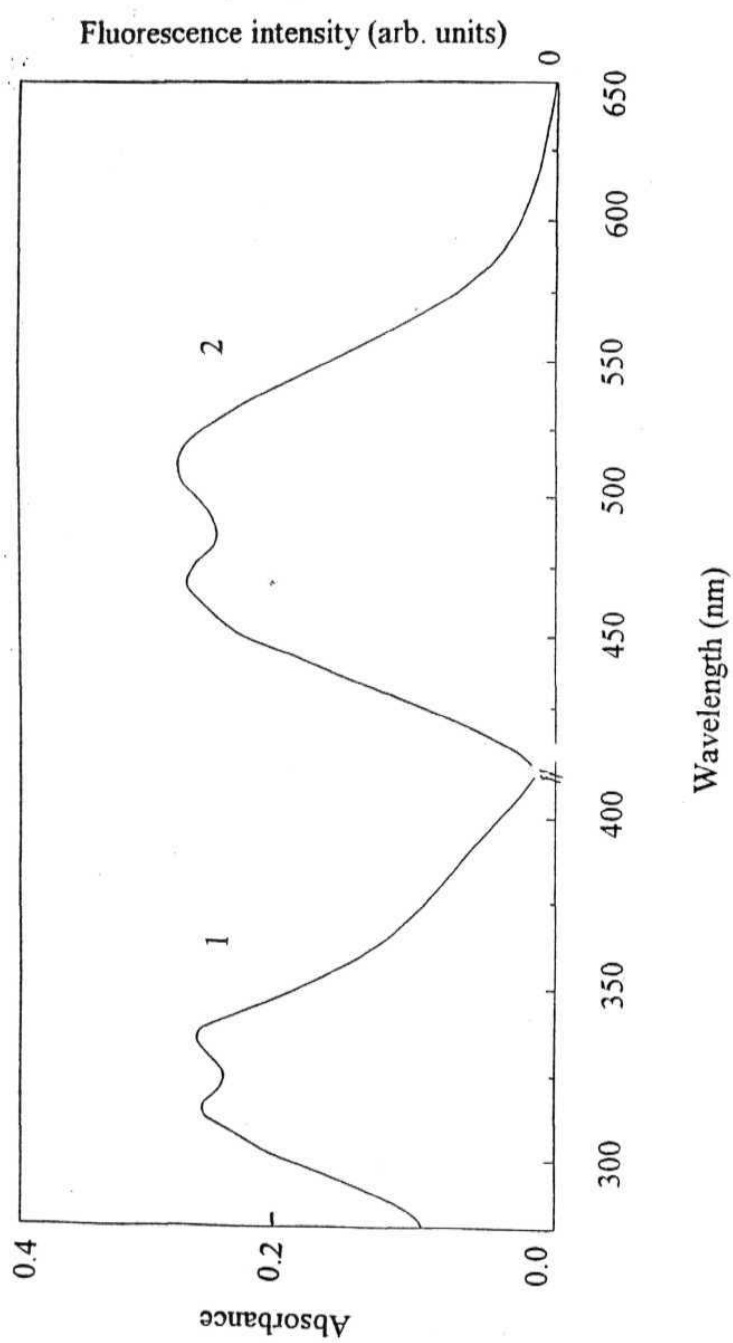
Fig 3.5(b). Absorption(1) and fluorescence(2) spectra of APNED in AN. The solution was excited at 380 nm for recording the fluorescence spectrum.

consists of two peaks appearing at around 469 nm and 513 nm in acetonitrile (fig. 3.5). Based on the solvatochromism of the longer wavelength unusual band and its relatively lower intensity in polar media such as AN, we attribute this band to an emission from the excited state of an intramolecular charge transfer complex formed between the fluorophore and naphthylamine receptor moiety. That the complex is formed in the ground state, though not very evident from the absorption spectrum, is confirmed by the existence of an additional peak in the longer wavelength side of the fluorescence excitation spectrum (when monitored at around 525 nm). The fluorescence excitation spectra of APNED in THF and AN are shown in fig. 3.6   illustarte this point.

Table 3.5. Spectral properties of AP and its derivatives in THF and AN.

System	THF		AN	
	λ_{max} (abs) (nm)	λ_{max} (flu)[a] (nm)	λ_{max} (abs) (nm)	λ_{max} (flu)[a] (nm)
AP[b]	358	455	359	460
APDEA	361	461	365	466
APDPA	365	465	365	478
APPED	366	463	366	468
APNED	315 335 375 (s)	465 500 ---	313 337 378 (s)	469 513 ---

[a]The excitation wavelength was 380 nm; [b]the data for AP have been collected from ref. 2

3.2.2.   *Fluorescence quantum yields and lifetimes*

Eventhough AP is highly fluorescent in aprotic solvents (ϕ_f values are 0.70 and 0.63 in THF and AN respectively),[2] the fluorescence yield of APDEA, APDPA, APPED and APNED are extremely low (Table 3.6). This is obviously due to PET in these multi-component systems. The fact that PET is much more efficient in these systems (compared
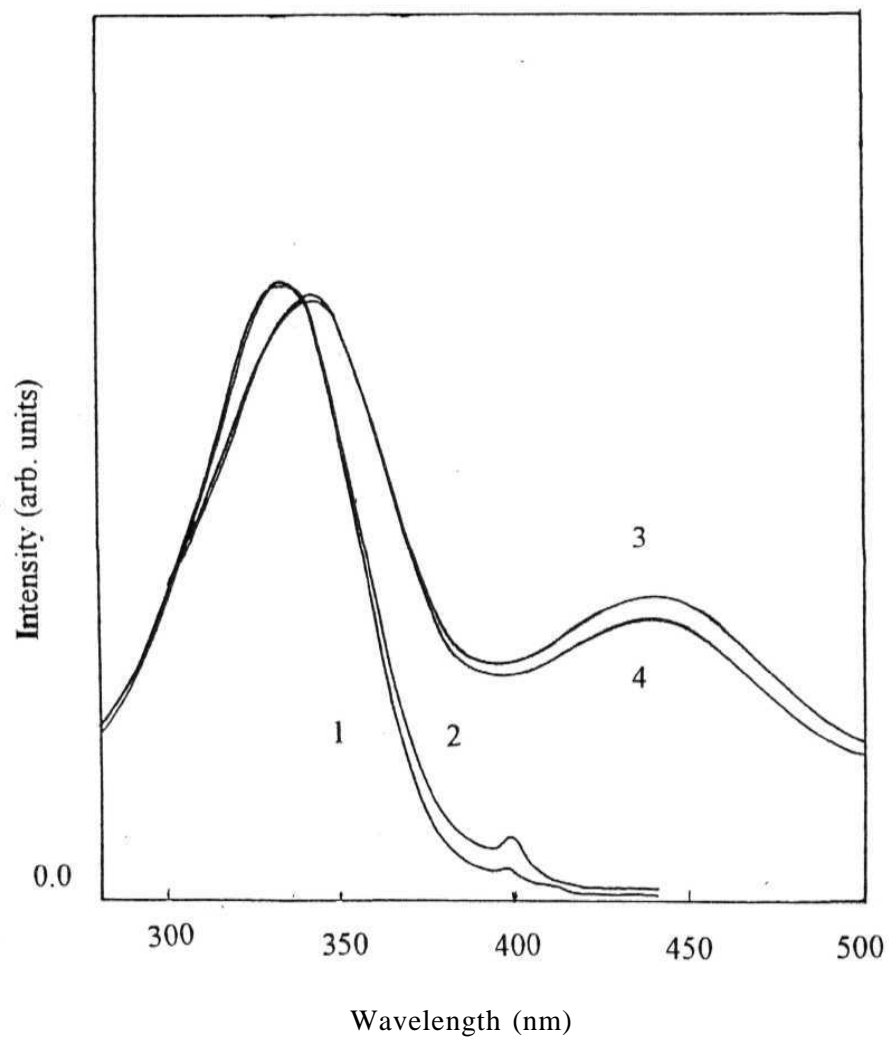
Fig.3.6. Fluorescence excitation spectra of APNED in THF(1, 3) and AN (2, 4). While 1 and 2 were obtained by monitoring fluorescence at 475 nm and 3 and 4 were recorded by monitoring at 525 nm.

Table 3.6. Fluorescence quantum yield[a]   and expected FE values (F) for the multi-component systems involving AP.

System	THF		AN	
	ϕ_f	F[b]		F[b]
AP	0.70	1	0.63	1
APDEA	2.3×10^{-2}	30	1.3×10^{-2}	50
APDPA	6.3×10^{-2}	11	2.3×10^{-2}	27
APPED	5.8×10^{-4}	2000	2.6×10^{-4}	2450
APNED	8.9×10^{-4}	785	5.1×10^{-4}	1230

[a]AP was used as the reference compound[2]; [b]F represents the ratio of the fluorescence quantum yield of the constituent fluorophore to that of the multi-component system.

to the ANP derivatives) is clearly evident from a comparison of the F values shown in Table 3.3 and 3.6. It is also clear from a comparison of the fluorescence yield of APDEA and APDPA that PET is more efficient for systems containing two mcthylene spacer units.

The fluorescence decay behaviour of the AP derivatives is illustrated in fig, 3.7 and the decay parameters are shown in Table 3.7. The decay behaviour of these systems is found to be very similar to that of the ANP derivatives except that the amplitude of the short-lived component is relatively higher and the lifetime of this component is relatively shorter in the case of AP derivatives. This observation once again confirms that PET is more favourable for systems involving the electron deficient fluorophore, AP.
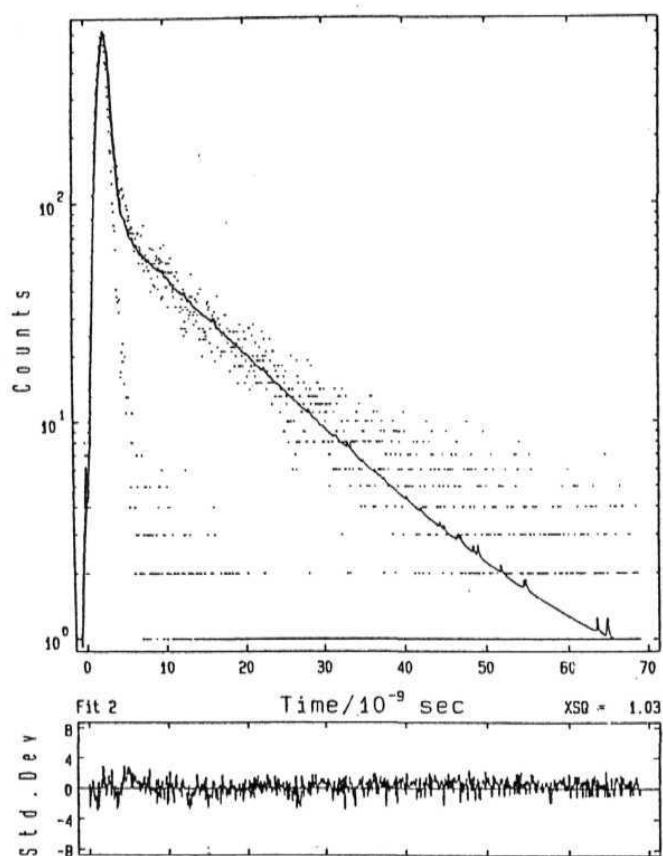
Fig 3.7. Fluorescence decay curve of APPED in AN. The Solid line indicates the best biexponential fit to the measured decay curve. Shown also in the figure is the exciting lamp profile. The excitation wavelength was 380 nm and the fluorescence was monitored at 475 nm.

Table 3.7. Fluorescence decay parameters of AP and its multi-component systems

System	THF		AN	
	τ_1 / ns	τ_2 / ns	τ_1 / ns	τ_2 / ns
AP[a]	14.0	---	12.4	---
APDEA[b]	0.7(48%)	13.0(52%)	0.5 (98%)	15.5(2%)
APDPA	4.8(5%)	13.8(95%)	0.8(64%)	11.2(36%)
APPED	0.9(95%)	12.2(5%)	0.15(99%)	12.1(1%)
APNED	2.2(81%)	12.4(19%)	0.5(91%)	10.2(9%)

[a] From ref. 2. All the AP derivatives were excited at 380 nm and the fluorescence monitored at 475 nm. The quantities shown within the brackets represent the relative weightages of the components.

3.2.3.   Effect of metal ions

3.2.3.1. Absorption spectra

The addition of the metal ions leads to changes in the absorption spectra of the multi-component systems. The effect of Ni^{+2} on APDEA is illustrated in fig. 3.8(a). Even though the spectral changes for APDEA, APPDA and APPED are quite similar in the presence of a given metal ion, those for APNED are found to be quite different. as can be seen from fig. 3.8(b). The fact that the absorption peaks at around 315 and 335 nm disappear in the presence of protons too, suggests that the spectral changes are most likely due to the protonation of the amino moiety connected to the naphthyl ring (in the case of protons) and coordination with the metal ions (in the case of the metal ions). In both cases, the lone pair of electrons get tied up. The above conjecture is supported by the observation that the addition of protons to a solution of 1-naphthylamine results in similar disappearance of the concerned band.
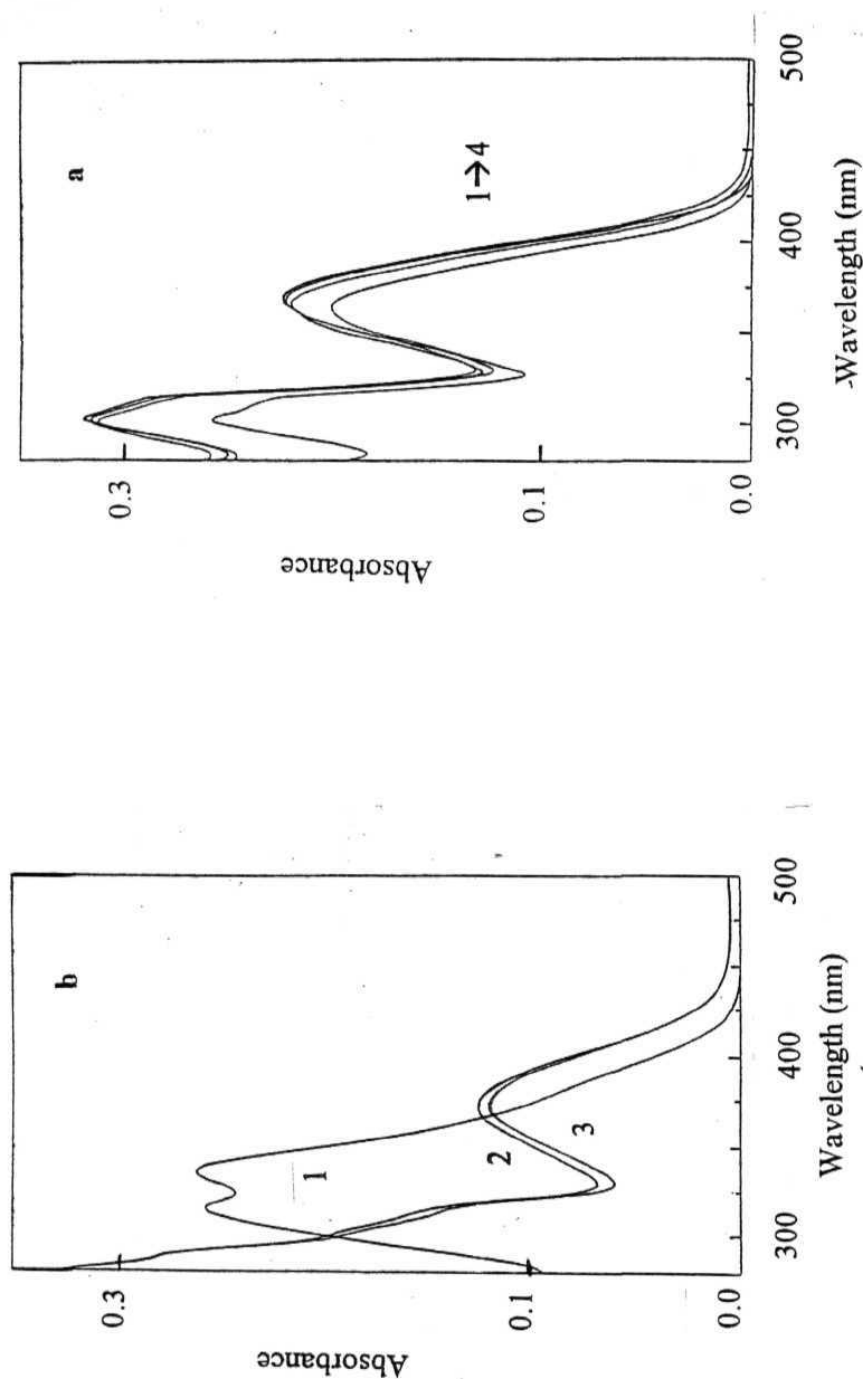
Fig 3.8. (a) Absorption spectra of APDEA in AN for different concentrations of Ni(H₂O)₆(ClO₄)₂. The concentrations of Ni⁺² for the spectra labelled 1 to 4 are 0, 1.8 x 10⁻⁴, 1.1 x 10⁻³ and 2.0 x 10⁻³ M respectively; (b) absorption spectra of APNED in AN in the presence of different amounts of Zn(H₂O)₆(ClO₄)₂.⁻The concentrations of Zn⁺² for the spectra labelled 1 to 3 are 0, 1.2 x 10⁻⁴ and 3.5 x 10⁻⁴ M respectively.

3.2.3.2. Changes in the fluorescence behaviour

Fig. 3.9 illustrates the effect of the metal ion on the fluorescence spectra of APDEA. The addition of the metal ions leads to FE and a red shift of the spectral maximum. The fluorescence spectral shift is found to be more prominent than that observed for the absorption spectra. This observation could be rationalised as follows. It is known that electronic excitation of AP increases the electron density on the carbonyl oxygen atoms.[2] Therefore, it is quite likely for these carbonyl oxygens of the multi-component systems to act as a coordinating site (in addition to the receptor moiety) in the excited state. The involvement of the carbonyl oxygens in coordination with the metal ions will help further separation of charge in the fluorophore leading to a Stokes shift of the fluorescence spectrum. The red-shift observed here for these systems is in accordance with the general guidelines for the spectral shift (induced by metal ions or protons) formulated by Valeur and co-workers for the electron donor-acceptor systems (vide section 1.3.4 for details).[11] Apart from the spectral shift, the addition of the metal ion is associated with a gradual increase in the fluorescence intensity until it reaches a limiting value. The FE values for different systems in THF and AN are collected in Table 3.8 and 3.9. Maximum FE could be observed with Zn^{+2} and Mn^{+2}. It is interesting to note that even efficient quenchers such as Fe^{+3}, Cr^{+3} and Co^{+2} show excellent enhancement.

Although complete recovery of fluorescence has been observed in the case of APDEA and APDPA in presence of nonquenching metal ions such as Zn^{2+}, both APPED and APNED display FE lower than the expected value. This is probably due to the fact that PET between the fluorophore and the receptor moieties could not be suppressed completely in these systems. Strong fluorophore-receptor interaction and weak binding of the metal ions with the receptor are perhaps responsible for this observation (vide later). It has been stated earlier that the fluorescence spectrum of APNED consists of two components. With increase in the concentration of the metal ions, the long wavelength
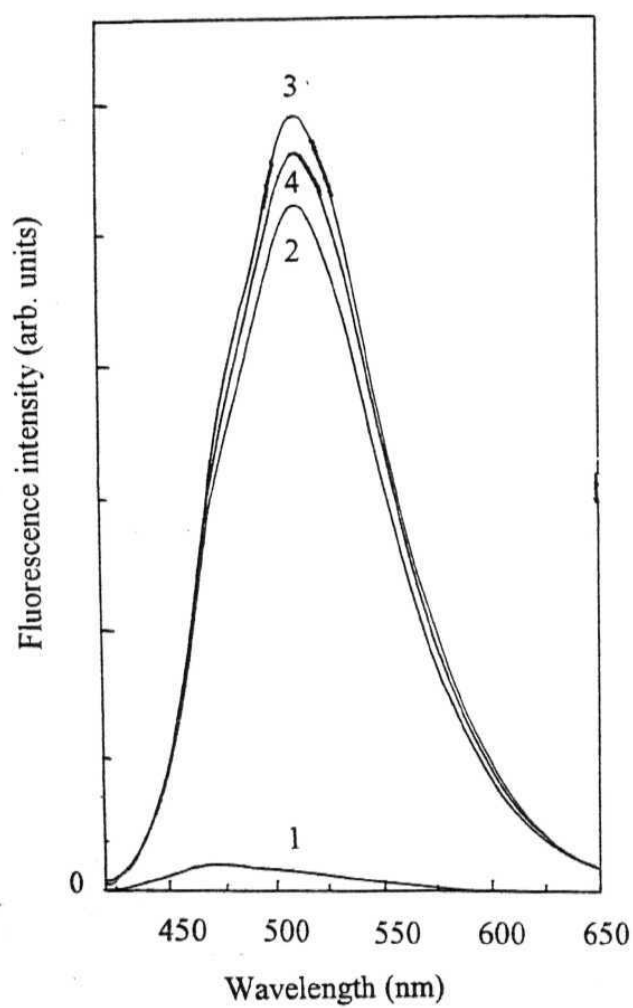
Fig 3.9. Fluorescence spectra of APDEA in acetonitrile for different concentrations of Fe(H₂O)₆(ClO₄)₃. The concentrations of Fe^{+3} for the spectra labelled 1 to 4 are 0, 5.3 x 10^5, 1.0 x 10^4 and 1.6 x 10^4 M respectively.

Table 3.8. Fluorescence enhancement (FE) values of APDEA and APDPA in the presence of various transition metal ions and protons.

Metal ion	APDEA				APDPA			
	THF		AN		THF		AN	
	[Salt]/M^a	FE^b	[Salt]/M^a	FE^b	[Salt]/M^a	FE^b	[Salt]/M^a	FE^b
Zn^{+2}	5.0×10^{-4}	18	3.9×10^{-4}	55	6.5×10^{-4}	9.0	6.8×10^{-4}	30
Cu^{+2}	3.7×10^{-3}	19	2.7×10^{-4}	41	2.0×10^{-3}	5.0	4.0×10^{-4}	.27
Ni^{+2}	2.2×10^{-3}	15	3.0×10^{-4}	37	3.0×10^{-3}	6.0	1.8×10^{-2}	22
Co^{+2}	3.1×10^{-3}	12	1.9×10^{-4}	38	1.3×10^{-3}	4.0	9.2×10^{-4}	12
Fe^{+3}	1.0×10^{-4}	33	1.0×10^{-4}	34	8.8×10^{-5}	11	1.0×10^{-4}	27
Mn^{+2}	3.9×10^{-4}	32	1.7×10^{-4}	32	2.6×10^{-4}	11	8.5×10^{-5}	19
Cr^{+3}	8.1×10^{-4}	38	1.2×10^{-4}	39	3.1×10^{-4}	12	1.1×10^{-4}	25
H^+	6.3×10^{-4}	16	3.0×10^{-5}	37	6.3×10^{-4}	9.0	3.0×10^{-4}	30

[a] The concentration of the metal salt/proton for which maximum fluorescence enhancement has been observed. A further increase in the concentration of the metal ions leads to fluorescence quenching. [b] FE values are calculated from the areas under the fluorescence curves of two solutions; one corresponding to the concentration of the metal ion/proton indicated in the second column of the Table and the other with no metal ion/proton (using equn. 2.14).

Table 3.9 Fluorescence enhancement (FE) values of APPED and APNED in the presence of various transition metal ions and protons.

Metal ion	APPED				APNED			
	THF		AN		THF		AN	
	[Salt]/M^a	FE^b	[Salt]/M^a	FE^b	[Salt]/M^a	FE^b	[Salt]/M^a	FE^b
Zn^{+2}	1.4×10^{-4}	85	1.2×10^{-4}	800	1.8×10^{-4}	4.0	3.1×10^{-4}	400
Cu^{+2}	4.1×10^{-4}	1.0	5.8×10^{-4}	230	1.0×10^{-4}	3.0	6.6×10^{-4}	17
Ni^{+2}	2.8×10^{-3}	10	7.7×10^{-4}	500	5.0×10^{-3}	11	3.2×10^{-3}	3.0
Co^{+2}	8.0×10^{-3}	103	6.1×10^{-3}	460	5.9×10^{-3}	115	7.6×10^{-3}	1.0
Mn^{+2}	9.7×10^{-3}	300	4.7×10^{-3}	680	1.1×10^{-2}	45	1.0×10^{-2}	285
Cr^{+3}	1.0×10^{-2}	130	3.8×10^{-3}	210	1.0×10^{-2}	8.0	5.1×10^{-3}	20
H$^+$	2.5×10^{-2}	45	2.5×10^{-3}	600	1.3×10^{-2}	3.0	2.5×10^{-3}	367

^{a}The concentration of the metal salt/proton for which maximum fluorescence enhancement has been observed. A further increase in the concentration of the metal ions leads to fluorescence quenching. ^{b}FE values are calculated from the areas under the fluorescence curves of two solutions; one corresponding to the concentration of the metal ion/proton indicated in the second column of the Table and the other with no metal ion/proton (using eqn. 2.14).

band disappears gradually with increase in the intensity of the short wavelength band (fig 3.10). This is simply an indication of the disappearence of the charge transfer complex (responsible for the second emission band), formed between the fluorophore and the receptor, as a result of coordination of the receptor moiety with the metal ion.

The metal ion induced changes in the fluorescence decay behaviour of APDEA and APDPA have been found to be similar (increase in lifetime and change from a biexponential to a single exponential decay) to those observed for ANPDEA and ANPPED. This is evident from the decay curves shown in fig.3.11. On the other hand, the fluorescence decay of both APPED and APNED could only be fitted to biexponential decay functions even in the presence of metal ions. Metal ion induced disappearance of the short-lived component, as seen in the previous cases, could not be observed with these two systems. This suggests that PET between the fluorophore and the receptor moieties could not be suppressed completely. Strong fluorophore-receptor interaction and weak binding of the metal ions with the receptor are perhaps responsible for this observation. The fluorescence decay behaviour helps in understanding why complete recovery of fluorescence intensity, as observed in the case of APDEA and APDPA, could not be achieved for APPED and APNED.
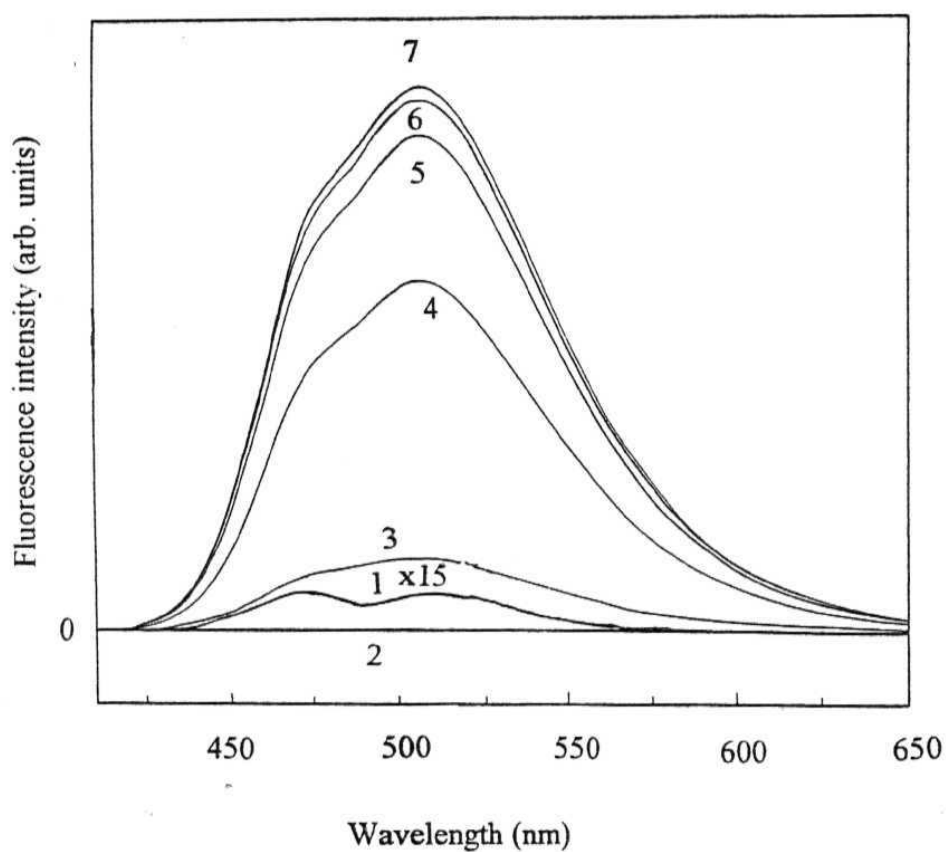
Fig 3.10. Fluorescence spectra of APNED in acetonitrile for different concentrations of Mn(H₂O)₆(ClO₄)₂. The concentrations of Mn⁺² are 1) 0, 2) 1.3 x 10³, 3) 3.6 x 10³, 4) 5.8 x 10³, 5) 8.1 x 10³, 6) 9.2 x 10³ and 7) 1.0 x 10² M.
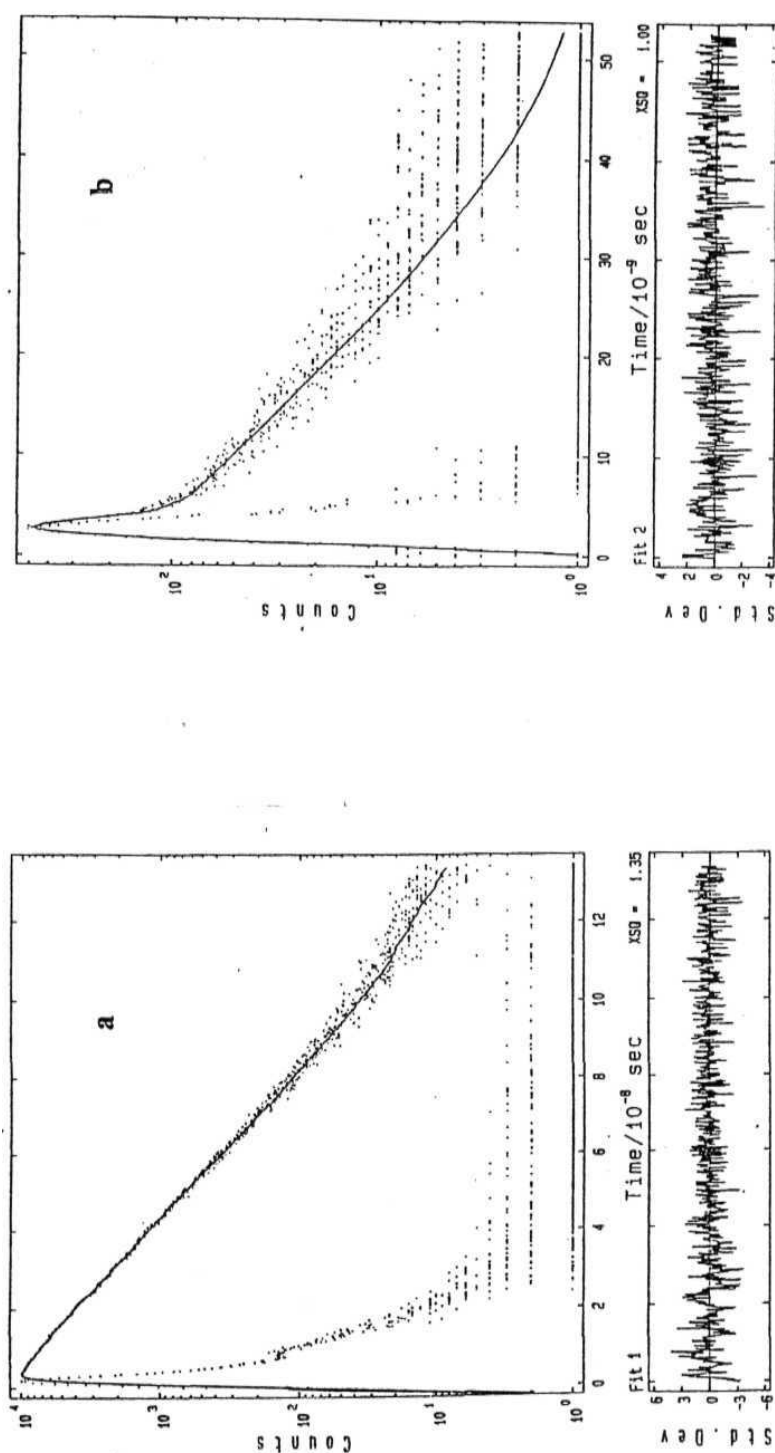
Fig 3.11. Fluorescence decay curves of APDEA and APPED in acetonitrile; (a) APDEA (10^{-5} M) in acetonitrile in the presence of 7.0×10^{-4} M of $Fe(H_2O)_6(ClO_4)_3$, and (b) APPED (10^{-5} M) in the presence of 1.5×10^{-3} M of $Ni(H_2O)_6(ClO_4)_2$. Shown also in the figure is the exciting lamp profile. While the decay profile for APDEA is fitted to a single exponential decay function ($\tau = 16.8$ ns), that for APPED is fitted to a biexponential decay function ($\tau_1 = 0.2$ (40%) and $\tau_2 = 12.0$ ns (60%)). The exciting wavelength was 380 nm and the fluorescence was monitored at 475 nm.

The multi-component systems, APDEA, APDPA and ANPDEA exhibit FE in the presence of protons as well. Since most of the transition metal salts are hydrated, they may contain proton as impurity. Therefore, one may argue that FE of these systems could be due to the contaminated protons rather than the metal ions. But such a possibility has been ruled out by the following observations. First, a freshly recrystallised transition metal salt when used in the experiment, the observed FE values were not very different from those observed with the nonrecrystallised sample. Second, the FE value observed with the hydrated salt of a metal ion (where protons are likely to be present as an impurity) is very close to that observed with the anhydrous salt of the same metal ion (which should be free from any impurities). Finally, as can be seen from Table 3.9, the FE values of APPED and APNED in the presence of the protons are lower than the FE values observed with some of the metal ions. Moreover, the proton concentrations necessary to obtain the observed FE values are much higher than those required for the metal ions.

In summary, the fluorescence properties of some multi-component systems involving ANP and AP as fluorophores have been investigated with a view to examine the potential of these systems as fluorosensors for the quenching transition metal ions. The results clearly show that, when an appropriate electron deficient fluorophore component is chosen, even a very simple *fluorophore-spacer-receptor* system can exhibit excellent fluorescence enhancement in the presence of quenching transition metal ions and as such there is no need to specially design a receptor to avoid the quenching influence of the transition metal ions.

3.4.   References

1. a) A. Pardo, J.M.L. Poyato, E. Martin, J.J. Camacho, D. Reyman, M.F. Brana, J.M. Castellano, *J. Photochem. Photobiol. A Chem.* 1986, *36,* 323; b) A. Pardo, E. Martin,

J.M.L. Poyato, J.J. Camacho, M.F. Brana, J.M. Castellano, *J. Photochem. Photobiol. A Chem.* 1987, *41,* 69; c) A. Pardo, E. Martin, J.M.L. Poyato, J.J. Camacho, J.M. Guerra, R. Weigand, M.F. Brana, J.M. Castellano, *J. Photochem. Photobiol. A Chem.* 1989, *48,* 259; d) A. Pardo, J.M.L. Poyato, E. Martin, J.J. Camacho, D. Reyman, *J. Lumin.* 1990, *46,* 381; e) D. Yuan, R.G. Brown, *J.Chem. Res (M).* 1994, 2337; f) M.S. Alexiou, V. Tychopoulos, S. Ghorbanian, J.H.P. Tyman, R.G. Brown, P.I. Brittain, *J. Chem. Soc. Perkin Trans. 2,* 1990, 837; g) E. Martin, R. Weigand, *Chem. Phys. Lett.* 1998, *288,* 52; h) A.P. de Silva, H.Q.N. Gunaratne, T. Gunnlagsson, P.L.M. Lynch, *New J. Chem.* 1996,20,871.

2. T. Soujanya, R.W. Fessenden, A. Samanta, *J. Phys. Chem.* 1996, *100,* 3507.

3. a) N. Noukakis, P. Suppan, *J. Lumin,* 1991, *47,* 285; b) E. Laitinen, K. Salonen, T.O. Harju, *J. Phys. Chem.* 1996, *104,* 6138; c) T. 0. Harju, A. H. Huzier, C.A.G.O. Varma, *Chem. Phys. Lett.* 1995, *200,* 215; d) S. Das, A. Datta, K. Bhattacharyya, *J. Phys. Chem.* 1997, *101,* 3299; e) H. Langhals, *Anal. Lett.* 1991, *23,* 2243; f) S. Aich, C. Raha, S. Basu, *J.Chem. Soc. Faraday Trans.* 1997, *93,* 2991.

4. a) G. Saroja, T. Soujanya, B. Ramachandram, A. Samanta, *J. Fluoresc.* 1998, *8,* 405; b) G. Saroja, A. Samanta, *Chem. Phys. Lett.* 1995, *246,* 506; c) G. Saroja, A. Samanta, *J. Chem. Soc. Faraday Trans.* 1996, *92,* 2697;

5. a) T. Soujanya, T. S. R. Krishna, A. Samanta, *J. Photochem. Photobiol. A: Chem.* 1992, *66,* 185; b) T. Soujanya, T. S. R. Krishna, A. Samanta, *J. Phys. Chem.* 1992, *96,* 8544.

6. a) W.R. Ware, S.K. Lee, G.J. Brant, P.P. Chow, *J. Chem. Phys.* 1971, *54,* 4729; b) V. Nagarajan, A.M. Brearly, T.J. Kang, P.F. Barbara, J. *Chem. Phys.* 1987, *86,* 3183; c) T. Hagan, D. Pilloud, P. Suppan, *Chem. Phys. Lett.* 1987, *139,* 499; d) N. Ghoneim, P. Suppan, *J. Lumin.* 1989, *44,* 83.

7. a) A. Weller, *Pure Appl. Chem.* **1968,** *16,* 115; b) **D.** Rehm, A. Weller, *Isr. J. Chem.* **1970,** *8,* 259.

8. **H.** Siegerman, in *Techniques of Chemistry,* Ed., NL. Weinberg, Wiley, New York, **1975,** Vol. V, part II, p 803.

9. K. Rechthaler, G. Kohler, *Chem. Phys.* **1994,** *189,* **99.**

10. a) A.W. Varnes, R.B. Dodson, E.L. Wehry, *J. Am. Chem. Soc.* **1972,** *94,* 946; b) J.A. Kemlo, T.M. Shepherd, *Chem. Phys. Lett.* **1977,** *47,* 158.

11. a) B. Valeur, In *Topics in Fluorescence Spectroscopy,* Ed., J.R. Lakowicz, Plenum Press, New York, **1994,** Vol. **IV,** p. 21; b) MM. Martin, P. Plaza, N. Dai Hung, Y.H. Meyer, J. Bourson, B. Valeur, *Chem. Phys. Lett.* **1993,** *202,* 425; c) M.M. Martin, P. Plaza, Y.H. Meyer, L. Begin, J. Bourson, B. Valeur, *J. Fluoresc.* **1994,** *4,* 271; d) M.M. Martin, P. Plaza, Y.H. Meyer, F. Badaoui, J. Bourson, J.P. Lefebvre, B. Valeur, J. *Phys. Chem.* **1996,***100,* 6879.

4-METHOXY-1, 8-NAPHTHALIMIDE DERIVATIVES AS FLUOROSENSORS FOR TRANSITION METAL IONS

The present chapter describes the Photophysical behaviour of *fluorophore-spacer-receptor* systems, OMNPDEA, OMNPDPA, OMNPPED and OMNPNED (Chart 4.1), involving 4-methoxy-1,8-naphthalimide as the fluorophore. This study has been undertaken with a view to explore the potential of these systems as fluorosensors for the transition metal ions.

The results described in the previous chapter clearly point to the need of an electron deficient fluorophore component for the construction of the multi-component sensor system. With an electron deficient fluorophore component, not only the desired PET communication between the fluorophore and the receptor in the sensor system is enhanced but also the undesired redox interaction (that perhaps leads to fluorescence quenching) between the fluorophore and the metal ion is decreased. While electron rich 4-amino-1,8-naphthalimido moiety is a poor fluorophore component, we thought that if the 4-amino group was replaced by some other group with less electron donating ability (such as a methoxy group), the resulting fluorophore would be relatively electron deficient.[1] With this idea we have obtained the *fluorophore-spacer-receptor* systems, OMNPDEA, OMNPDPA, OMNPPED and OMNPNED and studied their fluorescence response in the presence of the transition metal ion. While the fluorescence behaviour of a few systems based on 4- methoxy- 1,8-naphthalimide fluorophore in the presence of the protons has been reported in the literature, no studies have been made so far to find out whether these derivatives could be useful as fluorosensors **for the** detection of the **transition metal ions.**[2]
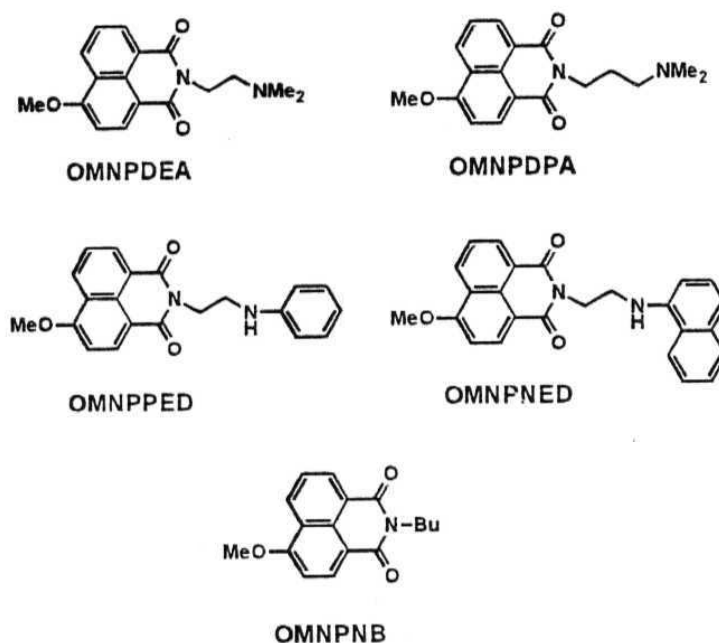
Chart 4.1

4.1. Spectral properties

4.1.1. *Absorption spectra*

The absorption spectra of the fluorophore, OMNPNB and the multi-component systems shown in Chart 4.1 were recorded in THF and AN. Representative absorption spectra of OMNPDEA in THF and AN are depicted in fig. 4.1 and those of OMNPDPA are presented in fig. 4.2. As can be seen from these figures, the absorption spectra are structured showing different vibronic transitions. A broadening of the absorption spectra could be observed with an increase in the polarity of the solvent. This is presumably due to the close proximity of two excited states; a $\pi\pi^*$ state and a ICT (from the methoxy group to the carbonyl oxygen) state. In nonpolar media, the TCTU* state is the lowest excited state. However, since in polar environment the ICT state is lower in energy than the $\pi\pi^*$ state, the spectral broadening in the longer wavelength side is observed.

Interestingly, the absorption spectra of OMNPNED in both polar and nonpolar
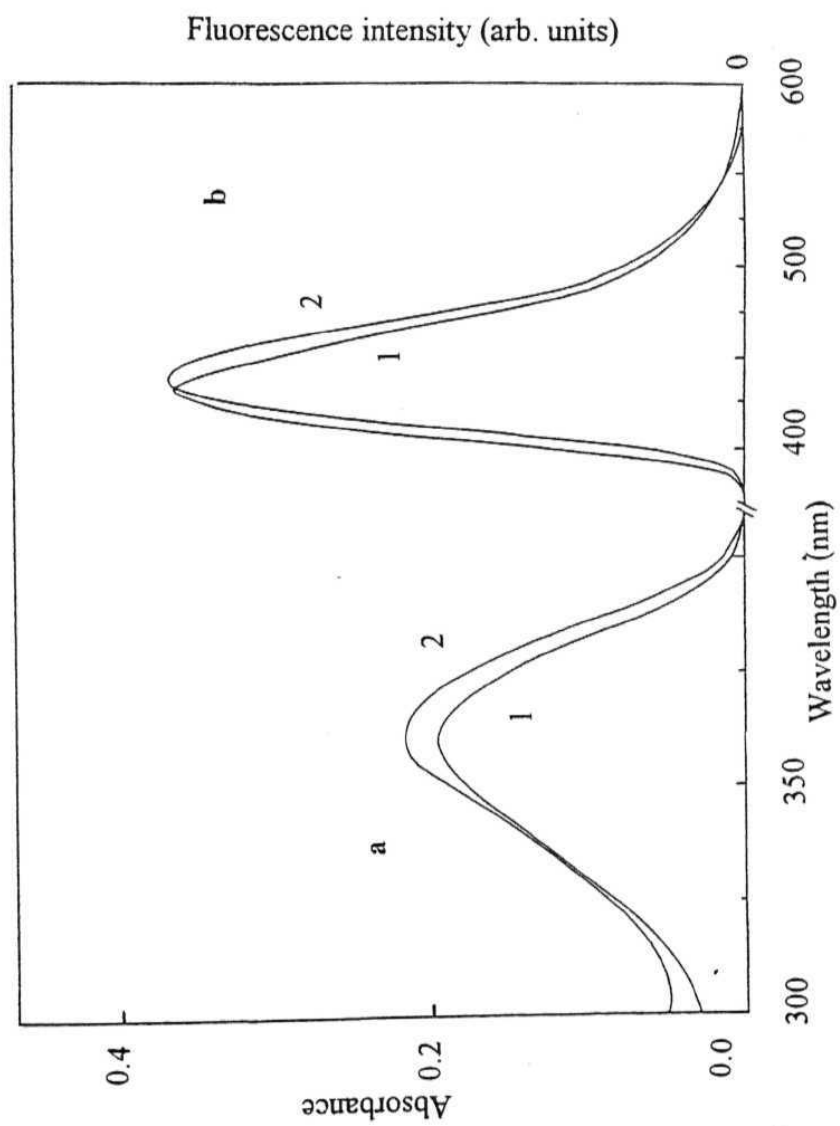
Fig. 4.1. Absorption (a) and fluorescence (b) spectra of OMNPDEA in 1) THF and 2) AN. λ_{ex} for obtaining the fluorescence spectra was 350 nm.
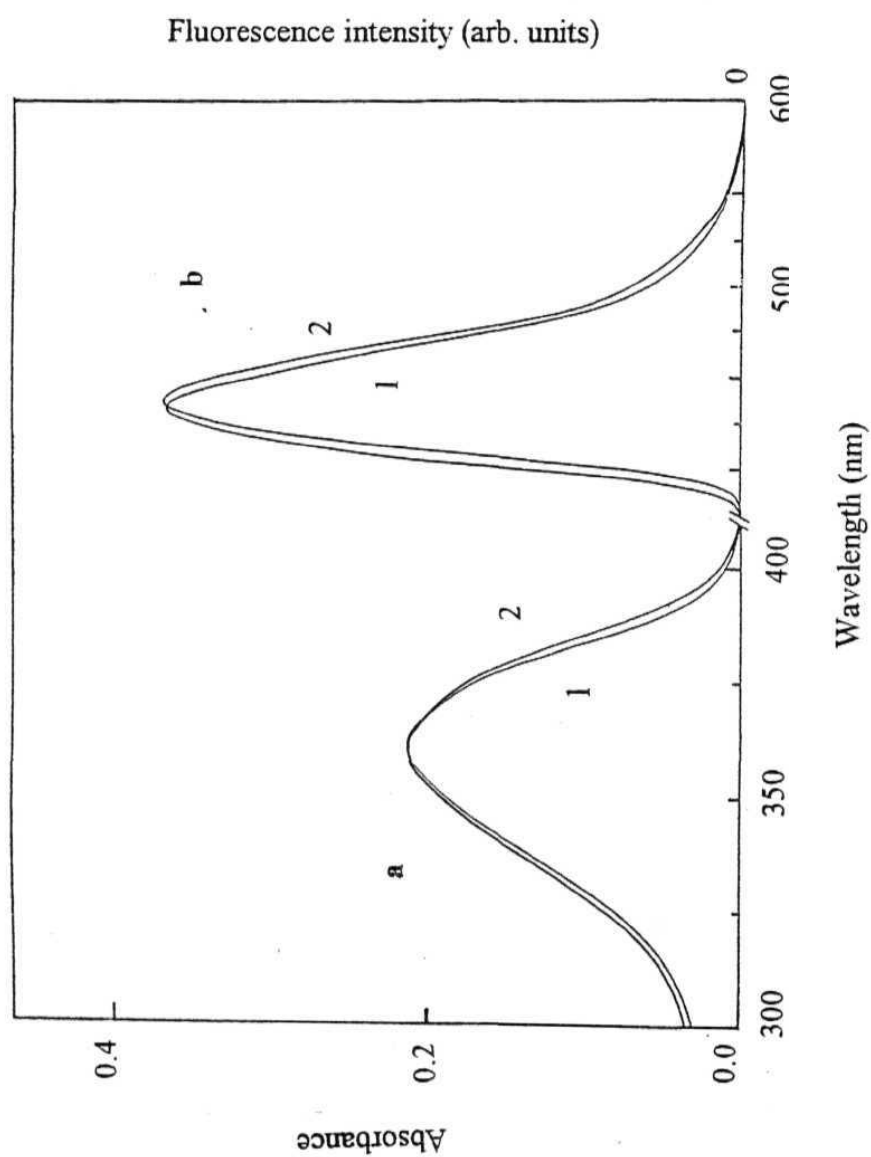
Fig. 4.2. Absorption (a) and fluorescence (b) spectra of OMNPDPA in 1) THF and 2) AN. λ_{ex} used for obtaining the fluorescence spectra was 350 nm.

media (fig. 4.3) are broader than those observed for its parent fluorophore (OMNPNB) and for all other multicomponent systems (OMNPDEA, OMNPDPA and OMNPPED). This is found to be partially due to the absorption by the aminonaphthyl moiety (that contributes around 250-350 nm) and an intramolecular charge transfer complex formed between the aminonaphthyl and methoxynaphthalimido moieties. The spectral properties of these systems are collected in Table 4.1.

4.1.2. *Fluorescence spectra*

The fluorescence spectra of all the systems are broad and devoid of any vibronic structure that is observed in the absorption spectra. The broadness of the band and solvatochromism of the fluorescence maxima indicate the charge transfer nature of the emission. Representative fluorescence spectra of OMNPDEA in THF and AN are showed in fig 4.1 and those of OMNPDPA are depicted in fig. 4.2. The fluorescence spectral data of the systems in THF and AN are presented in Table 4.1. The absorption and fluorescence maxima of the multi-component systems involving OMNP derivatives appear blue-shifted relative to those for the ANP derivatives. This indicates that intramolecular charge separation in the excited state of ANP is more than that in OMNPNB.[12] This is understandable as an amino group is better electron donor than a methoxy group.

The fluorescence spectra of OMNPNED in THF and AN, shown in fig. 4.3, consist of two clearly resolvable components. The short wavelength band is similar to that observed for OMNPDEA, OMNPDPA, OMNPPED and the parent fluorophore, OMNPNB. The long wavelength band arises from the intramolecular complex formed between the aminonaphthyl and 4-methoxy-1,8-naphthalimido moieties. The charge transfer nature of this band is also evident from its solvatochromic behaviour.
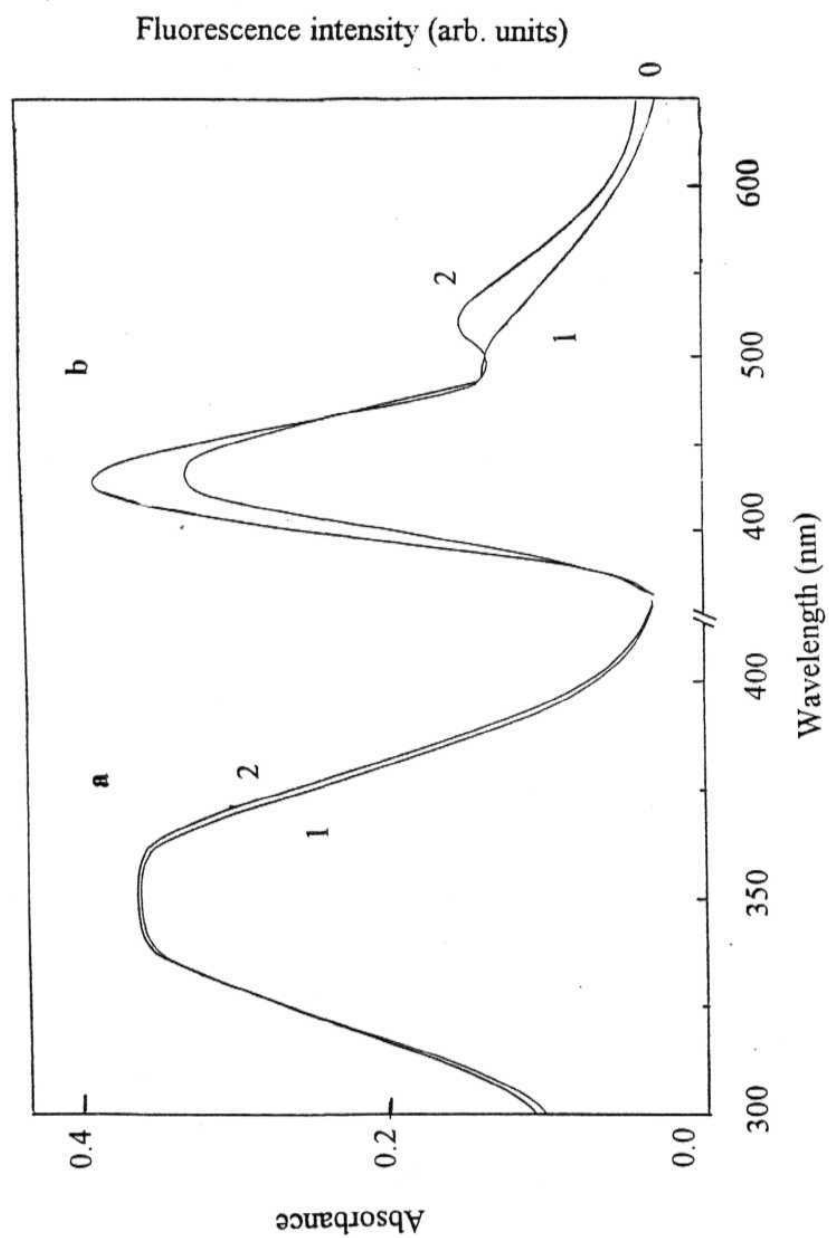
Fig. 4.3. Absorption (a) and fluorescence (b) spectra of OMNPNED in 1) THF and 2) AN. λ_{ex} for fluorescence was 350 nm.

4.1.3.   Fluorescence excitation spectra

With a view to establish the nature of the absorbing and emitting states, the fluorescence excitation spectra of these systems have been measured monitoring the fluorescence band(s). The spectral data have been collected in Table 4.1. It is interesting to note that the excitation maxima are clearly red shifted relative to the absorption maxima for any given system (fig. 4.4). This suggests that the fluorescence of these systems originates from a state that is different from the state observed most prominently in the absorption spectrum.

Table 4.1. Spectral properties of the multi-component systems and the fluorophore in
***THF and** AN.*

Solvent	Property	Compound				
		OMNPDEA	OMNPDPA	OMNPPED	OMNPNED	OMNPNB
THF	$\lambda_{max}(abs)$ $(nm)^a$	340 (s) 359 375 (s)	345 (s) 359 375 (s)	340 (s) 360 375 (s)	350(b)	345 (s) 354 375 (s)
	$\lambda_{max}(ex)$ $(nm)^b$	366	368	367	367 420	368
	$\lambda_{max}(em)$ $(nm)^c$	436	430	428	429 510	427
AN	$\lambda_{max}(abs)$ $(nm)^a$	345 (s) 360 375 (s)	345 (s) 360 375 (s)	340 (s) 362 375 (s)	356(b)	340 (s) 357 380 (s)
	$\lambda_{max}(ex)$ $(nm)^b$	367	368	368	367 439	368
	$\lambda_{max}(em)$ $(nm)^c$	439	438	437	436 535	438

[a]*The concentration of the solutions for the spectral measurements were in the range of 10^{-5} M.* [b]*The fluorescence excitation spectra of the compounds were recorded by monitoring at the fluorescence maxima.* [c]*The excitation wavelength was 350 nm for the measurement of the fluorescence spectra. 's' and 'b' in brackets indicate 'shoulder' and 'broad' respectively.*
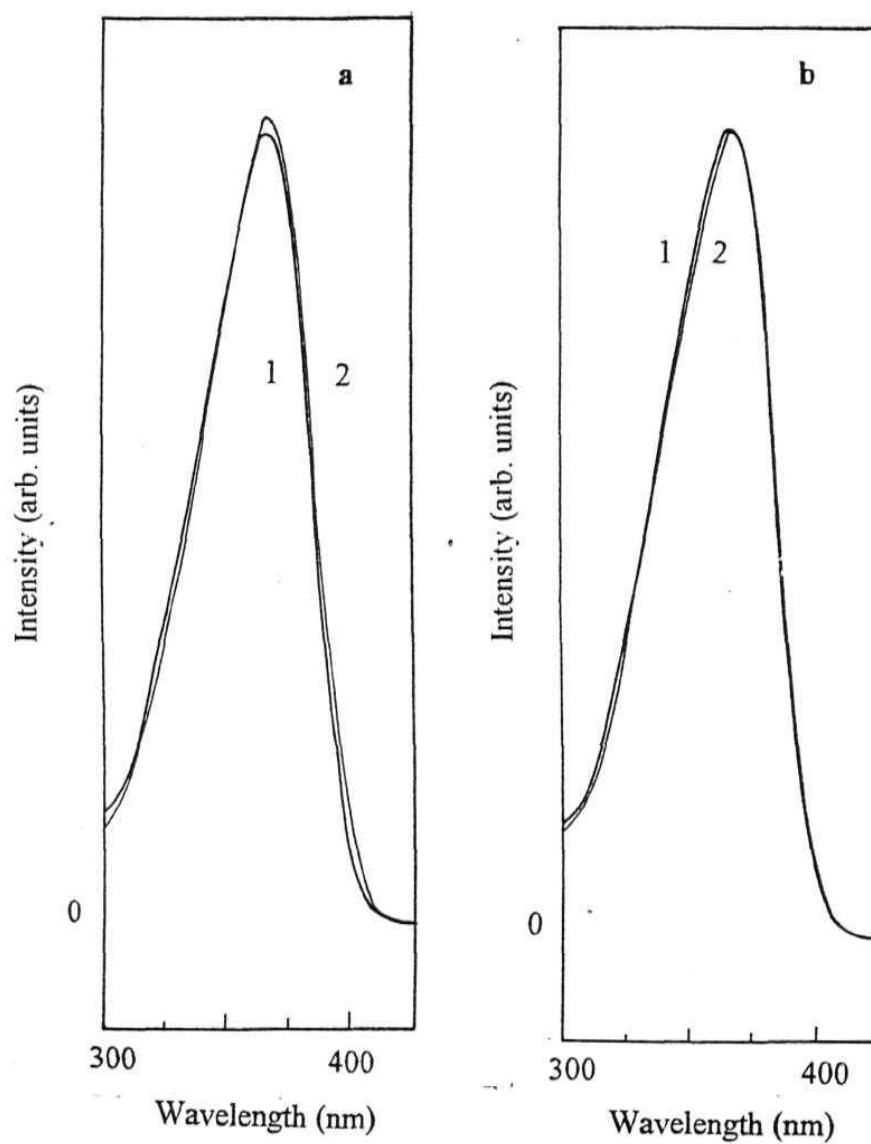
*Fig. 4.4. Fluorescence excitation spectra of **(a)** OMNPDEA (b) and **OMNPDPA** in 1) THF and 2) AN. Fluorescence was monitored at 450 **nm.***

The absorption, fluorescence and excitation spectral data suggest that the emission takes place from a ICT state that is just below the $\pi\pi^*$ state. The ICT state is not clearly resolvable in the absorption spectrum due to its close proximity with the strong $\pi\pi^*$ absorption band.

In the case of OMNPNED, the excitation spectra obtained on monitoring the two fluorescence bands are found to be different (fig. 4.5). The excitation spectrum corresponding to the higher energy emission band is very similar to that for the other multi-component systems. On the other hand, the excitation maximum corresponding to the longer wavelength emission band appears at a lower energy. This is due to the fact the latter emission arises from excitation of the charge transfer complex formed in the ground state between the aminonaphthyl and 4-methoxynaphthalimido moieties.

4.2.   Thennodynamic feasibility of PET in the multi-component systems

While oxidation of 4-amino-1,8-naphthalimide fluorophore was observed at 1.27 V, under the same measurement condition (details of which have been described in section 2.7) no oxidation of OMNPNB could be observed between 0 and 2 V. OMNPNB is therefore electronically deficient compared to ANP and hence, the right choice as the fluorophore component for the design of the PET fluorosensors for the transition metal ions. The reduction of OMNPNB is observed at 1.11 V.

The free energy change (AG*) for PET in the multi-component systems (estimated using equation. 2.13)[4] is found to be exergonic (Table 4.2). It is evident from a comparison of the calculated AG* values for the methoxy- and amino- derivatives of 1,8-naphthalimide that even though the latter derivatives are not suitable signalling agents, the systems based on methoxy derivatives are expected to be superior.
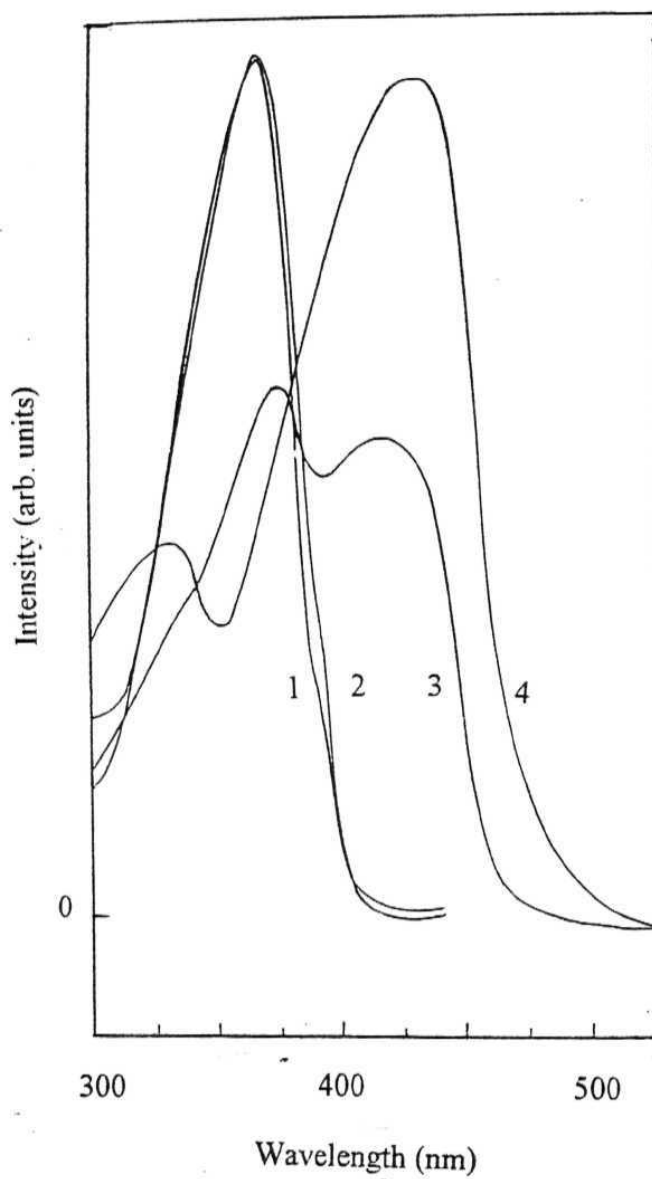
*Fig. 4.5. Fluorescence excitation spectra of OMNPNED in THF (1, 3), and AN (2, 4).
While 1 and 2 were obtained by monitoring fluorescence at 450 nm and 3 and 4 were
recorded by monitoring at 550 nm.*

Table 4.2. *Thermodynamic driving force (AG*) for the sensor systems and $E_{0,0}$ values of their parent fluorophore in acetonitrile.*

Sensor	E_{red} (fluor) $(V)^a$	$E_{0,0}$ $(kcal/mol)^b$	ΔG^* $(kcal/mol)^c$
OMNPDEA			
OMNPDPA	-1.11	65.3	-28.4
OMNPPED			-28.2
OMNPNED			-28.6
ANPDEA			-6.6
ANPPED	-1.61	55.04	-6.4

[a] E_{red} values (vs Ag/AgCl electrode) of the fluorophore components (OMNPNB **and** ANP) were measured following procedures as described in sec. 2.7, the cyclic voltammetric traces for the reduction of OMNPNB and ANP were found to be reversible and irreversible respectively; [b] $E_{0,0}$ was estimated from the mean position of the absorption and fluorescence maxima of the fluorophore components in acetonitrile. [c] ΔG^* calculations were made using **equn.** 2.13,[4] E_{ox} values of the receptor moieties (0.49, 0.50 and 0.48 V for triethylamine, N-methylaniline and N,N-dimethyl-1-aminonaphthalene respectively) were obtained from ref. 5. The oxidation potential of triethylamine was corrected for Ag/AgCl electrode by subtracting 0.27 V from the measured potential against SCE electrode. The free energy change values are applicable **in** polar solvents such as acetonitrile.

4.3.   Fluorescence quantum yield and lifetime

Eventhough OMNPNB is highly fluorescent (Table 4.3) in both polar and nonpolar media, the fluorescence quantum yields of the *fluorophore-spacer-receptor* systems involving this fluorophore are low (Table 4.4) indicating that intramolecular PET in these systems is quite efficient. The factor (F) by which the fluorescence yields of the multi-component systems are lower than that of the constituent fluorophore are also shown in Table 4.4. It is evident from the data that PET is most favourable for systems with two methylene spacer units. Further, PET is most efficient for systems involving the anilino or aminonaphthyl moiety.

Table 4.3. Fluorescence quantum yield of OMNPNB in various solvents.

Solvent	1,4-Dioxane	THF	AN	Methanol	Water
ϕ_f^a	0.76	0.76	0.78	0.85	0.46

$^a\phi_f$ is the fluorescence quantum yield of the system relative to that of 4-aminophthalmide (ϕ_f in acetonitrile is 0.63, ref.6).

Table 4.4. Fluorescence quantum yields of the multi-component systems and PET limiting values for the fluorescence enhancement (F).

Compound	Tetrahydrofuran		Acetonitrile	
	ϕ_f^a	F^b	ϕ_f^a	F^b
OMNPDEA	6.5×10^{-2}	12	3.0×10^{-2}	26
OMNPDPA	0.15	5	4.9×10^{-2}	16
OMNPPED	2.3×10^{-4}	3225	1.15×10^{-3}	680
OMNPNED	6.1×10^{-4}	1250	6.7×10^{-4}	1160
OMNPNB	0.76	1	0.78	1

$^a\phi_f$ is the fluorescence quantum yield of the system relative to that of 4-aminophthalmide (ϕ_f in acetonitrile is 0.63, ref.6). ^{b} F represents the ratio of the fluorescence quantum yield of the constituent fluorophore to that of the multi-component system.

The fluorescence decay behaviour of the various systems has been studied. Fig 4.6 shows the fluorescence decay profile of the fluorophore, OMNPNB in THF and the single exponential fit to the decay corresponding to a lifetime of 7.1 ns. On the other hand, the decay behaviour of the multi-component systems in THF and AN could be best fitted to the function, $I(t) = B_1 \exp(-t/\tau_1) + B_2 \exp(-t/\tau_2)$. Typical fluorescence decay behaviour of the multi-component systems is illustrated in fig. 4.7 and the decay parameters are collected in Table 4.5.
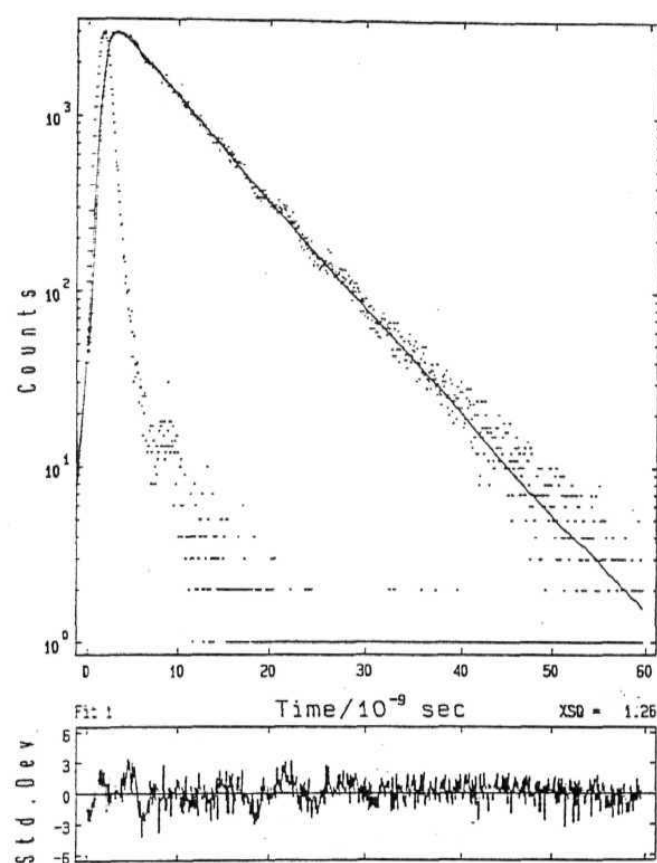
Fig. 4.6. Fluorescence decay profile of OMNPNB in THF. Solid line denotes the best fit (single exponential) to the measured decay curve. The excitation lamp profile is also shown in the figure. The excitation wavelength was 350 nm. The fluorescence was monitored at 450 nm.
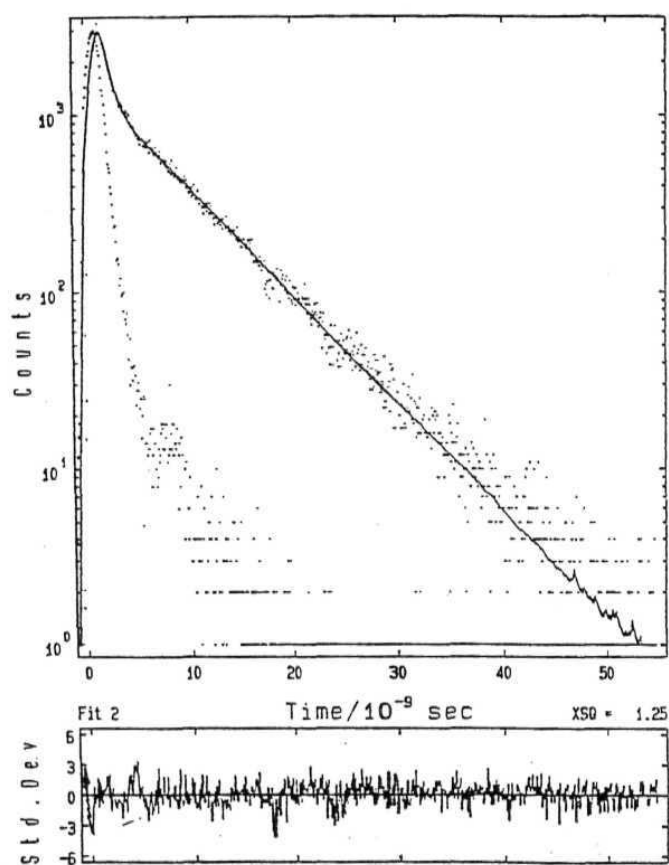
Fig. *4.7. The fluorescence decay curve of OMNPDPA in THF. The solid line indicates the fit to the measured decay curve. The excitation wavelength was 350 nm. TJte decay curve is fitted to a biexponential decay function. The excitation lamp profile is also shown in the figure, The fluorescence was monitored at 450 nm.*

Table 4.5. Fluorescence decay parameters of the sensor molecules and the fluorophore in THF and AM

Compound	THF		AN	
	τ_1 (ns)	τ_2 (ns)	τ_1 (ns)	τ_2 (ns)
OMNPDEA	0.4 (74%)	7.2 (26%)	0.1 (97%)	8.2 (3.0%)
OMNPDPA	0.4 (89%)	7.0 (11%)	0.4 (98.4%)	8.1 (1.6%)
OMNPPED	1.1 (46%)	7.2 (54%)	0.4 (89%)	8.2 (11%)
OMNPNED	0.5 (66%)	5.7 (44%)	1.7 (25%)	8.0 (75%)
OMNPNB	7.1	---	8.1	---

The quantities shown within the brackets represent the relative weightages of the components. Fluorescence was excited at 350 nm and monitored at 430 nm.

4 .4. Effect of the metal ions

4.4. J. A bsorption spectra

The effect of the transition metal ions on the absorption spectra of OMNPDEA in AN and OMNPDPA in THF are depicted in figs. 4.8 and 4.9 respectively. Since metal ion complexation is a ground state phenomenon, one expects changes in the absorption spectra of the systems on the addition of the metal salts. The spectral changes were found to be different for different metal ions and no general pattern could be observed. This behaviour is consistent with varied coordination chemistry of different metal ions, the difference in the stability of the complexes formed and also, due to the fact that some of the metal salts contribute to absorption in the spectral region investigated. The transition metal ion induced changes in the absorption spectra of OMNPNED were also found not to follow any general pattern. This has been illustrated in fig. 4.10.

4.4.2. Flu orescen ce properties

Unlike the multi-component systems involving ANP fluorophore, those containing the methoxy derivative exhibit excellent fluorescence enhancement in the
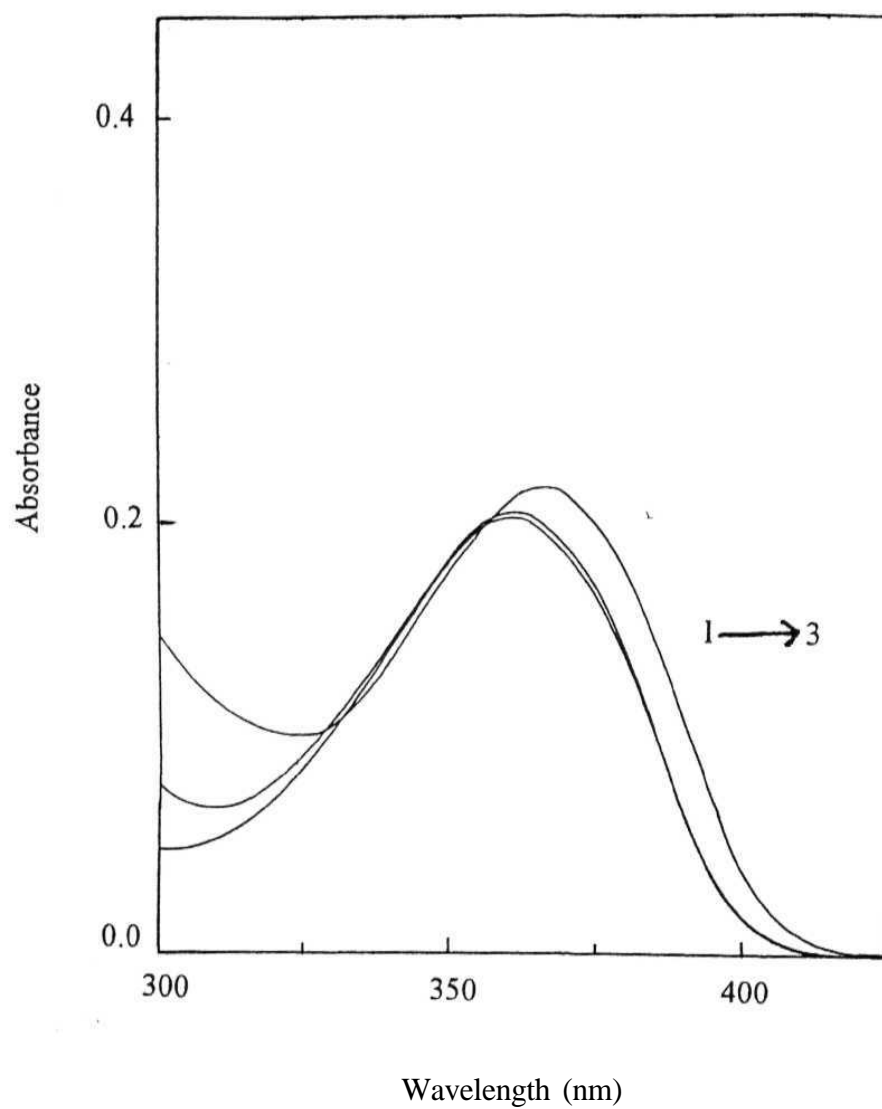
Fig 4.8. Absorption spectra of OMNPDEA in acetonitrile for various concentrations of Zn(H₂O)₆(ClO₄)₂ Zn⁺² concentrations are 1) 0, 2) 1.1 x 10⁻⁴ and 3) 4.4 x10⁻⁴ M.
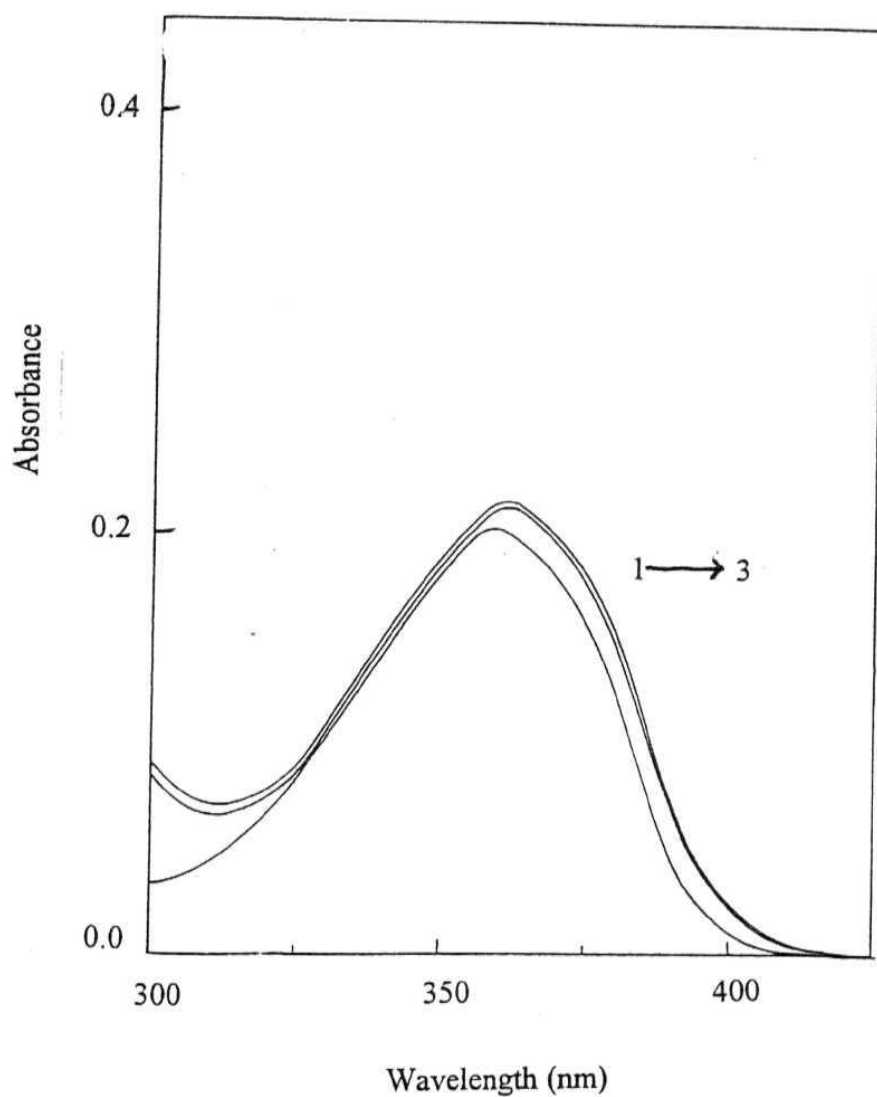
Fig 4.9. Absorption spectra of OMNPDPA in THF for various concentrations of Zn(H₂O)₆(ClO₄)₂ Zn⁺² concentrations are 1) 0, 2) 1.1 x 10⁻⁴ and 3) 4.5 x 10⁻⁴ M.
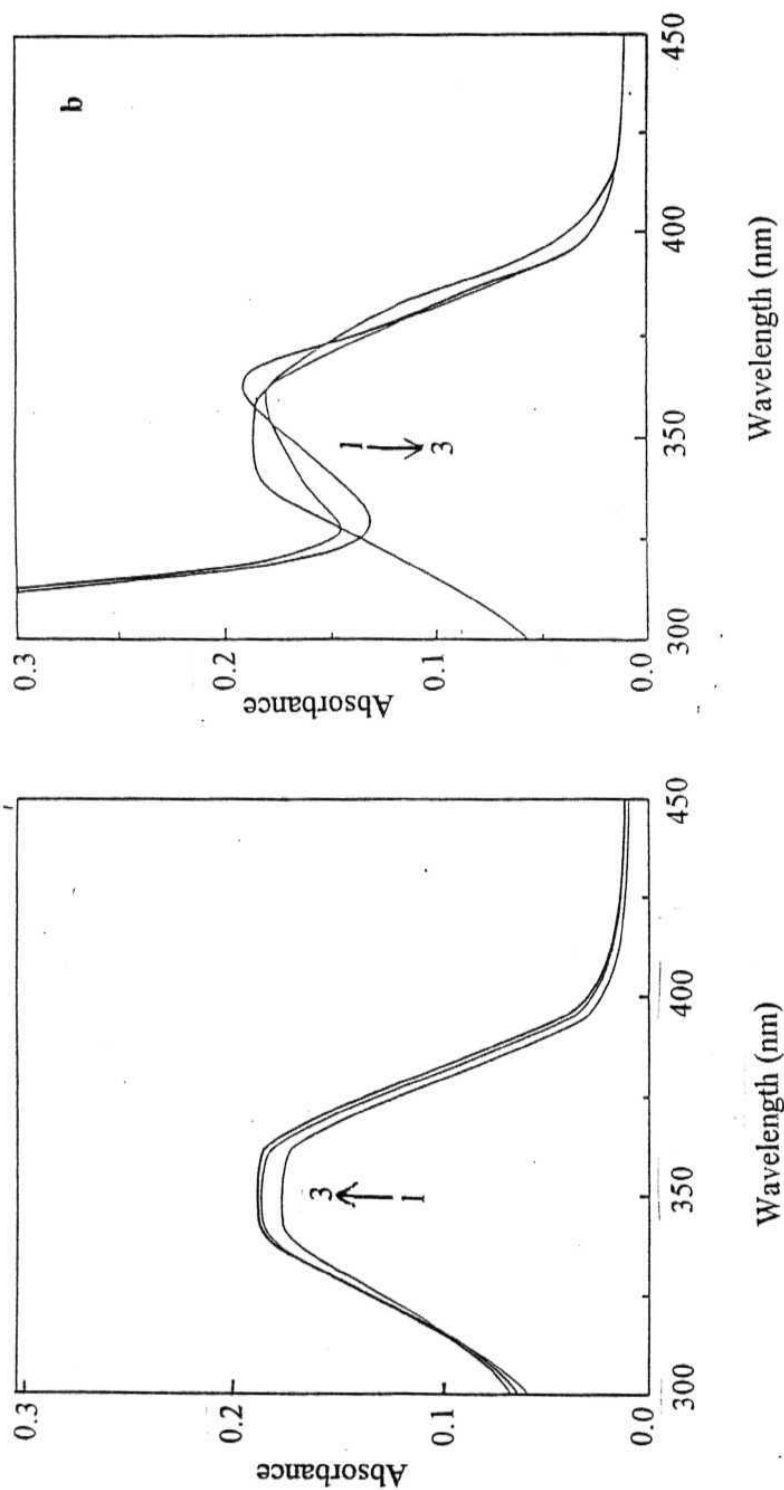
Fig 4.10. Metal ion induced changes in the absorption spectra of OMNPNED in THF; (a) in presence of $Zn(H_2O)_6(ClO_4)_2$. Zn^{+2} concentration are 1) 0, 2) 4.53 x 10^{-4} and 3) 5.7 x 10^{-4} M; (b) in presence of $Mn(H_2O)_6(ClO_4)_2$. Mn^{+2} concentrations are 1) 0, 2) 5.5 x 10^{-4} and 3) 5.9 x 10^{-3} M.

presence of the quenching transition metal ions. Figure 4.11 and 4.12 show typical changes in the fluorescence behaviour of these systems upon addition of a metal salt. For low concentration of the metal ions, the fluorescence intensity increases with increase in the concentration until it reaches a limiting value. A further increase in the concentration of the metal ions leads to fluorescence quenching. The limiting values of the fluorescence enhancement of OMNPDPA and OMNPDEA for different metal ions are collected in Table 4.6 and those for OMNPPED and OMNPNED in Table 4.7. The data clearly point to the ability of these systems in sensing the transition metal ions. The salient features of the data presented in these Tables are as follows: The FE values observed for OMNPDEA are higher than those observed in the case of OMNPDPA. Further, OMNPPED exhibits much higher FE values compared to either OMNPDEA or OMNPDPA. These observations are consistent with the extent of PET in the systems (vide Table 4.4). Further, for any given system, the highest FE has been observed for Zn^{+2}. This is also in accordance with the well-known nonquenching nature of this metal ion.[7] The fluorescence enhancement is associated with a red shift (ranges between 1.5 - 3 nm) of the fluorescence maximum. The metal ion induced red shift observed for these systems is in agreement with the fact that the binding of the metal ions takes place on the acceptor side of the EDA fluorophore (Section 1.3.5).[8]

As described in Section 4.1.2, the fluorescence spectrum of OMNPNED consists of two distinct emission bands with maxima at 436 and 535 nm in acetonitrile. The addition of the metal ion leads to a decrease in the intensity of the long wavelength band both in THF and AN. This is most likely due to the suppression of the formation of the charge transfer complex as a result of the addition of the metal ions. The first band, however, shows enhancement in the presence of any given metal ion. A comparison of the data presented in Table 4.4 and 4.7 reveals that, in the case of both OMNPPED and OMNPNED, fluorescence could not be completely recovered. This observation suggests
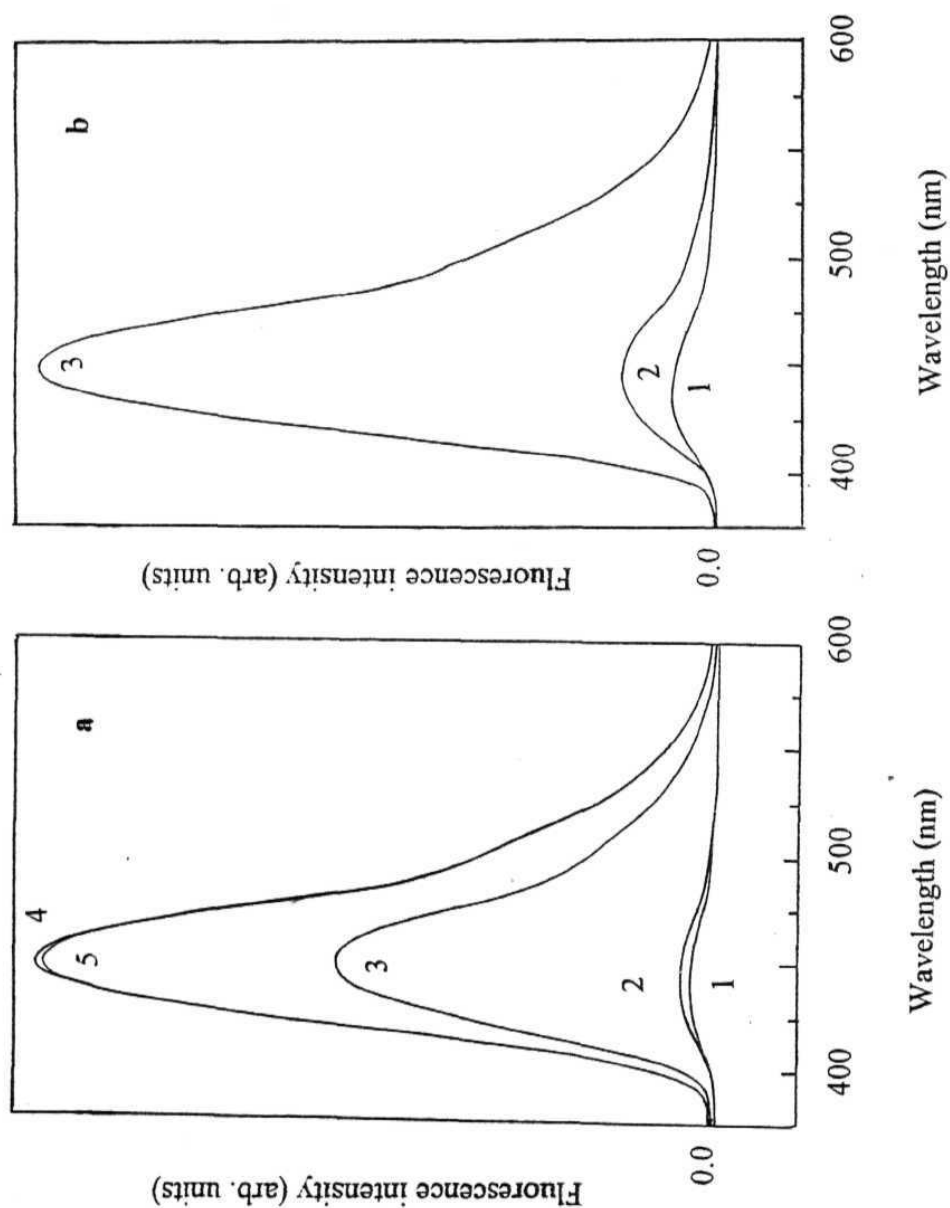
Fig. 4.11. Metal ion induced changes in the fluorescence spectra of the multi-component systems in acetonitrile; (a) OMNPDEA in the presence of Co(H₂O₆)(NO₃)₂, Co⁺² concentrations are 1) 0, 2) 1.6 x 10⁻⁴, 3) 3.1 x 10⁻⁴, 4) 4.7 x 10⁻⁴ and 5) 6.3 x 10⁻⁴ M; (b) OMNPDPA in the presence of Co(H₂O₆)(NO₃)₂, Co⁺² concentrations are 1) 0, 2) 1.6 x 10⁻⁴ and 3) 3.1 x 10⁻⁴M.
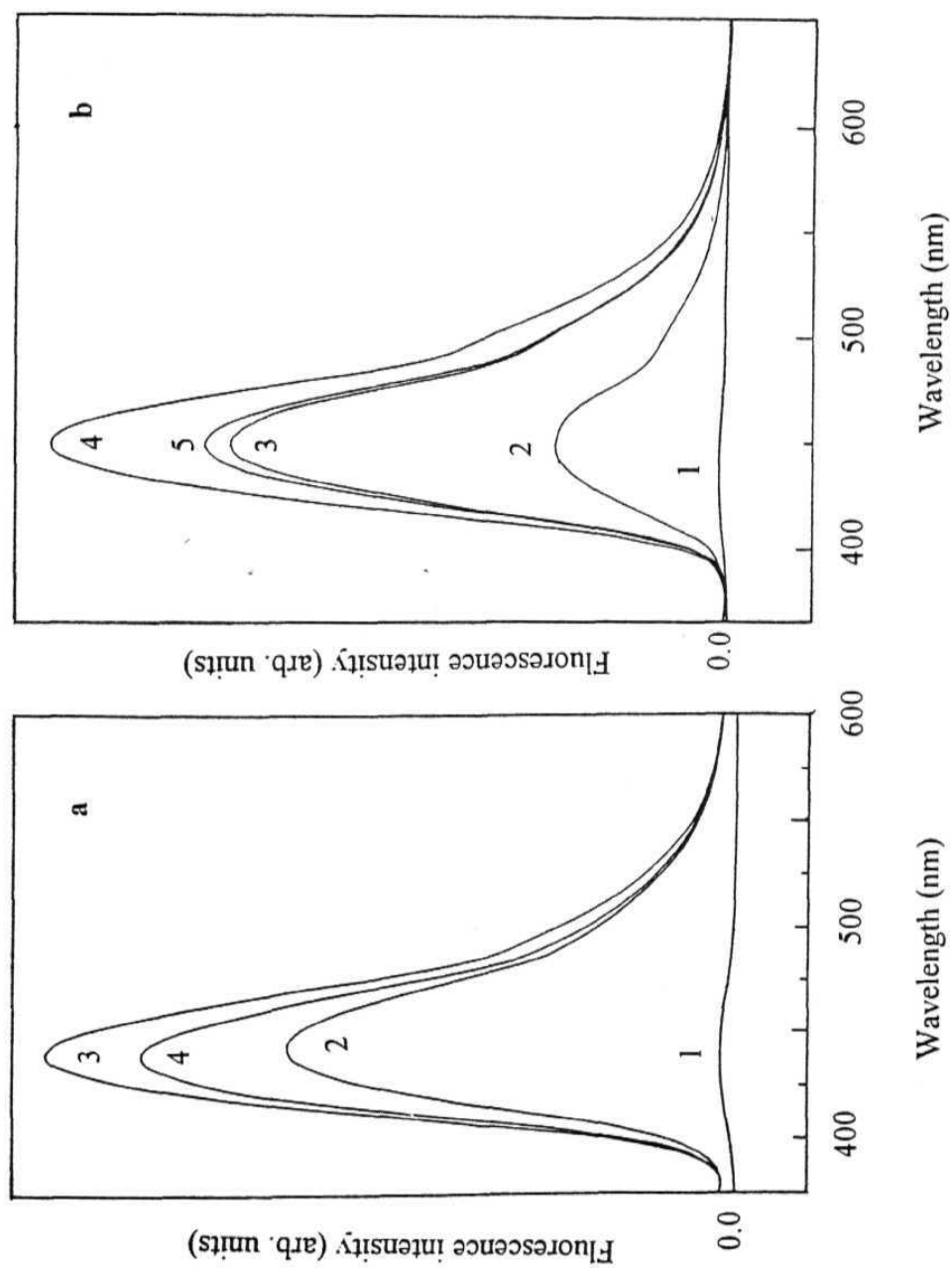
Fig. 4.12. Metal ion induced changes in the fluorescence spectra of the multi-component systems in acetonitrile; (a) OMNPPED with $Cu(H_2O)_3(NO_3)_2$ Cu^{+2} concentrations are 1) 0, 2) 1.2 x 10^{-4}, 3) 2.3 x 10^{-4} and 4) 4.7 x 10^{-4} M; and (b) OMNPNED in presence of $Fe(H_2O)_6(ClO_4)_3$, Fe^{+3} concentrations are 1) 0, 2) 1.1 x 10^{-4}, 3) 3.3 x 10^{-4}, 4) 4.4 x 10^{-4} and 5) 5.5 x 10^{-4} M.

Table 4.6. Fluorescence output of OMNPDEA and OMNPDPA in the presence of transition metal ions and proton as inputs.

Metal ion	OMNPDEA				OMNPDPA			
	THF		AN		THF		AN	
	[Salt]/M[a]	FE[b]	[Salt]/M[a]	FE[b]	[Salt]/M[a]	FE[b]	[Salt]/M[a]	FE[b]
Zn^{+2}	3.4×10^{-4}	13.0	3.3×10^{-4}	28.0	1.7×10^{-4}	6.0	4.4×10^{-4}	17.0
Cu^{+2}	3.5×10^{-4}	9.0	3.5×10^{-4}	23.0	2.9×10^{-4}	5.0	3.5×10^{-4}	15.0
Ni^{+2}	2.2×10^{-4}	12.0	7.1×10^{-4}	27.0	1.1×10^{-4}	6.0	5.1×10^{-4}	17.0
Co^{+2}	8.0×10^{-4}	10.0	4.7×10^{-4}	26.0	2.0×10^{-4}	5.0	3.3×10^{-4}	16.0
Fe^{+3}	6.25×10^{-5}	12.0	3.7×10^{-4}	15.0	3.1×10^{-4}	6.0	3.3×10^{-4}	10.0
Mn^{+2}	1.8×10^{-4}	12.0	6.0×10^{-4}	21.0	2.3×10^{-4}	6.0	4.0×10^{-4}	13.0
Cr^{+3}	4.6×10^{-4}	8.0	5.0×10^{-4}	26.0	3.0×10^{-4}	5.0	3.7×10^{-4}	16.0
H^{+}	5.0×10^{-4}	12.0	1.3×10^{-3}	28.0	2.5×10^{-4}	6.0	7.5×10^{-4}	17.0

[a]The concentration of the metal salt/proton for which maximum fluorescence enhancement has been observed. A further increase in the concentration of the metal ions led to fluorescence quenching. [b]FE values are calculated from the areas under the fluorescence curves of two solutions; one corresponding to the concentration of the metal ion/proton indicated in the second column of the Table and the other with no metal ion/proton (using equn. 2.14).

Table 4.7. Fluorescence enhancement (FE) values of OMNPPED and OMNPNED in the presence of various transition metal ions and protons in THF and ACN.

Metal ion	OMNPPED				OMNPNED			
	THF		AN		THF		AN	
	$[Salt]/M^a$	FE^b	$[Salt]/M^a$	FE^b	$[Salt]/M^a$	FE^b	$[Salt]/M^a$	FE^b
Zn^{+2}	1.1×10^{-4}	2420	5.5×10^{-4}	500	5.7×10^{-3}	4.0	6.35×10^{-3}	3.0
Cu^{+2}	1.2×10^{-3}	10.0	2.3×10^{-4}	50	1.2×10^{-4}	1.0	1.1×10^{-3}	15.2
Ni^{+2}	2.3×10^{-3}	19.0	2.0×10^{-3}	5.5	5.4×10^{-4}	2.0	1.5×10^{-3}	2.0
Co^{+2}	5.4×10^{-3}	112	4.7×10^{-3}	6.0	8.6×10^{-3}	33	2.2×10^{-3}	2.0
Fe^{+3}	1.3×10^{-4}	2000	3.9×10^{-4}	400	2.5×10^{-4}	122	4.4×10^{-4}	73
Mn^{+2}	2.4×10^{-3}	2660	2.0×10^{-3}	60	5.9×10^{-3}	260	5.0×10^{-3}	24
Cr^{+3}	1.0×10^{-2}	1450	4.3×10^{-3}	110	9.7×10^{-3}	17.0	6.2×10^{-3}	14.0
H^+	1.7×10^{-2}	515	5.0×10^{-4}	500	2.1×10^{-2}	27.0	2.5×10^{-3}	167

[a] The concentration of the metal salt/proton for which maximum fluorescence enhancement has been observed. A further increase in the concentration of the metal ions led to fluorescence quenching. [b] FE values are calculated from the areas under the fluorescence curves of two solutions; one corresponding to the concentration of the metal ion/proton indicated in the second column of the Table and the other with no metal ion/proton (using eqn. 2.14).

that for these systems the metal ion-receptor binding interaction is not strong enough so as to cut-off the fluorophore-receptor PET interaction completely.

The effect of the metal ions on the fluorescence decay profiles of the systems has been studied. A typical change in the fluorescence decay pattern of the systems in the presence of the metal ion is illustrated in fig.4.13. As observed in the case of the previously described systems, on addition of the metal salt the short-lived PET-quenched component disappears gradually and for a certain concentration of the metal ion, corresponding to almost complete recovery of fluorescence, the decay becomes single-exponential with lifetime similar to that of the fluorophore, OMNPNB. A further addition of the metal ions, however, leads to shortening of the fluorescence lifetime. Interestingly, metal ion induced change in the fluorescence decay behaviour of OMNPPED and OMNPNED is found to be quite different from that described for other systems. The decay behaviour of OMNPPED in acetonitrile is depicted in fig.4.14 to highlight this aspect. With an increase in the concentration of the metal ion, the percentage of the short-lived PET-quenched component is decreased gradually. However, the change of the decay pattern from biexponential to a single exponential one, as observed in the case of other multi-component systems, could not be observed for higher concentration of the metal ions. This can be rationalised taking into consideration the steady state fluorescence data, which indicated that in the case of OMNPPED, and OMNPNED, the fluorescence could not be completely recovered. The fluorescence decay behaviour of these two systems confirms that the PET communication between the fluorophore and the receptor could not be completely cut-off in the presence of metal ions. Quite obviously, the metal ion - receptor binding interaction is not strong enough to completely prevent the PET communication between the fluorophore and the receptor.
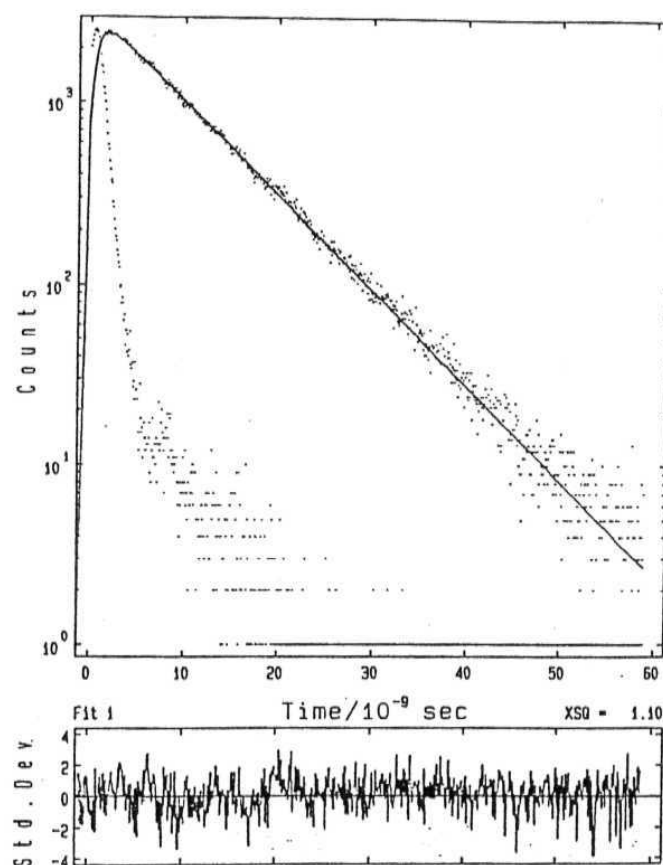
Fig. 4.13. Fluorescence decay curve *of OMNPDPA in* **THF** *in the presence* ^{of} **2.7 x10^{-4}** **M** *of* **Co(H$_2$O)$_6$(NO$_3$)$_2$** *Shown also in the figure are the exciting lamp profile and the single exponential* $_{fit}$ $(\tau = 8.1$ ns) to the fluorescence decay. The excitation wavelength was 350 nm and the fluorescence was monitored at 435 ^{nm}.
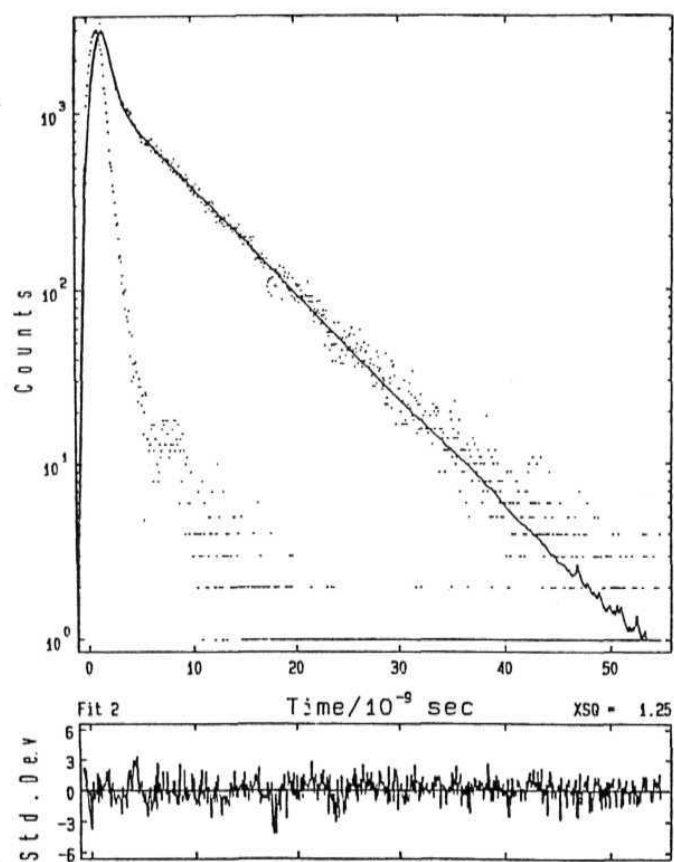
Fig. *4.14.* The *fluorescence* decay curve of OMNPPED in AN in presence of 2.2 x *10*
M *of Co(H₂O)₆(NO₃)₂* Shown also in the figure are the exciting lamp profile and the
biexponential *fit* to the fluorescence decay. The excitation wavelength was 350 nm and
the fluorescence was monitored at 435 *nm.*

It is to be noted that binding of the metal ions with the receptor (that leads to a decrease in the PET communication between the fluorophore and the receptor) leads to fluorescence recovery; on the other hand, fluorophore-metal ion interaction leads to fluorescence quenching. Therefore, whether the net result of the two opposing factors (which could be enhancement or quenching) depends on the relative magnitude of enhancement and quenching. It is clear from the results presented in this chapter that when PET is efficient in the multi-component system and the metal ion-receptor binding is strong, there is every possibility for even a structurally simple *fluorophore-spacer-receptor* system to exhibit transition metal ion induced fluorescence enhancement.

4.5. References

1. E. Martin, R. Weigand, *Chem. Phys. Lett.* 1998, *288*, 52.

2. a) A. Pardo, J.M.L. Poyato, E. Martin, J.J. Camacho, D. Reyman, M.F. Brana, J.M. Castellano, *J. Photochem. Photobiol. A Chem.* 1986, *36,* 323; b) A. Pardo, E. Martin, J.M.L. Poyato, J.J. Camacho, M.F. Brana, J.M. Castellano, J. *Photochem. Photobiol, A Chem.* 1987, *41,* 69; c) A. Pardo, E. Martin, J.M.L. Poyato, J.J Camacho, J.M. Guerra, R. Weigand, M.F. Brana, J.M. Castellano, *J. Photochem. Photobiol. A Chem.* 1989, *48,* 259; d) A. Pardo, J.M.L. Poyato, E. Martin, J.J. Camacho, D. Reyman, *J. Lumin.* 1990, *46,* 381; e) D. Yuan, R.G. Brown, *J. Chem. Res (M).* 1994, 2337; f) M.S. Alexiou, V. Tychopoulos, S. Ghorbanian, J.H.P. Tyman, R.G. Brown, P.I. Brittain, *J. Chem. Soc. Perkin Trans. 2,* 1990, 837.

3. *The Exciplex,* Eds., M. Gordon, W.R. Ware, Academic Press, New York, 1975 and references therein.

4. a) A. Weller *Pure Appl. Chem.* 1968, *16*, 115; b) D. Rehm, A. Weller, *Isr. J. Chem.* 1970, *8,* 259.

5. H. Siegerman, in *Techniques of Chemistry,* Ed., N.L. Weinberg, Wiley, New York, 1975, Vol. V, part II, p 803.

6. T. Soujanya, R.W. Fessenden, A. Samanta, *J. Phys. Chem.* 1996,*100, 3507*.

7. a) A.W. Varnes, R.B. Dodson, E.L. Wehry, *J. Am. Chem. Soc.* 1972, *94,* 946; b) J.A. Kemlo, T.M. Shepherd, *Chem. Phys. Lett.* 1977, *47,* 158.

8. a) B. Valeur, In *Topics in Fluorescence Spectroscopy,* Ed., J.R. Lakowicz, Plenum Press, New York, 1994, vol. IV, p 21; b) M.M. Martin, P. Plaza, N. Dai Hung, Y.H. Meyer, J. Bourson, B. Valeur, *Chem. Phys. Lett.* 1993, *202,* 425; c) M.M. Martin, P. Plaza, Y.H. Meyer, L. Begin, J. Bourson, B. Valeur, *J. Fluores.* 1994, *4,* 271; d) M.M. Martin, P. Plaza, Y.H. Meyer, F. Badaoui, J. Bourson, J.P. Lefebvre, B. Valeur, *J. Phys. Chem.* **1996,** *100,*6879.

FLUOROPHORE-SPACER-RECEPTOR SYSTEM INVOLVING 4-AMINO-7-NITROBENZ-2-OXA-l,3-DIAZOLE

Present chapter describes the fluorescence properties of two 7-nitrobenz-2-oxa-1,3-diazole (NBD) derivatives, 4-amino-7-nitrobenz-2-oxa-1,3-diazole (NAM) and the *fluorophore-spacer-receptor* system comprising NAM as the fluorophore component, 4-(N,N-dimethylethyIenediamino)-7-nitrobenz-2-oxa- J ,3-diazole (NEA), in the absence and in presence of the transition metal ions. The structures of the systems studied are shown in Chart 5.1. The results presented in the previous chapters have shown that the *jluorophore-spacer-receptor* systems involving an electron deficient fluorophore component exhibit excellent fluorescence 'off-on' signalling in the presence of quenching transition metal ions. The present study has been undertaken with a view to find out the suitability of NAM as the fluorophore component for the design of structurally simple multi-component fluorescence signalling systems for the d-block metal ions.
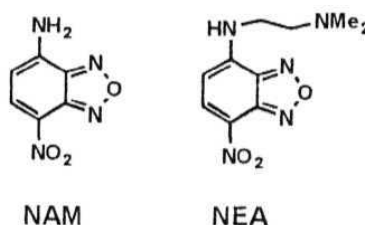
Chart 5.1

NBD fluorophores arc extensively used as fluorescence probes in biological studies such as membrane fusion, lipid motion, organisation of lipids and proteins in membranes, etc.[1-7] The highly reactive nature of the NBD halides towards various nucleophiles has been exploited in labelling studies of various biologically important molecules.[2] Excited state charge transfer and conformational change in some NBD derivatives have been investigated recently.[8] Amino-NBD derivatives also find application in various fields such as nonlinear optics[9] and sensor design for the detection

of various guest molecules such as metal ions.[10-13] For example, NBD fluorophore attached to 1-aza-18-crown-6 acts as a fluorosensor for the alkali metal ions, especially the potassium ions detection.[10]

5.1. Redox behaviour of NAM and free energy changes associated with PET in NEA

The reduction potential of NAM, estimated from the reversible reduction peaks, is measured to be - 0.91 V. Cyclic voltammogram exhibits an irreversible oxidation peak for NAM at 1.6 V. Since the oxidation potential of the fluorophore is higher than that for ANP and AP (whose oxidation potential values are 1.27 and 1.5 V respectively), from the point of view of electron deficiency in the fluorophore, NAM is expected to be superior to both ANP and AP as a fluorophore component for the design of a PET fluorosensor. On the other hand, NAM is not as good as a fluorophore component as OMNPNB (for which no oxidation could be observed between 0 and 2 V). Using equation 2.13,[14] $E_{red}(fluor)$ as -0.91 V, $E_{ox}(recep)$ as 0.49 V[15] and $E_{0,0}$ (estimated from the mean position of the absorption and fluorescence maxima in acetonitrile) as 58 kcal/mol, the free energy changes associated with intramolecular PET in NEA is measured to be - 26.2 kcal/mol in acetonitrile. Therefore, even though NAM is not an electron deficient fluorophore (compared to OMNPNB), its reduction potential and singlet state energy are such that PET is thermodynamically highly feasible in the multi-component system, NEA.

5.2. Spectral properties

The absorption and fluorescence spectra of NEA in acetonitrile are shown in fig 5.1. The lowest energy absorption band ($\varepsilon_{459} = 1.9 \times 10^4 M^{-1} cm^{-1}$) of this system can be attributed to an intramolecular charge transfer transition (between the 4-amino and 7-
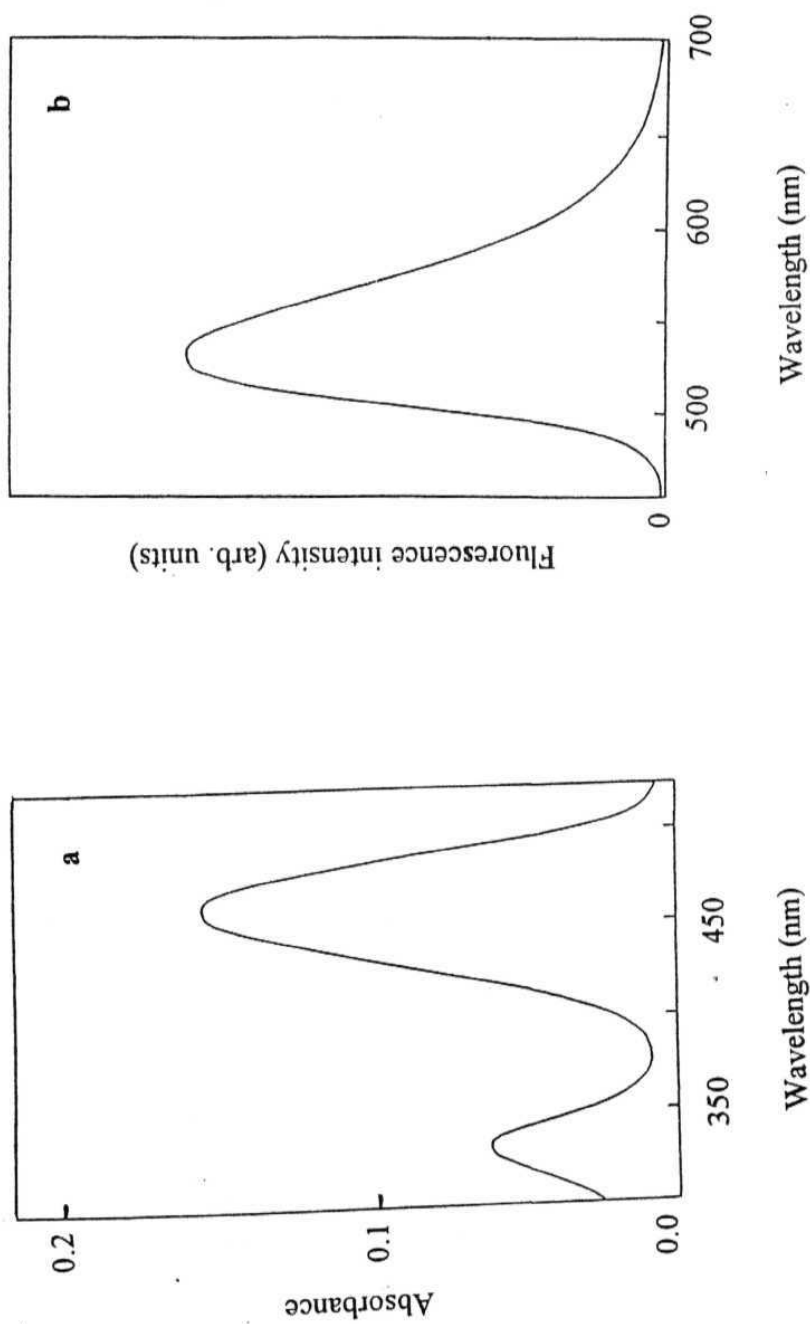
Fig. 5. 1. The absorption (a) and fluorescence (b) spectra of NEA in acetonitrile. The excitation wavelength for the measurement of the fluorescence spectrum was 440 nm.

nitro group of the fluorophore) on the basis of its solvatochromism, its broad structureless feature and the literature data on related NBD derivatives.[1-8] The absorption and fluorescence spectral data of NEA and NAM along with the literature data of 4-N-propylamino-NBD (NPR) have been collected in Table 5.1. It can be seen that the lowest energy absorption maxima of NEA and NPR are Stokes shifted relative to that of NAM in any given solvent. This is presumably due to the inductive influence of the alkylamino and the alkyl group. Interestingly, however, the fluorescence maxima of NEA are slightly blue-shifted with respect to those of NAM in both THF and AN. This small hypsochromic shift of the fluorescence band maximum of NEA relative to that of NAM is suggestive of a decrease in the excited state charge separation in the fluorophore. This could be due to a change in the excited state conformation of 4-N attached to the ring. A change in the pyramidalisation of this nitrogen or slight twisting of the alkylamino group relative to the ring system, which may be necessary for through-space overlap of the distal nitrogen lone pair orbital with the π-orbitals of the ring leading to intramolecular electron transfer in NEA (vide later), can lead to a decreased separation of charge in the NBD moiety and be responsible for the observed blue shift.

Table 5.1. Absorption and fluorescence spectral data of NBD derivatives in THF and AN.

Compound	THF		AN	
	λ_{max}(abs) in nm	λ_{max}(flu) in nm	λ_{max}(abs) in nm	λ_{max}(flu) in nm
NAM	445	525	447	532
NEA	455	522	459	529
NPR[a]	457	525	462	534

[a] *From ref.8a. The concentrations of the solutions used for spectral measurements were in the range of 10^{-5} M. The excitation wavelength for the fluorescence measurements was 440 nm.*

5.3.   Fluorescence yields and decay behaviour

NBD derivatives are usually highly fluorescent in non-hydrogen bonding solvents.[8] The measured ϕ_f values of NAM are 0.9 and 0.7 in THF and AN respectively.* Interestingly, the ϕ_f values of NEA are lower than those of NAM by nearly a factor of 125 in THF and 90 in AN. This unusually low fluorescence yield of NEA is obviously due to the receptor (amino group) induced PET quenching of the fluorescence.

The fluorescence decay behaviour of NEA further confirms PET-induced fluorescence quenching. While the fluorescence decay of NAM is single-exponential with lifetime of 11.7 ns and 11.4 ns in THF and AN respectively, NEA exhibits a biexponential decay behaviour consisting of a short-lived major component (~ 0.2 ns, 93 - 98%) and a minor long-lived component with lifetime ranging between 8.1 and 10.4 ns depending on the solvent (fig. 5.2 and 5.3). The predominant short-lived component clearly represents the lifetime of the PET-quenched fluorophore. The long-lived minor component can in principle arise from the products of the electron transfer reactions such as an exciplex. However, since no second component could be seen in the fluorescence spectrum of NEA (which is very similar to that of NAM) and the fact that the long-lived component in the fluorescence decay of NEA is also present in polar media such as in acetonitrile (where exciplexes are quite unstable), it is quite clear that this component can not be due to an exciplex, formed as a result of PET. The biexponential nature of the fluorescence decay of NEA can best be explained considering a through-space electron transfer mechanism involving the overlap of the lone pair orbital of the distal nitrogen and the rc-orbitals of the ring. The long-lived component arises from species in which the donor and acceptor groups are well separated, while the short component represents the

---

*The fluorescence quantum yields of the NAM and NEA were measured using coumarin-1 53 as the reference compound (ϕ_f in acetonitrile is 0.89).
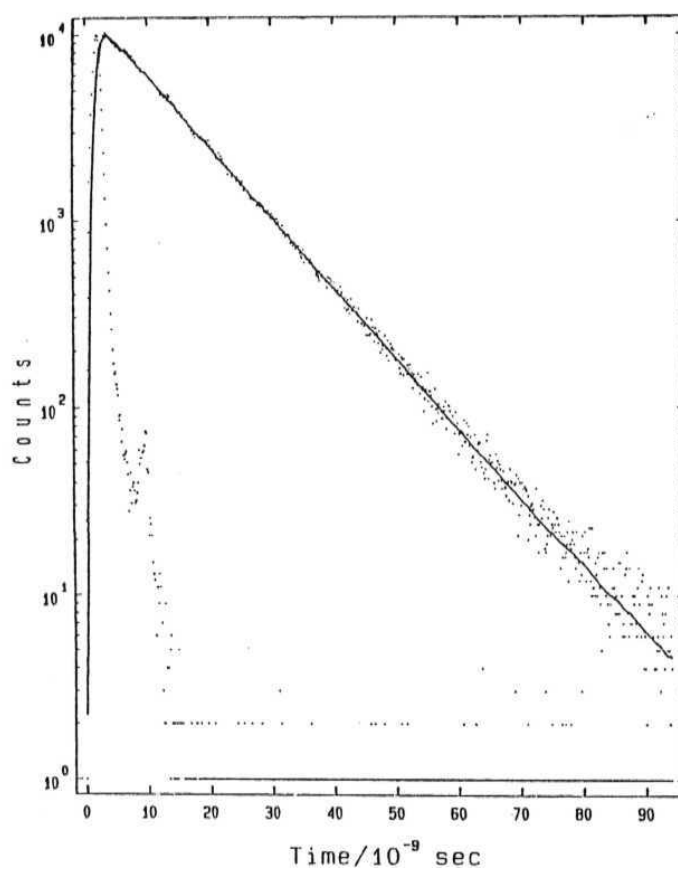
Fig. 5. 2. Fluorescence decay curve of NAM in acetonitrile. The excitation wavelength was 440 nm. The solid line indicates the fit to the measured decay trace. The decay curve was fitted to a single exponential decay function. The exciting lamp profile is also shown in the figure. The fluorescence was monitored at 530 nm.
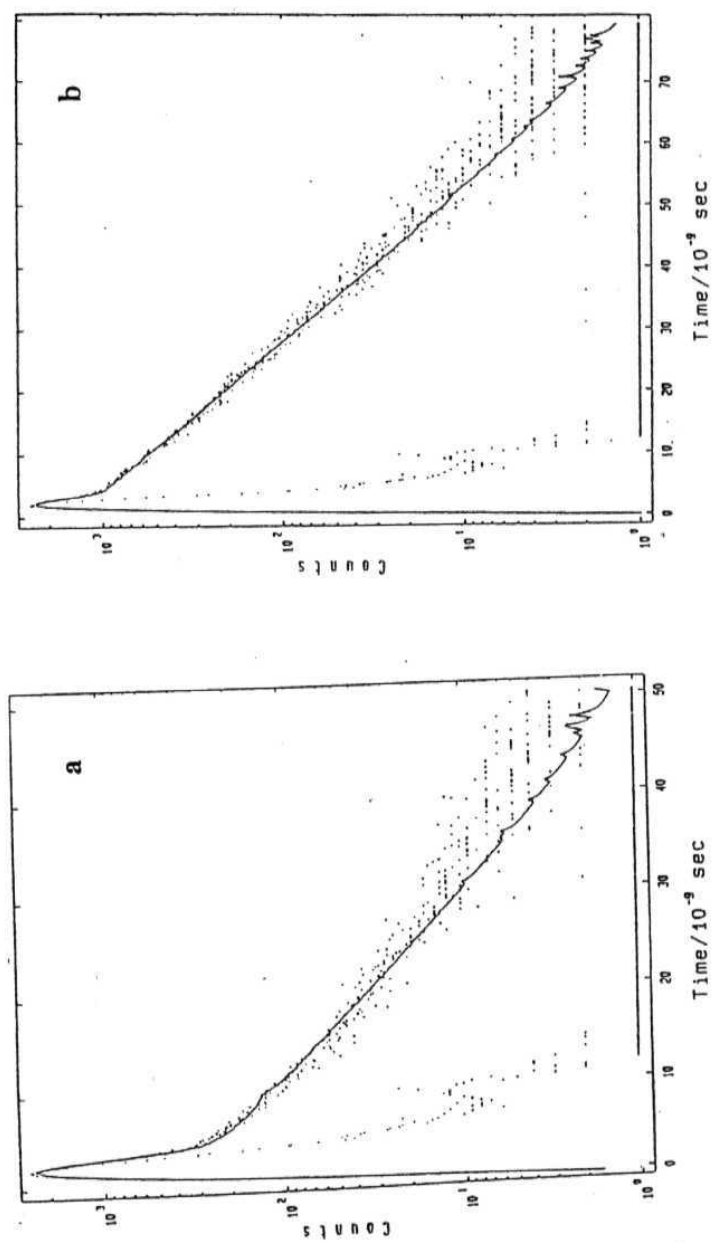
Fig. 5. 3 Fluorescence decay curves of NEA in THF (a) and AN (b). The excitation wavelength was 440 nm. Solid lines indicate the fit to the measured decay curves. The decay curves were fitted to biexponential decay functions. The exciting lamp profiles are also shown in the figure. The fluorescence was monitored at 530 nm.

quenched fluorophore in close proximity with the donor amine. A through-space electron transfer leading to a biexponential decay behaviour has also been observed for other flexible donor-acceptor systems such as ANP, AP and OMNP derivatives described in previous chapters.

5.4.   Effect of the metal ions

5.4.1.   Absorption spectra

It is generally believed that even though the metal ion binding with the receptor cuts off the PET communication between the fluorophore and the receptor, the fluorescence enhancement could not be observed in the presence of transition metal ions because of the quenching interaction between the fluorophore and the metal ions. In order to find out whether the present fluorophore interacts with the metal ions in the ground state, we have studied the changes in the absorption spectrum of NEA as a function of the metal ion concentrations. A parallel investigation has also been carried out on NAM that does not contain the receptor unit.

Fig. 5.4. illustrates the effect of the addition of some of the metal ions on the absorption spectrum of NAM. It may be noted that an isosbestic point was observed in the case of Cr^{3+} and Ni^{2+}. However, in most other cases no isosbestic point could be observed (fig 5.4). The absence of any common pattern of the spectral changes is a reflection of varied coordination chemistry of the transition metal ions and the stabilities of their complexes.[17] Since the coordination of the metal ions by a monodentate or bidentate ligand is a stepwise process with complexes of different stoichiometries are
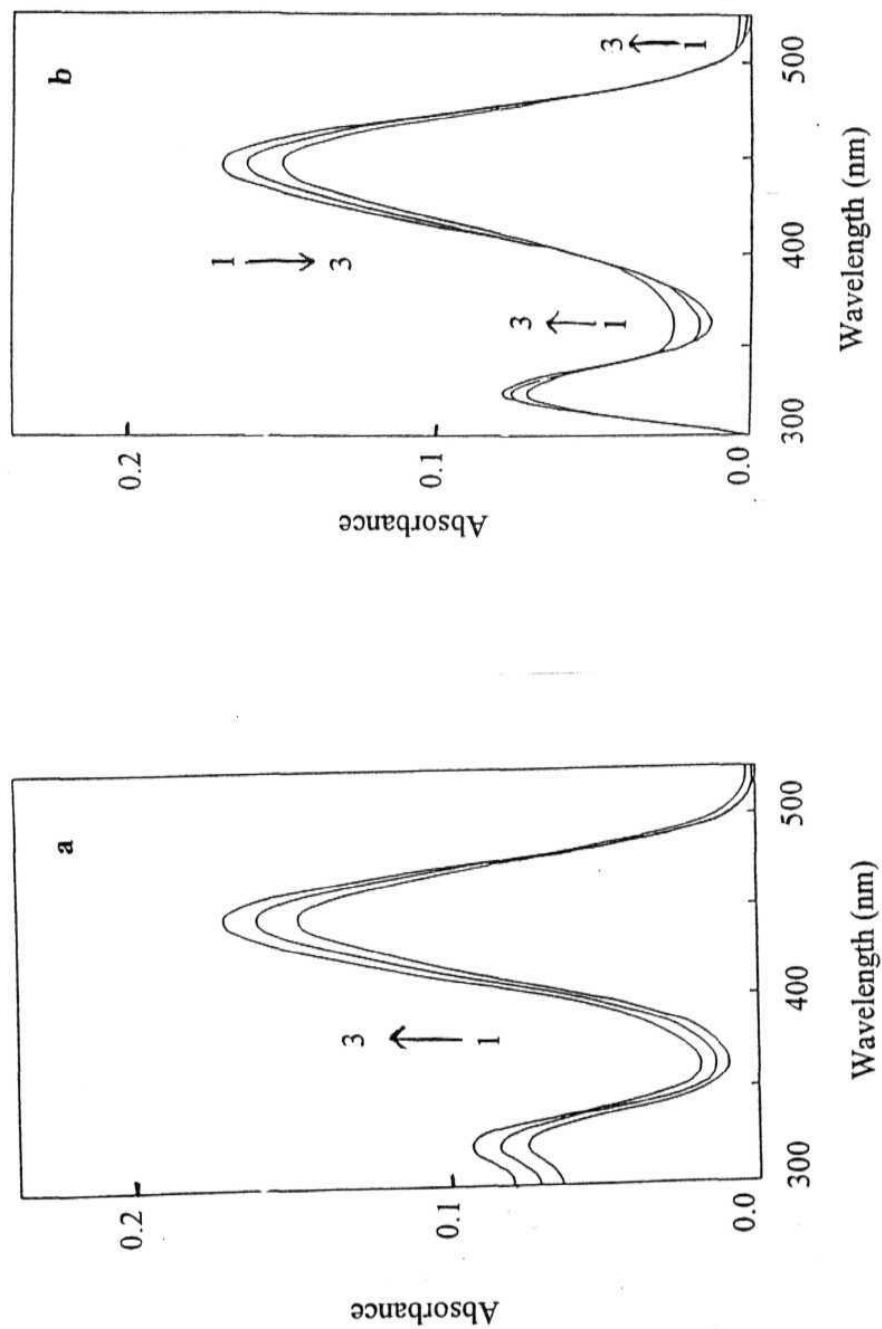
Fig. 5. 4. *Changes in the absorption spectrum of NAM on addition of different amount of* $Zn(H_2O)_6(ClO_4)_2$ *(a) and* $Ni(H_2O)_6(ClO_4)_2$ *(b) in acetonitrile. The concentration of* Zn^{2+} *corresponding to the spectra labelled 1, 2 and 3 are 0, 1.6 x 10^{-3} and 4.0 x 10^{-3} M respectively. The concentrations of* Ni^{2+} *were 1) 0, 2) 1.15 x 10^{-3} and 3) 2.87 x 10^{-3} M.*

expected to be present in the solution, one should not expect an isosbestic point over a large concentration range of the metal ions. However, an isosbestic point can be observed when only one of the various possible equilibria is dominant. It is important to note here that since the fluorophore concentration used in the measurements is rather low $(\sim 10^{-5}$ M), the concentration of the higher complexes could be too low and it may not always be possible to detect them spectrophotometrically under the present experimental condition.

Fig. 5.5 depicts typical effect of a metal ion on the absorption spectrum of NEA. Unlike in the previous case, the addition of the metal salts to NEA leads to a significant blue shift of the absorption maximum. The spectral shift for the various metal ions ranges between 9 to 16 nm in acetonitrile. The charge transfer bands are generally sensitive to small changes in the polarity of the medium. Since the salts used in the experiments contain water of crystallisation, one might expect the increase in the local polarity around the fluorophore (on addition of the salts) as responsible for the shift. However, for the NBD derivatives this would have resulted in a red shift of the maximum.[8] Further, since no shift could be observed on addition of these metal salts to NAM, which contains the same fluorophore, the spectral changes must be attributed to the binding of the metal ions with the fluorophore. If the distal dimethylamino receptor moiety alone gets bound to the metal ions (assuming NEA behaving as a monodentate ligand), the energy states of the fluorophore were not expected to be affected as the receptor is connected to the fluorophore by a non-conjugating spacer and there is no evidence of a through-bond transfer of charge. However, when the amino nitrogen atom (4-N) is involved in the coordination with the metal ions along with the distal receptor nitrogen, giving rise to a stable 5-membered chelate (Chart 5.2), the electron density available at 4-N for charge separation within the fluorophore decreases considerably leading to a blue shift of the spectral maxima. This interpretation of the spectral shift is in accordance

Chart 5 2
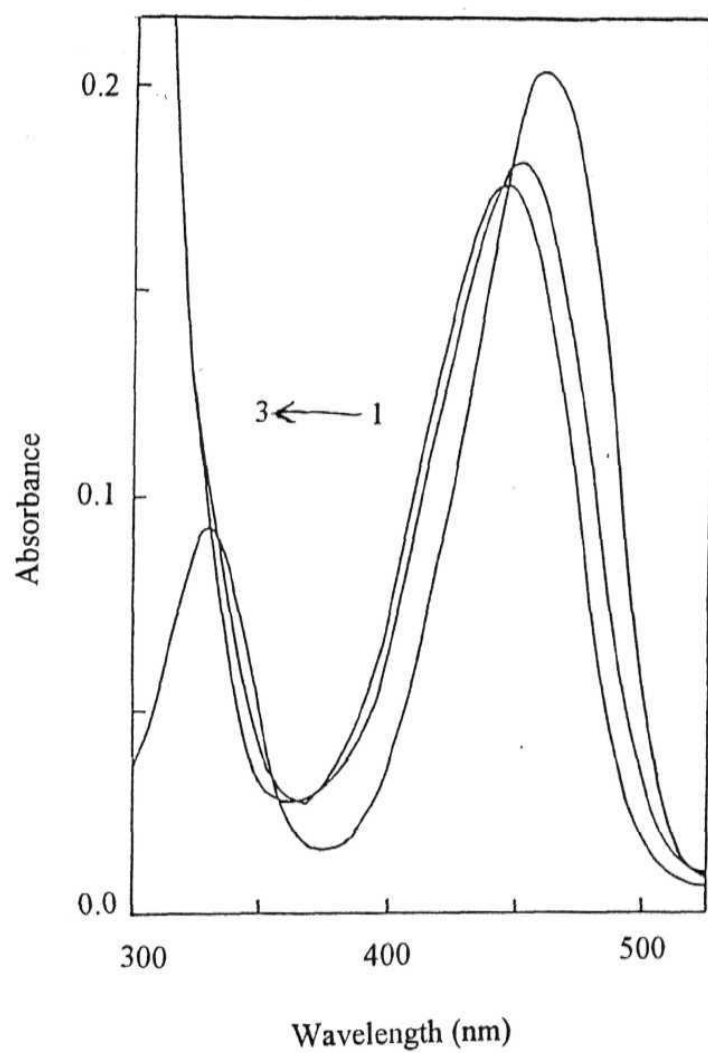
Fig. 5.5. Effect of Mn(H₂O)₆(ClO₄)₂on the absorption spectrum of NEA in acetonitrile.
The various concentrations of the metal ions are 1) 0, 2) 3.6 x 10⁻⁵ and 3) 1.1 x 10⁻⁴ M.

with the general principles framed by Valeur [18-21] and Lapouyade and Rettig.[22,24] In order to establish unequivocally the mode of binding of the metal ion to the multi-component system, we attempted to prepare the metal complexes in crystalline form. However, several such attempts were unsuccessful.   ,

5.4.2. Flu orescen ce spectra

The effect of the transition metal ions on the fluorescence spectrum of NAM is illustrated in fig.5.6. As can be seen from the figure, the addition of the transition metal ions to the NAM leads to expected fluorescence quenching with no noticeable change in the shape and the location of the spectrum. The quenching constants have been evaluated from a quantitative analysis of the fluorescence intensity data using Stern-Volmer equation $(VI = 1 + k_q \tau_0 [Q]$ where, I_0 and I are the fluorescence intensities in the absence and in presence of the metal ions respectively. $[Q]$ is the quencher concentration, k_q is the bimolecular quenching rate constant and τ_0 is the fluorescence lifetime of NAM in the absence of the quencher). A representative Stern-Volmer plot is shown in fig 5.7 and the quenching constants are collected in Table 5.2. As seen from the table, the quenching is pronounced in the case of Cr^{3+}, Co^{2+} and Cu^{2+} and minimum quenching is observed with Zn . The observed quenching efficiencies of the metal ions are found quite similar to those reported for other fluorophores [25,26] with Fe^{3+} is the only exception. Since the observed quenching is the result of the ground state interaction (evident from the absorption spectral changes) and dynamic interaction in the excited state, we have studied the variation of the fluorescence lifetime of NAM as a function of the metal ion concentration to extract the quenching constant that is solely a measure of the excited state interaction between the metal ions and the fluorophore. The contribution of the inner filter effect arising from the absorption of exciting light by the coloured metal salts appears to be negligible as the extinction coefficients of the metal salts (less than $100 \, M^{-1}$
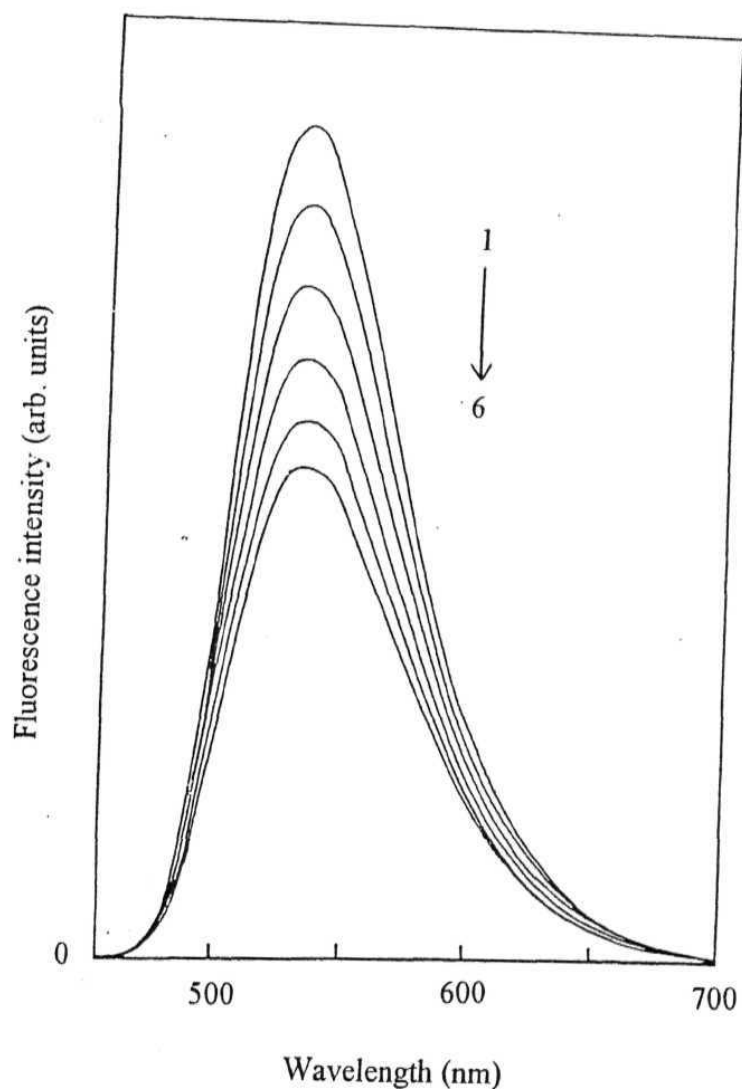
Fig.5.6. Fluorescence spectra of NAM in acetonitrile in the presence of $Co(H_2O)_6(NO_3)_2$. *The concentrations of the metal ions are 1) 0, 2) 4.97 x 10^{-4}, 3) 9.95 x 10^{-4}, 4) 1.5 x 10^{-3}, 5) 2.0 x 10^{-3} and 6) 2.5 x 10^{-3} M. The solution was excited at 440 nm.*
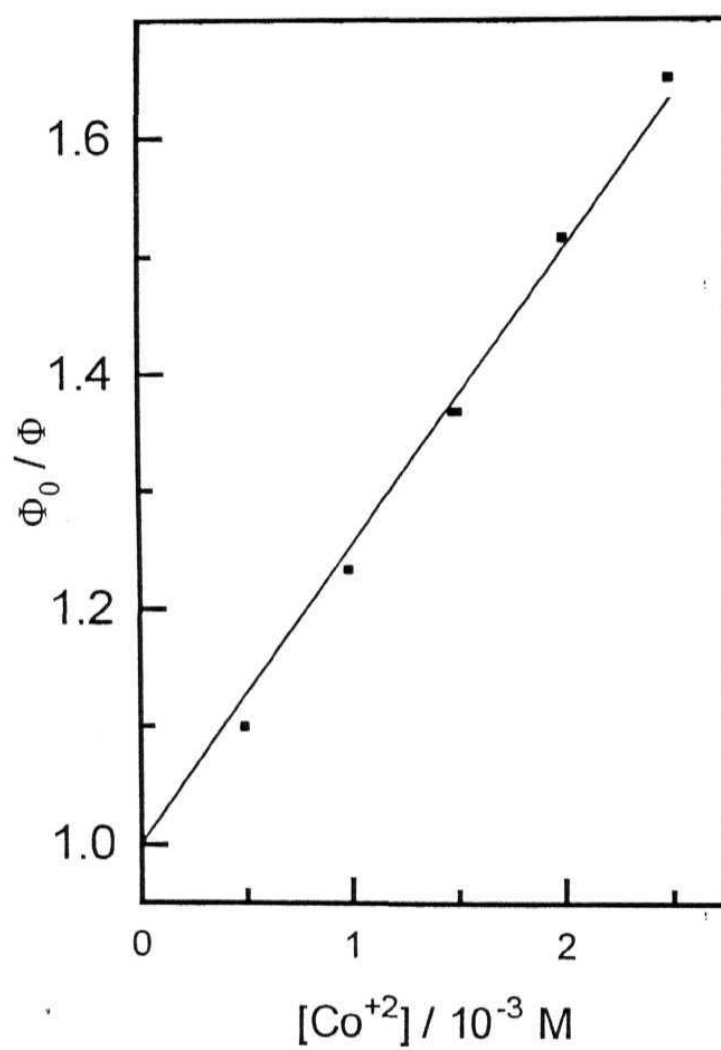
Fig. 5.7. Stern-Volmer plot for the quenching of the fluorescence intensity of NAM by $Co(H_2O)_6(NO_3)_2$ *in acetonitrile.*

cm^{-1}) at the exciting wavelength (440 nm) were measured to be much lower than that of the fluorophore (~10400 $M^{-1}cm^{-1}$).

A typical plot based on the equation, $\tau_0/\tau = 1 + k_q\tau_0[Q]$ is shown in fig. 5.8 and the quenching constants obtained from the lifetime data are collected in Table 5.2. As can be seen, the dynamic quenching constants are significantly lower than the overall quenching constants; however, the quenching trend remains almost the same.

That the NBD moiety interacts with the transition metal ions both in the ground and excited state with quenching constants in many cases close to the diffusion-limited values is clearly evident from the above data. Therefore, the choice of the NBD moiety as the fluorophore component of the supramolecular system, NEA may not be appropriate for the quenching metal ion sensing applications. Interestingly, however, NEA exhibits excellent fluorescence enhancement in the presence of all the transition metal ions studied. Fig 5.9 illustrates the effect of the addition of a metal ion on the fluorescence spectra of NEA. The enhancement is associated with a blue shift (ranging from 3 to 10 nm) of the spectra. The fluorescence spectral shift is found to be less pronounced than that observed for the absorption spectrum for any given metal ion. As stated in the earlier section, this can be rationalised by taking into consideration the fact that the excited state dipole moment of the NBD fluorophore is higher than the ground state dipole moment.[8] Since on electronic excitation, the charge density at 4-N is decreased, a weakening of the metal ion binding with the fluorophore takes place in the excited state which is responsible for a smaller shift of the fluorescence maximum. In this context, it is to be noted that using picosecond pump-probe teclmique, Valeur and co-workers demonstrated earlier that a metal ion bound to a donor-acceptor fluoroionophore can be ejected on electronic excitation because of weakening of the binding resulting from a decreased electron density available at the coordinating site of the fluorophore in the excited state.[19]
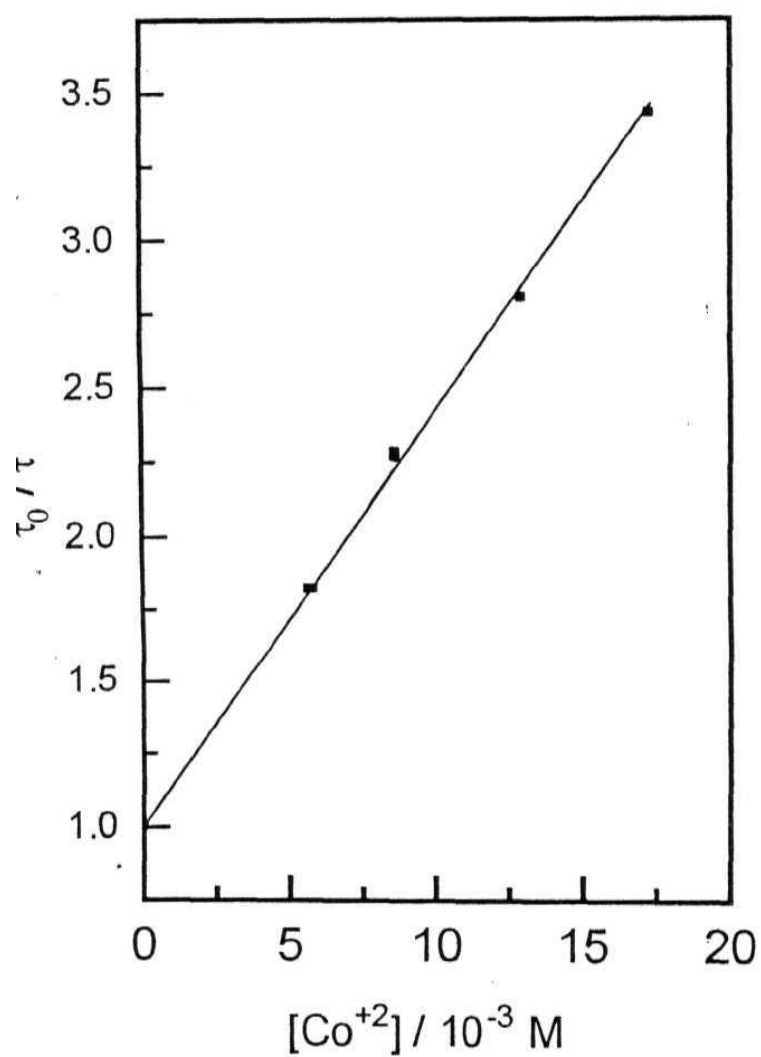
Fig. 5.8. A plot of τ_0/τ of NAM versus the concentration of the $Co(H_2O)_6(NO_3)_2$ in acetonitrile.

Table 5.2 Quenching constants obtained from the steady state and time-resolved measurements on NAM.

Metal Ion	Tetrahydrofuran				Acetonitrile			
	K_{SV} /M^{-1} (overall)	K_{SV} /M^{-1} (dynamic)	k_q^a /$10^9 M^{-1}s^{-1}$ (overall)	k_q^a /$10^9 M^{-1}s^{-1}$ (dynamic)	K_{SV} /M^{-1} (overall)	K_{SV} /M^{-1} (dynamic)	k_q^b /$10^9 M^{-1}s^{-1}$ (overall)	k_q^b /$10^9 M^{-1}s^{-1}$ (dynamic)
Zn^{+2}	70	3.3	6.0	0.3	31	10.6	2.74	0.9
Cu^{+2}	201	56.3	17.2	4.9	220	107	19.3	9.4
Ni^{+2}	122	23.2	10.5	2.0	130	76	11.4	6.6
Co^{+2}	268	115	23.0	10.0	255	142	22.4	12.4
Fe^{+3}	399	82	34.2	7.0	129	21.4	11.2	1.9
Mn^{+2}	59	5.9	5.1	0.5	60	10.8	5.25	0.9
Cr^{+3}	253	76.2	21.7	6.6	244	112	21.4	9.8

$^a \tau_0 = 11.7$ ns, $^b \tau_0 = 11.4$ ns. The excitation wavelength was 440 nm.
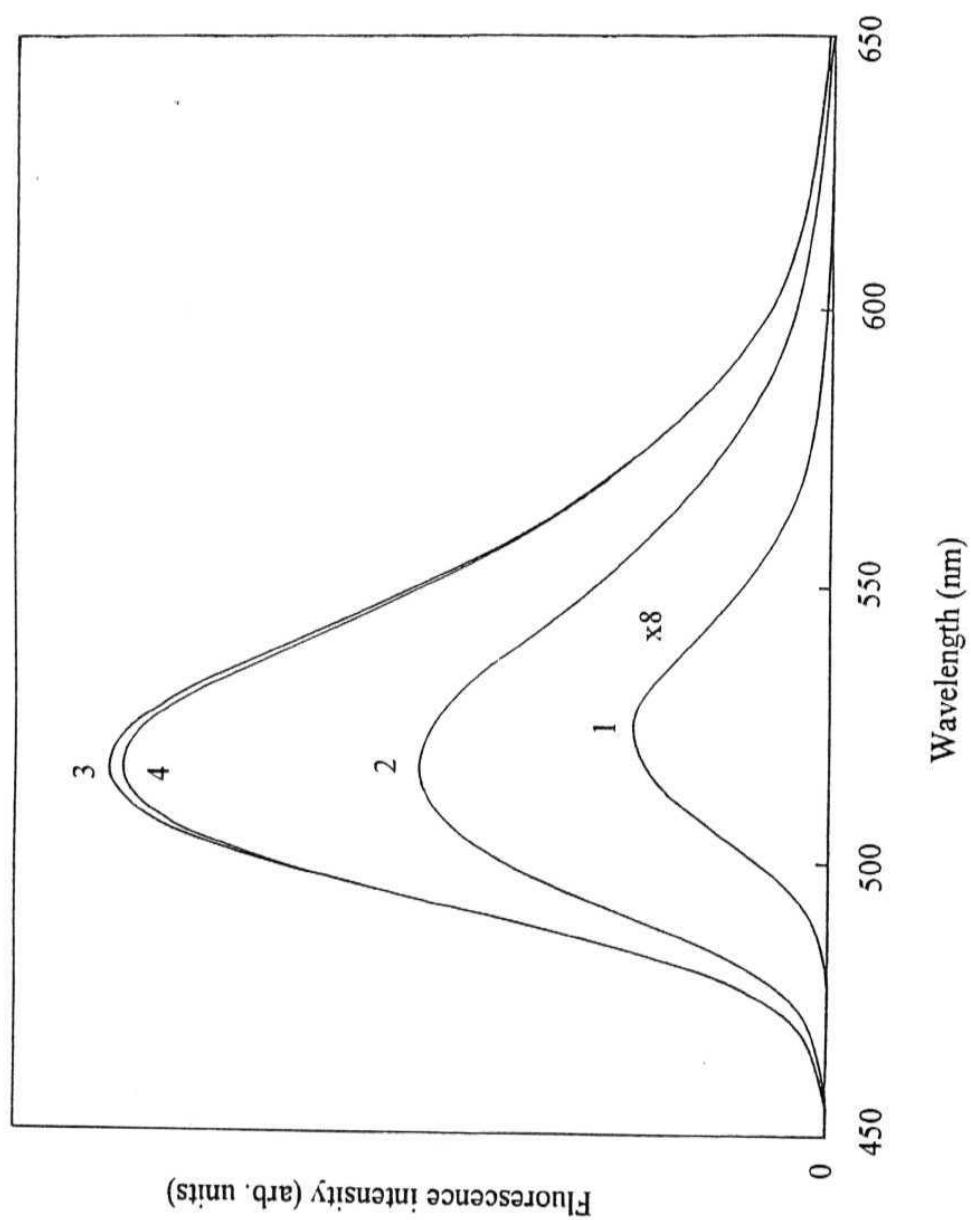
Fig.5.9. Fluorescence spectra of NEA in acetonitrile in the presence of Co(H₂O)₆(NO₃)₂. The various concentrations of the metal ions are 1) 0, 2) 1.3 x 10⁻⁴, 3) 1.2 x 10⁻³ and 4) 1.67 x 10⁻³ M. The excitation wavelength was 440 nm.

The fluorescence excitation spectra (fig. 5.10) obtained in the presence of the metal ions also display blue shift of magnitude similar to that observed for the absorption spectra. In addition to the shift of the spectral maxima that is observed, metal ion addition is associated with a gradual increase in the fluorescence intensity until it reaches a limiting value. It can be seen that the FE values observed with all the metal ions (Table 5.3) are quite high. While poor quenchers such as Zn^{2+} and Mn^{2+} show highest enhancement, as expected, it is interesting to note that some of the efficient quenchers also show excellent enhancement.

Table 5.3. Fluorescence enhancement (FE) values of NEA in the presence of different metal ions and protons in acetonitrile and tetrahydrofuran.

Metal Ion	THF		AN	
	[Salt]/ M[a]	FE[b]	[Salt]/ M[a]	FE[b]
Zn^{+2}	1.09×10^{-3}	295	6.8×10^{-5}	113
Cu^{+2}	3.47×10^{-3}	113	8.0×10^{-5}	43
Ni^{+2}	6.34×10^{-4}	247	6.3×10^{-3}	70
Co^{+2}	4.39×10^{-3}	81	1.2×10^{-3}	48
Fe^{+3}	2.85×10^{-5}	262	3.4×10^{-5}	113
Mn^{+2}	1.36×10^{-3}	258	8.6×10^{-4}	123
Cr^{+3}	4.5×10^{-4}	289	9.1×10^{-5}	70
H^{+}	9.0×10^{-5}	225	1.0×10^{-4}	105

[a]*The concentration of the metal salt or proton for which maximum fluorescence enhancement has been observed. A further increase in the concentration of the metal ion or proton leads to fluorescence quenching.* [b] *FE values are calculated from the areas under the fluorescence curves of two solutions; one corresponding to the concentration of the metal ion or proton indicated in the second column of the Table and the other with no metal ion or proton (using equn 2.14).*
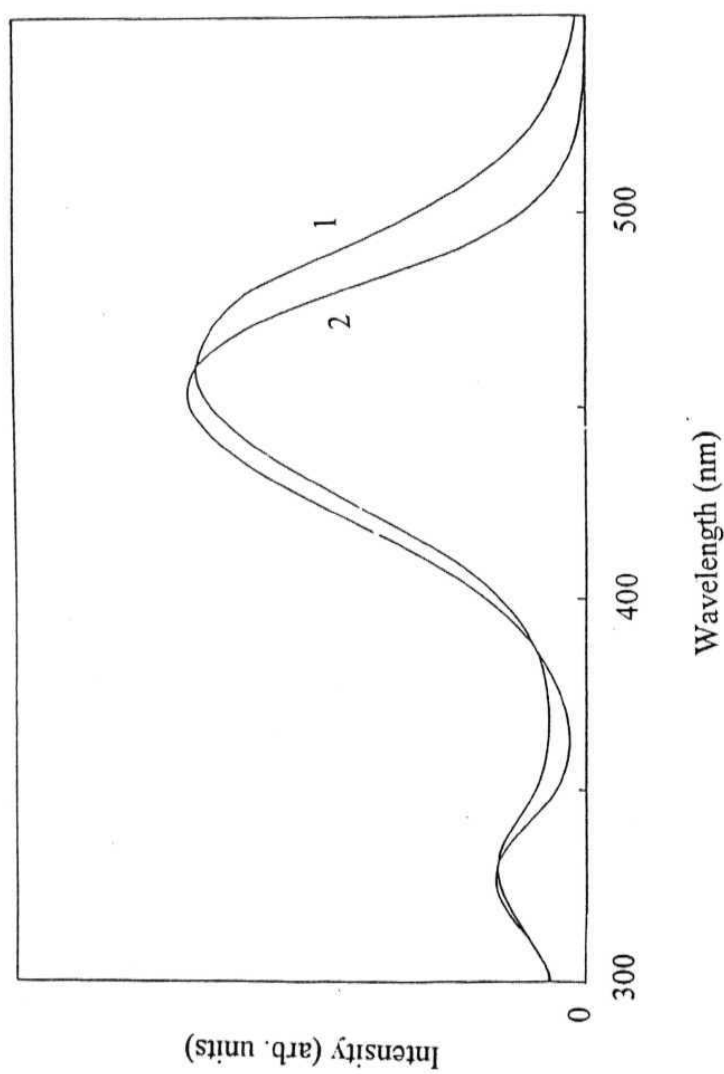
Fig. 5.10. Fluorescence excitation spectra of NEA in acetonitrile in the absence (1) and in presence (2) of 1.67 x 10⁻³ M of Co(NO₃)₂6H₂O. The fluorescence was monitored at 575 nm.

The changes in the fluorescence decay behaviour of NEA on the addition of the metal ions are illustrated in fig 5.11. It can be seen that with the addition of the salts the short-lived PET-quenched component disappears gradually and at a certain concentration of the metal ion, the decay becomes single-exponential with a lifetime very similar to that of NAM. This situation corresponds to complete recovery of the fluorescence. A further addition of the metal ions, however, leads to quenching of the fluorescence lifetime. The observation of significantly high FE in the presence of the quenching metal ions may appear quite unusual, particularly when the metal ion - fluorophore quenching interaction is taken into consideration. Since the experiments have been carried out with the hydrated salts of the metals, which may be contaminated with protons (resulting from partial hydrolysis of the salts), one can argue that the enhancement may result from the protonation of the dimethylamino group. In fact, we have observed that addition of protons also gives rise to considerable enhancement of the fluorescence signal. However, the possibility of the contaminated protons giving rise to FE has been discounted by some specific experiments. First, the proton concentration required for the same amount of FE is several folds higher than that of the metal ion concentration. Second, in most cases several times recrystallised salts showed FE not very different from those exhibited by nonrecrystallised salts. Third, one could hardly observe any difference in the FE values with a hydrated salt of cobalt, $[Co(H_2O)_6]Cl_2$ or its anhydrous salt prepared by following a standard procedure as described in chapter II. Fourth, in aqueous buffered solution of pH 7.5 (tris-buffered solution) when a majority of the receptor sites are protonated we could still observe 1.3-fold FE in the presence of Cu^{2+}. Since the fluorophore itself undergoes deprotonation at pH higher than 8, no experiment could be performed at higher pH required for this experiment.

We now attempt to rationalise whether it is possible to observe FE in the presence of the quenching ions. In the presence of the metal ions, the relative contribution
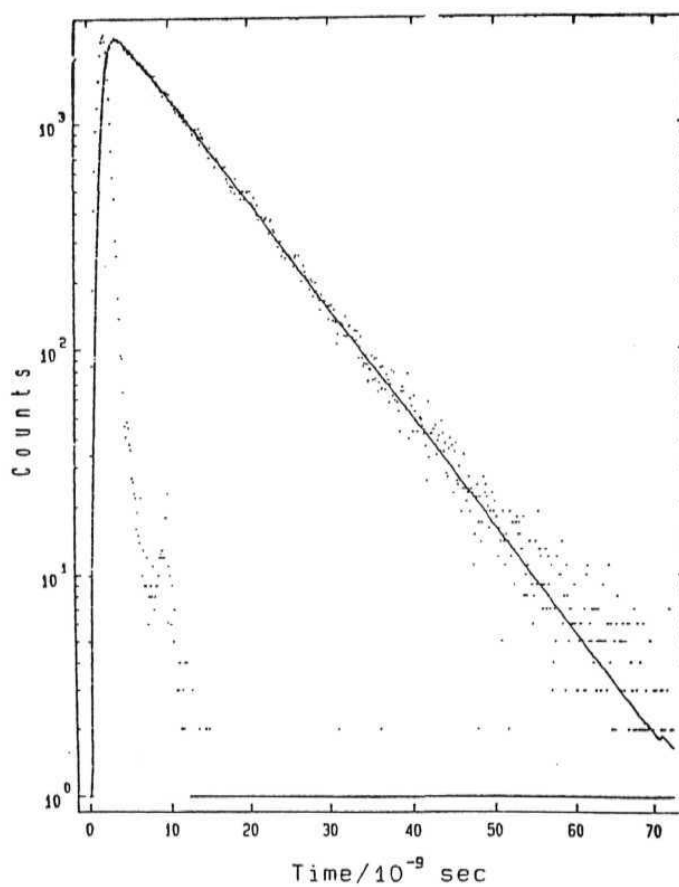
Fig. 5.11 Fluorescence decay curve of NEA in acetonitrile in the presence of 2.48 x 10^{-3} M of Co(NO$_3$)$_2$6H$_2$O. Shown also in the figure are the exciting lamp profile and the single exponential fit to the fluorescence decay. The fluorescence was monitored at 530 nm.

of two opposing factors, the metal ion - receptor binding that leads to enhancement of the fluorescence signal and the fluorophore-metal ion interaction that leads to fluorescence quenching, determines the net effect. It is therefore possible to observe a net FE in the presence of the quenching ions when the enhancement resulting from metal ion-receptor binding is greater than the reduction in the fluorescence intensity due to fluorophore-metal ion interaction. We note that even tliough the metal ions quench NAM fluorescence quite efficiently, they are not expected to be as efficient quenchers in the case of NEA, which contains the same fluorophore but with a short fluorescence lifetime. In the case of NAM, the fluorophore has a long lifetime of 11.4 ns in acetonitrile and 11.7 ns in tetrahydrofuran. On the other hand, the fluorescence lifetime of NEA is only ~ 0.2 ns. Since the lifetime of the two compounds differ by a factor of ≈ 55, then, according to Stern-Volmer equation, one needs 55-fold higher concentration of the metal ions in the case of NEA for identical reduction of the fluorescence intensity of the two compounds (assuming the quenching constant to be same in both cases). Obviously, the quenching influence of the metal ions becomes a less important factor for a system whose lifetime is quenched because of PET. That the quenching influence of a given metal ion is not very important in the case of a PET-quenched fluorophore can also be shown in the following manner. According to our quenching data, Co^{2+} is the most efficient quencher of NAM with k_q of 2.2 - 2.3 x 10^{10} $M^{-1}s^{-1}$. Therefore, according to Stern-Volmer equation, 1 mM concentration of Co^{2+} would quench the fluorescence intensity of NAM by 20.3 - 21.1 %. On the other hand, the same amount of Co^{2+} would reduce the fluorescence intensity of NEA by a factor of only ~ 0.4 %. It is therefore clear that for an already PET-quenched system, an otherwise strongly quenching metal ion acts as a poor quencher. In other words, the transition metal ions at moderate concentration can be treated as nonquenchers for an already PET-quenched system. Obviously, in the absence of quenching interaction, metal ion-binding with the receptor will only lead to fluorescence enhancement.

The results suggest that the simplest way to design an efficient fluorosensor for the quenching metal ion is to select the fluorophore and receptor component such that PET is maximised in the system. For an efficiently PET quenched system, the transition metal ions can be treated as nonquenching metal ions.

5.5.   References

1. a) A. Chattopadhyay, *Chem. Phys. Lipids,* 1990, *53,* 1; b) A. Chattopadhyay, *J. Biophys.* 1991, *191,* 59; c) A. Chattopadhyay, E. London, *Biochim. Biophys. Acta* **1988,** *938,* 24.

2. P.B. Ghosh, M.W. Whitehouse, *Biochem. J.* **1968,** *108,* 155.

3. K.J. Longmuir, O.C. Martin, R.E. Pagano, *Chem. Phys. Lipids,* 1985, *36,* 197.

4. N. Schmidt, G. Gercken, *Chem. Phys. Lipids,* 1985, *38,* 309.

5. J.R. Silvius, R. Leventis, P.M. Brown, M. Zuckermann, *Biochemistry,* 1987, *26,* 4279.

6. R.S. Fager, C.B. Kutina, E.W. Abrahamson, *Anal. Biochem.* 1973, *53,* 290.

7. S.J. Ferguson, W.J. Lloyd, G.K. Radda, *Biochem. J.* **1976,** *159,* 347.

8. a) S. Fery-Forgues, J.P. Fayet, A. Lopez, *J. Photochem. Photobiol. A: Chem.* 1993, *70,* 229; b) S. Saha, A. Samanta, *J. Phys. Chem.* **1998,** *102,* 7903.

9. J. Mori, T. Kaino, *Phys. Lett. A,* 1988, *127,* 259.

10. K.W. Streat, S.A. Krause, *Anal. Lett.* **1986,** *19,* 735.

11. S.D. Lytton, B. Mester, J. Libman, A. Shanzer, Z.I. Cabantchik, *Anal. Biochem.* 1992, *205,* 326.

12. S.D. Lytton, Z.I. Cabantchik, J. Libman, A. Shanzer, *Mol. Pharmacol.* 1991, *40,* 584.

13. H. Frost, R.E. Pacey, *Talanta,* 1989, *36,* 355.

14. a) A. Weller *Pure Appl. Chem.* **1968,** *16,* 115; b) D. Rehm, A. Weller, *Isr. J. Chem.* 1970, *8,* 259.

15. H. Siegerman, in *Techniques of Chemistry,* Ed., N.L. Weinberg, Wiley, New York, 1975, Vol. V, part II, p 803.

16. Rechthaler, K.; Köhler, G. *Chem. Phys.* **1994,** *189,* 99.

17. R.S. Drago, *Physical Methods in Chemistry,* Saunders College Publishing, Philadelphia, **1977.**

18. B. Valeur, In *Topics in Fluorescence Spectroscopy,* Ed., J.R. Lakowicz, Plenum Press, New York, **1994,** Vol. IV, p. 21.

19. M.M. Martin, P. Plaza, N. Dai Hung, Y.H. Meyer, J. Bourson, B. Valeur, *Chem. Phys. Lett.* **1993,** *202,* 425.

20. M.M. Martin, P. Plaza, Y.H. Meyer, L. Begin, J. Bourson, B. Valeur, *J. Fluores.* 1994,4,271.

21. M.M. Martin, P. Plaza, Y.H. Meyer, F. Badaoui, J. Bourson, J.P. Lefebvre, B. Valeur, *J. Phys. Chem.* 1996,*100,* 6879.

22. J-F. Letard, R. Lapouyade, W. Rettig, *Pure Appl. Chem.* 1993, *65,* 1705.

23. P. Dumon, G. Jonasauskas, F. Dupuy, P. Pee, C. Rulliere, J.-F. Letard, R. Lapouyade, *J. Phys. Chem.* **1994,** *98,* 10391.

24. R. Mathevet, G. Jonasauskas, C. Rulliere, J.-F. Letard, R. Lapouyade, *J. Phys. Chem.* 1995,99,15709.

25. A.W. Varnes, R.B. Dodson, E.L. Wehry, *J. Am. Chem. Soc.* 1972, *94,* 946.

26. J.A Kemlo, T.M. Shepherd, *Chem. Phys. Lett.* 1977, *47,* 158.

27. A.P. de Silva, H.Q.N. Gunaratne, J.L. Habib-Jiwan, C.P. McCoy, T.E. Rice, J.P. Soumillion, *Angew. Chem. Int. Ed Engl.* 1995, *34,* 1728.

1,8-NAPHTHALIMIDE AND 4-CHLORO-1,8-NAPHTHALIMDE
DERIVATIVES AS FLUOROSENSORS

The Photophysical behaviour and transition metal ion sensing ability of some *fluorophore - spacer - receptor* systems involving 1,8-naphthalimide (NP) and 4-chloro-1,8-naphthalimide (CNP) as the fluorophore component have been described in this chapter.

It is well known that the limiting value of FE of a *fluorophore - spacer - receptor* system in the presence of a guest is determined by the factor by which the fluorescence yield of the multi-component system is lower than that of the bare fluorophore.[1,2] Most often, one compares the fluorescence yields of the PET fluorosensor and the bare fluorophore to find out the upper limiting value of FE. Since FE can be induced by a number of mechanisms (stated in the first chapter of the thesis) other than the commonly used PET,[1,2] we thought that it might be possible to exceed the PET-limiting value of FE if one can couple some additional mechanism of FE with the PET. In order to explore the usage of more than one mechanism for the construction of the fluorosensors, that are expected to be more efficient than those involving only one mechanism, we have undertaken this work on the *fluorophore-spacer-receptor* systems (NPDEA, NPDPA, NPDBA, NPPED, NPNED, CNPDEA, CNPDPA, CNPPED and CNPNED), shown in Chart 6.1. The rationale behind the selection of these two fluorophores can be understood from the following discussion.

Realising that the transition metal salts are usually hydrated,[3] one expects the microscopic polarity around the fluorophore to increase on addition of these salts to a solution of the sensor in a nonpolar medium. Therefore, if the chosen fluorophore

NPDEA

NPDPA

NPDBA

NPPED

NPNED

CNPDEA

CNPDPA

CNPPED

CNPNED

NPNE

CNPNB
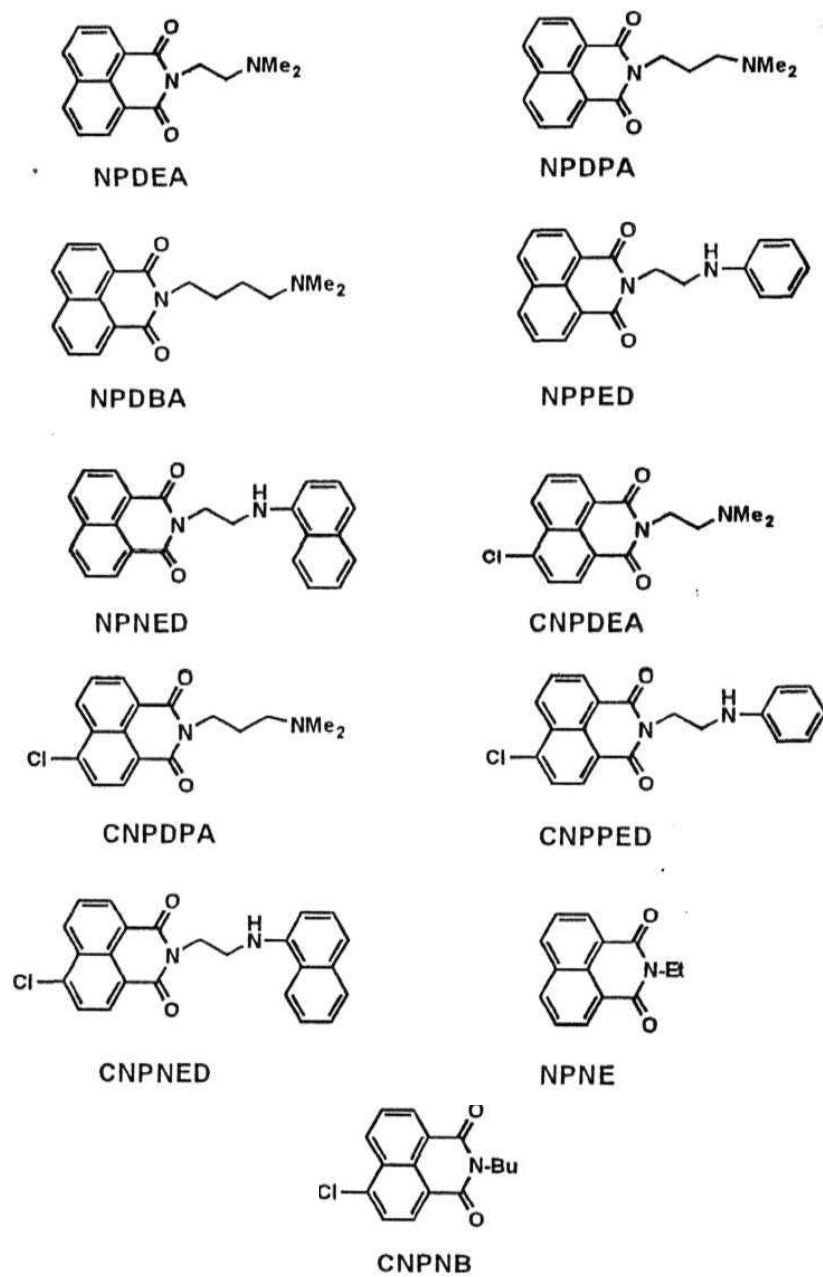
Chart 6.1

component for the design of the *fluorophore - spacer - receptor* system is such that its fluorescence efficiency in aqueous media is higher than that in nonpolar media, then, in the presence of the transition metal salts, one can expect FE due to (i) the suppression of intramolecular PET communication between the fluorophore and the receptor as a result of binding of the metal ions with the receptor moiety and (ii) a change of the microscopic polarity around the fluorophore. NP and CNP have been chosen as the fluorophore components for the construction of the multi-component systems, primarily because of the fact that it is known that the fluorescence yield of NP in polar media is considerably higher than that in a nonpolar environment*[4] Moreover, the chosen fluorophores are expected to be electron deficient compared to 4-amino-l,8-naphthalimide (ANP) and hence, they fulfil one of the important requirements for the design of efficient PET fluorosensors.

NP and CNP derivatives have been the subject of several investigations. Redmond and coworkers investigated the photoactive nature of the 1,8-naphthalimide and bisnaphthalimide derivatives in various biological environments.[4b] NP and bisnaphthalimide derivatives are used as effective anticancer agents.[5] Sulfonated derivatives of these compounds are good antiviral agents with selective *in vitro* activity against the human immunodeficiency virus, HIV-1.[6] Brominated mono and bisnaphthalimide derivatives have been used as photochemotherapeutic inhibitors for enveloped viruses in blood and blood products.[7] The high efficiency of the photoactivity and the DNA-intercalation has also prompted to use these derivatives as the sequence-specific DNA- photonucleases.[8] Amino derivatives of NP are known to exhibit polarity sensitive absorption and fluorescence spectra.[9] Kossanyi and coworkers observed dual emission for N-phenyl derivative of 2,3-naphthalimide.[10] The pH sensitive fluorescence response of CNPDEA has been reported earlier by Pardo[11] and de Silva.[12] However, no

---

*CNP *also exhibits a similar behaviour (vide section 6.3.3).*

studies have so far been undertaken on metal ion induced fluorescence response of this system and other systems depicted in Chart 6.1.

6.1.   Redox behaviour and driving force for PET

As stated in chapter III, ANP is a fairly electron rich fluorophore that shows an oxidation peak at 1.27 V. Considering that N-alkyl derivatives of NP and CNP would be the most appropriate reference fluorophore for the multi-component systems studied in this chapter, the redox behaviour of NPNE and CNPNB has been investigated. Interestingly, both of them show no oxidation peak between 0 and 2 V. Quite obviously, NPNE and CNPNB are electron deficient compared to ANP and certainly, are better fluorophore components for the design of PET fluorosensors. The reduction potentials have been measured to be -1.00 V and -0.85 V for NPNE and CNPNB respectively. Having measured these potentials, the thennodynamic driving force (AG*) for PET in the multi-component systems has been estimated using equn.2.13.[13] The various quantities used for the estimation of $\Delta G*$ values are indicated in Table 6.1. E_{ox} values for the receptors have been obtained from the literature.[14] Measured AG* values for various receptor-fluorophore combinations are collected in the Table 6.1. According to the data presented in this Table, PET is thermodynamically feasible for all the systems and AG* values are far more exergonic than those obtained in the case of ANPDEA and ANPPED[†], which contain a relatively electron rich fluorophore component, ANP.

6.2.   Molecular structures of NPDPA, NPPED and NPNED

Since it was possible to grow single crystals for NPDPA, NPPED and NPNED, the structures have been determined by X-ray crystallography. The motivation behind the structure determination of these multi-component systems was to find out whether most

---

[†]*ΔG* values for these systems are again shown in this Table for comparison.*

Table 6.1. Free energy changes (AG*) associated with PET in systems containing various fluorophores and receptors.

System	E_{red}(fluor) (V)[a]	$E_{0,0}$ (kcal/mol)[b]	AG* (kcal/mol)[c]
NPDEA			
NPDPA			-44.6
NPDBA	-1.0	79.0	
NPPED			-44.4
NPNED			-44.9
CNPDEA			
CNPDPA			-46.0
CNPPED	-0.85	76.9	-45.8
CNPNED			-46.2
ANPDEA	-1.61	55.04	-6.6
ANPPED			-6.4

[a] E_{red} values (vs Ag/AgCl electrode) of the fluorophore components (NPNE and CNPNB) were measured following procedures as described in sec. 2.7, the cyclic voltammetric traces for the reduction of NPNE and CNPNB were found to be reversible; [b] $E_{0,0}$ was estimated from the highest energy fluorescence maxima of the corresponding fluorophore components, NPNE and CNPNB in acetonitrile. [c] ΔG* calculations were made using equn. 2.13[13], E_{ox} values of the receptor moieties (0.49, 0.50 and 0.48V for triethylamine, N-methylaniline and N,N-dimethyl-1-aminonaphthalene respectively) were obtained from ref. 14. The oxidation potential of triethylamine was corrected for Ag/AgCl electrode by subtracting 0.27V from the measured potential against SCE electrode. The free energy change values are applicable in polar solvents such as acetonitrile.

of these systems exist in more than one conformation in the solid state as well.[¶] The existence of two definite conformers, one with a dihedral angle of 175° (N1, C13, C14 and N2) and the other with 71° (N3, C33, C34 and N4), is clearly evident from the

---

[¶] The biexponential nature of the fluorescence decay of most of the multi-component systems studied in the thesis is indicative of the existence of at least two conformers in the solution.

molecular structure of NPPED, shown in fig.6.1. Interestingly, however, for the two other systems, this behaviour could not be observed. This observation suggests that the molecular structure of a flexible system in the solution could be quite different from that in the solid state. The crystal structure data of these systems are presented in Table 6.2-6.4 and in the appendix.
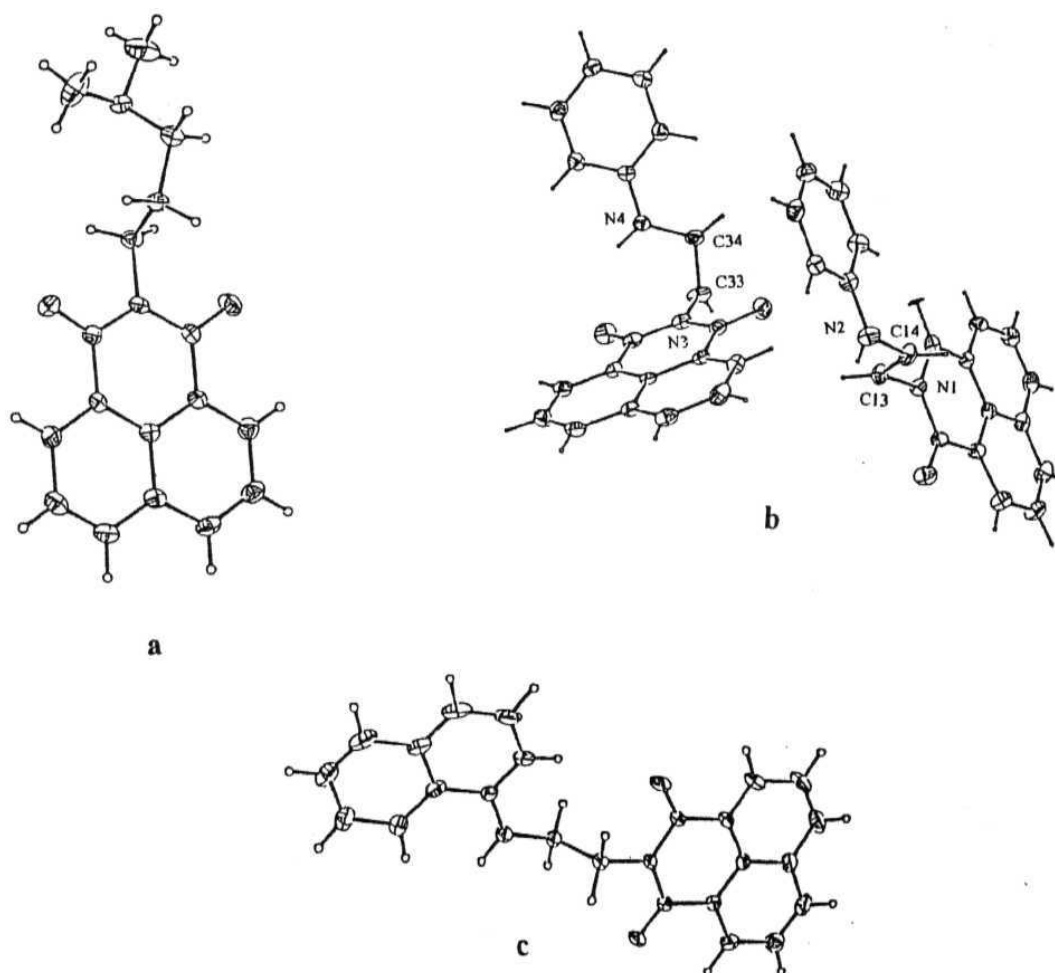
Fig. 6.1. Ortex diagrams of (a) NPDPA, (b) NPPED and (c) NPNED.

Table 6.2. Crystal data and structure refinement for the molecule, NPDPA.

Identification code	NPDPA
Empirical formula	$C_{17} H_{18} N_2 O_2$
Formula weight	282.33
Temperature	293(2) K
Wavelength	0.71073 Å
Crystal system	Monoclinic
Space group	P_2_1/a
Unit cell dimensions	a = 10.011(5) Å alpha = 90º
	b = 14.194(4) Å beta = 95.14(4)º
	c = 10.209(6) Å gamma = 90º
Volume	1444.8(12) Å^3
Z	4
Calculated density	1.298 Mg/m^3
Absorption coefficient	0.086 mm^{-1}
F(000)	600
Crystal size	0.48 x 0.40 x 0.70 mm
Crystal colour	Colourless
9 Range for data collection	2.00 to 27.47º
Index ranges	0<=h<=12, 0<=k<=18, -13<=l<=13
Reflections collected / unique	3489 / 3312 [R(int) = 0.0981]
Completeness to 29 = 27.47	96.1%
Refinement method	Full-matrix least-squares on F^2
Data / restraints / parameters	3312 / 0 / 193
Goodness-of-fit on F^2	1.137
Final R indices [I>2σ(I)]	R1 = 0.0601, wR2 = 0.1848

R indices (all data)	R1 = 0.1489, wR2 = 0.3010
Extinction coefficient	0.034(4)
Largest diff. peak and hole	0.720 and -0.674 e. A^{-3}

Table 6.3. Crystal data and structure refinement for molecule, NPPED.

Identification code	NPPED	
Empirical formula	$C_{20} H_{16} N_2 O_2$	
Formula weight	632.70	
Temperature	293(2) K	
Wavelength	0.71073 A	
Crystal system,	Triclinic	
Space group	P 1	
Unit cell dimensions	a = 8.520(11) A	alpha = 72.5885(3)°
	b= 13.391(3) A	beta = 83.0621(7)°
	c = 14.550(2) A	gamma = 81.2498(6)°
Volume	1561(2) A^3	
Z, Calculated density	2, 1.346 Mg/m^3	
Absorption coefficient	0.088 mm^{-1}	
F(000)	664	
Crystal size	0.44 x 0.52 x 0.60 mm	
θ range for data collection	1.61 to 24.99°	
Index ranges	0<=h<= 10, -15<=k<=15, -16<=l<=17	
Reflections collected / unique	5557 / 3060 [R(int) = 0.0000]	
Completeness to 2θ = 24.99	99.8%	
Refinement method	Full-matrix least-squares on F^2	

Data / restraints / parameters	3060 / 0 / 433
Goodness-of-fit on F^2	1.154
Final R indices [I>2σ (I)]	R1 = 0.0683, wR2 = 0.1991
R indices (all data)	R1 = 0.1151, wR2 = 0.2457
Largest diff. peak and hole	0.783 and -0.290 e. Å^{-3}

Table 6.4. Crystal data and structure refinement for molecule, NPNED.

Identification code	NPNED	
Empirical formula	$C_{24}H_{18}N_2O_2$	
Formula weight	366.40	
Temperature	293(2) K	
Wavelength	0.71073 Å	
Crystal system	Monoclinic	
Space group	$P2_1/c$	
Unit cell dimensions	a = 12.711(3) Å	alpha = 90°.
	b = 10.207(2) Å	beta = 105.97(5)°.
	c = 14.499(14) Å	gamma = 90°.
Volume	1808.5(19) Å^3	
Z	4	
Calculated density	1.346 Mg/m^3	
Absorption coefficient	0.087 mm^{-1}	
F(000)	768	
Crystal size	0.40 x 0.60 x 0.60 mm	
Crystal colour	Orange	
θ range for data collection	2.47 to 28.87°.	

Index ranges	-17<=h<=16, -3<=k<=12, 0<=l<=15
Reflections collected / unique	3318 / 3172 [R(int) = 0.0194]
Completeness to 2θ = 28.87	63.4%
Refinement method	Full-matrix least-squares on F^2
Data / restraints / parameters	3172 / 0 / 254
Goodness-of-fit on F^2	1.063
Final R indices [I>2σ(I)]	R1 = 0.0609, wR2 = 0.1694
R indices (all data)	R1 = 0.1136, wR2 = 0.2277
Extinction coefficient	0.011(3)
Largest diff. peak and hole	0.214 and -0.249 e.Å^{-3}

6,3.   Spectral characteristics

6.3.1. Absorption spectra

The UV-Vis absorption spectra of the multi-component systems have been studied in THF and AN. The absorption spectra of NPDPA and CNPDPA in THF are shown in fig.6.2 and those in AN are presented in fig. 6.3. The absorption spectra of these systems exhibit vibronic structures in both THF and AN. That the spectral behaviour of these multi-component systems is very similar to those of the respective fluorophore components is evident from fig. 6.4 where the spectral behaviour of NPNE in various solvents has been illustrated.

6.3.2. Flu orescen ce spectra

The fluorescence spectra of the multi-component systems have been studied in THF and AN. The fluorescence spectra of NPDPA and CNPDPA in THF are depicted in fig. 6.2 and those in AN are presented in fig 6.3. The spectral data have been collected in Table 6.5 and 6.6. Both NP and CNP derivatives display structured fluorescence in nonpolar media such as THF with the maximum appearing at around 380 nm and 388 nm
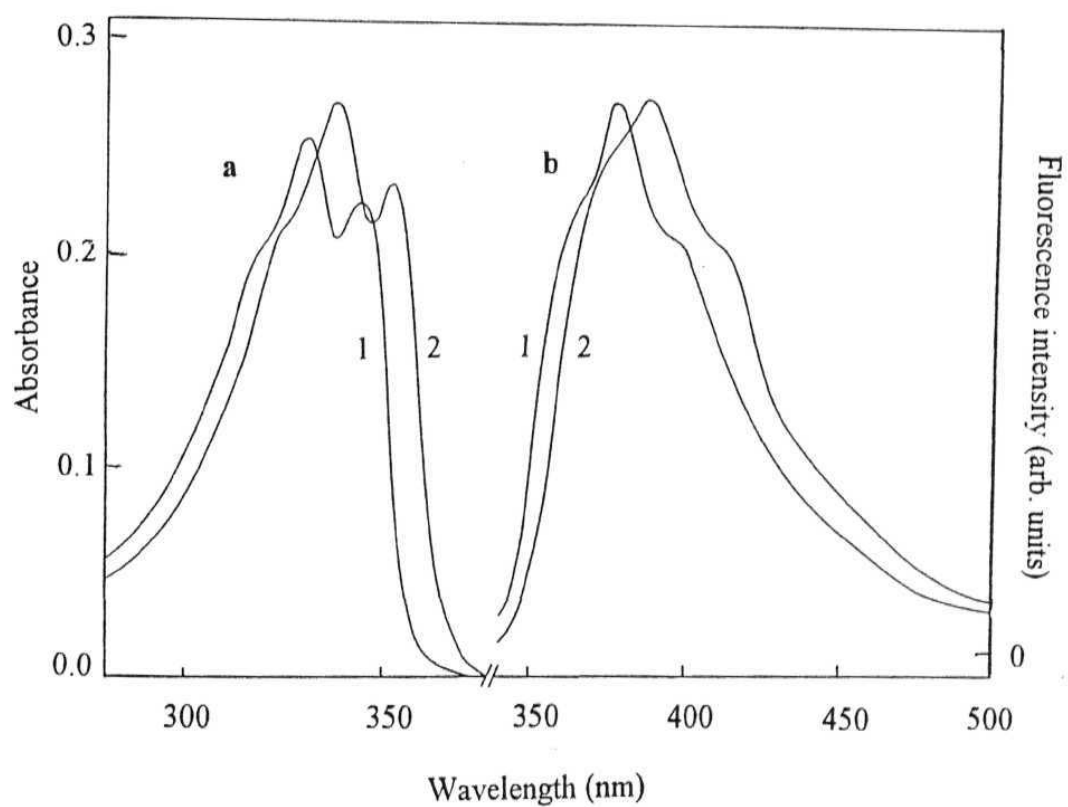
Fig. 6.2. Absorption (a) and fluorescence (b) spectra of NPDPA(J) and CNPDPA (2) in THF.

Fig. 6.3. Absorption (a) and fluorescence (b) spectra of NPDPA(1) and CNPDPA (2) in AN.
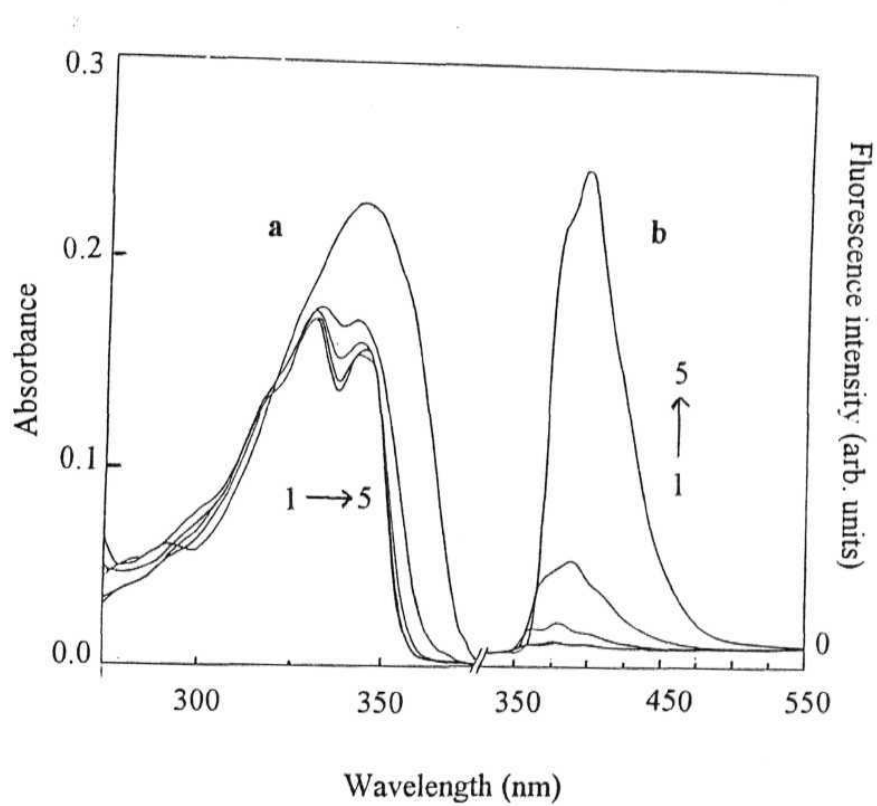
Fig. 6.4. Absorption (a) and fluorescence (b) spectra of NPNE in (1) 1,4-dioxane, (2) THF, (3) AN, (4) MeOH and (5) water. λ_{ex} was 320 nm.

Table 6.5 Absorption and fluorescence spectral data of NP derivatives in THF and AN.

Solvent	Property	Compound					
		NPDEA	NPDPA	NPDBA	NPPED	NPNED	NPNE
THF	$\lambda_{max}(abs)$	320 (s)	320 (s)	320 (s)	320(s)	320(s)	315 (s)
		330	330	330	331	332	330
	(nm)	341	342	340	342	343	343
	$\lambda_{max}(flu)$	357	357	356	356	355	360
		380	380	380	380	380	377
	(nm)	398(s)	398(s)	398(s)	399(s)	399(s)	396(s)
AN	$\lambda_{max}(abs)$	319(s)	319(s)	320(s)	320(s)	320(s)	315(s)
		330	330	330	330	331	330
	(nm)	341	341	340	341	340	343
	$\lambda_{max}(flu)$	362	363	363	364	363	362
		384	385	380	381	380	379
	(nm)	400(s)	400(s)	400(s)	400(s)	400(s)	400(s)

The concentrations of the solutions were ~ 10^{-5} M. λ_{ex} for the measurement of the fluorescence spectra was 320 nm.

Table 6.6 Absorption and fluorescence spectral data of CNP derivatives in THF and AN.

Solvent	Property	Compound				
		CNPDEA	CNPDPA	CNPPED	CNPNED	CNPNB
THF	$\lambda_{max}(abs)$	323(s)	325(s)	325(s)	326(s)	325(s)
		341	341	340	340	337
	(nm)	352	352	353	353	353
	$\lambda_{max}(flu)$	375	375	375	376	372
		388	388	390	391	387
	(nm)	412(s)	413(s)	415(s)	415(s)	400(s)
AN	$\lambda_{max}(abs)$	324(s)	324(s)	325(s)	325(s)	325(s)
		340	338	340	340	337
	(nm)	352	352	353	353	352
	$\lambda_{max}(flu)$	375	375	375	375	372
		387	390	391	390	389
	(nm)	413(s)	413(s)	414(s)	415(s)	400(s)

The concentrations of the solutions were ~ 10^{-5} M. λ_{ex} for the measurement of fluorescence spectra was 320 nm.

respectively. The vibronic band structures of NP and CNP derivatives disappear with increase in the polarity of the medium with no significant shift of the band maxima. For both NP and CNP derivatives, the fluorescence originates from a π-π^* state,[1] and as expected, there is a fairly good mirror image relationship between the absorption and the fluorescence spectra.

6.3.3.   *Fluorescence quantum yield*

The fluorescence quantum yields of NPNE and CNPNB have been measured in various solvents and the values are shown in Table 6.7. The fluorescence yield is relatively low in non-polar media such as THF; however, with an increase in the polarity of the media, the yield increases significantly. The fluorescence quantum yield of NPNE in water is higher than that in THF by a factor of 63, whereas this factor is 7.7 for CNPNB.

The fluorescence quantum yields of the multi-component systems are significantly lower than those of NPNE and CNPNB in any given solvent (Table 6.8) indicating that PET is efficient in the multi-component systems. The ratio (F) of the fluorescence yield of the constituent fluorophore to that of the *fluorophore-spacer-receptor* system that gives an indication of the extent of PET in the systems is also shown in Table 6.8. Evenjthough PET is thermodynamically highly feasible in all the systems; the actual extent of PET in any system depends on factors such as the fluorophore-receptor distance, the relative orientation of the two components, etc. It can be seen from Table 6.8 that among all the systems studied, F is the highest for NPPED. The extent of PET in CNPPED is also quite appreciable. These observations are consistent with the calculated AG* values for PET. Further, one can see that for a given set of compounds, say NP derivatives, the extent of PET is highest for the system with two methylene spacer

---

ǂ whereas in the case of the 4-methoxy-1,8- naphthalimide derivatives, the fluorescence was found to originate from a charge transfer state that is situated below the π-π^* state (chapter IV).

Table 6.7. Fluorescence quantum yield of NPNE and CNPNB in various solvents.[a]

Solvent	NPNE	CNPNB
1,4-Dioxane	3.1×10^{-3}	2.4×10^{-2}
Tetrahydrofuran	3.8×10^{-3}	2.0×10^{-2}
Acetonitrile	1.3×10^{-2}	6.0×10^{-2}
Methanol	4.4×10^{-2}	0.14
Water	0.24	0.15

[a]*1,8-Naphthalimide was used as the reference compound (ϕ_f of 5.0×10^{-2} in acetonitrile)[4a] for the measurements of the fluorescence quantum yields.*

Table 6.8. Fluorescence quantum yield of various systems and the factor (F) representing the ratio of the fluorescence yield of the constituent fluorophore to that of the multi-component system.

Compound	THF		AN	
	ϕ_f	F	ϕ_f	F
NPDEA	3.0×10^{-4}	37	6.9×10^{-3}	6
NPDPA	5.6×10^{-4}	20	9.6×10^{-3}	4
NPDBA	2.9×10^{-3}	4	9.1×10^{-3}	4
NPPED	2.8×10^{-3}	40	1.1×10^{-4}	360
NPNED	4.8×10^{-3}	2.3	3.5×10^{-3}	11.5
NPNE	1.1×10^{-2}	1	4.0×10^{-2}	1
CNPDEA	1.8×10^{-4}	105	5.4×10^{-4}	110
CNPDPA	1.1×10^{-3}	18	1.6×10^{-3}	38
CNPPED	3.1×10^{-4}	65	5.2×10^{-4}	115
CNPNED	2.2×10^{-3}	9	1.3×10^{-3}	46
CNPNB	2.0×10^{-2}	1	6.0×10^{-2}	1

1,8-Naphthalimide was used as the reference compound (ϕ_f of 5.0×10^{-2} in acetonitrile)[4a] for the measurements of the fluorescence quantum yields.

units. With an increase in the number of the methylene group! the fluorescence yield of the system increases indicating a decrease of PET in the system.

The fluorescence lifetimes of NPNE and CNPNB were found to be lower than the pulse width of the flash lamp used in the single photon counting instrument (vide chapter II). The fluorescence lifetimes of the multi-component systems were expected to be even lower due to PET. In view of this, the fluorescence decay behaviour of the systems could not be studied.

6.4.   The effect of the metal ions

6.4.1. A bsorption spectra

The transition metal ion induced changes in the absorption spectra of NPDPA and CNPDPA are illustrated in fig. 6.5 and 6.6 respectively. As observed with the earlier systems, the present systems too exhibit spectral changes on addition of the metal ions. The nature of the spectral changes was found to be different for different metal ions and in many cases, it was found that the nature of the spectral change was even different for different salts of a given metal ion. This observation is perhaps not surprising when taken into consideration that (i) many of these added salts contribute to the absorption in the spectral range of interest, (ii) the contribution to absorption is often different for different salts of a given metal ion and (iii) most importantly, the coordination chemistry of the metal ions studied is very different. In view of these, no quantitative information could be obtained from the metal ion induced changes in the absorption spectra of the systems.

6.4.2.   Fluorescence spectra

Representative spectra of the multi-component systems, NPDEA and CNPDEA in the presence of different concentrations of Ni^{+2} are shown in fig. 6.7 and 6.8 respectively to illustrate the effect of the transition metal ions on the fluorescence spectra of the systems. A definite pattern that emerges from the investigations carried out on
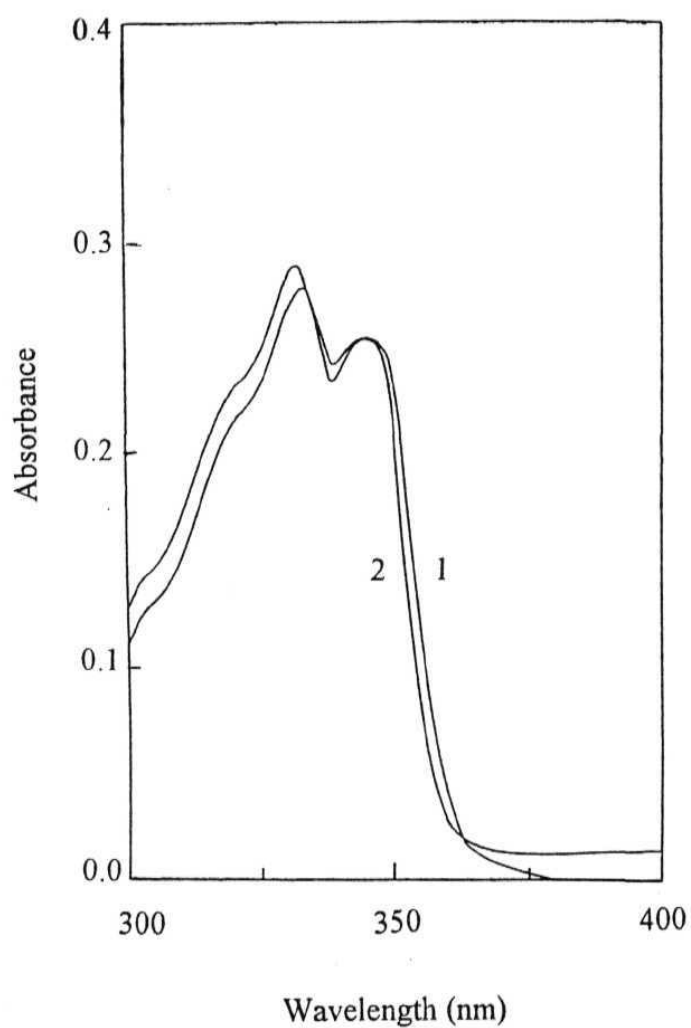
Fig. 6.5. Absorption spectra of NPDPA in AN for two different concentrations of
$Zn(H_2O)_6(ClO_4)_2$ *The concentrations of Zn^{+2} for the spectra labelled J and 2 are 0 and*
1.2 x 10^{-4} M respectively.
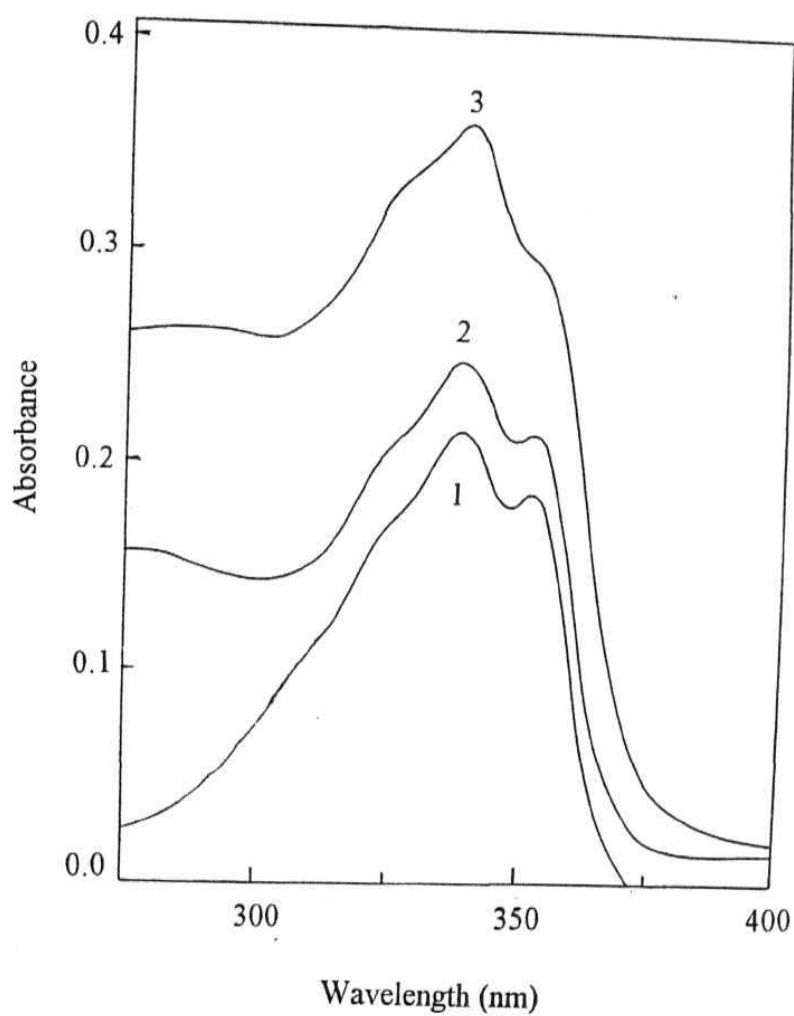
Fig. 6.6. Absorption spectra of CNPDPA in AN for different concentrations of $Cu(H_2O)_3(NO_3)_2$. The concentrations of Cu^{+2} for the spectra labelled 1 to 3 are 0, 5.9 x 10^{-5} and 1.8 x 10^{-4} M respectively.
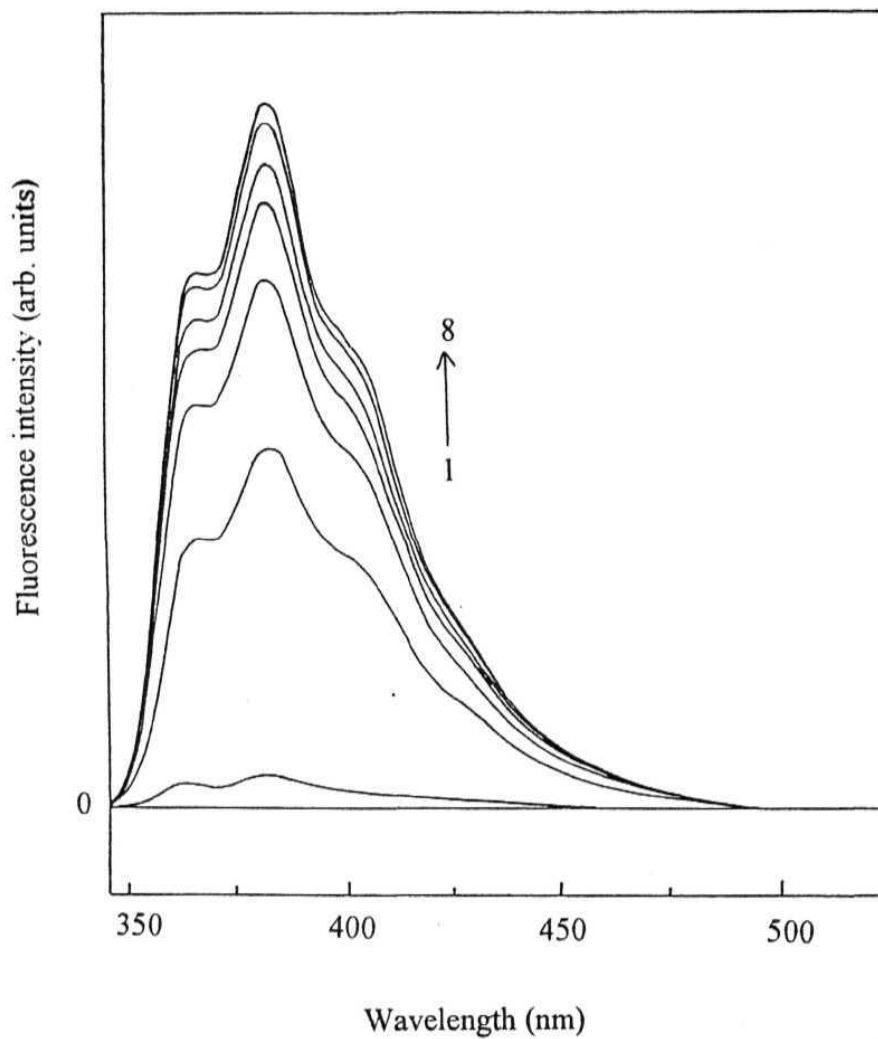
Fig. 6.7. Fluorescence response of NPDEA in THF (10^{-5} M) for different concentrations of Ni(H$_2$O)$_6$(ClO$_4$)$_2$. Ni^{+2} concentrations are 1) 0, 2) 3.8 x 10^{-5}, 3) 1.5 x 10^{-4}, 4) 1.9 x 10^{-4}, 5) 2.6 x 10^{-4}, 6) 3.8 x 10^{-4}, 7) 4.9 x 10^{-4} and 8) 8.7 x 10^{-4} M. λ_{ex} = 320 nm.
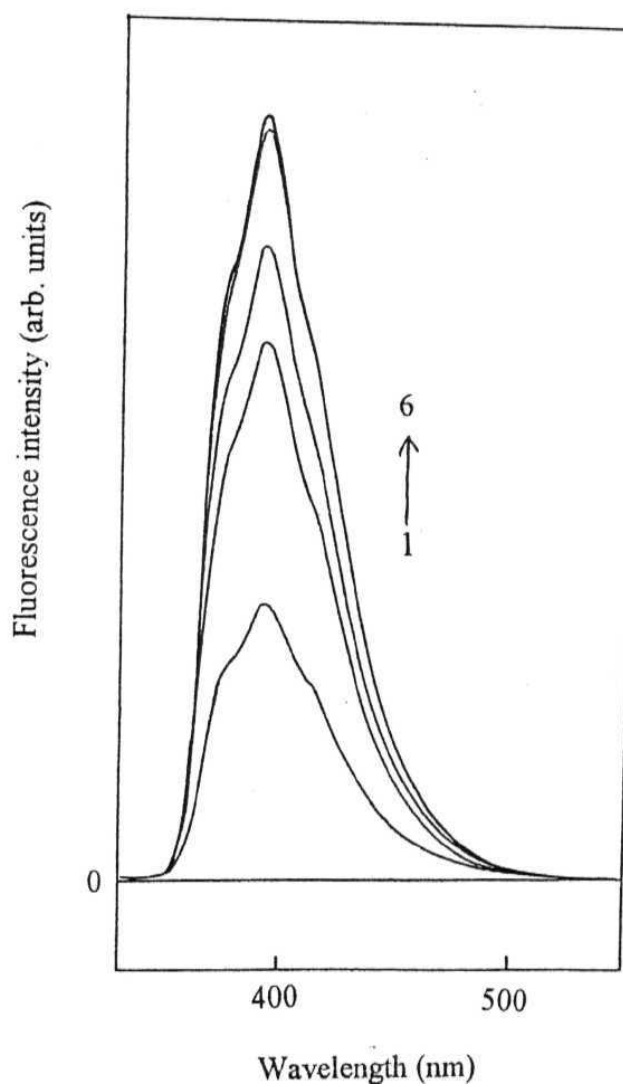
Fig. 6.8. Fluorescence response of CNPDEA in THF (10^{-5} M) in the presence of various concentrations of $Ni(H_2O)_6(ClO_4)_2$. Ni^{+2} concentrations are 1) 0, 2) 1.1 x 10^{-4}, 3) 2.2 x 10^{-4}, 4) 4.3 x 10^{-4}, 5) 1.3 x 10^{-3} and 6) 1.6 x 10^{-3} M. $\lambda_{ex} = 320$ nm.

these systems is that the addition of any metal ion at low concentration leads to an increase in the fluorescence efficiency of the system. Further addition leads to an increase in the intensity of fluorescence with less efficiency. Beyond a certain concentration of the metal ion, fluorescence quenching could be observed. No significant spectral shift could be observed with the present systems. The maximum FE values obtained for various derivatives of NP and CNP in the presence of different metal ions are collected in Table 6.9 - 6.12. In consistent with the observations made earlier for other systems, the FE values are the highest for systems with two methylene spacer units. The highest FE could be observed with NPDEA in the presence of nonquenching Zn^{+2} ion. It is noteworthy that even efficient quenching metal ions such as Fe^{+3} and Cr^{+3} give rise to excellent FE. However, the most interesting observation with the present systems is that the measured FE values are far in excess of the limiting values of FE determined by PET in the systems.

As evident from the studies made in the earlier chapters, there is nothing surprising in observing FE in the presence of metal ions that are well known for their quenching abilities.[15] It obviously means that FE resulting from the receptor-metal ion interaction is much more significant than the metal ion induced quenching of the fluorophore.

If one takes into account the PET mechanism alone, then assuming complete recovery, one expects only 37-fold FE for NPDEA and 20-fold FE for NPDPA (table 6.8) in the presence of the metal ions that do not have any quenching ability. Since Zn^{+2} ion is known to possess the lowest quenching ability among the d-block metal ions, one expects not more than 37-fold FE of NPDEA in the presence of Zn^{2+}. However, one can see from Table 6.9, the FE value observed for NPDEA is as high as 2150 with non-quenching Zn^{+2} and 1800 with Ni^{+2} in THF. With Fe^{+3} and Cr^{+3}, the most efficient quenchers among the first row of transition metal ions,[15] the observed FE values are 430 and 350 respectively.

Table 6.9 Fluorescence output of NPDEA, NPDPA and NPDBA as a function of different metal ion input in tetrahydrofuran and acetonitrile.[a]

Input Metal ion	NPDEA				NPDPA				NPDBA			
	THF		AN		THF		AN		THF		AN	
	[Salt][b] /M	FE[c,d]	[Salt][b] /M	FE[c,d]	[Salt][b] /M	FE[c,d]	[Salt][b] /M	FE[c,d]	[Salt][b] /M	FE[c,d]	[Salt][b] /M	FE[c,d]
Cr^{+3}	8.0×10^{-4}	350	6.0×10^{-5}	44	4.6×10^{-4}	50	2.0×10^{-5}	27	3.0×10^{-4}	1.0	2.5×10^{-4}	7.9
Mn^{+2}	1.6×10^{-4}	450	2.0×10^{-4}	65	4.1×10^{-4}	75	8.0×10^{-5}	110	5.5×10^{-4}	9.0	2.0×10^{-4}	8.9
Fe^{+3}	4.7×10^{-5}	430	3.4×10^{-5}	34	3.2×10^{-5}	70	1.7×10^{-5}	26	1.2×10^{-4}	7.9	1.1×10^{-4}	9.0
Co^{+2}	2.0×10^{-4}	450	1.2×10^{-4}	53	1.0×10^{-3}	60	4.9×10^{-5}	35	1.1×10^{-3}	6.1	3.1×10^{-4}	8.6
Ni^{+2}	9.7×10^{-4}	1800	1.8×10^{-4}	57	3.1×10^{-4}	120	8.8×10^{-5}	36	2.2×10^{-4}	8.8	2.0×10^{-4}	9.1
Cu^{+2}	5.9×10^{-4}	300	2.7×10^{-5}	48	2.8×10^{-4}	45	2.0×10^{-5}	34	4.6×10^{-4}	4.4	2.3×10^{-4}	1.3
Zn^{+2}	1.8×10^{-4}	2150	9.3×10^{-5}	50	1.2×10^{-4}	120	5.5×10^{-5}	35	6.8×10^{-4}	8.5	4.4×10^{-4}	9.4
H^{+}	1.7×10^{-2}	1775	5.4×10^{-4}	47	2.1×10^{-2}	340	5.4×10^{-4}	30	5.2×10^{-4}	40	5.2×10^{-4}	19.5

[a] *Experimental conditions: ~2×10^{-5} M solution of the compounds in tetrahydrofuran or acetonitrile was used at 298 K, λ_{ex} was 320 nm, excitation and emission band widths were 1.5 and 5 nm respectively;* [b] *represents the concentration of the metal ion for which maximum FE could be observed; any further increase in concentration led to fluorescence quenching;* [c] *with reference to the fluorescence intensity of the respective compounds in the absence of the metal ions,* [d] *± 15%.*

*Table 6.10 Fluorescence output of NPPED and NPNED as a function of different metal ion input in tetrahydrofuran and **acetonitrile.***

Input Metal Ion	NPPED				NPNED			
	THF		AN		THF		AN	
	[Salt] /M	FE	[Salt] /M	FE	[Salt] /M	FE	[Salt] /M	FE
Cr^{+3}	1.5×10^{-3}	1.3	2.5×10^{-3}	185	2.5×10^{-4}	1.6	1.2×10^{-4}	1.1
Mn^{+2}	2.3×10^{-3}	2.1	1.0×10^{-3}	900	7.5×10^{-3}	5.7	1.2×10^{-3}	7.1
Fe^{+3}	1.7×10^{-3}	2.0	2.2×10^{-3}	1140	6.5×10^{-4}	4.2	1.7×10^{-4}	4.8
Co^{+2}	2.0×10^{-3}	1.5	1.9×10^{-3}	7.5	5.4×10^{-4}	1.5	4.7×10^{-4}	1.1
Ni^{+2}	1.5×10^{-3}	1.2	4.1×10^{-4}	3.7	5.8×10^{-4}	1.4	1.0×10^{-4}	1.1
Cu^{+2}	3.3×10^{-3}	1.0	4.7×10^{-4}	136	2.0×10^{-4}	2.9	1.9×10^{-4}	2.6
Zn^{+2}	1.2×10^{-3}	1.1	3.1×10^{-3}	70	1.5×10^{-4}	26.0	6.6×10^{-4}	6.6
H^{+}	1.5×10^{-1}	25	4.0×10^{-2}	1930	6.8×10^{-2}	4.0	1.5×10^{-2}	9.1

Experimental conditions are described in the footnote of Table 6.9.

Table 6.11 Fluorescence output of CNPDEA and CNPDPA as a function of different metal ion input in tetrahydrofuran and acetonitrile.

Input Metal Ion	CNPDEA				CNPDPA			
	THF		AN		THF		AN	
	[Salt] /M	FE	[Salt] /M	FE	[Salt] /M	FE	[Salt] /M	FE
Cr^{+3}	6.1×10^{-4}	185	2.5×10^{-4}	260	1.5×10^{-4}	30	1.2×10^{-4}	90
Mn^{+2}	2.8×10^{-4}	780	1.0×10^{-4}	375	2.8×10^{-4}	70	1.0×10^{-4}	120
Fe^{+3}	1.3×10^{-4}	655	1.1×10^{-4}	315	1.3×10^{-4}	60	1.1×10^{-4}	115
Co^{+2}	5.4×10^{-4}	295	4.7×10^{-4}	375	8.0×10^{-4}	40	1.6×10^{-4}	125
Ni^{+2}	1.6×10^{-3}	660	2.5×10^{-3}	380	2.2×10^{-4}	68	2.0×10^{-4}	130
Cu^{+2}	5.8×10^{-4}	195	1.2×10^{-4}	320	2.3×10^{-4}	40	1.2×10^{-4}	100
Zn^{+2}	4.5×10^{-4}	735	1.1×10^{-4}	430	4.5×10^{-4}	70	2.2×10^{-4}	115
H^{+}	1.8×10^{-2}	761	1.3×10^{-3}	430	1.9×10^{-2}	85	6.25×10^{-4}	130

Experimental conditions are described in the footnote of Table 6.9.

Table 6.12 Fluorescence output of CNPPED and CNPNED as a function of different metal ion input in tetrahydrofuran and acetonitrile.

Input Metal Ion	CNPPED				CNPNED			
	THF		*AN*		*THF*		*AN*	
	[Salt]/M	FE	[Salt]/M	FE	[Salt]/M	FE	[Salt]/M	FE
Cr^{+3}	2.4×10^{-3}	50	2.0×10^{-3}	30	7.6×10^{-4}	5	1.2×10^{-4}	1.7
Mn^{+2}	3.1×10^{-3}	70	3.1×10^{-3}	50	4.1×10^{-4}	2	5.5×10^{-3}	9.5
Fe^{+3}	1.7×10^{-3}	80	7.1×10^{-4}	63	2.5×10^{-4}	8	1.1×10^{-4}	12
Co^{+2}	5.0×10^{-3}	45	5.8×10^{-3}	20	4.3×10^{-4}	3.5	8.0×10^{-4}	1.4
Ni^{+2}	6.0×10^{-3}	90	7.3×10^{-4}	46	6.2×10^{-3}	9	5.1×10^{-3}	30
Cu^{+2}	2.5×10^{-3}	15	8.6×10^{-4}	8	1.9×10^{-4}	2.5	8.6×10^{-4}	4
Zn^{+2}	3.0×10^{-3}	25	7.7×10^{-4}	20	5.4×10^{-4}	1.3	5.4×10^{-4}	1.2
H^{+}	1.0×10^{-2}	80	2.0×10^{-4}	95	1.0×10^{-2}	7	1.8×10^{-2}	11

Experimental conditions are described in the footnote of Table 6.9.

Even Mn^{+2} that contains five unpaired electrons in the high spin state, displays 450-fold enhancement. For NPDPA, even though the FE values are substantially lower in the range of 50-120, they are nevertheless much higher than the expected 20-fold FE. The FE values observed for NPDBA, CNPDEA and CNPDPA are also much higher than the PET limiting values. Interestingly, both NP and CNP derivatives containing anilino or naphthylamino receptor moieties exhibit rather low FE values (except for NPPED in AN). This observation perhaps suggests that the interaction between these electron deficient fluorophores and the aromatic amines (receptor) is strong enough not to allow efficient binding of the metal ions with these receptor moieties.

The extraordinarily large FE values, observed in the case of some NP and CNP derivatives, which are much in excess of the PET limiting values, might appear quite unusual. Neither the FE values of such large magnitude nor FE values higher than the

PET limiting values have been reported for any fluorophore metal ion combination, However, it is evident from the following discussion that this apparently unusual observation is simply the result of our novel sensor design principle in which two mechanisms of FE have been utilised, instead of commonly used PET mechanism alone.

Keeping in mind that the transition metal salts are usually hydrated, one expects an increase in the polarity of the immediate surroundings of the fluorophore on addition of the metal ions. We have chosen such fluorophore component in the design that apart from being electron deficient, displays fluorescence whose efficiency depends significantly on the polarity of the media. With increase in the polarity of the medium, the intersystem crossing efficiency in the fluorophore increases resulting in an increase in the fluorescence efficiency of the system.[4] It can be seen from Table 6.7 that for both NPNE and CNPNB, the fluorescence intensity is considerably higher in polar media. If it is assumed that the water molecules from the hydrated salts used in the study preferentially solvates the fluorophores by forming hydrogen bonds, then according to the data presented in Table 6.8, the fluorescence yield of the sensor systems NP as the constituting fluorophore unit can, in principle, go up by a factor ~63 in THF and 18 in acetonitrile. In such a situation, the observed FE, that is due to both metal ion binding and changes in the polarity of the microenvironment, can be as large as ~2300 (63 x 37) for NPDEA in THF, a value that is remarkably close to the maximum FE observed with this system in THF in the presence of non-quenching Zn^{+2}. In acetonitrile, while the expected maximum FE value for NPDEA is 108 (18 x 6), the observed value is 65. Taking into consideration of the two mechanisms of FE, the predicted values of FE for CNPDEA and CNPDPA (using the data from Table 6.7 and 6.8) in THF are 790 (7.5 x 105) and 135 (7.5 x 18). As can be seen, these values are not very different from the observed FE values.

The fact that a change in the microscopic polarity around the fluorophore induced

by the water molecules of the hydrated salts indeed leads to high FE values of the systems is also supported by the following observation. If our reasoning is correct, then one expects a significantly less FE with the anhydrous salts of the metals. Using anhydrous Co^{12} salt, the FE values observed for NPDEA and CNPDEA are only 9 and 2 respectively, whereas the FE values observed with the hydrated Co^{+2} salt are several folds higher. Second, multi-components systems involving a structurally related fluorophore but whose fluorescence efficiency does not depend on the polarity of the medium (e.g. OMNP derivatives), do not exhibit unusually high FE values.

In conclusion, the present chapter describes the metal ion sensing behaviour of some structurally simple NP and CNP derivatives. The magnitude of FE values observed for some of these systems in the presence of the quenching metal ions is quite unprecedented. Even though different mechanisms for the modulation of the fluorescence intensity of a given system are known for some time, this is the first time where more than one such mechanism have been used cooperatively to enhance the efficiency of a PET fluorosensor.

6.5. References

1. a) *Fluorescent Chemosensors for Ion and Molecular recognition*, ACS Symposium Series 538, Ed., A.W. Czarnik, American Chemical Society, Washington, DC, 1993. b) A.W. Czarnik, *Acc. Chem. Res.* 1994, *27,* 302; c) A.W. Czarnik, In *Topics in Fluorescence Spectroscopy,* Ed., J.R. Lakowicz, Plenum Press, New York, 1994, Vol. IV, p 49; d) M.E. Huston, K.W. Haider, A.W. Czarnik, *J. Am. Chem. Soc.* 1988, *110,* 4460.

2. a) A.P. de Silva, H.Q.N. Gunaratne, T. Gunnlaugsson, A.J.M. Huxley, C.P. McCoy, J.T. Rademacher, T.E. Rice, *Chem. Rev.* 1997, *97, 1515* and references therein; b) R.A. Bissel, A.P. de Silva, H.Q.N. Gunaratne, P.L.M. Lynch, G.E.M. Maguire, K.R.A.S. Sandanayake, *Chem. Soc. Rev.* 1992, *21,* 187; c) R.A. B.ssel, A.P. de Silva,

H.Q.N. Gunaratne, P.L.M. Lynch, G.E.M. Maguire, **K.R.A.S.** Sandanayake, *Top. Curr. Chem.* **1993,** *168,* 223; d) **A.P.** de Silva, H.Q.N. Gunaratne, G E M . Maguire, *J. Chem. Soc. Chem. Commun.* **1994,** 1213; e) A.P. de Silva, H.Q.N. Gunaratne, T. Gunnlaugsson, M. Nieuwenhuizen, *J. Chem. Soc, Chem. Commun.* 1996, 1967; f) A.P. de Silva, H.Q.N. Gunaratne, C. McVeigh, G.E.M. Maguire, P.R.S. Maxwell, E. Hanlon, *J. Chem. Soc, Chem. Commun.* 1996, 2191; g) A.P. de Silva, H.Q.N. Gunaratne, C.P. McCoy, *Nature* 1993, *364,* 42; h) A.P. de Silva, H.Q.N. Gunaratne, C.P. McCoy, *J. Chem. Soc. Chem. Commun.* 1996, 2399; i) A.J. Bryan, A.P. de Silva, S.A. de Silva, R.A.D.D. Rupasinghe, K.R.A.S. Sandanayake, *Biosensors,* 1989, *4,* 169.

3. a) **J.E. Huheey,** *Inorganic Chemistry: Principles of Structure and Reactivity,* **III** Ed., Harper and Row, New York, 1983; b) F.A. Cotton, G. Wilkinson, *Advanced Inorganic Chemistry: A Comprehensive Text,* Wiley-Interscience, New York, **1998,** p. 552.

4.   a) G. Saroja, A. Samanta, *J. Photochem. Photobiol. A: Chem.* 1994, *84,* 19; b) B.M. Aveline, S. Matsugo, R.W. Redmond, J. *Am. Chem. Soc.* **1997,** *119,* 11785.

5.   a) M.F. Brana, J.M. Castellano, C.M. Roldan, A. Santos, D. Vazquez, A. Jimenez, *Cancer Chemother. Pharmacal.* 1980, *4,* 61; b) M.F. Brana, J.M. Castellano, A.M. Sanz, CM. Roldan, *Eur. J. Med. Chem.* **1981,** *16,* 207.

6.   D. Rideout, R. Schinazi, CD. Pauza, K. Lovelace, L.C. Chiang, T. Calogeropoulou, M. McCarthy, J.H. Elder, *J. Cell Biochem.* **1993,** *51,* 446.

7.   a) T.C Chanh, D.E. Lewis, J.S. Allan, B.F. Sogandares, M.M. Judy, R.E. Utecht, J.L. Matthews, *AIDS Res. Hum. Retroviruses,* 1993, *9,* 891; b) T.C Chanh, B.J. Archer, R.E. Utecht, D.E. Lewis, M.M. Judy, J.L. Matthews, *Biomed. Chem. Lett.* **1993,** *3,* 555; c) **T.C.** Chanh, D.E. Lewis, M.M. Judy, B.F. Sogandares, G.R. Michalek, R.E. Utecht, H. Skiles, S.C. Chanh, J.L. Matthews, *Antiviral Res.* **1994,** *25,* 133.

8. C. Bailly, M. Brana, M.J. Waring, *Eur. J. Biochem.* **1996,** *240,* 195.

9. a) **D.** Yuan, R.G. Brown,./ *Phys. Chem. A,* 1997, *101,* 3461; b) D. Yuan, R.G. Brown, *J. Chem. Res (M).* 1994, 2337; c) M.S. Alexiou, V. Tychopoulos, S. Ghorbanian, J.H.P. Tynian, R.G. Brown, P.I. Brittain, *J. Chem. Soc. Perkin Trans.* 2, 1990, 837.

10. a) A. Demeter, T. Berces, L. Biczok, V. Wintgens, P. Valat, J. Kossanyi, *J. Phys. Chem.* 1996, *100,* 2001; b) A. Demeter, L. Biczok, T. Berces, V. Wintgens, P. Valat, J. Kossanyi,./. *Phys. Chem.* 1993, *97,* 3217; c) P. Valat, V. Wintgens, J. Kossanyi, L. Biczok, A. Demeter, T. Berces, *J. Am. Chem. Soc.* **1992,** *114,* 946.

11. a) A. Pardo, J.M.L. Poyato, E. Martin, J.J. Camacho, D. Reyman, M.F. Brana, J.M. Castellano, *J. Photochem. Photobiol. A: Chem.* 1986, *36,* 323; b) A. Pardo, E. Martin, J.M.L. Poyato, J.J. Camacho, M.F. Brana, J.M. Castellano, *J. Photochem. Photobiol. A: Chem.* 1987, *41,* 69; c) A. Pardo, E. Martin, J.M.L. Poyato, J.J. Camacho, J.M. Guerra, R. Weigand, M.F. Brana, J.M. Castellano, *J. Photochem. Photobiol. A: Chem.* 1989, *48,* 259; d) A. Pardo, J.M.L. Poyato, E. Martin, J.J. Camacho, D. Reyman, *J. Lumin.* 1990, *46,* 381.

12. L.M. Daffy, A.P. de Silva, H.Q.N. Gunaratne, C. Huber, P.L.M. Lynch, T. Werner, O.S. Wolfbeis, *Chem. Eur. J.* 1998, *4,* 1810.

13. a) A. Weller, *Pure Appl. Chem.* **1968,** *16,* 115; b) D. Rehm, A. Weller, *Isr. J. Chem.* **1970,** *8,* 259.

14. H. Siegerman, In *Techniques of Chemistry,* Ed., N.L. Weinberg, Wiley, New York, **1975,** Vol. V, part II.

15. a) A.W. Varnes, R.B. Dodson, E.L. Wehry, *J. Am. Chem. Soc.* **1972,** *94,* 946; b) J.A. Kemlo, T.M. Shepherd, *Chem. Phys. Lett.* **1977,** *47,* 158.

CONCLUDING REMARKS

A summary of the results presented in the thesis and the conclusion reached from this investigation have been described here. The scope of further work based on the present findings is also outlined in this chapter.

7.1.   Summary and Conclusion

The work embodied in this thesis deals with synthesis and study of the fluorescence response of some structurally simple multi-component systems with the *fluorophore-spacer-receptor* architecture in the presence of the first row of transition metal ions. The study has been undertaken with a view to find out whether it is possible to develop *simple* fluorescence 'off-on' signalling systems for the detection of the transition metal ions, well known for their fluorescence quenching abilities. Taking into consideration, the synthetic difficulties involved in developing fluorosensor for the transition metal ions following the 'receptor design' approach, where one is required to specially design a receptor to circumvent the quenching influence of the transition metal ions, we have concentrated on an alternative approach that mainly relies on right selection of the fluorophore component. The fluorophores have been chosen so as to maximise PET in the multi-component systems. The results amply demonstrate that it is possible for even the structurally simple *fluorophore-spacer-receptor* systems to exhibit excellent sensing behaviour towards the transition metal ions and that there is no need to specially design a receptor (following a synthetically more difficult route) just to circumvent the quenching influence of the transition metal ions.

The synthesis, purification and characterisation of the systems studied here comprise a significant part of the thesis work. First two multi-component systems, employing 4-amino-1,8-naphthalimide (ANP) moiety as the fluorophore component, have been synthesised and their fluorescence properties have been studied in the presence and absence of the transition metal salts. The sensing ability of the two systems, as evident from the metal ion induced fluorescence enhancement values, is extremely poor. The two factors that could be responsible for this behaviour have been identified as (i) inefficient PET in the multi-component system and (ii) fluorophore-metal ion quenching interaction because of electron rich nature of the constituting fluorophore, ANP.

Since the oxidation potential of 4-aminophthalimide, a fluorophore structurally very similar to ANP, is measured to be higher than that of ANP, one can expect the former to be relatively electron deficient. Consequently, the redox interaction between the fluorophore and the metal ion, which is often responsible for poor 'off-on' signalling ability of a multi-component system, is also expected to be reduced. Further, the electron deficient nature of the fluorophore is expected to enhance PET in the multi-component system and a relatively higher singlet state energy of 4-aminophthalimide (compared to ANP) is also likely to enhance PET in the system. In view of the above considerations, new multi-component systems using 4-aminophthalimide as the fluorophore have been synthesised and the fluorescence response of the systems has been studied in the presence and absence of the transition metal ions. This study shows that PET is most efficient for the systems with two methylene spacer units. The anilino moiety is found to be superior to the dialkylamino moiety as a receptor component. The fluorescence of the 4-aminophthalimide derivatives is 'switched on' in the presence of all the transition metal ions studied (including even Fe^{+3} and Cr^{+3}, reported to be highly efficient quenchers among the transition metal ions). The fluorescence enhancement is found to be associated with a red shift in the spectrum. This is most likely due to the metal ion

Concluding...

induced increase of the charge separation in the fluorophore. These results show for the first time that it is possible for the structurally simple multi-component systems to exhibit excellent sensory behaviour ('off-on') towards the quenching metal ions and as such there is no need to develop a receptor with special topology by following a relatively more complicated synthetic route.

Based on the above findings, we focussed our attention to another structurally similar fluorophore, 4-methoxy-l,8-naphthalimide. Unlike ANP (E_{ox} = 1.27 V), 4-methoxy-l,8-naph thalimide derivative, OMNPNB, does not show any oxidation in the range of 0 - 2 V. Quite obviously, this fluorophore is electron deficient when compared to ANP. Moreover, the charge separation in the excited state of this fluorophore is expected to be lower than that for the amino compound. One can therefore expect a higher energy for the fluorescent charge transfer state of the methoxy derivative. The higher singlet state energy and electron deficient nature of 4-methoxy-l,8-naphthalimide make it an ideal fluorophore component for the design of fluorosensor for the transition metal ions. Therefore, multi-component systems using 4-methoxy-l,8-naphthalimide fluorophore have been prepared and the Photophysical and metal sensing behaviour of these systems have been investigated. As in the previous case, PET is found to be most efficient for the system containing two methylene spacer units. The systems exhibit excellent fluorescence enhancement in the presence of various metal ions and protons. In the case of systems involving anilino and 1-naphthylamino receptor moieties, even though the fluorescence output in the presence of the transition metal ions is quite significant, the fluorescence could not be recovered completely. This behaviour has been rationalised taking into consideration two factors; metal ion-fluorophore binding and fluorophore-receptor interaction. It is suggested that for these two systems, the metal ion-receptor binding is not strong enough to cut-off completely the PET communication between the fluorophore and the receptor.

Amino-NBD derivatives represent one class of systems quite extensively used as fluorescence probes in biological studies. Quite naturally, we thought that it would be wortliwhile to explore the potential of amino NBD as a fluorophore component for the development of fluorosensor for the transition metal ions. The redox behaviour of 4-amino-NBD (NAM) has been studied first. The oxidation potential of NAM is found to be higher than that of ANP and AP. The multi-component system (NEA) involving NAM as the fluorophore component, dimethylamino group as the receptor and dimethylene group as the spacer has been synthesised. Photophysical investigation has been carried out on the constituting fluorophore, NAM as well. The steady state and time-resolved fluorescence experiments leave no doubt that the transition metal ions interact rather strongly with NAM both in the ground and excited state and thereby quench the fluorescence. A quantitative estimate of the quenching interaction of the fluorophore with the metal ions has been obtaincd by determining the quenching constants from the fluorescence intensity as well as the lifetime data. Even though the fluorescence quenching experiments suggest that NAM is not an appropriate fluorophore component for the design of transition metal ion sensor, interestingly however, NEA displays excellent fluorescence enhancement in the presence of the transition metal ions. The highest fluorescence output of NEA could be observed in the presence of nonquenching metal ion, Zn^{+2} and moderate values of fluorescence enhancement with other metal ions. Unlike the previous systems, the fluorescence enhancement of NEA is associated with a blue shift of the spectral maxima. This observation has been rationalised taking into consideration of the existing literature and likely binding site(s) of the metal ions. The results obtained with NEA may appear quite unusual for the fact that the fluorophore, NAM interacts strongly with the quenching metal ions both in the ground and excited state. The apparently puzzling observation has been accounted for taking into consideration of the difference in the fluorescence lifetime of the bare fluorophore and a

PET-quenched fluorophore. We have shown with the help of Stern-Volmer equation that the transition metal ions, which are generally very efficient quenchers of fluorescence, are not as efficient quencher in the case of an already PET-quenched fluorophore. This finding suggests the quenching influence transition metal ions need not be given any special consideration when PET in the multi-component system is very efficient. One should just ensure that the chosen fluorophore is such that PET between the receptor and the fluorophore is quite efficient.

Finally, we have developed systems based on fluorophores, 1,8-naphthalimide and 4-chloro 1,8-naphthalimide and studied their signalling abilities. While choosing these two fluorophores we were guided by the fact that these two systems, apart from being electron deficient, fluoresce strongly in polar environment. The addition of the transition metal salts, which are usually available in the hydrated form, is likely to enhance the fluorescence due to an increase in the microscopic polarity around the fluorophore. In other words, multi-component systems involving these two fluorophores provide an additional mechanism of fluorescence enhancement that was not possible with systems involving the fluorophores described so far.

It is gratifying to note that it is possible to observe fluorescence enhancement several folds higher than that suggested by the PET mechanism. Even though the microscopic polarity around the fluorophores (in the presence of the metal ions) is not known, it is observed in some cases that the FE values could best be explained assuming that the water molecules are in the close proximity of the fluorophores thereby creating a polarity not very different that of water.

7.2.   Scope of Further Work

The present investigation shows for the first time that it is possible for a structurally very simple system to exhibit 'off-on' fluorescence signalling for the

transition metal ions. One just needs to select a fluorophore so as to maximise **PET** in the *fluorophore-spacer-receptor* system. We have shown **that** the quenching interaction between the fluorophore and the metal ions becomes really unimportant in the case of a PET-maximised multi-component system and the transition metal ions can be treated as any other nonquenching metal ions for sensing applications. We have also demonstrated that by combining an additional mechanism of fluorescence enhancement with the already existing PET one can improve the sensing ability of the simple fluorophore-spacer-receptor systems quite significantly.

The results obtained from this study are likely to initiate further research in this area. One needs to play with many other fluorophores so as to develop even more efficient sensor systems. Mechanisms other than the polarity induced fluorescence enhancement should be examined (along with PET) to enhance the signalling ability of the systems. We have restricted ourselves to a limited number of metal ions. The potential of the present systems in sensing other metal ions of interest needs to be investigated. This study has been carried out in non-aqueous media. It is necessary to examine how good these systems are in sensing the metal ions in aqueous media.

Table A1. Atomic coordinates (x 10^4) and equivalent isotropic displacement parameters (Å^2 x 10^3) for NPDPA. U(eq) is defined as one third of the trace of the orthogonalized U_{ij} tensor.

	x	y	z	U(eq)
0(1)	-905(3)	5359(2)	1165(3)	65(1)
0(2)	3087(3)	6419(2)	3028(3)	71(1)
N(1)	1138(3)	5848(2)	2039(3)	47(1)
N(2)	679(3)	8170(2)	-839(3)	56(1)
C(1)	2184(3)	5100(2)	4038(3)	43(1)
C(2)	3204(4)	5053(3)	5029(4)	61(1)
C(3)	3229(5)	4331(3)	5964(4)	68(1)
C(4)	2251(5)	3681(3)	5918(4)	63(1)
C(5)	89(5)	3056(3)	4858(4)	61(1)
C(6)	-939(5)	3128(3)	3900(4)	67(1)
C(7)	-959(4)	3846(3)	2958(4)	58(1)
C(8)	59(3)	4491(2)	2984(3)	43(1)
C(9)	1136(3)	4436(2)	3973(3)	43(1)
C(10)	1157(4)	3708(2)	4932(3)	50(1)
C(11)	27(4)	5243(2)	1989(3)	47(1)
C(12)	2188(3)	5834(2)	3013(4)	48(1)
C(13)	1155(4)	6568(3)	1006(3)	55(1)
C(14)	428(4)	7460(2)	1345(3)	56(1)
C(15)	844(5)	8308(3)	568(4)	69(1)
C(16)	1326(7)	8927(4)	-1473(6)	111(2)
C(17)	-713(5)	8112(5)	-1307(5)	110(2)

Table A2. Bond lengths [A] and angles [°] for NPDPA

O(1)-C(11)	1.210(4)	C(16)-N(2)-C(15)	109.3(4)
O(2)-C(12)	1.223(4)	C(2)-C(1)-C(9)	120.3(3)
N(1)-C(12)	1.381(4)	C(2)-C(1)-C(12)	120.4(3)
N(1)-C(11)	1.402(4)	C(9)-C(1)-C(12)	119.3(3)
N(1)-C(13)	1.470(4)	C(1)-C(2)-C(3)	120.3(4)
N(2)-C(17)	1.434(6)	C(4)-C(3)-C(2)	120.7(4)
N(2)-C(16)	1.438(6)	C(3)-C(4)-C(10)	121.3(4)
N(2)-C(15)	1.444(5)	C(6)-C(5)-C(10)	120.7(4)
C(1)-C(2)	1.373(5)	C(5)-C(6)-C(7)	120.8(4)
C(1)-C(9)	1.408(5)	C(8)-C(7)-C(6)	120.6(4)
C(1)-C(12)	1.477(5)	C(7)-C(8)-C(9)	119.7(3)
C(2)-C(3)	1.399(6)	C(7)-C(8)-C(11)	120.1(3)
C(3)-C(4)	1.343(6)	C(9)-C(8)-C(11)	120.2(3)
C(4)-C(10)	1.420(5)	C(1)-C(9)-C(8)	120.9(3)
C(5)-C(6)	1.359(6)	C(1)-C(9)-C(10)	119.3(3)
C(5)-C(10)	1.411(6)	C(8)-C(9)-C(10)	119.8(3)
C(6)-C(7)	1.401(6)	C(5)-C(10)-C(4)	123.6(4)
C(7)-C(8)	1.369(5)	C(5)-C(10)-C(9)	118.4(3)
C(8)-C(9)	1.412(5)	C(4)-C(10)-C(9)	118.0(4)
C(8)-C(11)	1.471(5)	O(1)-C(11)-N(1)	120.1(3)
C(9)-C(10)	1.422(5)	O(1)-C(11)-C(8)	123.1(3)
C(13)-C(14)	1.516(5)	N(1)-C(11)-C(8)	116.8(3)
C(14)-C(15)	1.520(5)	O(2)-C(12)-N(1)	120.8(3)
		O(2)-C(12)-C(1)	121.2(3)
C(12)-N(1)-C(11)	124.6(3)	N(1)-C(12)-C(1)	118.0(3)
C(12)-N(1)-C(13)	118.0(3)	N(1)-C(13)-C(14)	112.3(3)
C(11)-N(1)-C(13)	117.4(3)	C(13)-C(14)-C(15)	112.5(3)
C(17)-N(2)-C(16)	110.9(4)	N(2)-C(15)-C(14)	113.6(3)
C(17)-N(2)-C(15)	111.1(4)		

Table A3. Anisotropic displacement parameters (A^2 x 10^3) for NPDPA. The anisotropic displacement factor exponent takes the form: $-2 n^2 [(ha^*)^2 U11 + ... + 2 h k a^* b^* U12]$

	un	U22	U33	U23	U13	U12
0(1)	66(2)	70(2)	56(2)	6(1)	-8(1)	3(1)
0(2)	65(2)	58(2)	89(2)	2(2)	7(2)	-15(1)
N(1)	56(2)	38(1)	48(2)	5(1)	11(1)	-1(1)
N(2)	57(2)	58(2)	53(2)	14(1)	8(1)	4(2)
C(1)	45(2)	38(2)	46(2)	-4(1)	7(1)	6(1)
C(2)	54(2)	60(2)	66(2)	-7(2)	0(2)	5(2)
C(3)	71(3)	73(3)	58(2)	4(2)	-9(2)	15(2)
C(4)	78(3)	57(2)	54(2)	10(2)	6(2)	21(2)
C(5)	80(3)	42(2)	63(2)	9(2)	26(2)	5(2)
C(6)	66(3)	55(2)	83(3)	0(2)	19(2)	-14(2)
C(7)	51(2)	62(2)	60(2)	0(2)	4(2)	-8(2)
C(8)	46(2)	37(2)	47(2)	-1(1)	9(1)	2(1)
C(9)	46(2)	41(2)	45(2)	-4(1)	12(1)	10(1)
C(10)	59(2)	43(2)	51(2)	2(2)	14(2)	16(2)
C(11)	56(2)	43(2)	41(2)	-3(2)	7(2)	2(2)
C(12)	48(2)	40(2)	58(2)	-3(2)	8(2)	-1(2)
C(13)	67(2)	51(2)	48(2)	10(2)	18(2)	4(2)
C(14)	69(2)	48(2)	53(2)	5(2)	12(2)	8(2)
C(15)	80(3)	52(2)	73(3)	5(2)	2(2)	3(2)
C(16)	149(6)	74(3)	120(4)	36(3)	59(4)	13(4)
C(17)	73(3)	175(6)	79(3)	-10(4)	-13(3)	20(4)

Table A4. Hydrogen coordinates (x 10^4) and isotropic displacement parameters (Å^2 x 10^3) for NPDPA.

	x	y	z	U(eq)
H(2)	3881	5503	5079	73
H(3)	3930	4302	6625	82
H(4)	2291	3204	6544	75
H(5)	89	2572	5472	73
H(6)	-1639	2695	3870	81
H(7)	-1671	3885	2309	69
H(13A)	736	6314	188	65
H(13B)	2078	6720	874	65
H(14A)	613	7588	2278	67
H(14B)	-530	7364	1169	67
H(15A)	315	8848	790	83
H(15B)	1777	8451	830	83
H(16A)	1309	8800	-2398	167
H(16B)	2240	8980	-1103	167
H(16C)	863	9506	-1340	167
H(17A)	-1176	8656	-1018	165
H(17B)	-1095	7553	-966	165
H(17C)	-798	8090	-2251	165

Table A5. Atomic coordinates (x 10^4) and equivalent isotropic displacement parameters (Å^2 x 10^3) for molecule NPPED. U(eq) is defined as one third of the trace of the orthogonalized Uij tensor.

	x	y	z	U(eq)
N(1)	1687(3)	7130(2)	4629(2)	44(1)
0(1)	1723(3)	8737(2)	4840(2)	31(1)
C(8)	-203(4)	6886(3)	3595(3)	46(1)
0(2)	1795(3)	5563(2)	4334(2)	66(1)
N(2)	5973(4)	6527(3)	5235(3)	60(1)
N(3)	1352(4)	6596(2)	9196(2)	50(1)
0(4)	2258(4)	7235(2)	7632(2)	74(1)
0(3)	444(4)	5963(3)	10768(2)	75(1)
N(4)	1269(4)	8257(2)	10247(2)	55(1)
C(1)	-365(4)	8587(3)	3955(2)	43(1)
C(2)	-1076(5)	9593(3)	3854(3)	52(1)
C(3)	-2381(5)	9991(3)	3298(3)	64(1)
C(4)	-2957(5)	9382(4)	2852(3)	62(1)
C(5)	-2754(5)	7673(4)	2451(3)	66(1)
C(6)	-2006(5)	6695(4)	2524(3)	69(1)
C(7)	-721(5)	6291(4)	3097(3)	62(1)
C(9)	-942(4)	7932(3)	3499(2)	42(1)
C(10)	-2253(5)	8331(3)	2929(3)	51(1)
C(11)	1154(4)	6466(3)	4203(3)	45(1)
C(12)	1077(5)	8203(3)	4512(3)	50(1)
C(13)	3033(4)	6716(3)	5238(3)	50(1)
C(14)	4627(5)	6854(3)	4645(3)	56(1)
C(15)	6578(4)	7190(3)	5637(3)	46(1)
C(16)	5808(5)	8190(3)	5632(3)	59(1)
C(17)	6505(6)	**8818(4)**	6035(3)	68(1)
C(18)	7916(6)	8472(4)	6465(3)	66(1)
C(19)	8668(5)	7483(4)	6478(3)	60(1)
C(20)	7995(4)	6847(3)	6079(3)	52(1)
C(21)	3430(4)	5541(3)	8456(3)	44(1)
C(22)	4461(5)	5430(3)	7681(3)	' 54(1)
C(23)	5521(5)	4514**(4)**	7753(3)	63(1)
C(24)	5580(5)	3724(3)	8597(3)	58(1)
C(25)	4645(5)	3038(3)	10328(3)	58(1)

C(26)	3676(5)	3190(3)	11111(3)	61(1)
C(27)	2595(5)	4097(3)	11026(3)	56(1)
C(28)	2477(4)	4859(3)	10167(3)	47(1)
C(29)	3476(4)	4741(3)	9344(3)	40(1)
C(30)	4568(4)	3815(3)	9419(3)	46(1)
C(31)	1333(4)	5834(3)	10086(3)	53(1)
C(32)	2325(5)	6513(3)	8380(3)	49(1)
C(33)	208(5)	7562(3)	9105(4)	68(1)
C(34)	976(5)	8461(3)	9247(3)	57(1)
C(35)	1881(4)	8970(3)	10581(3)	45(1)
C(36)	2439(5)	9881(3)	9957(3)	53(1)
C(37)	3114(5)	10550(3)	10323(3)	60(1)
C(38)	3211(5)	10347(3)	11301(3)	56(1)
C(39)	2652(5)	9460(3)	11914(3)	59(1)
C(40)	1989(5)	8779(3)	11564(3)	54(1)

Table A6. Bond lengths [A] and angles [º] for molecule, NPPED.

N(1)-C(11)	1.379(4)	C(22)-C(23)	1.392(6)
N(1)-C(12)	1.418(5)	C(23)-C(24)	1.361(6)
N(1)-C(13)	1.472(4)	C(24)-C(30)	1.412(6)
O(1)-C(12)	1.196(5)	C(25)-C(26)	1.371(6)
C(8)-C(7)	1.373(5)	C(25)-C(30)	1.418(6)
C(8)-C(9)	1.418(5)	C(26)-C(27)	1.392(6)
C(8)-C(11)	1.479(5)	C(27)-C(28)	1.360(5)
O(2)-C(11)	1.218(4)	C(28)-C(29)	1.418(5)
N(2)-C(15)	1.386(5)	C(28)-C(31)	1.489(5)
N(2)-C(14)	1.450(5)	C(29)-C(30)	1.417(5)
N(3)-C(32)	1.386(5)	C(33)-C(34)	1.530(5)
N(3)-C(31)	1.388(5)	C(35)-C(40)	1.388(5)
N(3)-C(33)	1.479(5)	C(35)-C(36)	1.394(5)
O(4)-C(32)	1.221(4)	C(36)-C(37)	1.391(5)
O(3)-C(31)	1.212(5)	C(37)-C(38)	1.377(6)
N(4)-C(35)	1.382(4)	C(38)-C(39)	1.367(6)
N(4)-C(34)	1.444(5)	C(39)-C(40)	1.384(5)
C(1)-C(2)	1.363(5)		
C(1)-C(9)	1.418(5)		
C(1)-C(12)	1.493(5)	C(11)-N(1)-C(12)	125.6(3)
C(2)-C(3)	1.397(6)	C(11)-N(1)-C(13)	118.2(3)
C(3)-C(4)	1.358(6)	C(12)-N(1)-C(13)	116.2(3)
C(4)-C(10)	1.421(6)	C(7)-8C-C(9)	119.6(3)
C(5)-C(6)	1.346(6)	C(7)-8C-C(11)	120.9(3)
C(5)-C(10)	1.412(6)	C(9)-8C-C(11)	119.4(3)
C(6)-C(7)	1.398(6)	C(15)-N(2)-C(14)	123.5(3)
C(9)-C(10)	1.414(5)	C(32)-N(3)-C(31)	125.4(3)
C(13)-C(14)	1.523(5)	C(32)-N(3)-C(33)	117.4(3)
C(15)-C(20)	1.387(5)	C(31)-N(3)-C(33)	117.2(3)
C(15)-C(16)	1.397(5)	C(35)-N(4)-C(34)	122.5(3)
C(16)-C(17)	1.391(6)	C(2)-C(1)-C(9)	120.4(3)
C(17)-C(18)	1.375(7)	C(2)-C(1)-C(12)	119.1(3)
C(18)-C(19)	1.377(6)	C(9)-C(1)-C(12)	120.4(3)
C(19)-C(20)	1.383(5)	C(1)-C(2)-C(3)	120.4(4)
C(21)-C(22)	1.373(5)	C(4)-C(3)-C(2)	120.5(4)
C(21)-C(29)	1.411(5)	C(3)-C(4)-C(10)	121.4(4)
C(21)-C(32)	1.470(5)	C(6)-C(5)-C(10)	121.5(4)
		C(5)-C(6)-C(7)	120.6(4)

C(8)-C(7)-C(6)	120.5(4)	C(26)-C(25)-C(30)	120.1(4)
C(10)-C(9)-C(1)	119.6(3)	C(25)-C(26)-C(27)	120.8(4)
C(10)-C(9)-8C	119.6(3)	C(28)-C(27)-C(26)	120.9(4)
C(1)-C(9)-8C	120.8(3)	C(27)-C(28)-C(29)	120.0(4)
C(5)-C(10)-C(9)	118.2(4)	C(27)-C(28)-C(31)	120.6(4)
C(5)-C(10)-C(4)	124.1(4)	C(29)-C(28)-C(31)	119.4(3)
C(9)-C(10)-C(4)	117.7(4)	C(21)-C(29)-C(28)	121.1(3)
O(2)-C(11)-N(1)	120.1(3)	C(21)-C(29)-C(30)	119.3(3)
O(2)-C(11)-8C	121.9(3)	C(28)-C(29)-C(30)	119.5(3)
N(1)-C(11)-8C	118.0(3)	C(24)-C(30)-C(25)	122.8(4)
O(1)-C(12)-N(1)	120.1(3)	C(24)-C(30)-C(29)	118.6(4)
O(1)-C(12)-C(1)	124.5(3)	C(25)-C(30)-C(29)	118.6(4)
N(1)-C(12)-C(1)	115.4(3)	O(3)-C(31)-N(3)	121.6(4)
N(1)-C(13)-C(14)	111.6(3)	O(3)-C(31)-C(28)	121.6(4)
N(2)-C(14)-C(13)	112.9(3)	N(3)-C(31)-C(28)	116.8(3)
C(20)-C(15)-N(2)	119.1(3)	O(4)-C(32)-N(3)	120.3(4)
C(20)-C(15)-C(16)	118.1(4)	O(4)-C(32)-C(21)	122.0(4)
N(2)-C(15)-C(16)	122.8(3)	N(3)-C(32)-C(21)	117.7(3)
C(17)-C(16)-C(15)	119.5(4)	N(3)-C(33)-C(34)	111.8(3)
C(18)-C(17)-C(16)	121.8(4)	N(4)-C(34)-C(33)	110.7(4)
C(17)-C(18)-C(19)	118.6(4)	C(40)-C(35)-N(4)	119.9(3)
C(20)-C(19)-C(18)	120.3(4)	C(40)-C(35)-C(36)	117.9(3)
C(19)-C(20)-C(15)	121.6(4)	N(4)-C(35)-C(36)	122.2(3)
C(22)-C(21)-C(29)	120.1(3)	C(37)-C(36)-C(35)	120.2(4)
C(22)-C(21)-C(32)	120.3(3)	C(38)-C(37)-C(36)	121.1(4)
C(29)-C(21)-C(32)	119.6(3)	C(37)-C(38)-C(39)	418.8(4)
C(21)-C(22)-C(23)	120.5(4)	C(38)-C(39)-C(40)	120.9(4)
C(24)-C(23)-C(22)	120.7(4)	C(35)-C(40)-C(39)	121.1(4)
C(23)-C(24)-C(30)	120.7(4)		

Table A7. Anisotropic displacement parameters (Å^2 x 10^3) for molecule, NPPED. The anisotropic displacement factor exponent takes the form: $-2\pi^2[(ha^*)^2\ U11 + ... + 2\ h\ k\ a^*\ b^*\ U12]$

	U11	U22	U33	U23	U13	U12
N(1)	40(2)	49(2)	47(2)	-19(1)	-7(1)	1(1)
0(1)	30(2)	29(2)	46(2)	-26(1)	-14(1)	-5(1)
C(8)	41(2)	48(2)	52(2)	-21(2)	-2(2)	-5(2)
0(2)	59(2)	54(2)	94(2)	-34(2)	-21(2)	8(1)
N(2)	46(2)	56(2)	85(2)	-33(2)	-19(2)	4(2)
N(3)	43(2)	47(2)	65(2)	-25(2)	-12(2)	3(1)
0(4)	88(2)	60(2)	68(2)	-12(2)	-23(2)	8(2)
0(3)	63(2)	87(2)	79(2)	-40(2)	16(2)	-5(2)
N(4)	64(2)	44(2)	61(2)	-20(2)	-8(2)	-6(2)
C(1)	39(2)	47(2)	44(2)	-17(2)	0(2)	-5(2)
C(2)	54(2)	47(2)	56(2)	-21(2)	-2(2)	0(2)
C(3)	65(3)	55(2)	65(3)	-13(2)	-4(2)	8(2)
C(4)	50(2)	77(3)	50(2)	-10(2)	-11(2)	9(2)
C(5)	52(3)	91(3)	61(3)	-28(2)	-18(2)	-2(2)
C(6)	62(3)	83(3)	81(3)	-46(3)	-26(2)	-3(2)
C(7)	58(3)	67(3)	74(3)	-37(2)	-11(2)	-5(2)
C(9)	39(2)	47(2)	38(2)	-13(2)	1(1)	-2(2)
C(10)	41(2)	66(3)	45(2)	-17(2)	-2(2)	-3(2)
C(11)	43(2)	42(2)	54(2)	-22(2)	-3(2)	-2(2)
C(12)	45(2)	52(2)	46(2)	-10(2)	4(2)	5(2)
C(13)	39(2)	66(3)	43(2)	-11(2)	-10(2)	-2(2)
C(14)	41(2)	79(3)	48(2)	-20(2)	-9(2)	-2(2)
C(15)	38(2)	50(2)	49(2)	-17(2)	0(2)	-4(2)
C(16)	50(2)	56(2)	70(3)	-19(2)	-8(2)	-3(2)
C(17)	67(3)	58(3)	80(3)	-25(2)	9(2)	-15(2)
C(18)	69(3)	78(3)	59(3)	-27(2)	5(2)	-31(3)
C(19)	51(2)	81(3)	48(2)	-16(2)	-7(2)	-14(2)
C(20)	47(2)	53(2)	50(2)	-9(2)	-5(2)	-4(2)
C(21)	45(2)	45(2)	50(2)	-21(2)	-10(2)	-7(2)
C(22)	54(2)	64(3)	47(2)	-20(2)	-4(2)	-9(2)
C(23)	51(3)	86(3)	60(3)	-39(2)	-1(2)	-3(2)
C(24)	48(2)	58(3)	80(3)	-39(2)	-14(2)	3(2)
C(25)	59(3)	41(2)	81(3)	-19(2)	-27(2)	-4(2)

C(26)	68(3)	52(2)	61(3)	-3(2)	-18(2)	-19(2)
C(27)	60(3)	60(3)	55(2)	-19(2)	-1(2)	-23(2)
C(28)	44(2)	48(2)	55(2)	-20(2)	-7(2)	-13(2)
C(29)	41(2)	37(2)	50(2)	-20(2)	-11(2)	-7(2)
C(30)	42(2)	43(2)	59(2)	-21(2)	-14(2)	-4(2)
C(31)	41(2)	63(3)	67(3)	-37(2)	-2(2)	-12(2)
C(32)	50(2)	50(2)	54(2)	-19(2)	-17(2)	-5(2)
C(33)	49(3)	56(2)	114(4)	-45(3)	-34(3)	17(2)
C(34)	66(3)	42(2)	65(3)	-16(2)	-19(2)	-2(2)
C(35)	37(2)	42(2)	56(2)	-20(2)	0(2)	3(2)
C(36)	55(2)	48(2)	52(2)	-13(2)	-5(2)	-1(2)
C(37)	65(3)	44(2)	72(3)	-18(2)	-5(2)	-9(2)
C(38)	55(2)	53(2)	65(3)	-25(2)	-9(2)	-6(2)
C(39)	65(3)	63(3)	52(2)	-23(2)	-8(2)	1(2)
C(40)	57(2)	49(2)	54(2)	-15(2)	6(2)	-8(2)

Table A8. Hydrogen coordinates (x 10^4) and isotropic displacement parameters (Å^2 x 10^3) for molecule, NPPED.

	x	y	z	U(eq)
H(2)	6420	5887	5340	72
H(4)	1054	7669	10651	66
H(2)	-691	10017	4156	62
H(3)	-2859	10678	3234	77
H(4)	-3830	9659	2488	74
H(5)	-3620	7922	2077	80
H(6)	-2347	6284	2191	83
H(7)	-214	5614	3140	74
H(13)	2925	6408	5903	60
H(14)	4726	7120	3976	67
H(16)	4837	8433	5362	71
H(17)	6002	9491	6012	81
H(18)	8353	8898	6743	79
H(19)	9632	7241	6756	72
H(20)	8504	6175	6109	62
H(22)	4451	5970	7104	64
H(23)	6196	4442	7219	75
H(24)	6294	3118	8633	70
H(25)	5353	2424	10393	70
H(26)	3742	2680	11706	73
H(27)	1945	4184	11565	68
H(33)	-850	7616	8977	82
H(34)	1220	9057	8756	68
H(36)	2359	10040	9296	63
H(37)	3507	11146	9899	72
H(38)	3649	10805	11540	67
H(39)	2719	9312	12576	71
H(40)	1608	8183	11995	65

Table A9. Atomic coordinates (x 10^4) and equivalent isotropic displacement parameters (Å^2 x 10^3) for NPNED. U(eq) is defined as one third of the trace of the orthogonalized Uij tensor.

	x	y	z	U(eq)
N(1)	2117(2)	8229(2)	3023(2)	51(1)
N(2)	1572(2)	11788(3)	3288(2)	61(1)
0(1)	542(2)	7716(2)	2567(2)	71(1)
0(2)	3684(2)	8803(3)	3442(3)	93(1)
C(1)	3270(2)	6771(3)	2538(3)	58(1)
C(2)	4193(3)	6487(4)	2513(3)	85(1)
C(3)	4399(4)	5310(5)	2068(4)	102(2)
C(4)	3689(4)	4433(5)	1640(4)	90(1)
C(5)	1960(4)	3828(4)	1199(3)	72(1)
C(6)	1049(3)	4129(4)	1172(3)	75(1)
C(7)	847(3)	5315(3)	1599(3)	66(1)
C(8)	1571(2)	6178(3)	2072(2)	49(1)
C(9)	1355(2)	7403(3)	2554(2)	51(1)
C(10)	3071(2)	7993(3)	3033(3)	60(1)
C(11)	2527(2)	5879(3)	2089(2)	51(1)
C(12)	2728(3)	4691(3)	1638(3)	63(1)
C(13)	2349(2)	12532(3)	3826(3)	56(1)
C(14)	3275(3)	12118(4)	3951(3)	76(1)
C(15+)	4060(3)	12888(5)	4524(4)	98(2)
C(16)	3915(4)	14065(5)	4963(4)	99(2)
C(17)	2817(5)	15788(5)	5253(3)	92(2)
C(18)	1928(5)	16227(4)	5145(4)	90(1)
C(19)	1138(4)	15465(4)	4647(3)	78(1)
C(20)	1261(3)	14251(4)	4230(3)	65(1)
C(21)	2177(3)	13771(3)	4294(3)	56(1)
C(22)	2979(3)	14545(4)	4845(3)	73(1)
C(23)	1675(2)	10572(3)	2749(3)	59(1)
C(24)	1917(2)	9436(3)	3557(3)	56(1)

Table A10. Bond lengths [Å] and angles [°] for molecule, NPNED.

N(1)-C(10)	1.233(3)	C(1)-C(2)-C(3)	120.9(4)
N(1)-C(9)	1.322(4)	C(4)-C(3)-C(2)	127.4(4)
N(1)-C(24)	1.513(4)	C(12)-C(4)-C(3)	114.0(4)
N(2)-C(13)	1.318(4)	C(6)-C(5)-C(12)	115.0(4)
N(2)-C(23)	1.492(4)	C(5)-C(6)-C(7)	119.9(4)
O(1)-C(9)	1.087(3)	C(8)-C(7)-C(6)	127.8(3)
O(2)-C(10)	1.178(4)	C(11)-C(8)-C(7)	112.6(3)
C(1)-C(2)	1.219(4)	C(11)-C(8)-C(9)	119.9(3)
C(1)-C(11)	1.345(5)	C(7)-C(8)-C(9)	127.5(3)
C(1)-C(10)	1.495(5)	O(1)-C(9)-N(1)	111.7(3)
C(2)-C(3)	1.422(6)	O(1)-C(9)-C(8)	123.5(3)
C(3)-C(4)	1.301(6)	N(1)-C(9)-C(8)	124.8(3)
C(4)-C(12)	1.249(5)	O(2)-C(10)-N(1)	112.4(3)
C(5)-C(6)	1.189(5)	O(2)-C(10)-C(1)	130.6(3)
C(5)-C(12)	1.338(5)	N(1)-C(10)-C(1)	117.0(3)
C(6)-C(7)	1.415(5)	C(8)-C(11)-C(1)	113.3(3)
C(7)-C(8)	1.321(4)	C(8)-C(11)-C(12)	119.5(3)
C(8)-C(11)	1.245(4)	C(1)-C(11)-C(12)	127.2(3)
C(8)-C(9)	1.495(4)	C(4)-C(12)-C(5)	116.6(4)
C(11)-C(12)	1.434(5)	C(4)-C(12)-C(11)	118.3(4)
C(13)-C(14)	1.215(4)	C(5)-C(12)-C(11)	125.1(3)
C(13)-C(21)	1.479(5)	C(14)-C(13)-N(2)	115.2(4)
C(14)-C(15+)	1.359(6)	C(14)-C(13)-C(21)	119.2(3)
C(15+)-C(16)	1.396(7)	N(2)-C(13)-C(21)	125.6(3)
C(16)-C(22)	1.254(6)	C(13)-C(14)-C(15+)	114.1(4)
C(17)-C(18)	1.185(6)	C(14)-C(15+)-C(16)	127.5(4)
C(17)-C(22)	1.438(6)	C(22)-C(16)-C(15+)	120.9(4)
C(18)-C(19)	1.317(6)	C(18)-C(17)-C(22)	121.3(5)
C(19)-C(20)	1.406(5)	C(17)-C(18)-C(19)	113.9(5)
C(20)-C(21)	1.244(5)	C(18)-C(19)-C(20)	126.7(4)
C(21)-C(22)	1.362(5)	C(21)-C(20)-C(19)	121.9(4)
C(23)-C(24)	1.617(5)	C(20)-C(21)-C(22)	110.4(4)
		C(20)-C(21)-C(13)	123.8(3)
		C(22)-C(21)-C(13)	125.7(3)
C(10)-N(1)-C(9)	117.4(3)	C(16)-C(22)-C(21)	112.4(4)
C(10)-N(1)-C(24)	117.1(3)	C(16)-C(22)-C(17)	121.8(4)
C(9)-N(1)-C(24)	125.5(2)	C(21)-C(22)-C(17)	125.7(4)
C(13)-N(2)-C(23)	129.0(3)	N(2)-C(23)-C(24)	104.1(3)
C(2)-C(1)-C(11)	112.2(4)	N(1)-C(24)-C(23)	103.8(3)
C(2)-C(1)-C(10)	120.3(4)		
C(11)-C(1)-C(10)	127.5(3)		

Table A11. Anisotropic displacement parameters ($\text{Å}^2 \times 10^3$) for molecule, NPNED. The anisotropic displacement factor exponent takes the form: $-2\pi^2[(ha^*)^2 U11 + .., + 2hk\ a^* b^* U12]$

	un	U22	U33	U23	U13	U12
N(1)	30(1)	38(1)	85(2)	1(1)	16(1)	2(1)
N(2)	36(1)	45(2)	96(2)	-5(2)	10(1)	0(1)
0(1)	30(1)	60(2)	122(2)	-3(1)	20(1)	3(1)
0(2)	32(1)	71(2)	173(3)	-18(2)	20(1)	-9(1)
C(1)	37(1)	53(2)	86(3)	11(2)	21(2)	9(1)
C(2)	40(2)	87(3)	127(4)	9(3)	25(2)	15(2)
C(3)	59(2)	106(4)	150(5)	8(3)	44(3)	38(3)
C(4)	87(3)	76(3)	115(4)	4(3)	43(3)	37(3)
C(5)	98(3)	45(2)	80(3)	⊤3(2)	36(2)	3(2)
C(6)	73(2)	60(3)	94(3)	-10(2)	25(2)	-11(2)
C(7)	55(2)	53(2)	91(3)	-6(2)	21(2)	-11(2)
C(8)	44(2)	43(2)	63(2)	9(2)	17(2)	0(1)
C(9)	34(1)	42(2)	76(2)	6(2)	15(2)	1(1)
C(10)	32(1)	51(2)	96(3)	9(2)	16(2)	4(1)
C(11)	46(2)	44(2)	66(2)	10(2)	21(2)	⁓9(1)
C(12)	69(2)	50(2)	75(3)	6(2)	29(2)	15(2)
C(13)	38(2)	50(2)	75(2)	11(2)	9(2)	-9(1)
C(14)	43(2)	70(3)	112(3)	8(2)	18(2)	-12(2)
C(15+)	42(2)	114(4)	134(4)	9(3)	17(2)	-22(2)
C(16)	68(3)	108(4)	116(4)	-8(3)	18(3)	-50(3)
C(17)	117(4)	76(3)	88(3)	-26(3)	37(3)	-54(3)
C(18)	134(4)	55(3)	91(3)	-18(2)	48(3)	-26(3)
C(19)	101(3)	52(2)	84(3)	•2(2)	31(2)	2(2)
C(20)	63(2)	51(2)	78(3)	1(2)	14(2)	-1(2)
C(21)	58(2)	45(2)	60(2)	5(2)	10(2)	-16(2)
C(22)	70(2)	71(3)	77(3)	1(2)	20(2)	-30(2)
C(23)	40(2)	42(2)	91(3)	-4(2)	13(2)	0(1)
C(24)	38(1)	41(2)	88(3)	-2(2)	15(2)	HO

Table A12. Hydrogen coordinates (x 10^4) and isotropic displacement parameters (Å^2 x 10^3) for NPNED.

	x	y	z	U(eq)
H(2)	913	12038	3241	73
H(2A)	4771	7047	2789	101
H(3)	5124	5148	2085	122
H(4)	3880	3681	1362	108
H(5)	2127	3052	935	87
H(6)	469	3585	870	90
H(7)	117	5511	1539	80
H(14)	3431	11343	3679	91
H(15)	4778	12596	4636	118
H(16)	4521	14499	5348	118
H(17)	3420	16255	5609	110
H(18)	1800	17035	5389	108
H(19)	426	15761	4562	94
H(20)	639	13795	3897	78
H(23A)	2273	10646	2456	71
H(23B)	1004	10395	2252	71
H(24A)	2555	9647	4080	67
H(24B)	1294	9312	3813	67